

MARINE AEROSOLS, THEIR PRECURSORS AND THEIR
INFLUENCE ON CLOUDS OVER THE GLOBAL OCEAN

MARÍA ARÁNZAZU LANA CELAYA

DR. RAFAEL SIMÓ Y DR. JORDI DACHS

20 DE DICIEMBRE DE 2011

ACTA DE QUALIFICACIÓ DE LA TESI DOCTORAL

Reunit el tribunal integrat pels sota signants per jutjar la tesi doctoral:

Títol de la tesi: Marine aerosols, their precursors and their influence on clouds over the global ocean.....

Autor de la tesi: María Aránzazu Lana Celaya.....

Acorda atorgar la qualificació de:

No apte

Aprovat

Notable

Excel·lent

Excel·lent Cum Laude

Barcelona, de/d' de

El President

El Secretari

.....
(nom i cognoms)

.....
(nom i cognoms)

El vocal

El vocal

El vocal

.....
(nom i cognoms)

.....
(nom i cognoms)

.....
(nom i cognoms)



UNIVERSITAT POLITÈCNICA
DE CATALUNYA
BARCELONATECH



Institut de Ciències del Mar

Marine aerosols, their precursors and their influence on clouds over the global ocean

María Aránzazu Lana Celaya

Tesis Doctoral presentada por D^a M. Aránzazu Lana Celaya para obtener el grado de Doctor por la Universitat Politècnica de Catalunya, Programa de Doctorado en Ciències del Mar

Directores: Dr. Rafel Simó y Dr. Jordi Dachs

Universitat Politècnica de Catalunya
Institut de Ciències del Mar (ICM-CSIC)

En Barcelona, a de de 2011

La Doctoranda
M. Aránzazu Lana

El Director
Rafel Simó

El Codirector
Jordi Dachs

A mis padres y hermanos,
a mis carnales...

Contents

Resumen/Summary	10/11
General Introduction	13
Aims of the Thesis	45
Chapter 1 An updated climatology of surface dimethylsulphide concentrations and emission fluxes in the global ocean	51
Chapter 2 Re-examination of global emerging patterns of ocean DMS concentration	93
Chapter 3 Natural seasonal feedback on shortwave solar radiation by low marine clouds	113
Chapter 4 Biogenic influence on cloud microphysics over the global	131
Conclusions and Discussion	161
References	181

La técnica era complicada, pero permitía introducir cada palabra pronunciada, en una gotita de agua. Cuando había suficientes como para llenar un vaso, se arrojaban al mar. Por esa razón cada mañana el olor de la bruma les hacía más sabios y precisos.

Jesús Lana.

Resumen

Los aerosoles marinos tienen un gran potencial para influir en el clima de la Tierra a través de sus efectos en las propiedades de las nubes. La hipótesis de CLAW va más allá y sugiere que los aerosoles marinos formados por el ciclo del azufre en océanos y atmósfera actúan como un mecanismo para la regulación del clima de la Tierra. Este efecto se produce a través de la influencia de las emisiones de plancton de compuestos de azufre en la formación de nubes. El fitoplancton produce sulfuro de dimetilo (DMS), un compuesto de azufre altamente volátil. Una vez en la atmósfera, el DMS se oxida y se convierte en la principal fuente de sulfatos naturales atmosféricos. Estos sulfatos actúan como núcleos de condensación, partículas esenciales para la formación de nubes. Estas partículas presentes en la atmósfera marina juegan un papel importante en el ciclo radiativo de la Tierra. Indirectamente, producen una mayor cantidad de gotas de las nubes. Mayor número de núcleos de condensación en las nubes implica gotas de nubes más pequeñas. La eficacia de las pequeñas gotas en reflejar la radiación solar incidente es mayor, lo que resulta en un aumento del albedo de las nubes, produciendo un efecto de enfriamiento en la superficie de la Tierra.

Para estudiar adecuadamente los aerosoles marinos necesitamos tener un correcto conocimiento de la distribución oceánica global de los precursores de aerosoles. Nuestro trabajo se ha centrado en las emisiones del océano a la atmósfera de DMS y otros gases biogénicos que puede tener un impacto en la microfísica de nubes. Durante la tesis se ha actualizado la climatología mensual global de DMS, aprovechando el aumento en tres veces del número de observaciones y una mejor distribución global de las mismas, en la base de datos de DMS. Los patrones emergentes encontrados con las versiones anteriores de la base de datos y de la climatología se han re-evaluado con la versión actualizada. Las relaciones estadísticas encontradas entre la evolución temporal de las concentraciones de DMS y las dosis de radiación solar y concentraciones de clorofila han sido re-examinadas. Los análisis de nueve años de datos de satélite sugieren que existe una correlación inversa entre la cubierta espacial de nubes marinas bajas y el tamaño de las gotas de nubes, relacionado con la presencia de aerosoles pequeños. Esta estacionalidad acoplada conduce al albedo de las nubes a contribuir a un forzamiento radiativo negativo superior en verano, y más bajo en invierno. Esta relación se interrumpe en las regiones de la atmósfera marina con un alto impacto de los aerosoles antropogénicos. En consecuencia, la posible influencia de los precursores de aerosoles marinos en las nubes se ha analizado en una atmósfera marina limpia y contaminada, por separado. Los 9 años de datos satelitales globales y climatologías oceánicas se han utilizado para derivar las parametrizaciones de los flujos de producción de aerosoles secundarios, formados por la oxidación de DMS, y otros compuestos volátiles orgánicos biogénicos. Además, los flujos de emisiones biogénicas de aerosoles primarios orgánicos y aerosoles de sal marina expulsados por acción del viento sobre la superficie del mar se ha estudiado también a nivel global. Las series semanales de las estimaciones de estos flujos se han correlacionado con las series temporales de los radios de las gotas de nubes. El resultado de los análisis estadísticos ha indicado que el azufre orgánico y otros aerosoles secundarios pueden ser importantes en la nucleación y la activación de sus gotas sobre las regiones oceánicas no contaminadas en latitudes medias y altas. Por el contrario, aerosoles primarios (orgánico y la sal del mar) han mostrado que, a pesar de que contribuyen a una gran proporción de la masa de aerosol marino, no parecen ser los principales motores de la variabilidad de la microfísica de nubes.

Nuestros resultados proporcionan un apoyo parcial a la viabilidad de la hipótesis de CLAW a escala estacional. A pesar de que el DMS ha llamado mucho la atención sobre los vínculos entre la biota marina y la regulación del clima, la implicación de otros precursores biogénicos en la formación de nubes ofrece y sugiere un mayor alcance en la formulación de esta hipótesis.

Summary

Marine aerosols have a large potential to influence the Earth's climate through their effects on cloud properties. The CLAW hypothesis goes further, and suggests that marine aerosols formed by the sulphur cycle of the ocean and the atmosphere act as a mechanism for regulating the Earth's climate. This effect is produced through the influence of plankton emissions of sulphur compounds on cloud formation. Phytoplankton produces dimethylsulphide (DMS), a highly volatile sulphur compound. Once in the atmosphere, DMS is oxidized and becomes the main source of natural atmospheric sulphates. These sulphates act as condensation nuclei, particles that are essential for the formation of clouds. Those marine particles in the atmosphere play an important role in the Earth's radiation budget. Indirectly they produce a greater amount of cloud droplets. Higher cloud condensation nuclei imply smaller cloud droplets. The efficiency of smaller droplets in reflecting incident solar radiation is greater, resulting in an increase in cloud albedo, producing a cooling effect on the Earth's surface.

To properly study the marine aerosols we need accurate knowledge of the global seawater distribution of the aerosol precursors. Our work focused on the ocean-to-atmosphere emissions of DMS and other biogenic gases that can have an impact on cloud microphysics. During the thesis we updated the monthly global DMS climatology taking advantage of the three-fold increased size and better resolved distribution of the observations available in the DMS database. The emerging patterns found with the previous versions of the database and climatology were explored with the updated version. The statistical relationships between the seasonalities of DMS concentrations and solar radiation doses and chlorophyll *a* concentrations were here re-examined. Analyses of nine years of satellite data suggested that there is a natural inverse correlation between the spatial cover of low marine clouds and the cloud droplet size, which is related to the presence of small aerosols. This coupled seasonality pushes cloud albedo to contribute higher negative radiative forcing in summer and lower in winter. This relation is disrupted in the marine atmosphere regions heavily impacted by anthropogenic aerosols. Consequently, the potential influence the aerosol precursors have on marine clouds was next analysed over unpolluted and polluted ocean, separately. The 9 years of global satellite data and ocean climatologies were used to derive parameterizations of the production fluxes of secondary aerosols formed by oxidation of DMS and other biogenic organic volatiles. Further, the emission fluxes of biogenic primary organic and sea salt aerosols ejected by wind action on sea surface were also globally studied. Series of weekly estimates of these fluxes were correlated to series of cloud droplet effective radius. The outcome of the statistical analyses indicated that sulphur and organic secondary aerosols might be important in seeding cloud nucleation and droplet activation over mid and high latitude unpolluted oceanic regions. Conversely, primary aerosols (organic and sea salt) showed that, despite contributing to large shares of the marine aerosol mass, they do not seem to be major drivers of the variability of cloud microphysics.

Our results provide partial support for the feasibility of the CLAW hypothesis at the seasonal scale. Despite that DMS has drawn much of the attention on the links between marine biota and climate regulation, the implication of other biogenic precursors on cloud formation provides and suggests a wider scope on the formulation of such hypothesis.

General Introduction

The self-regulating Earth

The Earth's atmosphere is completely unstable, continuously consuming and replacing gases and particles that coexist within it. Its composition is surprisingly anomalous compared with the atmosphere expected for a planet located between Mars and Venus. Despite the changes occurred since the Earth was formed, the atmosphere has been kept appropriate for life for most of the time. And in turn, most of the chemical changes produced in the atmosphere over the Earth's history, in direction and/or amplitude, were a direct or indirect result of the developing biosphere. Apparently, the Earth maintains a stable and homeostatic system through all the processes among its components (upper lithosphere, hydrosphere, cryosphere, atmosphere and biosphere), with biosphere playing a pivotal role. This idea of the Earth as a self-regulating system was the premise of the Gaia hypothesis [Lovelock and Margulis, 1974], which later became theory. According to this theory, the Earth is a self-regulating system comprised of physical, chemical and biological components, all conforming a whole entity called Gaia. James Lovelock, the father of this theory, suggested that Gaia has developed the ability to regulate the chemical composition of its components, the surface pH and possibly, the climate [Lovelock and Margulis, 1974].

Gaia became an intuitive theory, difficult to prove in many aspects. However, for an increasing part of the scientific community, it became a trigger for a different –more holistic- view of the Earth system, and has been a valuable seed for modern biogeochemical and environmental sciences [Lovelock, 2003].

The understanding of this complex system begins with the knowledge of all the biogeochemical cycles that take place in it, which involve the physical, chemical, geological and biological processes among all the components of the Earth. Since the oceans cover the 70% of the Earth's surface, the processes and exchanges of particles and gases between the oceans and the atmosphere play an important role in the biogeochemical cycles of the Earth, and on its self-regulating behavior.

Aerosols

The particles suspended in the atmosphere are called aerosols. The aerosols play an important role on the physical and chemical characteristics of the Earth's atmosphere, and hence, on the Earth's radiation budget.

There are two different ways through which aerosols can be formed:

Directly - as particles, injected to the atmosphere from the land or surface ocean. These aerosols are called primary aerosols.

Indirectly - by chemical gas transformation into particles through nucleation or coalescence, in which case they are called secondary aerosols.

The aerosols found in the marine atmosphere can also be classified according to their origin. They can be continental aerosols, transported into the marine atmosphere by wind speed or atmospheric currents, and marine aerosols, originally formed at the sea surface, either directly or from gaseous precursors.

Continents are a large source of aerosols to the marine atmosphere. The continental aerosols are mainly formed by dust, biological (fungi, spores, seeds), biomass burning and urban and suburban particles, and secondary aerosols formed by gas-to-particle conversion processes [Kinne et al., 2003], see Figure 1 for a scheme of natural aerosols. The human activity has a very important impact in the amount of these aerosols. The desertification of the continents, the increase of human population, and industry are just a few examples of the immediate causes that would influence the amount of continental aerosols in the atmosphere.

Dust is composed by mineral aerosols ejected from the land into the atmosphere, where they remain suspended. Dust is dominated by coarse (large sized) aerosols and it is the major continental aerosol contributor to aerosol optical depth (the satellite-derived metrics that serves as a proxy of aerosol abundance), followed by biomass burning. Biomass burning is produced by the burn of vegetation, mostly due to human agricultural activity, and less to natural fires. The purpose of this burn is the elimination of dry vegetation to prepare the fields to cultivation, or other agricultural finalities. This activity is particularly widespread in Centre and South Africa, Southern Asia and

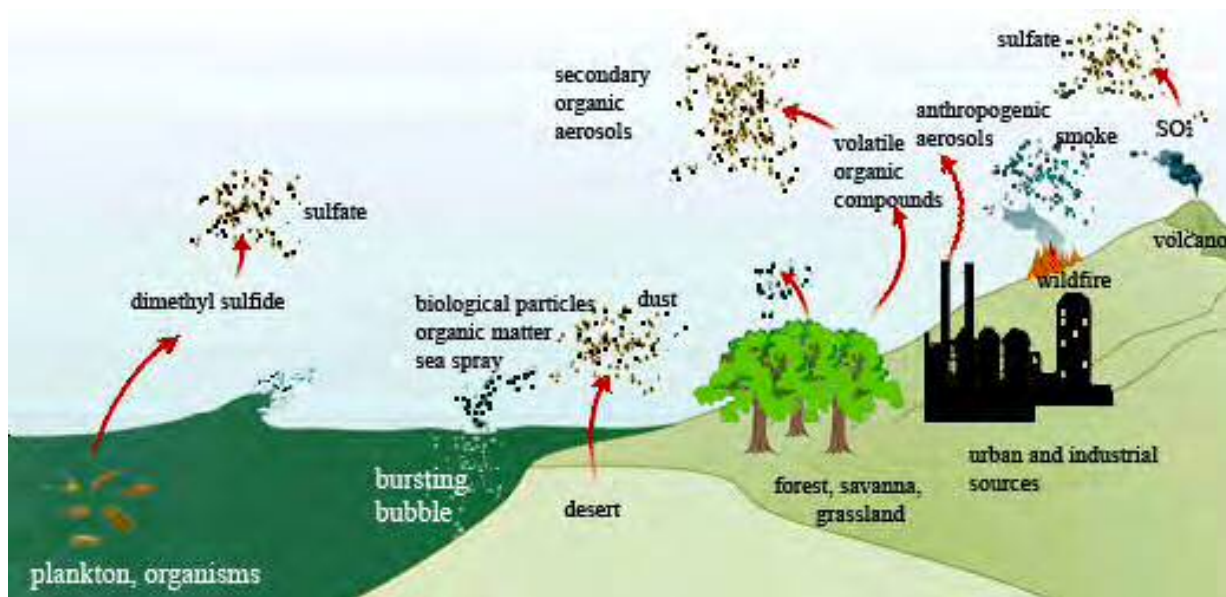


Figure 1. Scheme of primary and secondary aerosol sources (modified from Andreae, 2007).

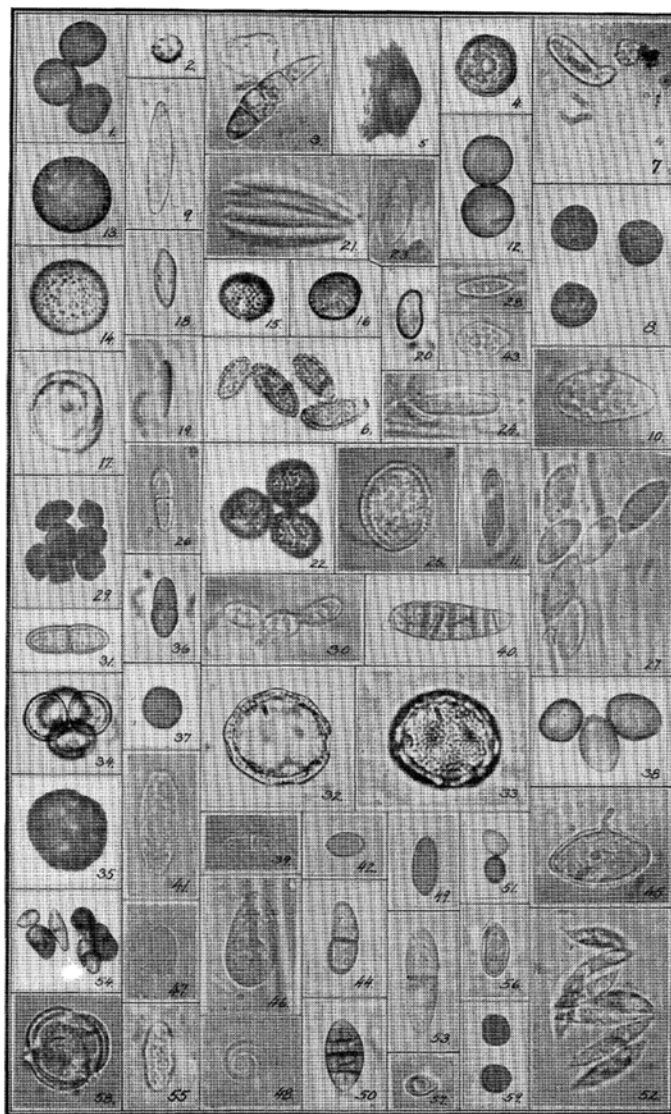
Central America. Biomass burning aerosols are dominated by fine particles. Urban and suburban aerosols, mainly produced by the combustion of fossil fuels, have a very variable influence in the aerosol optical depth. They are also dominated by fine sizes, with a consequent impact on human health. Marine aerosols mainly consist of sea salt crystals in all size ranges, yet dominant among coarse particles, small secondary or semi-secondary particles formed from gaseous precursors and biogenic polymers, and biological particles of all sizes, such as virus, bacteria and protists. The aerosol size and its proximity to potential continental sources are properties that can be used to distinguish continental and marine aerosols over the ocean by remote sensing. However, complete segregation is difficult to achieve, because, as mentioned above, both coarse and fine particles concur in both continental and marine aerosols. Also anthropogenic (continental) aerosols are difficult to distinguish from biogenic aerosols from either continental or marine origin. Anthropogenic contributions to aerosols are mainly sulfate, organic carbon, black carbon, nitrate, and dust from land mobilization and some industrial activities like concrete production. The amount of anthropogenic aerosols has largely increased since the Industrial Revolution, and with the land-use change associated with the increase in human population. Since most

anthropogenic aerosols are characterized by their small dimension, their localized sources and their pulsed emission, one can base their remote sensing characterization upon observations of size, connectivity to source points, and temporal variability [Kaufman, 2005]

Over the vast areas of the ocean far away from land, low particle numbers occur in the atmosphere. Even though aerosols are scarce in the pristine marine air compared with continental air, the oceanic atmosphere comprises an area two fold larger than that over land. Hence, marine aerosols have a larger impact in the Earth's atmosphere than the ones from continental origin.

In 1830 Ehrenberg published the first study of microscopic objects found in the marine atmosphere [Ehrenberg, 1830]. In 1846 Charles Darwin wrote: “Professor Ehrenberg has examined dust collected by L. James and myself, and he finds that it is in considerable part composed by infusoria, including no less than sixty-seven different forms” [Darwin, 1846]. Infusoria was a term, now obsolete, used to designate aquatic creatures like ciliates, euglenoids, protozoa, and unicellular algae. The aerosols recollected by Darwin and colleagues were from the African side of the Atlantic Ocean, a region heavily influenced by continental sources. Almost a hundred years had to pass before the pristine marine atmosphere started to be studied. In 1935 Meier and other scientists made simultaneous measurements from ship and airplane in the North Atlantic Ocean, visiting areas never studied before. Surprisingly, they found similar results to those obtained by Darwin [Meier, 1935]. They found a wide variety of micro-organisms present in the atmosphere – fungi, unicellular algae, diatoms, volcanic ash and glass, and other microscopic debris over the coast of Greenland, above the Arctic Circle, at 3,000 feet (914.4 m) above the sea level – see Figure 2.

The study of aerosols had scientific importance since the first studies, either because of their influence on human health, their interest for agriculture, or their key role in the physical and chemical characteristics of the atmosphere. Recently, aerosols have deserved further interest because of their ability to affect the climate through a wide variety of paths that will be explained below.



Photomicrographs by F. C. Meier

Figure 2. Plate with examples of particles found in the Arctic atmosphere [Meier, 1935]. Photomicrographs by F.C. Meier.

Aerosols and clouds

Cloud formation

Aerosols are needed to form clouds since water molecules in the atmosphere need somewhere to condense. Without aerosols, normal thermodynamic conditions in the atmosphere are too unfavorable for water to condense and clouds to form. There must be particles that act as cloud condensation nuclei.

The requirement of particles in the process of cloud formation was discovered by P.J. Coulier in 1875. He was, by then, a professor at a Parisian hospital, interested in the behavior of clouds. He made a few experiments to form clouds in a crystal flask – see Figure 3. By regulating the pressure inside the flask, which had some water, he observed that he was able to form clouds. Initially, the flask was filled with room air. When negative pressure was applied at the outlet of the flask, the air from the laboratory was drawn inside the flask, where it got saturated with water vapor. By closing the inlet to build up vacuum, the air expanded and cooled, forming a dense visible fog, a

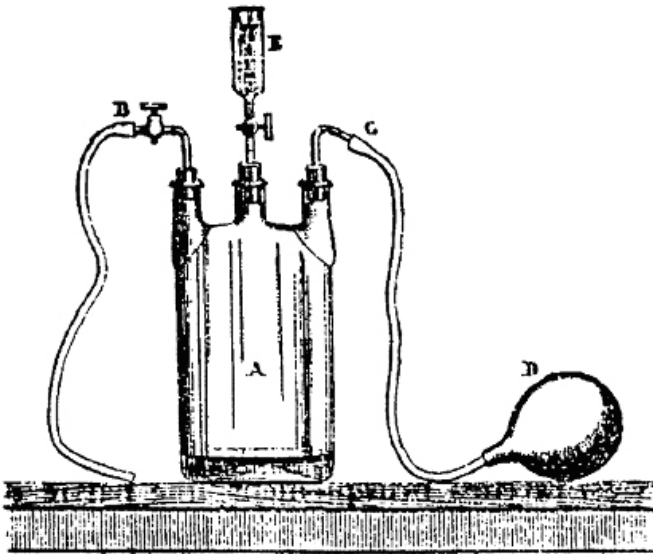


Figure 3. Apparatus used by P.J. Coulier for his studies on water vapour condensation [Coulier, 1875].

kind of artificial cloud. By contrast, if he filtered the air as it was drawn into the flask, he could not find cloud generation. This observation pointed to the existence of something in the air that enabled clouds to condense [Coulter, 1875]. A few years later, the Scottish researcher J. Aitken conducted the same experiment, with much more repercussion of his findings. Aitken, a brilliant scientist interested in a wide variety of atmospheric subjects, condensed in three affirmations the results of his first, of so many, experiments in cloud formation [Aitken, 1880]:

- when water vapor condenses in the atmosphere, it always does so on some solid nucleus;
- the dust particles in the air form the nuclei on which it condenses;
- if there was no dust in the air there would be no fogs, no clouds, no mists, and probably no rain.

Aerosols and cloud albedo

What Coulter and Aitken called dust, nowadays are called aerosols. Aerosols have a great impact on the Earth's radiation budget mainly in two ways [Penner et al., 2001] (see Figure 4):

Directly: The aerosols interfere with the incoming solar radiation. They can either absorb part of it, thus heating the troposphere, or scatter it, thus reflecting it back to space and cooling the troposphere.

Indirectly: Through the big influence they have on cloud formation. The physical and chemical characteristics of the aerosols modify cloud microphysics, producing changes in cloud optical properties (albedo) and lifetime.

C 

The albedo is a measure of the fraction of the solar radiation reflected back by a surface. Surfaces with high albedo reflect most of the solar radiation. The planetary albedo is the fraction of solar radiation reflected back to space by all components of a planet's surface and atmosphere. Most of the surfaces that cover the Earth have very low albedo, which means that they absorb most of the incident radiation and dissipate it as heat, thus causing warming. The darker the surface is,

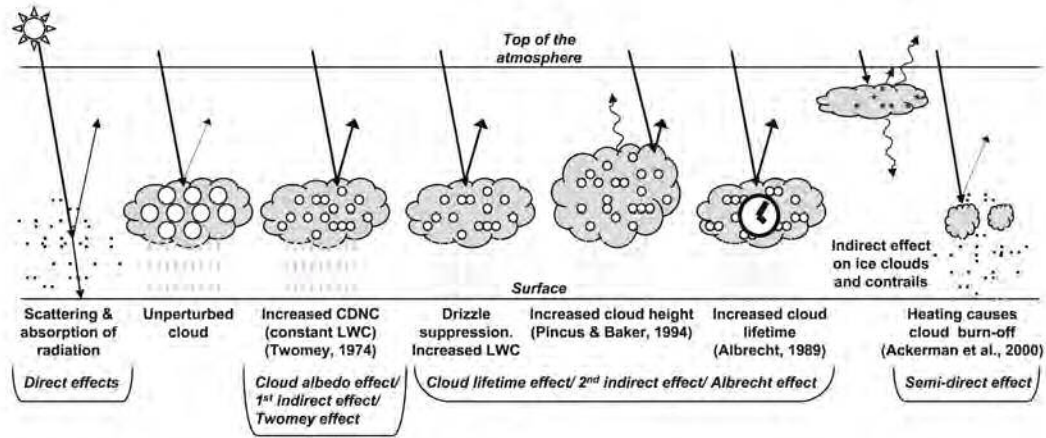


Figure 4. Scheme modified from Haywood and Boucher, 2000. It represents indirect radiative mechanisms associated with significant liquid clouds effects in relation to aerosols. Small black dots: aerosols. Open circles: cloud droplets. [Forster et al., 2007].

the lower its albedo, the larger its warming effect. Forests have different albedos according to the kind of trees they harbor; while coniferous forests have albedos between 0.05-0.15, deciduous forests reflect more radiation, with values ranging between 0.15-0.20. Other dry surfaces like sand or soil have a large variability with values varying between 0.1-0.4. The surface that covers most of the Earth, the dark ocean, has very low albedo, ranging from 0.06 to 0.1. Therefore, an Earth without clouds would have an average albedo of 0.15 and would absorb on average 85% of the incident radiation. However, since clouds have albedos between 0.4 and 0.8, and about half of the Earth is covered by clouds, our planet has an actual overall albedo of 0.30. This means that clouds have a very important role in the regulation of the amount of shortwave solar radiation that reaches the Earth's surface, acting as a parasol during the day and producing a cooling effect. Clouds also retain longwave radiation that leaves the Earth's surface during the night but their net effect is to cool the planet [Ramanathan et al., 1989, Harrison et al., 1990].

The net radiative behavior of clouds depends on the cloud type. Cloud type distributions differ over land and ocean. Water vapor and cloud nuclei supply have much to say in that distribution [Sassen and Wang, 2008], but essentially it is cloud altitude and thickness that determines the radiative properties of a cloud. High altitude clouds transmit large part of the short-wave incoming radiation (have low albedo), and retain the outgoing low-wave radiation – the one reflected by

the Earth's surface. So, their net balance is to warm the Earth, letting the solar radiation going in and not letting it going back to space. Deep convective (storm) clouds are as efficient at reflecting short-wave radiation as at retaining long-wave radiation, and their net effect on the radiative budget is virtually null. On the other hand, low clouds, and particularly layer clouds (stratiform clouds such as stratus and stratocumulus) have very high albedo. They reflect much of the incident shortwave radiation and are less efficient at retaining the long-wave radiation, so they cool the surface underneath. Solely low stratiform clouds are present 39.4% of the time over the ocean [Sassen and Wang, 2008]; therefore, these clouds largely reduce the amount of solar radiation absorbed by the dark oceans, that otherwise would have been 90% all over.

The cooling effect that low clouds have on Earth might play a fundamental role in a global warming scenario should cloud cover change significantly with warming. This will depend on changes in the water evaporation rates and the mobilization of water vapor, but also on changes in the amount of aerosols available for cloud condensation. The knowledge of the impact that the primary and secondary aerosols from the oceans have on cloud formation is therefore very important to the understanding of the Earth's radiation budget and its biogeochemical cycles.

The chemical composition of the aerosols (proportions of organic and inorganic components, water solubility, acidity) and the physical characteristics (size, surface tension...) are key parameters to take into account in the study of their role as potential cloud condensation nuclei. However, aerosol properties are highly variable. The aerosol size distribution can be classified in three main modes, as a function of their diameter size (d): Aitken ($d < 0.1 \mu\text{m}$), accumulation ($0.1\text{-}1 \mu\text{m}$) and coarse ($d > 1 \mu\text{m}$). Figure 5 shows examples of marine aerosols classified into the major size classes by columns. Aitken mode aerosols are mainly formed upon growth of nanoparticles evolved through particle nucleation; these serve as nuclei for the condensation of volatile substances until they reach the Aitken mode diameter [Hoppel et al., 1994; Weber et al., 1998]. Aitken particles move in the atmosphere by Brownian motion. Coagulation caused by the continuous collision between the particles is the most usual scavenging process for these fine particles, which thus evolve into larger (accumulation mode) aerosols. Coarse mode particles, mostly of primary origin, are highly affected by gravitational settling, hence, their residence in the atmosphere is shorter compared with the other aerosols [Kreidenweis et al., 1999]. The accumulation mode aerosols have the proper size to stay long in the atmosphere with a low number of collisions between particles [Saltzman, 2009a]. These aerosols tend to accumulate in the atmosphere, having an important role in the cloud formation, being potentially activated as cloud droplets with the proper humidity conditions. However, the understanding of cloud

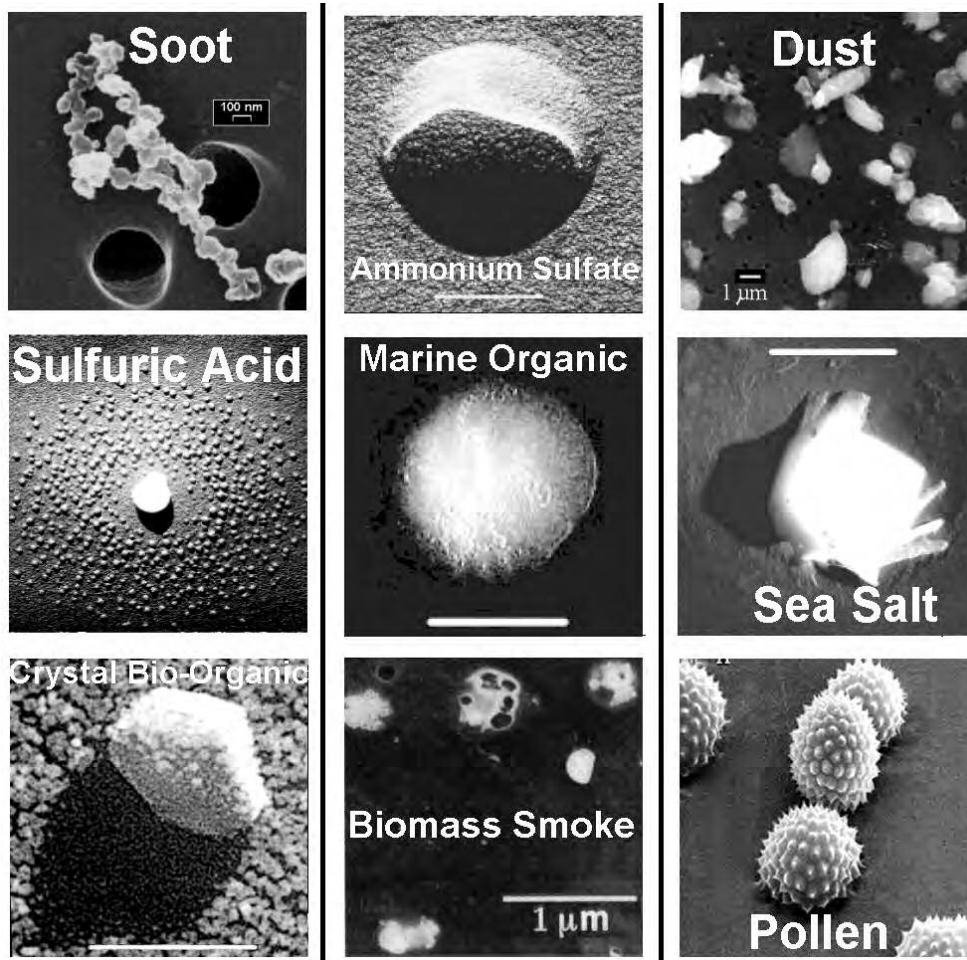


Figure 5. Examples of different aerosols from the marine atmosphere, classified by columns in the three main size modes: Aitken (left), accumulation (middle) and coarse (right). Modified from Brasseur et al., 2003.

formation also requires information about the aerosol number concentration, their size, their vertical velocity and their chemical composition. The prediction of the evolution of these aerosol characteristics is one of the largest sources of uncertainty in global warming models [Roesler and Penner, 2010].

Two main effects of aerosols on cloud formation constitute the aerosol indirect effect outline above [Lohmann, 2005]:

- **Cloud albedo effect:** Twomey's effect (also called *first indirect effect*).

Cloud microphysical properties are altered by aerosols. The size of the cloud droplets has a significant role in the Earth's albedo. The solar radiation reflected back to the space by a cloud depends greatly on the size and concentration of the cloud droplets. The smaller cloud droplets are, the higher is the amount of solar radiation reflected (higher albedo). With the same amount of liquid water, if there is an increase in the number of cloud droplets, these will be smaller, and the cloud albedo will increase [Twomey, 1974]. The presence of aerosols suited to act as cloud condensation nuclei will modify the amount of cloud droplets in the atmosphere. With a higher amount of aerosols, there will be a potential increase in the number of cloud droplets; hence they will have smaller size, and consequently higher albedo. This effect, called the Twomey's indirect effect, can be easily shown in the ship tracks – see Figure 6. The increase of the pollution injected by the ship into the atmosphere (primary and secondary aerosols) affects the cloud properties, producing brighter cloudy track.

- **Cloud lifetime effect:** Albrecht's effect (also called *second indirect effect*).

The clouds modified by an increase in the number of aerosols are more persistent because their smaller droplets will take longer to grow up to precipitable (raindrop) sizes [Albrecht 1989]. The amount of cloudiness due to the increase of aerosols has a large effect on the solar radiation reflected, not only producing clouds with higher albedo, but also extending their presence in the atmosphere.



Figure 6. Ship tracks in the coast of California, USA. Along the tracks the number of aerosols are higher, producing an increase in the number of cloud droplets, and hence smaller droplets, for a given liquid water content. Smaller droplets produce clouds with higher albedo, as it can be observed by the bright ship tracks.

M

P

At the sea surface, wind friction causes the entrance of air bubbles into the water. Bubble bursting produces the ejection of particles from the ocean directly into the atmosphere. The aerosols that compose the so-called sea spray are formed by organic and inorganic compounds. Marine primary organic aerosols are formed by virus and bacteria [Christner et al., 2008], plus polymeric organic material of biological origin [Leck and Bigg, 2005]. The inorganic fraction of the sea spray is composed by sea salt, which dominates the mass of primary aerosols in the marine atmosphere. Despite the importance of wind speed in sea-spray flux estimation [Geever, 2005],

sea-spray aerosol parameterization should also require the understanding of wave breaking, bubble formation, bubble bursting, aerosol ejection, deposition, and entrainment into the boundary layer [Saltzman, 2009a].

Marine organic sea-spray has not been incorporated in the large-scale models until very recently [O'Dowd et al., 2008], due to the difficulties to obtain a proper parameterization. It has been observed that the organic matter content of the sea-spray correlate with wind speed and the organic matter of surface seawater [O'Dowd et al., 2004]. Organic compounds have the largest contribution during high biological activity, while sea salt dominates the sea-spray during the periods of low biological activity [O'Dowd et al., 2008]. The global emission of organic matter in the submicron size range of sea-spray has been estimated at 8.2 Tg/yr, much lower than that of fine sea-salt, which accounts for 24 Tg/yr [Vignati et al., 2010].

Sea salt accounts for the largest mass emission of all the marine aerosols. Most of its mass corresponds to supermicron particles (see Figure 7), but its highest number concentration occurs in the submicron range [O'Dowd and De Leeuw, 2007, Andreae and Rosenfeld, 2008]. They seem to have an important role in the growth of sulfate aerosols [Pirjola et al., 2000].

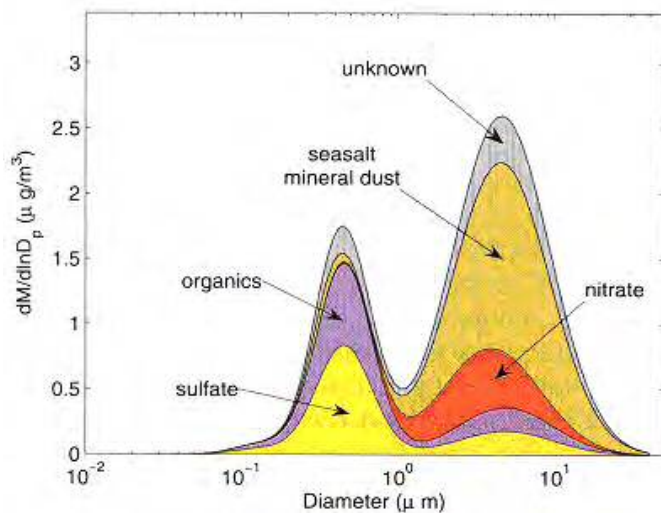


Figure 7. Size distribution of the mass of various marine aerosol components [Saltzman, 2009].

Sulfate aerosols

There are gases which have been suggested to play a role in cloud formation over the marine atmosphere. Gases emitted from the ocean are converted in the atmosphere - after some chemical processes - into aerosols. There are two ways this conversion can occur: a) via the nucleation of stable clusters or b) via heterogeneous reactions and aqueous phase oxidation of dissolved gases in existing aerosol particles [O'Dowd and Leeuw, 2007].

Sulfate aerosols have an important impact on the radiation budget, because they have large single-particle scattering and they are very efficient as CCN. The oceans are the main natural source of volatile sulfur [Simó, 2001, Gondwe et al., 2003], which enters in the atmosphere mainly through the emissions of dimethylsulfide (DMS). DMS is a gas generated by marine plankton. Its emission accounts for >90% of the oceanic emission of volatile sulfur. It is also the most studied marine aerosol precursor as it will be explained in the next section.

Marine algae also emit biogenic iodocarbons, which are suggested to play an important role in the formation of new particles over the coastal ocean [O'Dowd et al., 2002, Hughes et al., 2008]. Photolysis products of these biogenic iodocarbons, iodine-containing vapors, are responsible for new particle formation. Also ammonia and ammonium are produced in the sea surface, by the biological reduction of nitrate. There is an exchange of their gas form (ammonia) between ocean and atmosphere that can go in both directions depending on the water temperature and productivity [Johnson et al., 2008]. Part of the ammonia emitted to the atmosphere is incorporated into particles, generally as ammonium that neutralizes sulfuric acid into sulfate, which has an effect in the sulfur cycle and cloud formation [Quinn et al., 1988, Liss and Galloway, 1993]. Volatile organic compounds, such as isoprene, terpenes, and short-chained non-methane hydrocarbons, are also suggested to be a potential precursor to secondary organic aerosols. Recent studies [Saiz-Lopez et al., 2004, Greenberg et al., 2005, Palmer and Shaw, 2005] estimate that the organic volatile fluxes from marine biota seem to account for a significant share of the marine aerosol sources. However, it is still unclear if the oxidation products of volatile organics actually contribute significantly to nucleation of new particles [Vattovaara et al., 2006], or to the growth of recently formed aerosols. The potential role of biogenic volatiles, once emitted and oxidized in the atmosphere, in the formation of secondary organic aerosols was studied by Meskhidez and Nenes [2006] in an area characterized by an intense and recurrent chlorophyll *a* bloom in the Southern Ocean. Using remote-sensing and model simulations they concluded that

plankton-associated emissions may have a considerable role in Earth's radiation budget through their formation of secondary organic aerosols that can act as CCN, and subsequent effects on cloud albedo.

The linkages between marine aerosol precursors and their influence on cloud formation remain unclear. Deciphering the sources, chemical composition, chemical processes and formation and growth of marine aerosols are formidable challenges that require a whole lot of interdisciplinary and multiple-scale studies.

DMS: the missing link in the CLAW hypothesis

Hitherto, DMS has been the most deeply studied among marine organic volatiles, and particularly among secondary aerosol precursors. One reason for this interest lies on the fact that it occurs at concentrations 10 to 100 as high as those of other individual aerosol-forming volatiles [Simó, 2011]. But the most important reason is to be found in the hypothesis, released 24 years ago, that DMS could be a key piece of a gear by which biosphere-atmosphere interactions contribute to regulate the Earth's climate.

The CLAW hypothesis

In 1987 James Lovelock, together with Robert Charlson, Meinrat Andreae and Stephen Warren, hypothesized about a biological control of the Earth's climate, propounding the widely studied CLAW hypothesis (the acronym is based on the initials of the author's surnames; Charlson et al., 1987). According to this hypothesis, DMS emitted by the ocean acts as the main gaseous precursor of cloud condensation nuclei in the remote unpolluted marine atmosphere. Atmospheric DMS oxidation gives rise to sulfuric acid, among other products. Sulfuric acid nucleates to form new particles in the marine boundary layer. Actually, biogenic sulfate is ubiquitous as a component of the marine aerosol, usually neutralized with ammonium [Froyd et al. 2009], and at the time the CLAW hypothesis was released it was thought to be the main source of new CCN. Therefore, any increase in the oceanic DMS concentration and its emission flux, would produce an increase in the number of condensation nuclei of marine stratiform clouds, which would lead to smaller cloud droplets according to the Twomey's effect. This change would cause an increase in the cloud

albedo, reducing the input of light and heat into the oceans. Shading and cooling of the oceans could reduce biological DMS production and its emission to the atmosphere, thus completing a negative feedback [Charlson et al., 1987], see Figure 8.

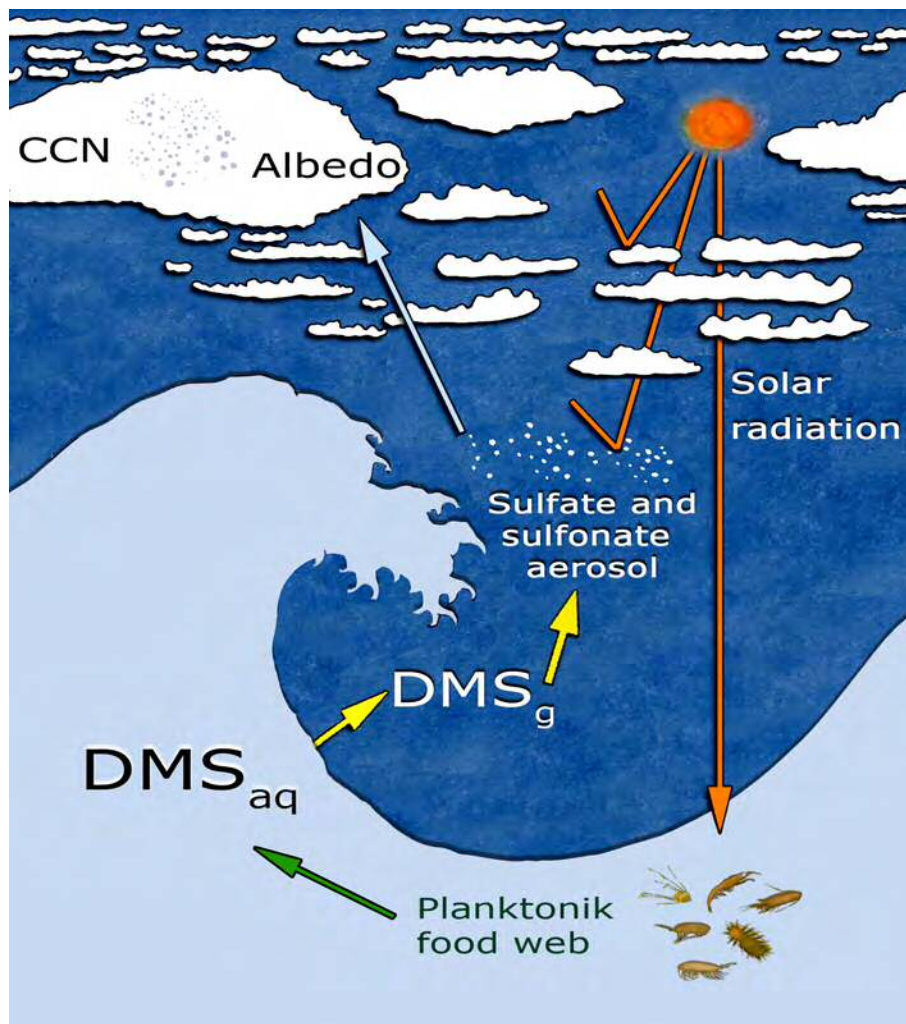


Figure 8. Schematic loop of the postulated DMS role in climate, according to the CLAW hypothesis.

DMS production and atmospheric transport

DMS is a biogenic gas naturally produced as a sub-product of food-web processes and as a product of stressed phytoplankton. The main precursor of DMS is the microalgal metabolite dimethylsulfoniopropionate (DMSP). Dissolved DMSP in the ocean can be transformed into DMS by extracellular and bacterial enzymes [Stefels et al. 2007, Vila-Costa et al., 2007, Howard et al., 2008]. There are multiple interactions among phytoplankton, zooplankton, bacteria and environmental forcing such as sunlight involved in the transformation of DMSP into DMS and the subsequent transformation of the latter. Eventually, only a small fraction of the DMS produced in the ocean escapes into the atmosphere [Simó, 2001, Vila-Costa et al., 2006].

The sea-air transfer of DMS is extremely difficult to measure *in situ*. There are many mechanisms to take into account, related to kinetic and thermodynamic constraints. One of the algorithms widely used to calculate DMS emission fluxes to the atmosphere is a function of sea surface temperature, wind speed and DMS seawater concentration [Nightingale et al., 2000]. Before this thesis, global oceanic DMS emissions had been estimated at approximately 15 – 21 TgS/year, depending on the parameterization used [Kettle and Andreae, 2000].

Global distribution of seawater DMS concentrations

The global distribution of seawater DMS concentrations is not accurately known, despite the multiple efforts invested so far. In 1999 A.J. Kettle and M.O. Andreae compiled the existing DMS measurements since 1972 with the aim to construct a database, and subsequently a climatology. Such database, still maintained at the NOAA-PMEL (<http://saga.pmelnoaa.gov/dms>), is widely used, and currently contains more than 48,000 DMS data. The DMS measurements, added to the database by individual contributors, are obtained from oceanographic cruises and time series stations over the ocean. The data are mainly collected in the top ten meters of the water column, where DMS occurs at nanomolar concentrations, i.e., about two orders of magnitude higher than most of other individual trace gases. The DMS data coverage of the ocean is not enough to derive a reliable global distribution by direct spatial interpolation/extrapolation, because there is a total lack of measurements in many areas of the ocean – see Figure 9. Also the temporal coverage in many regions is too poor to derive DMS seasonality by direct temporal interpolation.

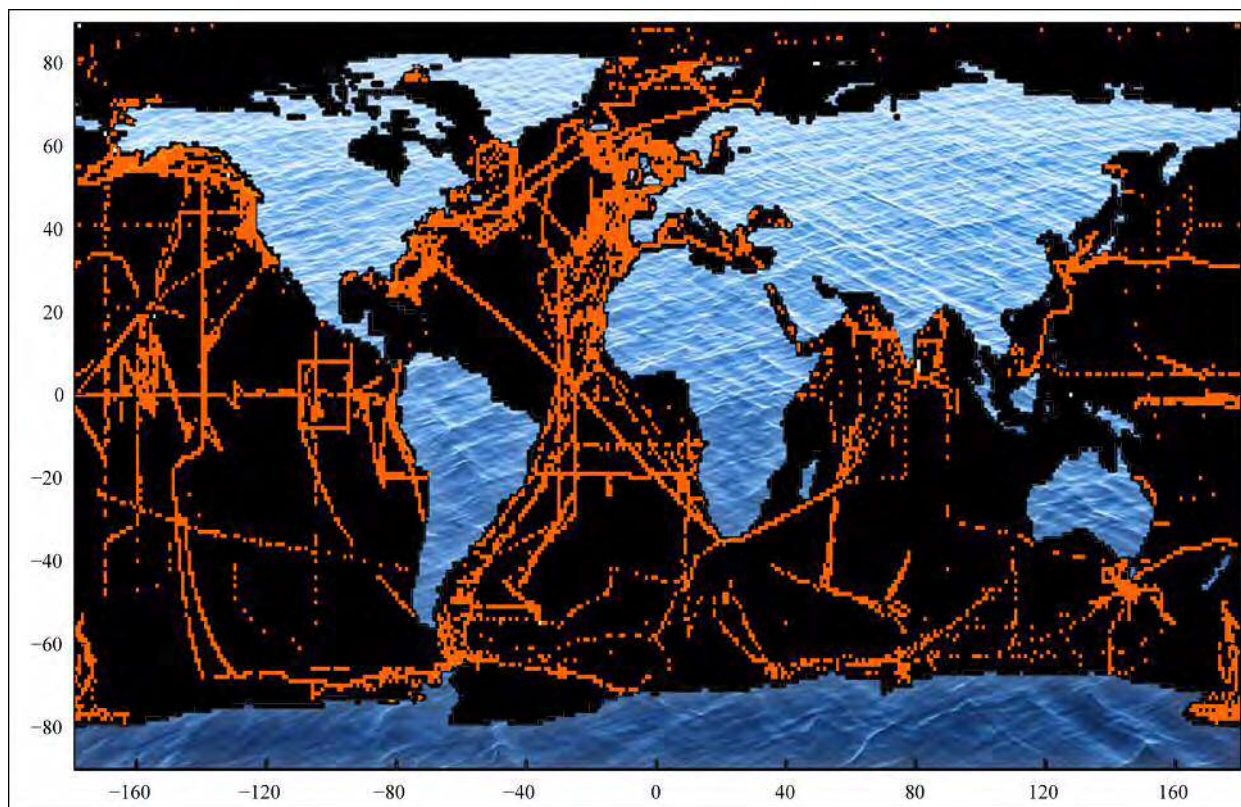


Figure 9. Distribution of $1^\circ \times 1^\circ$ latitude-longitude pixels with seawater DMS data (orange dots).

To be able to construct a climatology from the existing data, some kinds of mapping criteria and objective analysis techniques have to be applied. The original climatology was constructed initially with approximately 15,000 DMS concentration measurements [Kettle et al., 1999]. That climatology was updated one year later with the inclusion of approximately 1,500 new measurements [Kettle and Andreae, 2000]. Since then, the number of measurements available in the database has increased considerably. The scientific community has worked with the SOLAS (Surface Ocean Lower Atmosphere Study) Integration Project with the aim to further update the database and to create an updated climatology that better represents the current DMS distribution over the global ocean. The effort for the construction of the new climatology has been part of this thesis and will be reported here.

In spite of the existing uncertainties in the detailed spatial and temporal DMS distribution, the original DMS climatology [Kettle et al. 1999] and subsequent work [e.g., Vallina et al. 2007] revealed some emerging patterns. DMS concentration follows a strong seasonal pattern at high latitudes, with higher values during each hemispheric summer. During the winter DMS concentration is low, reflecting low levels of biological activity. At low latitudes the seasonality is less pronounced and the maximum spring-summer concentrations are lower (generally $< 5\text{nM}$). At low temperate and subtropical latitudes, interestingly, DMS follows more closely the monthly variation of sunlight than that of plankton biomass.

3.1.2 Atmospheric Chemistry of DMS

Once in the atmosphere after emission across the air-sea interface, DMS is oxidized by free radicals. The atmospheric chemistry of DMS is more complicated than originally proposed by the CLAW hypothesis. There are two main reaction pathways in the atmospheric DMS oxidation. The ‘addition pathway’ is initialized by an added O atom. After chemical transformations into water soluble products (dimethyl sulfoxide (DMSO), dimethyl sulfone (DMSO_2), methylsulfinic acid (MSIA) and methanesulfonic acid (MSA)), these seem to have a key role in the growth of existing particles. The ‘abstraction pathway’ begins with the abstraction of a H atom. After that first step, chemical transformations lead to the formation of H_2SO_4 or MSA [von Glasow, 2007].

The OH radical is the main DMS oxidant; it acts through both the addition and the abstraction pathways [von Glasow and Crutzen, 2004]. According to laboratory and model studies [Barnes, 1991; Bedjanian et al., 1996; Ingham et al., 1999; Nakano et al., 2001] BrO also seems to play a role in the oxidation of DMS. The influence of NO_3 , Cl, and $\text{O}_{3,\text{aq}}$ in the atmospheric chemical processes have been also studied based on chemical models outputs [von Glasow and Crutzen, 2004]. After the OH, and in the absence of halogens, NO_3 is the major oxidant of DMS. The reaction with NO_3 proceeds via abstraction and occurs in polluted regions and during night time when the concentrations of NO_3 are high. However, the impact of those atmospheric components on DMS oxidation is still poorly quantified [von Glasow, 2007].

For the sake of this thesis and its global perspective, we adapt our study to some simplifications, and omit some unclear details that should be important for quantifying the production of aerosols, but probably not for studying their seasonal variability. Our first simplification is to consider OH

as the only DMS oxidant.

The main products of DMS oxidation are MSA, an exclusive product of DMS, and sulfuric acid and non-sea-salt- SO_4^{2-} particles that can act as cloud condensation nuclei. Other products include dimethylsulfoxide and dimethylsulfone. DMS oxidation can hardly be explained by gas-phase reactions exclusively, and multiphase chemistry has to be considered [Barnes, 2006].

The knowledge of the chemical DMS transformations in the atmosphere and its end products still holds a lot of uncertainties. Transport processes, aerosol-cloud interactions, and atmospheric conditions such as temperature, pressure, air humidity and the presence of other molecules, all suppose serious difficulties to obtain *in situ* data to validate laboratory and modeling results. Increasing our understanding of the atmospheric chemistry of DMS is however essential to ascertain its role in the formation of new particles and the growth of existing particles, which is largely relevant to cloudiness over, and insolation into the oceans.

Observations of biogenic sulfur in the atmosphere and the CLAW hypothesis

Despite the uncertainties in the global distribution and the atmospheric chemistry of DMS, a number of results, particularly from the last decade, have provided evidence in support of the involvement of this gas in a CLAW-like feedback mechanism. These are just some of the most significant:

A recent study using global DMS observations and satellite-derived data suggest that biogenic sulfur from the oceans represents a major source of cloud-forming aerosols over much of the pristine southern hemisphere oceans [Vallina et al., 2006; 2007]. According to this study, oxidation of biogenic DMS seems to largely contribute to the CCN numbers but more importantly to drive their seasonal variability over the remote ocean. Regional positive correlation between climatological seawater DMS concentration, its emission to the atmosphere, and satellite-derived cloud condensation nuclei agree with *in situ* measurements [Andreae et al., 1995]. This is compatible with one of the postulates of the CLAW hypothesis, by which changes in DMS emission cause changes in CCN numbers over the ocean.

Model simulations [Thomas et al., 2010] and satellite-derived data [Meskhidze and Nenes, 2006] reproduce an increased number of smaller sized cloud droplets during high biological surface

ocean activity. Emissions of DMS (and potentially other biogenic trace gases and primary aerosols) seem to affect cloud microphysics over pristine areas of the marine atmosphere not affected by continental aerosols. This supports another postulate of the CLAW hypothesis by which marine biogenic emissions have an influence on cloud microphysics and optics.

A global study by Vallina and Simó [2007a] concluded that regional monthly DMS concentrations are positively correlated with the daily amount of solar radiation received in the upper mixed layer of the open ocean, irrespectively of the latitude, plankton biomass or temperature. This is a necessary condition for the CLAW negative feedback to occur, as it implies that changes in the amount of solar radiation reaching the surface ocean have a consequence on the amount of DMS produced and emitted.

The lack of DMS data in some areas of the ocean, the parameterizations needed to estimate the biogenic aerosols emissions to the atmosphere, our incapacity to measure some chemical processes in the atmosphere, and our virtual ignorance of the potential quantitative contribution of other trace gases and primary particles to aerosol production and cloud microphysics, are all uncertainty sources that are difficult to overcome. There is still much to improve in the knowledge of the involvement that marine aerosols have on the biogeochemical cycles of the Earth. In the words of a scientist that deeply studied the first steps of this subject, Aitken: “Much, very much, still remains to be done. Like a traveler who has landed in an unknown country, I am conscious my latering steps have extended but little beyond the starting point”.

Chapter I. Datasets

The four studies presented in this thesis are based mainly, yet not only, on the use of satellite data. Orbital satellites provide physical and radiative global cloud properties for the last decade, as well as some sea surface properties. However, not all the desired variables are measurable from satellite on a global scale. Sometimes it is useful to turn to climatologies, or to reanalyse *in situ* and satellite data through models.

The variables used in the four chapters of the thesis are summarised in the table below, with the source they were obtained from, the time span and the temporal resolution used in each study.

Variable	Source	Years	Temporal Resolution	Chapter 1	Chapter 2	Chapter 3	Chapter 4
DMS	GSS DMS database ⁽¹⁾	1972-2009	Monthly-Annual				
		1972-2009	Climatology				
	Simó and Dachs 2002	Climatology					
Sea Ice	CERSAT/Ifremer ⁽²⁾	1992-2009	Climatology				
Sea Surface Temperature	NCEP/NCAR Reanalysis ⁽³⁾	1978-2008	Climatology				
		2001-2009	Monthly				
Wind Speed	NCEP/NCAR reanalysis ⁽³⁾	1978-2008 2001-2009	Climatology Monthly				
Chlorophyll <i>a</i>	SeaWiFS ⁽⁴⁾	1997-2009	Climatology				
		2001-2009	Monthly				
Nitrate	WOA 2009 ⁽⁵⁾	2009	Climatology				
Phosphate	WOA 2009 ⁽⁵⁾	2009	Climatology				
Mixed Layer Depth	Modified from de Boyer Montégut et al. (2004)		Climatology				

Solar Radiation Dose	Calculated as in Vallina and Simó (2006)		Climatology				
Cloud Condensation Nuclei	MODIS-Terra ⁽⁶⁾	2001-2009	Weekly				
		2001-2009	Monthly				
Cloud Effective Radius	MODIS-Terra ⁽⁶⁾	2001-2009	Weekly				
		2001-2009	Monthly				
Cloud Fraction Liquid	MODIS-Terra ⁽⁶⁾	2001-2009	Weekly				
Aerosol Optical Thickness	MODIS-Terra ⁽⁶⁾	2001-2009	Monthly				
Aerosol Optical Thickness Standard Deviation	MODIS-Terra ⁽⁶⁾	2001-2009	Monthly				
Fraction Optical Depth Submicron Aerosol	MODIS-Terra ⁽⁶⁾	2001-2009	Monthly				
Firecounts	World Fire Atlas ATSR ⁽⁷⁾	2001-2009	Monthly				
Land Cover	IGBP land cover classification ⁽⁸⁾		Climatology				
Albedo	CERES ⁽⁹⁾	2001-2009	Weekly				
		2001-2009	Daily				
Angstrom Exponent Ocean	MODIS-Terra ⁽⁶⁾	2001-2009	Monthly				
OH	GEOS-Chem ⁽¹⁰⁾	2001	Monthly				
MSA	UMAG network ⁽¹¹⁾ plus other stations		Monthly				

(1) The GSS DMS database

The GSS DMS (Global Sea Surface Dimethylsulfide) database of surface seawater DMS concentrations was constructed initially in 1999 by Dr. Jamie Kettle and has been updated ever since. The data contributed by individual researchers have been collected between March 1972 and June 2010 (mostly since April 1980). The data used in our studies (47,313 DMS seawater concentration measurements) consist of DMS measurements, reported in nanomolar (nM) concentrations, from depths of 0–10 meters.

The database is today maintained at NOAA-PMEL (National Oceanic and Atmospheric Administration-Pacific Marine Environmental Laboratory).

For further information, visit: <http://saga.pmel.noaa.gov/dms/>

(2) CERSAT/Ifremer.

CERSAT (Centre ERS d'Archivage et de Traitement - French ERS Processing and Archiving Facility) is part of IFREMER (French Research Institute for Exploitation of the Sea).

Sea Ice concentration products are obtained for both, North and South poles, with polar stereographic 12.5 km resolution grids, from the 85 GHz channel of SSM/I (Special Sensor Microwave/Imager) onboard DMSP (Defense Meteorological Satellite Program) satellite. The daily maps are processed from the daily brightness temperature maps from NSIDC (National Snow and Ice Data Center), using the Artist Sea Ice (ASI) algorithm developed at University of Bremen (Germany).

For further information, visit: <http://www.ifremer.fr/cersat/en/index.htm>

(3) NCEP reanalysis Model

The National Centers for Atmospheric Prediction (NCEP) and the National Center for Atmospheric Research (NCAR) have accomplished different re-analysis/forecast projects to perform data assimilation of global data sets for 1948 to present for atmospheric parameters. This model used to create the reanalysis is initialized with measured data from different sources, including observations from weather stations, ship, aircraft, radiosondes, and satellite.

Daily time series and monthly means of sea surface temperature and wind speed at 10 m over sea level are calculated with $2.5^\circ \times 2.5^\circ$ spatial resolution. A subset of the NCEP/NCAR Reanalysis has been processed to create monthly means of the original data, and in some cases, derived variables or other statistics.

The project development has been supported by the National Ocean and Atmospheric Administration's (NOAA) Office of Global Programs.

For further information, visit: <http://www.esrl.noaa.gov/psd/data/gridded/data.ncep.reanalysis.html>

(4) SeaWiFS

Sea-viewing Wide Field-of-view Sensor (SeaWiFS) is the instrument on board the Orbview-2 spacecraft. SeaWiFS is basically formed by a rotating optical scanner which measures radiances in 8 spectral bands (from 0.40 to 0.88 μm).

Based in the strong absorption of chlorophyll *a* concentration on the blue (435 nm) band and a minimum absorption in the green (565 nm), the chlorophyll *a* concentration in the global surface ocean can be estimated from the water-leaving radiance near these two visible wavelengths.

The data we use are Level 3, which has been statistically processed at 4 km and 9 km spatial resolution to produce global analyses.

For further information, visit: <http://oceancolor.gsfc.nasa.gov/>

(5) WOA 2009

The World Ocean Atlas 2009 (WOA 2009) is a set of objectively analyzed (1° grid) climatological fields based on *in situ* data at standard depth levels for annual, seasonal, and monthly compositing periods for the World Ocean.

The global maps are obtained using an objective analysis scheme to produce global fields from one degree square means of data values at standard values. The profile used is defined as a set

of measurements for a single variable at discrete depths taken as an instrument drops or rises vertically in the water column. The nutrient data used in this atlas were typically obtained by means of analysis of serial (discrete) samples.

The global maps we used (surface nitrate and phosphate concentrations) are based on historical oceanographic nutrient data obtained from the NODC/WDC (the U.S. National Oceanographic Data Center/World Data Center System) archives and include all data gathered as a result of the Intergovernmental Oceanographic Commission (IOC) GODAR (Global Oceanographic Data Archaeology and Rescue) project and WOD (World Ocean Database project).

For further information, visit: http://www.nodc.noaa.gov/OC5/WOA09/pr_woa09.html

(6) MODIS-Terra

The MODIS (Moderate-resolution imaging spectroradiometer) instrument is operating on the Terra and Aqua spacecraft. We used cloud and aerosol data provided by Terra. Its detectors measure 36 spectral bands between 0.405 and 14.385 μm , and it acquires data at three spatial resolutions -- 250m, 500m, and 1,000m. The MODIS is composed of two mutually supporting sensors that cover a swath width of 2,330 km to provide nearly complete two-day global coverage from a polar-orbiting, sun-synchronous, serviceable platform.

Along with all the data from other instruments on board the Terra spacecraft, MODIS data are transferred to ground and transformed into Level 3 data, produced by the MODIS Adaptive Processing System (MODAPS), and then are parceled out among three DAACs (Distributed Active Archive Centers) for distribution.

For further information, visit: <http://modis.gsfc.nasa.gov>

(7) World Fire Atlas ATSR

The ATSR (Along Track Scanning Radiometer) World Fire Atlas (WFAA) provides global monthly maps of fires. Maps are available for years since 1995. ATSR instruments produce infrared images of the Earth at a spatial resolution of one kilometre. The ATSR channels are at wavelengths of 1.6 μm (visible) and three thermal bands at 3.7 μm , 11 μm , and 12 μm .

Fire-counts are determined from nighttime ATSR data as the record having a brightness temperature in the 3.7 micron channel above 308K.

For further information, visit: <http://dup.esrin.esa.it/ionia/wfa/index.asp>

(8) IGBP land cover classification

The IGBP (International Geosphere Biosphere Programme) land cover classification maps are derived from 1 kilometer Advanced Very High Resolution Radiometer (AVHRR) data using all available bands and derived Normalized Difference Vegetation Index (NDVI). All 5 spectral bands of the AVHRR were used as inputs: channel 1 (visible red reflectance, 0.58-0.68 microns), channel 2 (near infrared reflectance, 0.725-1.1 microns), channel 3 (thermal infrared, 3.55-3.93 microns), channel 4 (thermal, 10.3-11.3 microns), channel 5 (thermal, 11.5-12.5 microns) and the NDVI (channel 2- channel 1)/(channel 2 + channel 1). The multi-spectral measurements have been proven to be suitable for the quantitative measurement of a number of parameters that AVHRR was originally not designed for.

The data sets of the obtained land cover classification are provided at three spatial resolutions of 0.25, 0.5 and 1 degrees lat./long. For each spatial resolution there is a land cover type classification layer (with numbers from 0 to 14) and 15 associated layers that provide the fraction, from 0 to 100, of each land cover type per cell.

For further information, visit: <http://edcdaac.usgs.gov/modis/mod12q1v4.asp>

(9) CERES

The CERES (Clouds and the Earth's Radiant Energy System) is a key component of the Earth Observing System (EOS) program. CERES instruments were launched aboard the Tropical Rainfall Measuring Mission (TRMM) in November 1997 and on the EOS Terra satellite in December 1999, and two additional instruments are flying on the EOS Aqua spacecraft since 2002. Multiple satellites are needed to provide adequate temporal sampling since clouds and radiative fluxes vary throughout the day.

The CERES instruments provide radiometric measurements of the Earth's atmosphere from three

broadband channels -- a shortwave channel to measure reflected sunlight, a longwave channel to measure Earth-emitted thermal radiation in the 8-12 μm “window” region, and a total channel to measure all wavelengths of radiation.

CERES products include both solar-reflected and Earth-emitted radiation from the top of the atmosphere to the Earth’s surface. Cloud properties are determined using simultaneous measurements by other EOS instruments such as the Moderate Resolution Imaging Spectroradiometer (MODIS).

Top-of-Atmosphere (TOA) and Surface Products use cloud imager data for scene classification and CERES measurements to provide radiative fluxes for both cloudy and clear sky conditions.

For further information, visit: <http://ceres.larc.nasa.gov/index.php>

(10) GEOS-Chem

GEOS–Chem is a global 3-D chemical transport model (CTM) for atmospheric composition driven by meteorological input from the Goddard Earth Observing System (GEOS) of the NASA Global Modeling and Assimilation Office. It is applied by research groups around the world to a wide range of atmospheric composition problems.

The GEOS meteorological data archive has a temporal resolution of 6 hours (3 hours for surface quantities and mixing depths). Standard global GEOS–Chem simulations use $2^\circ \times 2.5^\circ$ or $4^\circ \times 5^\circ$ grid resolution by aggregating GEOS meteorological data.

GEOS–Chem includes detailed HO_x–NO_x–VOC–ozone tropospheric chemistry. Stratospheric chemistry in GEOS–Chem is based on climatological representation of species sources and sinks.

The model is managed by the GEOS–Chem Support Team, based at Harvard University and Dalhousie University with support from the US NASA Earth Science Division and the Canadian National and Engineering Research Council.

For further information, visit: <http://acmg.seas.harvard.edu/geos/index.html>

(11) UMAG

The UMAG (University of Miami Aerosol Group) began to develop networks of aerosol monitoring stations at various ocean sites beginning in the early 1980's. Aerosols are collected by high-volume filter samplers.

All samples are analyzed for the major aerosol species: nss-SO₄⁼, NO₃⁻, NH₄⁺, sea-salt components. A large subset of the samples are also analyzed for methanesulfonate (MSA).

For further information, visit: http://gacp.giss.nasa.gov/data_sets/Joseph_Prospiero.html

Aims of the Thesis

2.1.1. Main objective

The main objective of this thesis was to improve our knowledge of the influence that the emissions of DMS and other marine aerosol precursors have on cloud microphysics over the ocean. This broad aim can be divided into four major questions that correspond to the four chapters of the thesis:

Why is the global precipitation chemistry of DMS and other marine aerosol precursors important for cloud microphysics over the ocean? How do the emissions of DMS and other marine aerosol precursors vary in space and time? How do the emissions of DMS and other marine aerosol precursors vary in space and time? How do the emissions of DMS and other marine aerosol precursors vary in space and time?

Chapter 1. How do the emissions of DMS and other marine aerosol precursors vary in space and time? How do the emissions of DMS and other marine aerosol precursors vary in space and time? How do the emissions of DMS and other marine aerosol precursors vary in space and time?

A threefold increase in DMS data in the last decade prompted us to update the existing DMS climatology, created ten years ago by Kettle et al. [1999]. To this aim we used the Global Surface Seawater DMS Database contributed by researchers from all over the world. The objective analysis methodologies and interpolation schemes used in the original climatology had to be revised, with application of our current knowledge of ocean biogeochemistry and DMS variability. The new climatology should be instrumental to re-calculate the DMS emission fluxes to the atmosphere, to explore the statistical relationship of DMS to other oceanic and environmental variables, and to raise awareness of those areas with sparse sampling coverage that deserve prioritized consideration in the planning of new fieldwork efforts.

How do the emissions of DMS and other marine aerosol precursors vary in space and time? How do the emissions of DMS and other marine aerosol precursors vary in space and time? How do the emissions of DMS and other marine aerosol precursors vary in space and time?

Chapter 2. How do the emissions of DMS and other marine aerosol precursors vary in space and time? How do the emissions of DMS and other marine aerosol precursors vary in space and time? How do the emissions of DMS and other marine aerosol precursors vary in space and time?

The construction of the updated climatology prompted us to revise the emerging patterns found with previous versions of the DMS database and climatology, and to revisit the statistical between DMS and environmental variables that could provide insights on the drivers of DMS production.

estimated essentially from the seawater chlorophyll *a* concentration and the wind speed. And the variability of the small sea salt particle flux was derived from the wind speed. A running-window correlation approach was used to investigate if there was a statistical relationship between the production of each marine aerosol type and the size of liquid cloud droplets.

Chapter I

An updated climatology of surface dimethylsulphide concentrations and emission fluxes in the global ocean.

A. Lana, T. G. Bell, R. Simó, S. M. Vallina, J. Ballabrera-Poy, A. J. Kettle, J. Dachs, L. Bopp, E. S. Saltzman, J. Stefels, J. E. Johnson and P. S. Liss.

☒ b☒☒☒☒☒

The potentially significant role of the biogenic trace gas dimethylsulphuride (DMS) in determining the Earth's radiation budget makes it necessary to accurately reproduce seawater DMS distribution and quantify its global flux across the sea/air interface. Following a threefold increase of data (from 15,000 to over 47,000) in the global surface ocean DMS database over the last decade, new global monthly climatologies of surface ocean DMS concentration and sea-to-air emission flux are presented as updates of those constructed 10 years ago. Interpolation/extrapolation techniques were applied to project the discrete concentration data onto a first guess field based on Longhurst's biogeographic provinces. Further objective analysis allowed us to obtain the final monthly maps. The new climatology projects DMS concentrations typically in the range of 1–7 nM, with higher levels occurring in the high latitudes, and with a general trend toward increasing concentration in summer. The increased size and distribution of the observations in the DMS database have produced in the new climatology substantially lower DMS concentrations in the polar latitudes and generally higher DMS concentrations in regions that were severely undersampled 10 years ago, such as the southern Indian Ocean. Using the new DMS concentration climatology in conjunction with state-of-the-art parameterizations for the sea/air gas transfer velocity and climatological wind fields, we estimate that 28.1 (17.6–34.4) Tg of sulphur are transferred from the oceans into the atmosphere annually in the form of DMS. This represents a global emission increase of 17% with respect to the equivalent calculation using the previous climatology. This new DMS climatology represents a valuable tool for atmospheric chemistry, climate, and Earth System models.



The ocean surface plays an important role in the global biogeochemical cycle of sulphur. Oceanic dimethylsulphuride (DMS) emission is the main natural source of atmospheric sulphur [Bates et al., 1992; Simó, 2001]. Once in the atmosphere, DMS is oxidized to form sulphuric and methanesulphuronic acids, which contribute to new particle formation and growth to maintain the pool of cloud condensation nuclei (CCN) that is necessary for cloud formation [Andreae and Crutzen, 1997]. The number of these small-sized atmospheric particles affects the radiation budget of the Earth, directly by scattering solar radiation and indirectly by influencing cloud microphysics and albedo [Andreae and Rosenfeld, 2008]. The CLAW hypothesis, acronym based on the initials of the authors surnames [Charlson et al., 1987], postulates a climate feedback loop between phytoplankton, DMS emissions, CCN, and cloudiness. The feasibility of such a feedback loop at the local scale has been challenged by state-of-the-art atmospheric model outcomes showing limited new particle formation in the marine boundary layer (MBL). According to these models, DMS contribution to CCN numbers would only occur at large supraregional scales after long range transport in the free troposphere and reentrainment into the MBL [e.g., Carslaw et al., 2010].

The main precursor of DMS is the microalgal metabolite dimethylsulphuroniopropionate (DMSP). Intracellular DMSP breakdown leads to the production of DMS by phytoplankton [Stefels et al., 2007]. Microalgae also release untransformed DMSP through exudation and mortality, and part of this dissolved DMSP is converted to DMS by extracellular and bacterial enzymes [Stefels and Dijkhuizen, 1996; Kiene et al., 2000; Yoch, 2002; Stefels et al., 2007; Vila-Costa et al., 2007; Howard et al., 2008]. DMS, in turn, is oxidized by photochemical reactions [Brimblecombe and Shooter, 1986; Toole et al., 2003] and metabolized by heterotrophic bacteria. Finally, only a small fraction of the DMS produced escapes to the atmosphere [Simó, 2001; Vila-Costa et al., 2006]. The tight coupling between DMS production and loss makes it challenging to study the driving factors and the dynamics of DMS emission from the ocean surface. However, large-scale

observations of ocean surface DMS reveal macroscale patterns of variability such as a global proportionality between DMS concentration and average daily solar radiation in the surface mixed layer [Vallina and Simó, 2007a]. This provides partial support for the CLAW hypothesis.

The potentially significant role of DMS in climate regulation has encouraged the community to provide an accurate representation of both DMS seawater concentration and sea/air DMS flux distribution on a global scale. There have been multiple efforts to accurately represent the global DMS distribution. The main effort, initiated by A.J. Kettle and M.O. Andreae, was to compile a now freely available database using archived DMS measurements. The Global Surface Seawater DMS Database (GSSDD), currently maintained at the NOAA-PMEL, is constructed from data contributions by individual scientists and made available to the scientific community (<http://saga.pmel.noaa.gov/dms/>). The data are sparsely distributed in both space and time, as is shown in the DMS data footprint on the $1^\circ \times 1^\circ$ annual global map (Figure S1). The map shows that the coverage is not enough to resolve the global distribution of DMS on a monthly basis, whereas the importance of global emissions maps for climate models necessitates the formulation of a gridding procedure by the best means possible. Therefore, extensive data treatment or modeling is required to produce global DMS and emission fluxes climatologies from the database.

Several methods have been proposed to obtain realistic global DMS distributions. Some of them rely on the relationship between the DMS concentration and other variables for which global distributions exist or can be modeled: Anderson et al. [2001] computed DMS from chlorophyll, light and nutrients; Simó and Dachs [2002] used a two-equation algorithm to derive surface DMS from surface chlorophyll a and the mixed layer depth; Aumont et al. [2002] and Belviso et al. [2004a] developed nonlinear parameterizations to compute DMS from chlorophyll a and an index representing the community structure of marine phytoplankton. Other approaches are totally or partially based on numerical models: Chu et al. [2003], Six and Maier-Reimer [2006], Kloster et al. [2006], Elliott [2009], Bopp et al. [2008] and Vogt et al. [2010] used prognostic biogeochemical formulations for DMS production and removal processes within global ocean circulation models.

The most widely used global DMS climatology, derived exclusively from the database, was published a decade ago (Kettle et al. [1999] and Kettle and Andreae [2000]; hereafter referred to as K99 and K00, respectively). The number of data used was initially 15,617 (K99), to which approximately 1,500 extra seawater DMS concentration measurements from the period 1996–

1998 were added to produce an updated climatology (K00). Since then, the scientific community has worked with SOLAS Integration (Surface Ocean Lower Atmosphere Study, http://www.bodc.ac.uk/solas_integration/) to update the database, increasing the number of DMS measurements in the ocean surface three fold (47,250 in April 2010). The aim of this work is to create an updated monthly DMS concentration climatology for the global ocean, and an associated DMS emission flux climatology. Objective data analysis and interpolation schemes in concert with current knowledge of ocean biogeochemistry and DMS dynamics have enabled the construction of a new climatology. Novel distribution patterns, differences with the original climatology, and the resulting reestimate of the global annual emission flux are discussed.

DMS Data Methodology

Data

The data used (47,313 DMS seawater concentration measurements) are entirely from the Global Surface Seawater DMS Database (<http://saga.pmel.noaa.gov/dms/>) plus 63 additional measurements in the South Pacific [Lee et al., 2010], not included in the database. The data contributed by individual researchers have been collected between March 1972 and February 2009 (mostly since April 1980); see Table S1. The data consist of DMS measurements, reported in nM, from depths of 0–10 meters.

There is no quality control in the database. This is worth stressing because there is no unification of the DMS measurement protocol, and very few intercalibration exercises have been conducted in the last 30 years. A number of sampling and analytical issues have been reported or communicated in recent years. For example, the use of HgCl_2 as a sample preservative can result in anomalously high DMS values by transformation of DMSP into DMS [Curran et al., 1998]; or, in the presence of thick blooms of high DMSP producers like *Phaeocystis* sp., a lack of sample prefiltration may produce continuous and abundant DMS during purging [del Valle et al., 2009]. Despite these recognized concerns, information is still too sparse to provide robust criteria for the selection or elimination of historical data. Hence, no data from the database has been flagged. However, to avoid the undesirable effects that potentially erroneous and very high values might produce during the objective analysis, data that were above the 99.9 percentile are removed. The 0.1%

eliminated were seawater DMS concentrations greater than 148 nM.

To create the climatology we first stratified data according to the sampling month, and averaged to $1^\circ \times 1^\circ$ bins, which are the input to the objective analysis. If there was only one DMS datum within the $1^\circ \times 1^\circ$ square, the pixel value would be the value of that datum. The objective analysis scheme used is described by Barnes [1964], which is the same employed by K99 for DMS. This method is used as well by other authors for temperature, salinity, oxygen and nutrients in the last version of the World Ocean Atlas [Locarnini et al., 2010] and previous editions (WOA94, WOA98, WOA01, WOA05). The purpose of this method is to create a gridded field of a variable from sparse in situ data. A key element of the objective analysis is the firstguess field, which is subsequently corrected with the help of the available observations.

Firstguess fields are produced by the following procedure:

As described by Daley [1993], there are several methods to obtain the continuous monthly background fields that will be subsequently reshaped with in situ data: an existing climatology, the short forecast of an assimilation model, or some optimum blend of the two. In our case, using the earlier K99 climatology was not appropriate because we were using all of those same data in the updated climatology, and also because we were aiming at improving the first guess fields of K99. The authors of the World Ocean Atlas [Locarnini et al., 2010] used a single annual analysis based on zonal annual means as the first guess field for all of the seasonal climatologies. In our case, however, data are so spaced out in distance and time that direct interpolation between local annual means without consideration of physical and biological regionalization of the oceans would produce anomalous geographical representation. Furthermore, regional DMS concentrations vary so much among months that it was considered more appropriate to construct monthly first guess fields. For this purpose we adopted K99's use of the Longhurst's division of the oceans into static biogeographic provinces [Longhurst, 1998], each representing an oceanic region with coherent biogeochemical characteristics (e.g., chlorophyll, nitrate, mixing, etc.) distinguishable from those of its neighbor regions. These, in their author's words, offer the degree of formalism and partition in a constantly changing system that helps us to comprehend changes in such a vastly complex interacting whole [Longhurst, 2007].

The province approach, which has been helpful to partially overcome the problem of undersampling, also carries its own limitations. Provinces have been defined as static features in the sea, with well defined borders that do not shift from month to month. Satellite imagery reveals

that provinces, as recurrent coherent features, do exist, but also show that they are dynamic. In recent years there have been multiple efforts to define dynamic ocean provinces based on satellite measurements [e.g., Devred et al., 2007; Alvain et al., 2008; Hardman-Mountford et al., 2008; Oliver and Irwin, 2008]. However, because of the impossibility to attribute historical DMS data to their contemporary dynamic provinces, we decided to stay with the static provinces.

Therefore, we divided the oceans into the 54 biogeographic provinces proposed by Longhurst [1998] (see Table 1). The monthly mean DMS concentration was calculated for each province (Figure 1). White regions indicate provinces with not enough data (<3). However, in order to create a complete climatology, these areas need to be given a first-guess concentration.

As in K99, temporal interpolation and substitution schemes were employed to fill the gaps and solve this problem. Firstly, an annual cycle was generated using the monthly means for each ocean province. Where a monthly gap occurred, it was filled by interpolating from the adjacent months. The interpolation method was a piecewise cubic Hermite technique [Fritsch and Carlson, 1980]. If there were three or fewer measurements per month per province, these values were not taken into account to generate the temporal evolution because they would have a disproportionate influence on the creation of the first-guess field and, consequently, in the objective analysis. In provinces that lacked enough months with data to construct a robust annual mean, the temporal evolution of a similar province was used and scaled with the few data of the original province. Provinces with enough data to complete the annual cycle solely by interpolation were not substituted. We tried to ensure that as many provinces as possible in the first guess field represented the data from that province; substitution was applied to 10 provinces (18% of the total; see Table 1), whereas the provinces substituted in K99 were 52% of the total. [14] The choice of each substitution province was a subjective process based on a combination of criteria: similarity of chlorophyll concentration patterns, latitude, geographical proximity, as well as the choice made by K99. The whole series of resulting annual cycles are shown in Figure 2. The coastal Atlantic provinces GUIN and GUIA were substituted by the large provinces that are directly adjacent, ETRA and WTRA, respectively. The Indian Ocean Coastal Biome contains very little data despite its relative importance: EAFR, REDS and INDE all do not have enough data and were substituted by ARAB, with the exception of EAFR, which was substituted by ISSG. In the Pacific Ocean, PSAW was substituted by PSAE as both are part of the Pacific Westerly Wind Biome and have more similarities than differences in terms of the annual cycles of mixed layer and euphotic depths, surface chlorophyll and primary productivity [Longhurst,

Province Name	Acronym	Number	Number of data	Number of months	Shape Substitute
S. Pacific Subtropical Gyre	SPSG	37	3982	8	-
Subantarctic Water Ring	SANT	52	4156	9	-
Antarctic	ANTA	53	1035	8	-
South Atlantic Gyral	SATL	10	1102	10	-
Indian S. Subtropical Gyre	ISSG	23	367	6	-
S. Subtropical Convergence	SSTC	51	820	12	-
Indian Monsoon Gyres	MONS	22	266	9	-
N. Pacific Tropical Gyre (East)	NPTE	38	933	10	-
Pacific Equatorial Divergence	PEQD	40	2550	10	-
N. Pacific Tropical Gyre (West)	NPTW	35	352	5	-
W. Pacific Warm Pool	WARM	41	993	5	-
Boreal Polar	BPLR	1	777	7	-
N. Pacific Equatorial Countercurrent	PNEC	39	1114	9	-
Archipelagic Deep Basins	ARCH	42	50	5	-
Austral Polar	APLR	54	1310	8	-
N. Atlantic Tropical Gyral	NATR	7	549	10	-
N. Pacific Transition Zone	NPPF	34	331	7	-
Sunda-Arafura Shelves	SUND	48	16	2	*
N. Atlantic Subtropical Gyral (West)	NASW	6	987	11	-
Western Tropical Atlantic	WTRA	8	420	7	-
Eastern Tropical Atlantic	ETRA	9	180	5	-
Caribbean	CARB	17	599	7	-
N. Atlantic Subtropical Gyral (East)	NASE	18	1226	9	-
N. Pacific Epicontinental Sea	BERS	30	2708	7	-
E. Africa Coastal	EAFR	24	195	2	ISSG
N. Atlantic Drift	NADR	4	1304	9	-
NW Arabian Upwelling	ARAB	26	149	7	-
Atlantic Arctic	ARCT	2	858	8	-
Mediterranean Sea, Black Sea	MEDI	16	623	11	-
Kuroshio Current	KURO	33	1087	8	-
Pacific Subarctic Gyres (East)	PSAE	31	745	9	-
California Current	CALC	44	2118	9	-
Australia-Indonesia Coastal	AUSW	29	7	1	AUSE+SUND
Humboldt Current Coastal	HUMB	46	544	6	-
Atlantic Subarctic	SARC	3	1403	5	-
Pacific Subarctic Gyres (West)	PSAW	32	54	2	PSAE
NW Atlantic Shelves	NWCS	15	2522	11	-
Tasman Sea	TASM	36	116	1	SSTC
NE Atlantic Shelves	NECS	11	2191	11	-
Guinea Current Coastal	GUIN	13	30	3	ETRA
SW Atlantic Shelves	FKLD	20	166	4	-
Central American Coastal	CAMR	45	97	2	CALC
Guianas Coastal	GUIA	14	20	1	WTRA
Brazil Current Coastal	BRAZ	19	100	4	-
New Zealand Coastal	NEWZ	50	6	1	AUSE+SUND
Benguela Current Coastal	BENG	21	182	5	-
East Australian Coastal	AUSE	49	26	2	*
Gulf Stream	GFST	5	231	7	-
China Sea Coastal	CHIN	47	141	5	-
E. India Coastal	INDE	27	88	2	ARAB
W. India Coastal	INDW	28	93	9	-
Alaska Downwelling Coastal	ALSK	43	4582	6	-
Eastern Canary Coastal	CNRY	12	681	8	-
Red Sea, Persian Gulf	REDS	25	11	1	ARAB

* The annual pattern in these provinces was constructed by combining DMS data from AUSE and SUND provinces.

Table 1. The Biogeochemical Provinces suggested by *Longhurst* [1998] (in order of decreasing areal extent) with their name, abbreviation, reference number in Figure 2, number of DMS data, number of months with DMS data and, where appropriate, the province used as a substitute (see text for details).

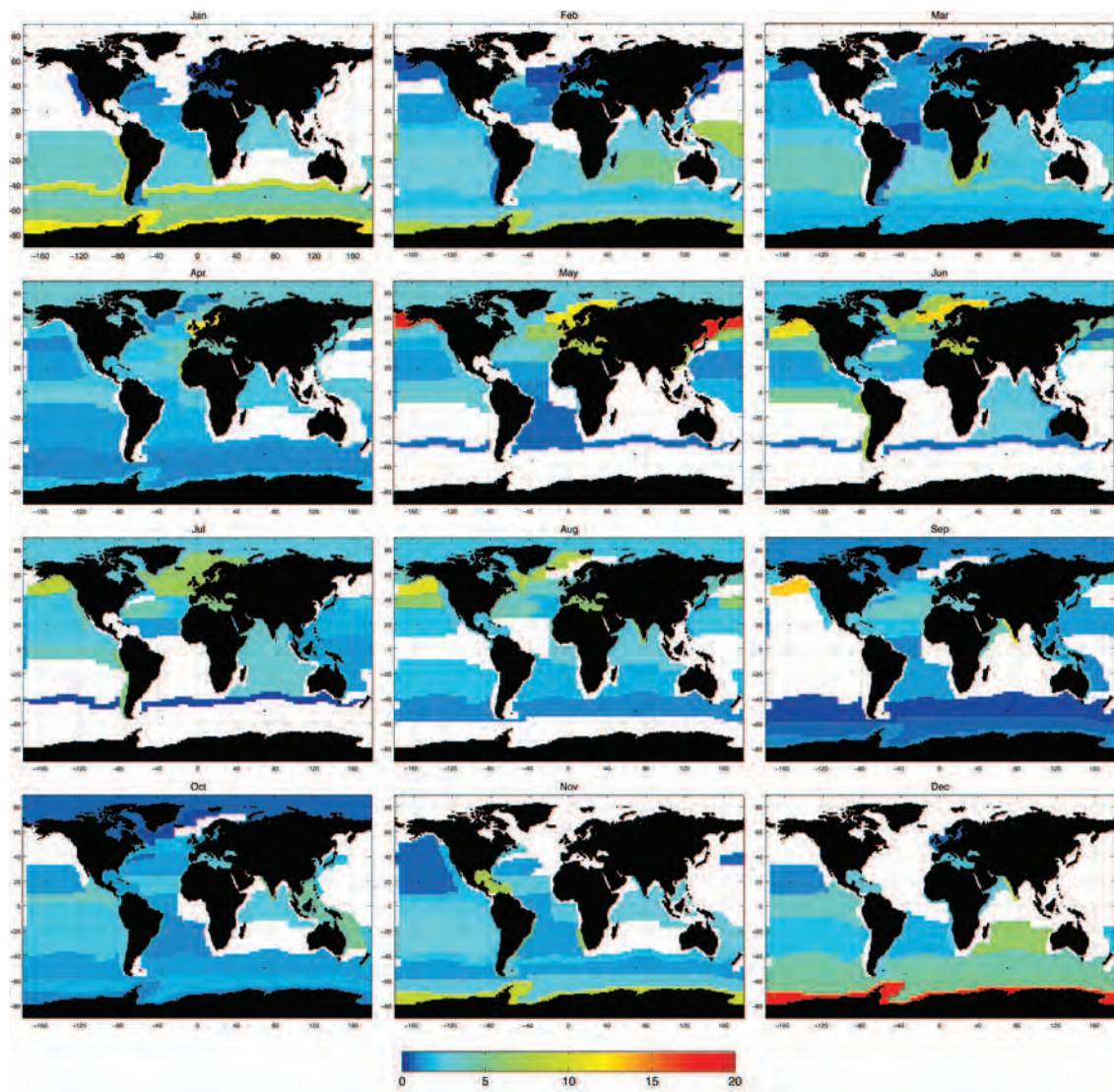


Figure 1. Monthly maps of average DMS concentrations (nM) for each biogeochemical province. Note that provinces that are white contain zero data for that calendar month.

1998]. In equatorial regions, the coastal province CAMR was substituted by CCAL following K99. The provinces AUSE and SUND were merged together into a single region, which was then used to substitute for AUSW and NEWZ. TASM is substituted by SSTC. TASM is a very small province that has its own particularities [Longhurst, 1998] but is expected to be largely affected by the processes and characteristics of its neighbor SSTC.

ObjXXXXXXXXXXXXXXXXXXXX

By filling the monthly gaps in the annual cycle for each province as described above, twelve global first-guess maps with the monthly mean DMS were constructed in each province. Transitions across province borders were smoothed using an unweighted 11 point filter based on the work of Shuman [1957]. Cressman [1959] proposed an iterative application of this distance-weighted interpolation method, with successive corrections. We tested several variants, based either on single-pass analysis [Barnes, 1964], or multiple-pass analysis for successive corrections [Cressman, 1959; Barnes, 1994; Koch et al., 1983], and with different weight functions, different filters, and different radius of influence. The technique we found to be most appropriate was the one applied by K99, with a radius of influence of 555 km and a single-pass correction.

Finally, the uniform-within-province global monthly maps (Figure S2) were updated with in situ data using the distance-weighted interpolation scheme of Barnes [1964]. This method determines the variable at grid points as the sum of the weighted values of the departures of individual in situ data to the first-guess field. The closer a data point is to a certain grid point, the greater the influence the Batum exerts to the grid point (inversely proportional to the exponential of the square of the distance). The radius of influence was chosen to be 555 km, so that data beyond that distance from the grid point were not taken into account.

The resulting global map was once again smoothed by a 5 point median filter, and by a 11 point unweighted smoothing filter, with both filters applied following the methodology used in the World Ocean Atlas [Locarnini et al., 2010].

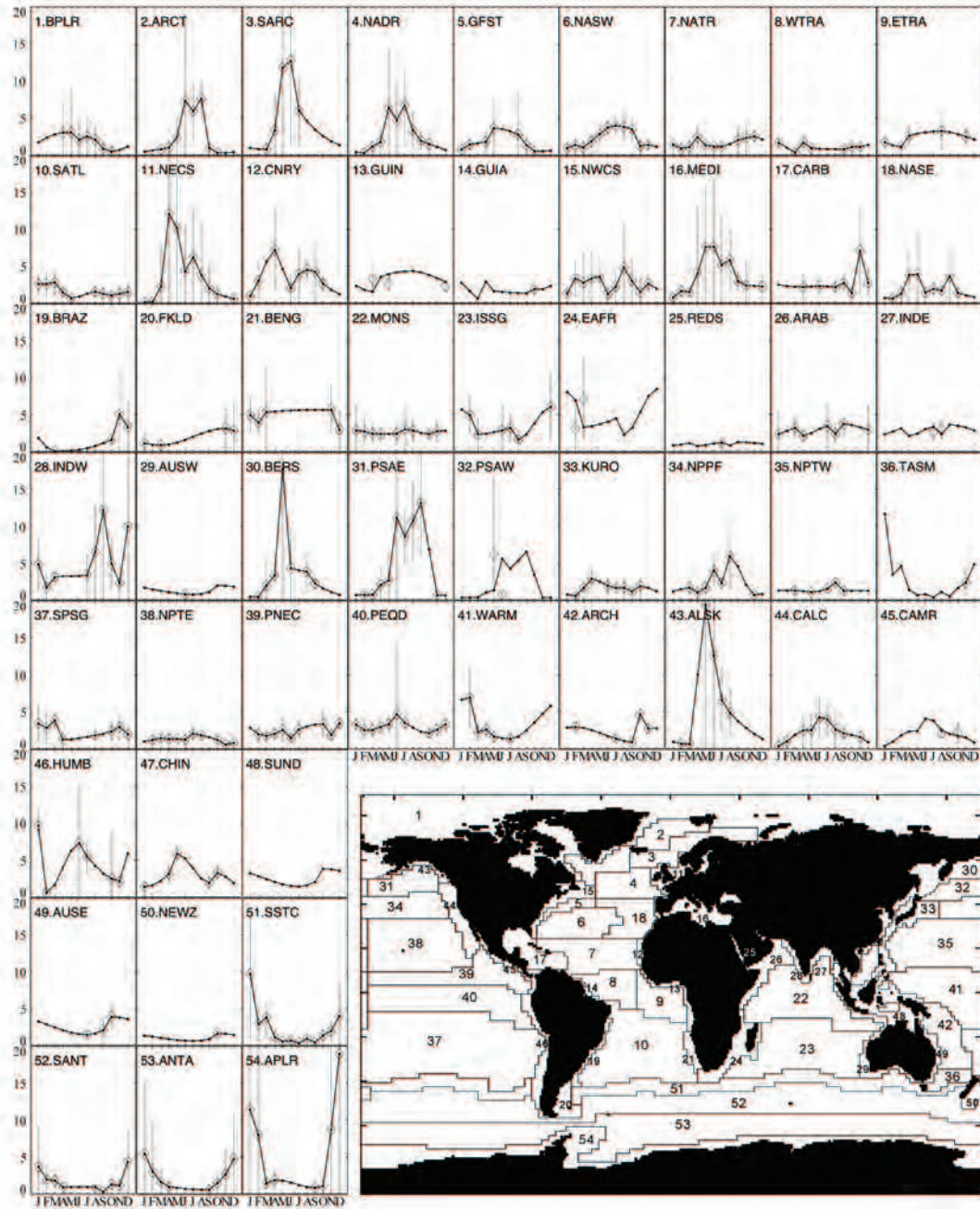


Figure 2. Time series of sea surface DMS concentration (nM) for each biogeochemical province. Calculated average values (open diamonds) plus one standard deviation are overlain with the seasonal cycle (dots and solid line) used to construct the L10 climatology. See text for details of interpolation and substitution methods.

Uncertainty

An estimate of the uncertainty in DMS concentration for each $1^\circ \times 1^\circ$ bin was made using the standard deviation (SD) of the log transformed monthly observations for each biogeographic province that contained data. The mean value plus/minus the SD of the log-transformed data is hereafter referred to as the upper/lower “bounds,” respectively. These DMS concentration bounds for each month in each province thus capture approximately 68% of the available data and are asymmetric about the mean, which accurately reflects the positive skew in the data set distribution. For each month, in each province, the upper and lower bounds were normalized to the monthly average concentration and the mean of all of these taken to represent global average upper and lower bounds. The normalized average bounds were then applied to all provinces with months that contained ≤ 3 data points and where a mean value had been interpolated or substituted. The interpolated or substituted mean value and the average normalized bounds were then used to convert back to an appropriately scaled upper and lower bound for that specific month and province.

In the substituted provinces, certain months still contained some data. Whenever processing these, the logtransformed SD was always applied to the substituted mean in preference to applying the global average bound values. After having produced bounds for all months in all provinces including all those that had been interpolated or substituted, the relative confidence in the mean values was assessed using the number of data points contained within each province in each month. Each upper and lower bound value was divided by the square-root of the number of data points (n). Provinces with months containing ≤ 3 data points not used in the first-guess used $n = 3$. We used these new climatologies of upper and lower bounds as a data based estimate of uncertainty in the climatology. The monthly maps and related data will be available along with the concentration climatology itself on the SOLAS Project Integration Web site (http://www.bodc.ac.uk/solas_integration/implementation_products/group1/#dms).

Other ocean variables

For the sake of statistical comparison with DMS distributions, state-of-the-art global climatologies of ocean variables were extracted and converted into $1^\circ \times 1^\circ$ monthly fields. The chlorophyll a concentration climatology for the years 1997–2009 was obtained from the SeaWiFS Project (GSFC, NASA). Cumulative climatologies of phosphate and nitrate concentrations were obtained

from the World Ocean Atlas 2009 [Garcia et al., 2010]. The SST climatology (1978–2008) was taken from the NCEP/NCAR reanalysis project, as above. The solar radiation dose (SRD) climatology was that computed by Vallina and Simó [2007a]. The mixed layer depth (MLD) climatology was the same used by Vallina and Simó [2007a] after modification of that by de Boyer-Montégut et al. [2004]. All data, including DMS, were log transformed before correlation to overcome nonnormal distribution.

RESULTS AND DISCUSSION

DMS CLIMATOLOGY

The original data available to construct our revised DMS climatology (hereafter referred to as L10) were 47,313 surface seawater DMS concentration values, which were reduced to 47,266 after the data removal procedure described earlier. Although the time span of data collection is greater than three decades, more than half of the data are from the last 8 years. This is due to an obvious increase in the sampling effort, but also to the development of automatic and semiautomatic DMS analysis systems [e.g., Marandino et al., 2009; Saltzman et al., 2009; Archer et al., 2009]. The data are plotted in monthly $1^\circ \times 1^\circ$ fields. Even though the overall data is distributed fairly well throughout most of the global oceans, monthly distribution shows a remarkable lack of data in some regions and months: see Figure 1 and Table 1. As much as 64% of the data have been collected in the Northern Hemisphere, half of them during the boreal late spring and summer months (May–August). The Southern Hemisphere, despite its larger contribution to the global ocean surface area, contains only one third of the total data, with almost half of them collected during austral spring/summer (November through February).

DMS CLIMATOLOGY AND OTHER OCEANIC VARIABLES

An attempt was made to compare climatological DMS concentrations with other oceanic variables by means of Pearson's correlations of log transformed data. Due to the enormous number of data, all correlations were significant with probabilities $>99.99\%$. Low negative correlations were found with surface nitrate and phosphate ($r = -0.09$ and -0.109 , respectively, $n = 491,460$). Low positive correlations were obtained with SST ($r = 0.181$, $n = 420,127$) and chlorophyll a ($r = 0.147$,

$n = 397,751$), while much higher correlations were found with MLD ($r = -0.47$, $n = 471,419$) and SRD ($r = 0.58$, $n = 452,269$). Kettle et al. [1999] also attempted correlation analyses with global climatologies, and found a similar result with chlorophyll *a*. They also found a negative correlation, yet lower, with the MLD, and a positive correlation with light, although they used surface irradiance rather than radiation dose. A remarkable difference between K99 and our study was the correlations to nitrate and phosphate, which were positive. It has to be stressed, however, that the data used by Kettle et al. [1999] were not log transformed despite the lack of normal distribution. The results of our correlation analysis support the suggestion (challenged by some authors [e.g., Derevianko et al., 2009] that the MLD and the SRD play prominent roles in driving monthly surface DMS concentrations [Simó and Pedrós-Alió, 1999; Simó and Dachs, 2002; Vallina and Simó, 2007a; Miles et al., 2009]).

Seasonal and monthly DMS concentrations by province

The high-latitude provinces in the North Atlantic and North Pacific Oceans (e.g., SARC, NADR, BERS, PSAE) show a common pattern of high average DMS concentrations (>5 nM) during the boreal summer, with either unimodal or bimodal maxima between May and September (Figure 2). The Arctic Ocean (BPLR) exhibits a similar seasonal cycle, but with lower average maxima in spring/summer (<4 nM). Moving South toward northern temperate and subtropical provinces (e.g., NASW, NASE, NPPF, NPTW, NPTE), the seasonal pattern becomes less pronounced and the average spring/summer maximum concentrations are lower (generally <5 nM). The seasonal cycle is almost lost in most of the tropical provinces around the equator in both hemispheres (e.g., NATR, WTRA, ETRA, MONS, NPTE, PNEC, PEQD, WARM), where average DMS concentrations are from moderate to low (1–4 nM) throughout the year. The southern subtropical provinces of the Atlantic, Pacific and Indian Oceans (SATL, ISSG, SPSG) recover a slight seasonality with austral summer maxima at concentrations generally below 5 nM. The same seasonal pattern is much more pronounced in the four provinces of the Southern Ocean (SSTC, SANT, ANTA, APLR), with summer maxima occurring at concentrations of 5 nM that peak most sharply in Antarctic waters (Figure 2).

Monthly DMS concentrations by province

The annual patterns shown in Figure 2 are used to create the monthly first-guess fields (see Figure S2). These are adjusted with real data at the local scale to obtain more realistic distributions.

After 5 point median and 11 point unweighted filter smoothing, the monthly global maps of the climatology were produced (Figure 3). The remarkable spottiness of the maps is due to the differences between the first-guess background (which is the province monthly mean concentration) and the measurements made at the local scale. Spottiness must be regarded, hence, as a sign of fidelity to the measurements in the database.

The monthly climatology maps (Figure 3) show the temporal (seasonal) and spatial variability of DMS concentrations. The salient features are (1) concentrations are in the range 1–7 nM for the global oceans most of the time; only 1% of the climatology's values are >10 nM whereas 50% are <2 nM, paralleling data distribution in the original database; (2) higher concentrations are found at high latitudes (polar and subpolar) and in some regions close to continents; (3) existence of a general trend toward increasing concentrations in summer in both hemispheres. The global map of annually averaged concentrations (Figure 4) is fairly homogeneous, with few regions with values below 1 nM or above 5 nM.

RgXXXXXXXXXXXX

In the high-latitude Northern Hemisphere, DMS concentrations follow a strong seasonal pattern. They increase in the warmer and more illuminated months from late spring through late summer, although the timing of the concentration peak varies among regions (Figures 2 and 3). In the northern Gulf of Alaska and the Bering and Barents Seas, observed DMS is high in May, coinciding with documented blooms of strong DMS producers, *Phaeocystis pouchetii* and coccolithophores [Barnard et al., 1984; Iida et al., 2002; Matrai et al., 2007], and the summer maxima in June and July also accompanies the persistence of coccolithophores [Iida et al., 2002]. In the NW Atlantic and around the Iceland Basin, DMS concentrations are moderate in April–May and September and peak in June–July, at the time of maximum development of recurrent coccolithophore and flagellate blooms, which cooccur with dinoflagellates to yield high DMS concentrations [e.g., Matrai and Keller, 1993; Scarratt et al., 2007; Lizotte et al., 2008; Yang et al., 2009]. In the open ocean waters of the central Gulf of Alaska, concentrations are high throughout the summer and well into September for reasons not fully ascertained [Wong et al., 2005]. Much of the data from this latter region have been collected recently and thus summer DMS levels for the PSAE province in our new climatology are remarkably higher than those in the original climatology, K99.

Temperate low latitudes and northern subtropical regions typically follow a seasonal pattern with higher DMS concentrations in summer despite low chlorophyll *a* concentrations, a feature that has been coined the “summer DMS paradox” [Simó and Pedrós-Alió, 1999]. In the large subtropical Pacific (NPTW, NPTE) the summer maximum occurs, yet very subtly. In the subtropical Atlantic there is a remarkable difference between the seasonality of the western side (NASW) and that of the eastern side (NASE). While in the NASW the summer maximum is clear [Dacey et al., 1998], in the NASE DMS concentrations are higher, yet more variable, in spring (April-May) than in late summer [Belviso and Caniaux, 2009].

The eastern equatorial Pacific between 10°N and 10°S is one of the most visited regions over three decades. DMS concentrations in the region are relatively constant throughout the year [Bates and Quinn, 1997], which is clearly apparent in our climatological monthly maps. In the western equatorial Pacific, increased DMS concentrations in the period November–February have been observed, although it should be noted that the number of observations is low and the equatorial province (WARM) extends as far south as 18°S. As in the Pacific, the main equatorial province of the Atlantic (WTR) also does not show a marked seasonality. The neighboring eastern province, ETRA, has fewer data. There, higher DMS levels have been observed to occur between April and September, coinciding with climatological satellite observations of increased chlorophyll *a* concentrations between June and September due to a strengthening of the zonal winds and associated upwelling [Pérez et al., 2005].

The equatorial Indian Ocean (MONS) shows a slight trend toward higher DMS levels during the boreal summer. Concentrations are always above 2–3 nM throughout the year. This is a remarkable difference with respect to the concentration given by K99, which was constructed almost without any data in this region and which predicted very low DMS levels over long periods of the year. The lack of data prompted K99 to attribute to MONS the patterns observed in the Arabian Sea (ARAB) and the coastal Indian provinces (INDE and INDW). The amount of data collected in MONS, ARAB and INDE has increased considerably in recent years. The new data demonstrates that DMS concentrations are typically elevated during the southwest monsoon (June to September), particularly on the West Indian shelf [Shenoy and Kumar, 2007]. On the eastern side of India, the few existing measurements in the Bay of Bengal point to more moderate concentrations all year round.

The Indian subtropical gyre (ISSG) shows a marked seasonality with average DMS concentrations

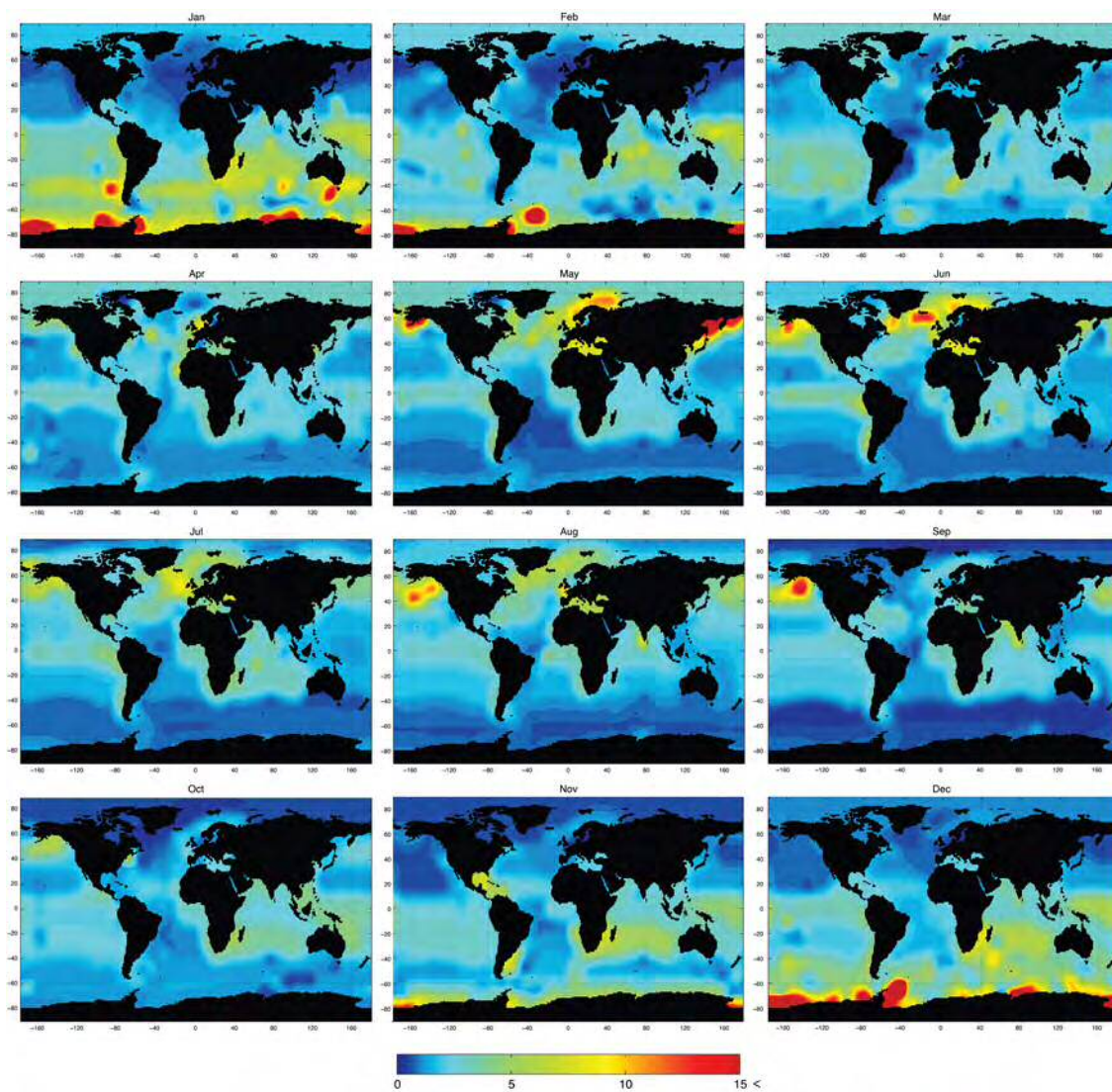


Figure 3. Monthly climatology (L10) of DMS concentrations (nM). Note that the scale is capped at 15 nM to ensure readability of the plots, although only a few specific regions exceed 15 nM DMS concentration.

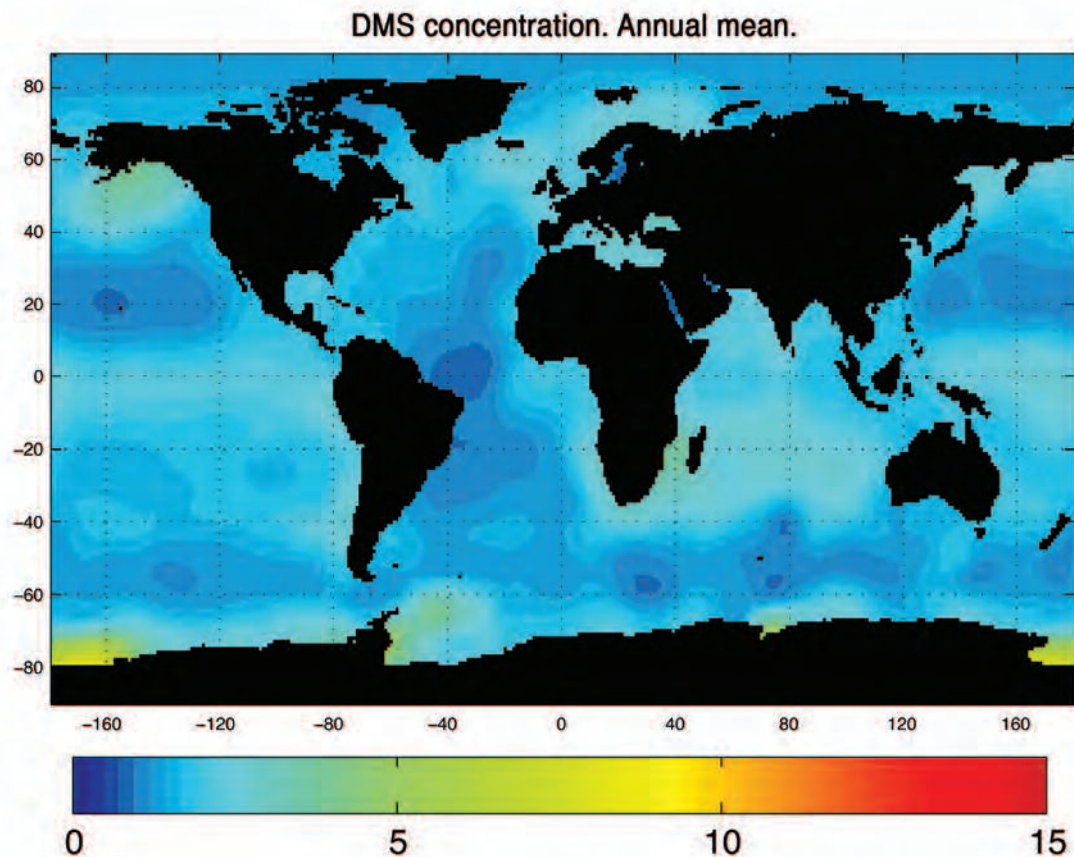


Figure 4. Annual global mean climatology (L10) of DMS concentrations (nM).

in the austral summer 6 times as high as the winter ones (6 and 1 nM, respectively). Such a seasonal pattern is coincident with that of the shoaling of the mixed layer and opposite to that of chlorophyll *a* concentrations [Longhurst, 1998], thus setting the conditions for the so-called “summer DMS paradox” [Simó and Pedrós-Alió, 1999]. A noticeable increase in data coverage now provides a reasonably good description of DMS distribution in this large region. In K99, there were data only in two months and ISSG had to be substituted by its neighboring province to the South (SSTC), a region with completely different biogeochemistry. The semiempirical models of Aumont et al. [2002] and Simó and Dachs [2002] already predicted higher DMS concentrations in the southern Indian Ocean than K99. These predictions are borne out by the

new climatology.

The large ultraoligotrophic subtropical gyre provinces of the South Atlantic and South Pacific (SATL and SPSG) show a similar seasonality to ISSG, with higher DMS levels coincident with the shoaling of the mixed layer [Longhurst, 1998], yet with lower maximum concentrations [e.g., Bell et al., 2006]. It is worth mentioning that, in K99, both provinces had very little data and were adjusted to the seasonal pattern of the circumglobal province SSTC. Although in the last 10 years the number of measurements in these regions has increased considerably, SPSG is still one of the more poorly sampled open ocean regions (Table 1).

DMS seasonality in the coastal Pacific upwelling region, Humboldt Current coastal province (HUMB), appears very marked but is highly uncertain because of the lack of data during half of the year. High, but variable, concentrations are found in June-July along the Peruvian coastal upwelling [Andreae et al., 1995], and low concentration levels are observed all along the province in October-November (J. Johnson, unpublished data, 2006, 2007) and in the southernmost part in February [Lee et al., 2010]. A very strong “hotspot” of DMS is apparent off the southern coast of Chile in January (Figure 3). Concentrations as high as 22 nM were measured in a few samples through the transition between the HUMB and the South Subtropical Convergence province (SSTC). Since there was no associated signal in chlorophyll a, hydrography or atmospheric DMS concentrations, these observations may have corresponded to a highly localized patch [Marandino et al., 2009]. Further visits should help decipher if this hotspot is a recurrent feature.

The Southern Ocean, as a whole, has enough data coverage to construct reliable monthly DMS maps. The seasonalities of the four provinces (SSTC, SANT, ANTA and APLR) are in phase, with concentrations increasing in the austral summer. High DMS levels (around 10 nM) are found southwest of Australia in January, coinciding with minimal mixed layer depths and maximal chlorophyll a concentrations [Longhurst, 1998]. Moving southward, DMS levels decrease across the subantarctic current and increase again in Antarctic waters [McTaggart and Burton, 1992]. A similar pattern is found along transects from the subtropical convergence off South Africa or on either side of South America toward Antarctic waters [Liss et al., 2004]. The highest concentrations of the Southern Hemisphere (>20 nM) are found in Antarctic coastal seas (APLR) in the period November-February. Those high DMS values are driven by the strong phytoplankton blooms in the sea-ice breakout season [Trevena and Jones, 2006]. Throughout the rest of the year DMS concentrations are low, reflecting the low levels of biological activity due

to increased ice cover and reduced light levels.

Average summer DMS concentrations in Antarctic waters (APLR) have been reduced significantly with respect to those in K99. Ten years ago, average concentrations in December and January were larger than 40 nM throughout most of the province, reaching regional maxima of up to 160 nM (K99). With the recent increase in measurements, the new climatology contains a monthly average concentration of ca. 20 nM in December, with a regional maximum of ca. 50 nM.

Ocean-atmosphere DMS fluxes

Ocean-atmosphere DMS fluxes are computed as the product of the air/sea concentration difference and gas transfer velocity, as follows: $F = kT(C_w - C_{ga})$, where the gas transfer coefficient, kT , is the reciprocal of the total resistance to gas transfer on both sides of the air/sea interface [Liss and Slater, 1974]. DMS fluxes are generally parameterized assuming water side resistance only, but as demonstrated by McGillis et al. [2000], air side resistance can also be significant at cold temperatures and high wind speeds. Atmospheric DMS levels are typically orders of magnitude lower than those in the surface ocean, and are assumed to be zero for these calculations.

The waterside DMS gas transfer velocity was based on the 10 m wind-speed-based parameterization of Nightingale et al. [2000] (hereafter N00), for a Schmidt number of 600 ($k_{600} = 0.222U_{10}^2 + 0.333U_{10}$). These were normalized to the Schmidt number of DMS as follows: $k_w = k_{600} (Sc_{DMS}/600)^{-1/2}$, where Sc_{DMS} is a function of SST according to Saltzman et al. [1993].

Total gas transfer velocities for DMS were computed using the atmospheric gradient fraction (ga): $kT = k_w (1 - ga)$, where ga is defined by $ga = 1/(1 + ka/akw)$, using the approach of McGillis et al. [2000]. In this expression ka is the airside transfer coefficient, which was based on neutral stability water vapor bulk transfer coefficients from Kondo [1975] and a is the DMS solubility, from Dacey et al. [1984].

The DMS flux is calculated with the DMS concentration values obtained from this study and the total transfer velocity. This approach is slightly different than that of K00, who assumed only water side resistance to the air/sea flux under conditions of high wind speeds and cold SST. On an annual basis, the flux computed including air side resistance was 7.4% less than computed assuming water side resistance only.

SST and wind speed climatologies were obtained from the NCEP/NCAR reanalysis project (<http://www.esrl.noaa.gov/>) for the period 1978–2008. Most of the DMS data used to generate the climatology were measured during that period. We applied a monthly sea-ice mask to set DMS emission fluxes to zero in ice-covered waters. Data on ice extent and concentration (percentage of the local ocean surface covered by sea ice) were provided by IFREMER/CERSAT (<http://cersat.ifremer.fr/>) upon analyses of the 12.5 km resolution data from the US SSM/I sensor since 1992. We assumed negligible DMS emission fluxes where the sea ice concentration is higher than 75%. All SST, wind speed and sea ice coverage data are converted to a $1^\circ \times 1^\circ$ resolution using a cubic spline interpolation that avoids the problem of distortions near the edges of the global map.

Because k_w has a nonlinear dependence on wind speed, the use of monthly averaged wind speeds introduces a bias into the flux calculation. The flux was corrected for this effect assuming that instantaneous winds follow a Rayleigh distribution, using the approach of Simó and Dachs [2002]. To compare with K00, monthly global fields of DMS emission fluxes were also computed using the parameterizations of Liss and Merlivat [1986] and Wanninkhof [1992].

L10 v ~~XXXXX~~ K00

In order to evaluate the influence of a 3-fold increase in measurements to the predicted monthly global distributions of DMS, we now compare the updated climatology (L10) with the reference climatology that is widely used at present (K00). The differences are summarized with graphical representations of the latitudinal annual means (Figure 5a) and the latitudinal means for the periods December–February (DJF) and June–August (JJA) (Figure 5b). Note that the concentration difference between K00 and L10 versus latitude can also be plotted for every individual month (see Figure S3). Large differences in the annual average distribution are found in the high latitudes ($\geq 65^\circ$) of both summer hemispheres, where K00 predicted much higher DMS concentrations than L10. Clearly, the inclusion of new data has led to a substantial decrease of the high-latitude average DMS concentration, partly because data in K00 were dominated by coastal and ice-edge measurements.

There are two latitudinal bands where L10 predicts higher annual mean concentrations than K00. One is around 50° – 60° N, where the incorporation of a great number of measurements in

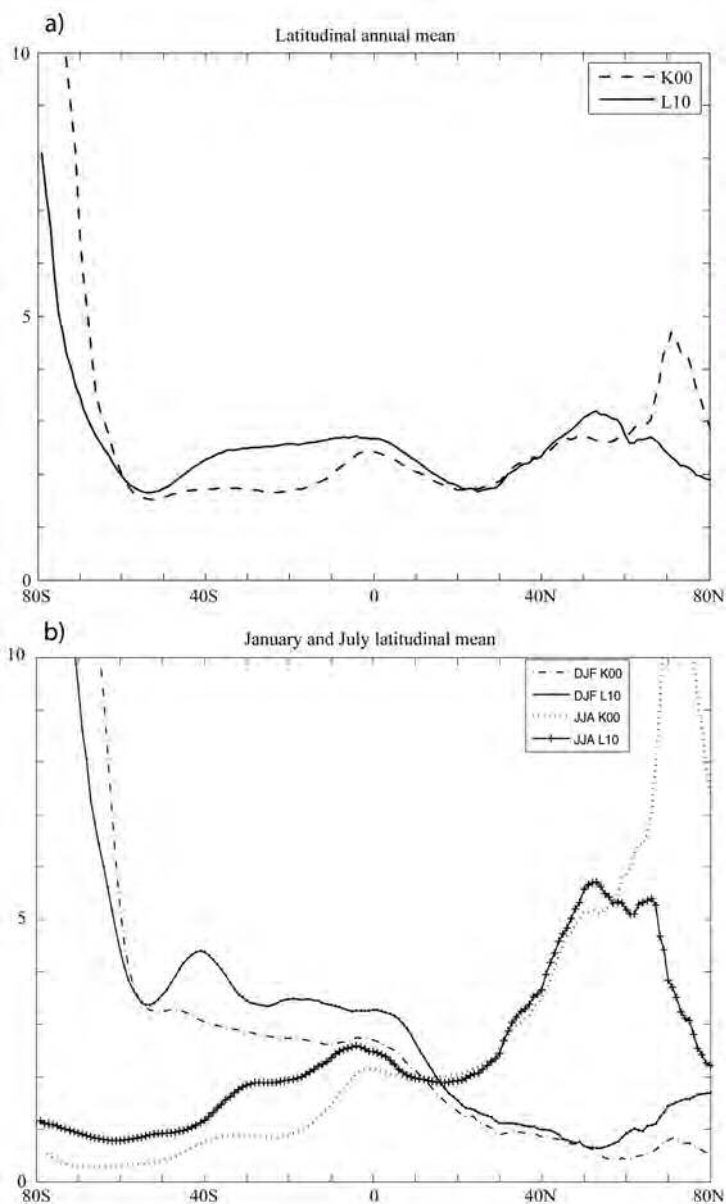


Figure 5. Comparison between K00 (dashed line) and L10 (solid line) climatological DMS concentration data (nM) in terms of (a) annual latitudinal mean concentrations; and (b) summer and winter (i.e. December- January-February, DJF, and June-July-August, JJA) latitudinal mean concentrations.

the DMS-rich Alaska coastal province ALSK (J. Johnson et al., unpublished data, 2002, 2003) has increased the regional mean (Figure 2). The other band occurs between the equator and 40°S, where new data in the Indian Ocean (MONS and ISSG) and Pacific Warm Pool (WARM) provinces raise the annual mean.

The plot of the latitudinal seasonal means (Figure 5b) shows how DMS concentrations oscillate seasonally between lower values in the hemispheric winters and higher values in the hemispheric summers. The two climatologies predict almost identical concentrations in both seasons within the region comprised between 10°N and 50°N. Figure 5b clearly illustrates the substantial reduction in summer values and increase in winter values at both poles (i.e., greater than 60°N and S), as well as the year-round increase between 10°N–50°S, particularly in the Southern Hemisphere.

DMS flux

Local ocean-to-atmosphere DMS fluxes were computed from surface ocean concentrations using the parameterization suggested by Nightingale et al. [2000]; see section 2. A climatological monthly sea ice mask was applied with the assumption that fluxes across the sea ice cover are greatly reduced or completely blocked, even though DMS concentrations measurements exist from the waters underneath. Emissions from the sea ice itself would also increase the amount of DMS fluxes to the atmosphere. Recent laboratory and in situ experiments [Zemmelink et al., 2008; Loose et al., 2009] indicate that gas emission can occur through or from complete or partial ice cover and this should be taken into account. However, this poses an obvious difficulty when we are to apply a general parameterization of the gas transfer coefficient. Computed fluxes with and without the ice cover mask, and the resulting global annual emissions, are not substantially different at the global scale (9.8% higher without ice mask). The difference at high latitudes (60°–90°N and 60°–90°S) is significant, 47.5% higher without the ice mask. The fluxes calculated here are capped by the use of an ice cover mask, but further work is required to better quantify the effect of sea ice on the sea-to-air flux of DMS.

In northern latitudes, emission fluxes follow the seasonality of surface concentrations (see Figure 6). This is also true of the high latitudes in each hemispheric summer. The Southern Ocean emissions stand out because high summer concentrations coincide with strong winds all year round. In the subtropical Indian Ocean, the combination of moderate DMS concentrations and persistent high wind speeds throughout most of the year leads to a strong flux. The Pacific Warm

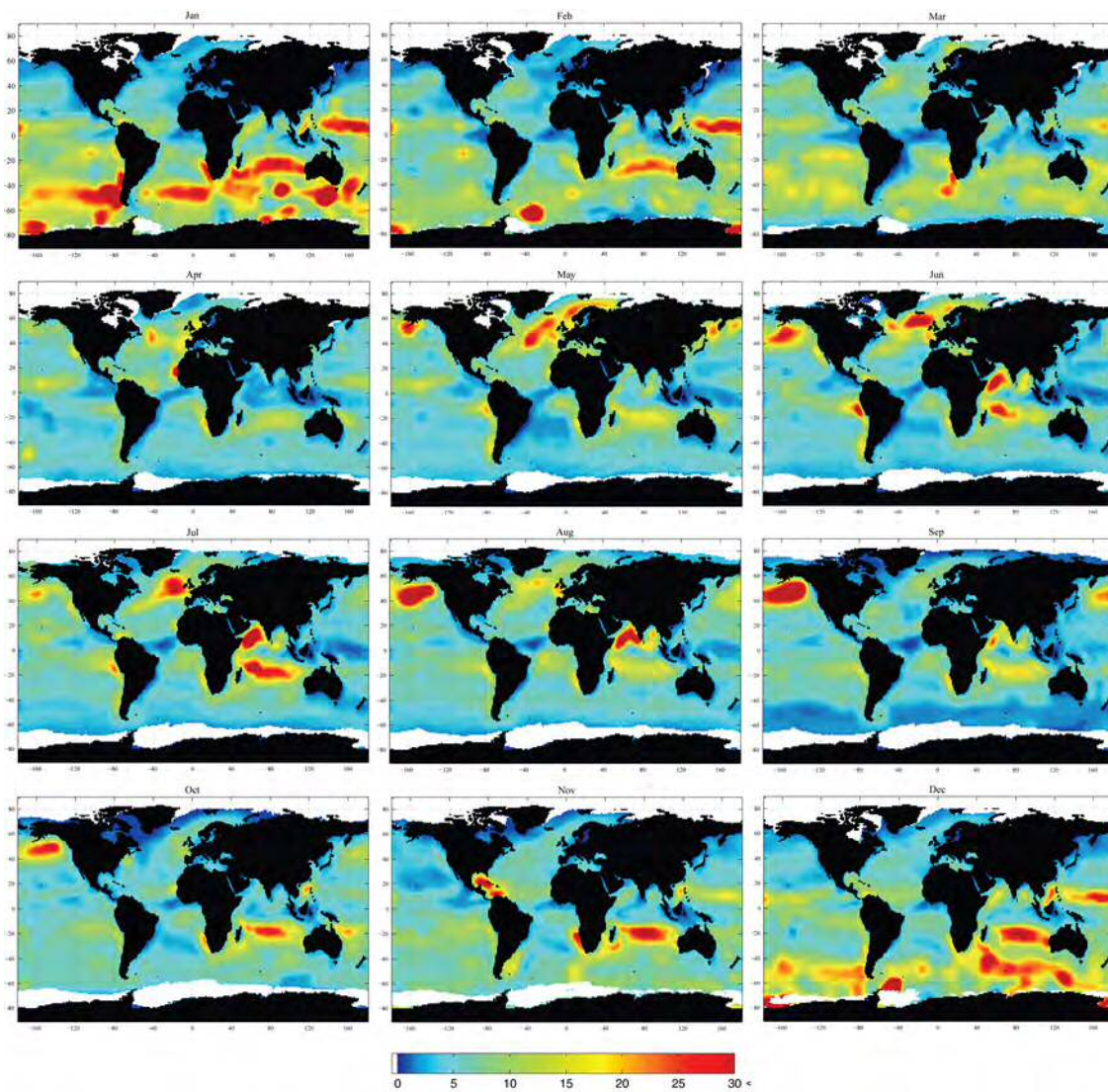


Figure 6. Monthly climatology of DMS fluxes ($\mu\text{molS}/\text{m}^2 \text{d}$). Note that the scale is capped at 30 $\mu\text{molS}/\text{m}^2 \text{d}$ to ensure readability of the plots, although only a few specific regions exceed this value.

Table 2. Annual DMS flux (TgS/yr) per 10 degree latitudinal band after this study (L10) and the Kettle and Andreae [2000] (K00) climatology, computed with the Nightingale et al. [2000] parameterization of the piston velocity. Total global DMS fluxes calculated using the Liss and Merlivat [1986] and Wanninkhof [1992] parameterization are provided for comparison.

<i>Latitude</i>	<i>Nightingale et al. [2000]</i>	
	K00	L10
90°-80°N	0.0	0.0
80°-70°N	0.2	0.1
70°-60°N	0.2	0.2
60°-50°N	0.7	0.9
50°-40°N	1.4	1.5
40°-30°N	1.5	1.5
30°-20°N	1.4	1.4
20°-10°N	2.4	2.6
10°-0°N	2.3	2.6
0°-10°S	1.9	2.2
10°-20°S	2.3	3.5
20°-30°S	1.9	3.0
30°-40°S	1.9	2.7
40°-50°S	2.4	2.8
50°-60°S	2.0	2.1
60°-70°S	1.2	0.9
70°-80°S	0.2	0.1
80°-90°S	0.0	0.0
Total	24.0	28.1

	<i>Liss and Merlivat [1986]</i>	
	K00	L10
Total	15.0	17.6

	<i>Wanninkhof [1992]</i>	
	K00	L10
Total	29.4	34.4

Pool (WARM) fluxes are characterized by the coincidence of large concentrations and wind speeds between November and February, which renders high seasonal fluxes. In contrast, the waters East of Somalia, despite having quite constant predicted DMS concentrations throughout the year, become an important region of sulphur emissions during the boreal summer due to the strengthening winds caused by the southwest monsoon.

Integrated DMS emission fluxes were computed using N00 and the classical parameterizations of Liss and Merlivat [1986] and Wanninkhof [1992], hereafter LM86 and W92, respectively. For the sake of comparison, and to provide a range of DMS flux estimates, we recalculated emissions for K00 with the three gas transfer parameterizations. Table 2 reports the results of annually integrated emissions by 10° latitudinal bands resulting from applying the different parameterizations to K00 and L10.

Annually integrated latitudinal emissions depend on the magnitude and persistence of local fluxes but also on the ocean area occupied by each latitudinal band. In K00, the tropics and Southern Ocean contribute the largest share of the global DMS emission. In L10, the southern subtropical latitudes also contribute substantially. Together, the Southern Hemisphere oceans contribute 61%–62% (depending on the parameterization) of the global annual DMS emissions in L10 whereas their contribution was around 56%–57% in K00. As a result of the differences in DMS concentration distribution discussed above, the global annual DMS emission in L10 is 15%–17% higher than that of K00. Taking N00 as an intermediate and probably more realistic parameterization of the transfer coefficient [Marandino et al., 2009], the updated revision of the global oceanic DMS emission is estimated at 28.1 TgS/yr. Following the classification of Longhurst [1998] we computed the oceanic DMS emission fluxes from the coastal and upwelling areas. Nearly 11% of the global annual emissions occur in coastal provinces, which occupy nearly 10% of the global ocean area.

Analysis of the variability in the underlying data used to construct the climatology shows that the range in total global flux estimates due to data variability is, at least, as large as the range due to uncertainty in the air/sea gas transfer velocity parameterization. DMS emission fluxes calculated by applying the N00 parameterization to the upper and lower bounds of the climatology uncertainty span a range of 24.1 to 40.4 TgS/yr.



The aim of this study was to construct a more accurate climatology of global monthly distributions of surface ocean DMS concentration based on state-of-the-art data, and to calculate associated sea-to-air emission fluxes. The new L10 climatology has been constructed using data contributed by researchers from all over the world and archived in the Global Surface DMS Database (see Table S1), and can be regarded as an updated and refined version of the former climatology (K00) assembled by A.J. Kettle and others (K99 and K00).

Climatological DMS concentrations increased in regions and months that were severely under-sampled 10 years ago, as for example in the subtropical Indian Gyre. Conversely, data additions

have substantially decreased climatological concentrations in regions where K99 showed extremely high values, namely polar waters. In this sense, a climatology constructed exclusively from available DMS measurements is very sensitive to the number of data, as pointed out by Belviso et al. [2004b]. Although the number of new DMS measurements in the Northern Hemisphere was around 50% higher than that in the Southern Hemisphere, the largest differences between L10 and K00 are found in the South.

Assessing the data coverage in oceanic provinces with the greatest areal extent (and consequently the largest influence on DMS flux) has led to the realization that they are not always the most comprehensively sampled. In many cases, the measurements are poorly distributed in space and time (see Table 1). For example, the South Pacific Subtropical Gyre (SPSG) is undersampled despite containing data from eight calendar months. The data is sufficient to make a first-guess construction but only with a large associated uncertainty. Another example is the Indian Subtropical Gyre (ISSG), which still lacks data for half of the year despite a significant effort to increase the number of measurements in the last decade. Also the western North Pacific provinces, from the subarctic (PSAW) to the Tropical Gyre (NPTW) through the Transition Zone (NPPF), show a serious lack of data relative to the surface area they represent. This means that the obtained climatological patterns have been constructed using interpolated data and should be used with caution and urgently revised as more measurements are made.

The L10 climatology offers more reliable representation of sea surface DMS concentrations in the global oceans than the widely used former climatology (K00) mainly because of an increased number of measurements and improvements in their spatial and temporal coverage. It is expected to be used as an input field for global atmospheric models and as a reference for global comparisons with oceanic and atmospheric variables. K00 has also been used to validate the output of oceanic DMS models [Le Clainche et al., 2010] despite the uncertainty associated with the data analysis. As a parallel product to the L10 climatology, we have created a $1^\circ \times 1^\circ$ binned monthly climatology of the original data which can be used for model validation (see http://www.bodc.ac.uk/solas_integration/). This work confirms the central role of DMS in the transport of sulphur from the biosphere into the atmosphere. The updated estimates given here indicate that the annual global DMS emissions are even larger than previously thought, with our best estimate suggesting 28.1 TgS/yr (17 % higher than estimated with K00). Owing to the potentially important influence of ocean-atmosphere DMS emissions for global sulphur cycling, aerosol formation, cloud microphysics, and radiative balance, the L10 will be useful for assessing the environmental factors controlling the DMS distribution and for validation of ocean

biogeochemical models.

Acknowledgments. The authors are indebted to each of the individual contributors that generously submitted their data to the Global Surface Seawater Dimethylsulphuride Database (GSSDD) (see details in Table S1) and to T.S. Bates (NOAA/PMEL) for the maintenance and personal implication in the GSSDD. We thank the NCEP/NCAR Reanalysis Project for the production and free distribution of the SST and wind speed data used in the present work. We thank the Ocean Biology Processing Group at GSFC for the production and distribution of the chlorophyll a climatology, and Ocean Climate Laboratory at the NODC for the distribution of the World Ocean Atlas 2009 phosphate and nitrate's climatologies used in this study. We also wish to thank the Centre de Recherche et d'Exploitation Satellitaire (CERSAT), at IFREMER, Plouzané, France, for providing the Ice Climatology, and specially F. Girard-Ardhuin for her help with the data. A. Longhurst kindly provided the biogeographic provinces data. This work was the core of DiMethylSulphuride concentrations and emission fluxes in the Global Ocean (DMS-GO), a joint initiative of the SOLAS Integration Project and the EU projects COST Action 735 and EUR-OCEANS. Tom Bell, Peter Liss, and SOLAS Project Integration are supported by a U.K. SOLAS Knowledge Transfer grant (NE/E001696/1). Further support was provided by the Spanish Ministry of Science and Innovation through the projects MIMOSA, Malaspina 2010, and a Ph.D. studentship to A.L.

Supplementary Material

This supplementary material contains a table showing the individual contributors who submitted DMS data to the Global Surface Seawater Dimethylsulfide Database. Their data were used to create the updated DMS climatology in this study. The supplementary material also contains three figures that represent: (S1) the location of the $1^\circ \times 1^\circ$ pixels with DMS data, (S2) the smoothed monthly first-guess fields of sea surface DMS concentration (nM), and (S3) the latitudinal difference between the previous climatology (K00) and that obtained in the present study (L10). Figure S1 was constructed by pooling together all existing DMS data in 1° latitude \times 1° longitude squares; the map shows the squares where DMS data exist. The monthly maps of Figure S2 were created from the annual cycles of each biogeographical province by computing the province monthly mean concentrations either from *in situ* data or by interpolation or substitution where there were no data; transitions across province borders were smoothed using an unweighted 11-point filter. Figure S3 shows the % of difference between K00 and L10 of monthly DMS concentrations in 1° latitudinal bands.

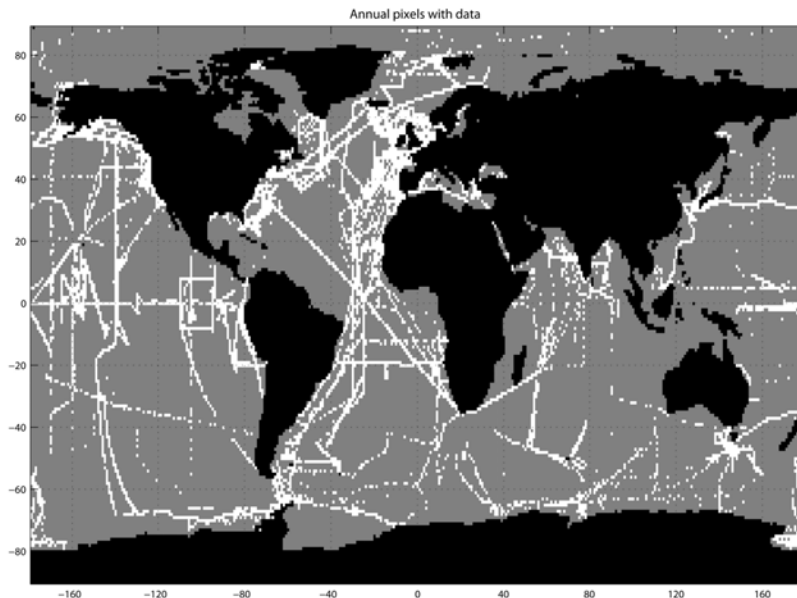


Figure S1. Annual map of the location of the $1^\circ \times 1^\circ$ ocean pixels with DMS data.

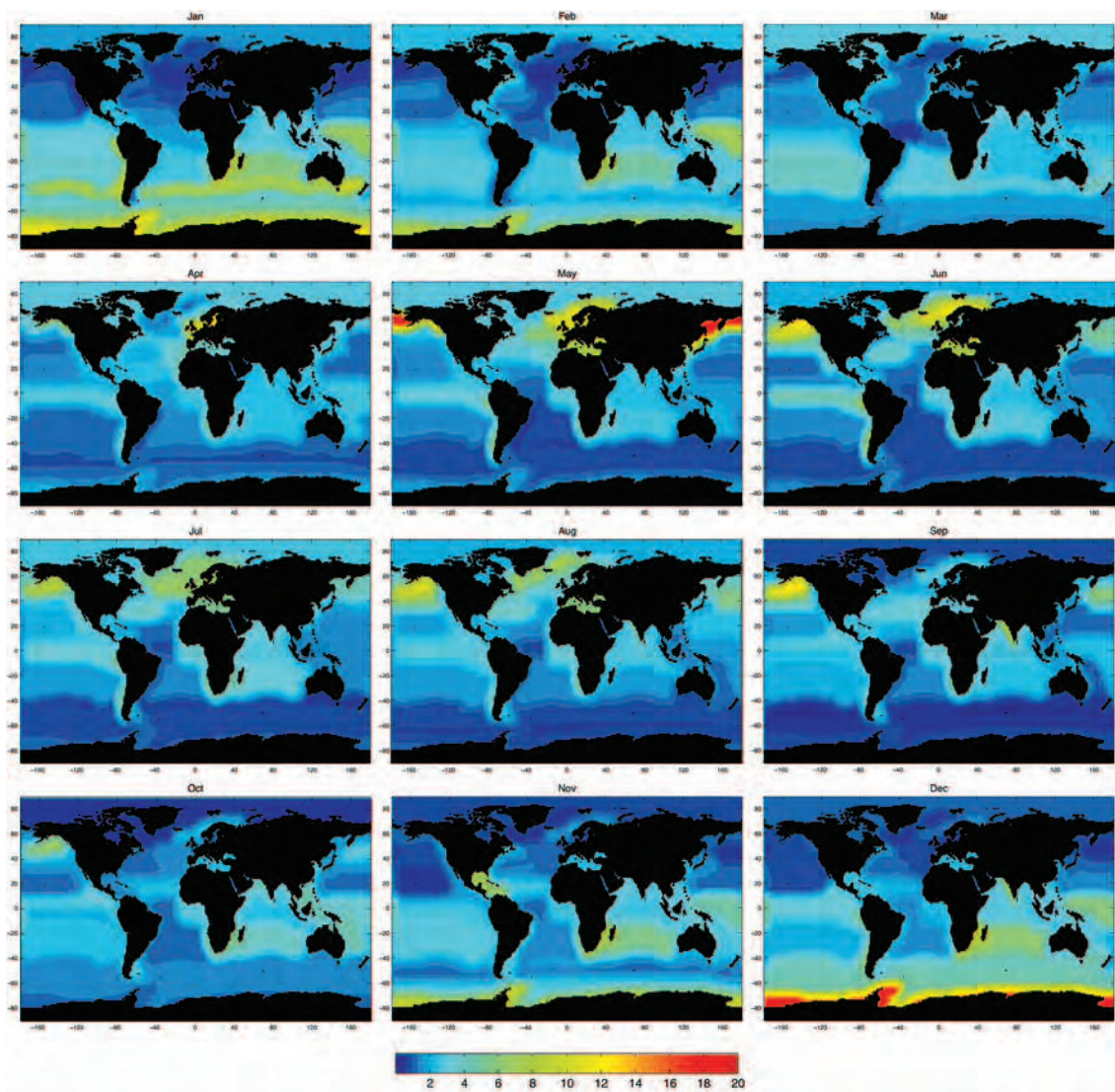


Figure S2. Smoothed monthly first-guess fields of sea surface DMS concentration (nM).

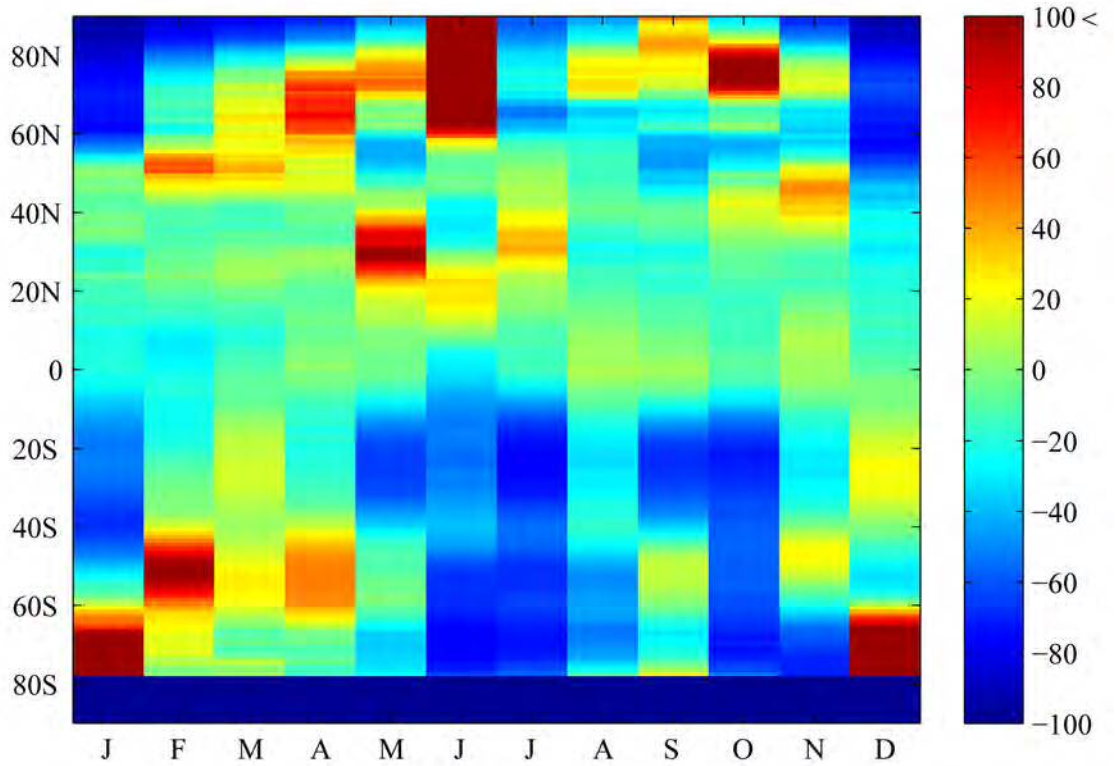


Figure S3. Monthly latitudinal comparison between K00 and L10 in % of the difference (using L10 as the reference). Note that K00 > L10 is capped at 100% for readability.

Table S1: List of the data contributors to the DMS database, with their contributor number, sampling region, number of samples, dates, and references.

CN	Contributor	Region	Samples	Start-End dates	Reference(s)
1	KettleD	Atlantic	20	1972-03-11 1972-04-03	<i>Lovelock et al.</i> [1972], <i>Liss et al.</i> [1997]
2	KettleD	Atlantic, Indian	19	1977-03-15 1978-05-15	<i>Nguyen et al.</i> [1978]
3	Andreae	Florida Strait	40	1980-04-07 1980-04-16	<i>Andreae and Raemdonck</i> [1983]
4	Andreae	Atlantic	231	1980-10-09 1980-11-07	<i>Barnard et al.</i> [1982], <i>Andreae and Barnard</i> [1984]
5	Andreae	Bering Sea	13	1981-05-04 1981-05-24	<i>Barnard et al.</i> [1984]
6	Andreae	Sargasso Sea	67	1981-09-18 1981-09-28	<i>Andreae and Barnard</i> [1984]
7	Andreae	Charlotte Harbour	30	1981-10-31 1981-10-31	<i>Frolich et al.</i> [1985]
8	Bates	Pacific	70	1982-05-08 1982-05-21	<i>Cline and Bates</i> [1983], <i>Bates et al.</i> [1987], <i>Bates and Quinn</i> [1997]
9	Andreae	Peru Shelf	294	1982-06-23 1982-08-06	<i>Andreae</i> [1985], <i>Andreae and Raemdonck</i> [1983]
10	Bingemer	Southern, Atlantic	89	1983-01-04 1983-01-19	<i>Bingemer</i> [1984], <i>Bingemer and Ockelmann</i> [1987]
11	Bates	Pacific	24	1983-03-04 1983-03-20	<i>Bates and Quinn</i> [1997], <i>Bates et al.</i> [1987]
12	Bingemer	Southern, Atlantic	79	1983-03-30 1983-04-22	<i>Bingemer</i> [1984], <i>Bingemer and Ockelmann</i> [1987]
13	Bates	Pacific	267	1983-04-02 1983-05-01	<i>Bates and Quinn</i> [1997], <i>Bates et al.</i> [1987]
14	Bates	Pacific	123	1983-05-13 1983-05-22	<i>Bates et al.</i> [1987], <i>Bates and Cline</i> [1985], <i>Bates et al.</i> [1990]
15	Andreae	Bahamas	99	1983-11-06 1983-11-22	<i>Andreae</i> [1985]
16	Bates	Pacific	48	1984-02-15 1984-02-23	<i>Bates et al.</i> [1987], <i>Bates and Quinn</i> [1997], <i>Bates and Cline</i> [1985]
17	Bates	Pacific	7	1984-03-20 1984-03-22	<i>Bates et al.</i> [1987], <i>Bates and Quinn</i> [1997]
18	Bates	Pacific	53	1984-04-02 1984-04-28	<i>Bates et al.</i> [1987], <i>Bates and Quinn</i> [1997]
19	Andreae	Atlantic	97	1984-04-24 1984-05-11	<i>Andreae</i> [1985]
20	KettleD	English Channel	27	1984-06-18 1984-06-19	<i>Holligan et al.</i> [1987]
21	Bates	Pacific	62	1984-08-28 1984-09-27	<i>Bates and Cline</i> [1985], <i>Bates et al.</i> [1987], <i>Bates et al.</i> [1990]
22	Turner	English Channel	176	1985-01-06 1985-01-19	<i>Turner et al.</i> [1988], <i>Turner et al.</i> [1989]
23	Turner	Oosterschelde	64	1985-05-01 1985-05-03	unpublished
24	Bates	Pacific	116	1985-05-14 1985-06-09	<i>Bates et al.</i> [1987], <i>Bates et al.</i> [1990]
25	Bates	Pacific, Arctic	211	1985-06-29 1985-10-08	<i>Bates et al.</i> [1987], <i>Bates et al.</i> [1990]
26	Turner	around Britain	186	1985-07-10 1985-08-02	<i>Turner et al.</i> [1988]
27	Andreae	Mid-Atlantic Bight	224	1986-02-03 1986-02-15	<i>Iverson et al.</i> [1989], <i>Berresheim et al.</i> [1991]
28	Berresheim	Southern	141	1986-03-21 1986-04-26	<i>Berresheim et al.</i> [1989], <i>Berresheim</i> [1987]
29	Bates	Pacific	53	1986-04-22 1986-04-30	<i>Bates et al.</i> [1990]
30	Andreae	Mid-Atlantic Bight	114	1986-04-22 1986-05-02	<i>Iverson et al.</i> [1989], <i>Berresheim et al.</i> [1991]
31	Turner	southern North Sea	151	1986-05-01 1986-05-13	<i>Turner et al.</i> [1989], <i>Berresheim et al.</i> [1991]
32	Bates	Pacific	27	1986-06-11 1986-06-14	<i>Bates et al.</i> [1990]
33	Andreae	Mid-Atlantic Bight	153	1986-09-02 1986-09-13	<i>Iverson et al.</i> [1989], <i>Berresheim et al.</i> [1991]
34	KettleD	Baltic Sea	24	1987-03-28 1988-06-09	<i>Leck et al.</i> [1990]
35	KettleD	Indian	23	1987-04-01 1988-02-26	<i>Nguyen et al.</i> [1990]
36	Bingemer	Atlantic	98	1987-03-23 1987-04-17	<i>Burgermeister et al.</i> [1990]
37	Nguyen, Putaud, Mihalopoulos	Indian Ocean, Mediterranean	66	1986-04-03 1987-07-25	<i>Mihalopoulos</i> [1989], <i>Mihalopoulos et al.</i> [1992]

... Table S1: (continued) ...

38	Turner	northern North Sea	162	1987-04-23	1987-05-10	Turner et al. [1989]
39	KettleD	Antarctica	14	1987-05-12	1988-01-21	Gibson et al. [1988]
40	Bates	Pacific	55	1987-05-14	1987-05-21	Bates et al. [1990]
41	Turner	NE Atlantic	158	1987-06-09	1987-07-01	Turner et al. [1989]
42	Bates	Indian, Pacific	100	1987-06-16	1987-07-24	unpublished
43	KettleD	Baltic Sea	14	1987-09-01	1987-09-01	Leck et al. [1990]
44	KettleD	Pacific	21	1988-01-26	1988-03-10	Uchida et al. [1992]
45	KettleD	Indian	22	1989-02-15	1990-11-15	Nguyen et al. [1992]
46	Bates	Pacific	70	1988-04-08	1988-05-05	Quinn et al. [1990], Bates and Quinn [1997]
47	Turner	North Sea	55	1988-04-08	1988-04-23	unpublished
48	Leck	Baltic Sea	24	1988-07-12	1988-07-12	Leck and Rodhe [1991]
49	KettleD	Pacific	29	1988-07-08	1988-07-30	Watanabe et al. [1995]
50	Leck	Baltic Sea	35	1988-07-19	1988-07-20	Leck and Rodhe [1991]
51	Leck	North Sea	30	1988-07-26	1988-07-26	Leck and Rodhe [1991]
52	KettleD	Pacific	37	1988-08-05	1988-08-23	Watanabe et al. [1995]
53	Bingemer	Atlantic	60	1988-09-17	1988-10-05	Staubes and Georgii [1993], Staubes-Diederich [1992], Staubes and Georgii [1993]
54	McTaggart	Southern	44	1988-11-06	1989-01-24	McTaggart and Burton [1992]
55	Turner	North Sea	798	1989-01-29	1989-10-02	Turner et al. [1996a], Liss et al. [1993]
56	Bates	Pacific	108	1989-02-17	1989-04-20	Bates et al. [1992], Bates and Quinn [1997]
57	KettleD	Atlantic	83	1989-03-14	1989-04-03	Tanzer and Heumann [1992]
58	Matrai	Sargasso Sea	39	1989-04-22	1989-04-25	Matrai et al. [1996]
59	Bates	Pacific	62	1989-05-31	1989-06-09	unpublished
60	Staubes	Atlantic	102	1989-08-06	1989-09-01	Staubes-Diederich [1992], Staubes and Georgii [1993], Staubes and Georgii [1993]
61	Matrai	near New Jersey	9	1989-08-24	1989-09-03	Georgii [1993]
62	Matrai	New England	12	1989-08-21	1989-08-23	Matrai et al. [1993]
63	Helas, Schebeske, Andrae	Southern	62	1990-01-29	1990-03-06	Matrai et al. [1993]
64	Bates	Pacific	744	1990-02-20	1990-03-09	Bates et al. [1993], Bates and Quinn [1997]
65	Bates	Pacific	136	1990-04-09	1990-04-26	unpublished
66	KettleD	Mediterranean Sea	17	1991-05-16	1991-05-22	Belviso et al. [1993]
67	Matrai	Gulf of Maine	8	1990-07-08	1990-07-13	Matrai and Keller [1993]
68	Keller	Gulf of Maine	10	1990-07-08	1990-07-13	Matrai and Keller [1993]
69	Staubes	Greenland Sea	85	1990-07-12	1990-08-09	Staubes and Georgii [1993], Staubes and Georgii [1993], Staubes-Diederich [1992]
70	Keller	Gulf of Maine	27	1990-08-07	1991-10-07	unpublished
71	Staubes	Southern, Atlantic	210	1990-10-22	1990-12-22	Staubes and Georgii [1993], Staubes and Georgii [1993], Staubes-Diederich [1992]
72	Andrae	Atlantic	342	1991-02-12	1991-03-20	Andrae et al. [1994]
74	Bates	Pacific	616	1991-04-16	1991-05-01	Bates et al. [1994]

... Table S1: (continued) ...

75	Keller	Gulf of Maine	38	1991-04-23	1991-04-29	unpublished
76	Turner	Atlantic	152	1991-06-14	1991-06-27	Holligan <i>et al.</i> [1993]
77	Keller	Gulf of Maine	39	1991-07-06	1991-07-14	unpublished
78	Leck	Arctic	303	1991-08-04	1991-10-06	Leck and Persson [1996]
79	Nguyen, Putaud,	Atlantic	110	1991-09-18	1991-10-23	Putaud <i>et al.</i> [1993a], Putaud <i>et al.</i> [1993b]
80	Mihalopoulos	North Sea	27	1991-11-14	1993-06-11	Kwint and Kramer [1996]
81	Rapsomanikis	Southern	52	1991-12-11	1991-12-28	Kirst <i>et al.</i> [1993]
82	KettleD	Sargasso Sea	44	1992-01-29	1993-10-25	Siegel and Michaels [1996]
83	DiTullio	Ross Sea	30	1992-02-07	1992-02-26	DiTullio and Smith [1993], DiTullio and Smith [1995]
84	Bates	Pacific	952	1992-02-22	1992-03-20	Kieber <i>et al.</i> [1996], Yvon <i>et al.</i> [1996]
85	Kiene	Pacific	26	1992-02-24	1992-03-08	unpublished
86	Keller	Gulf of Maine	8	1992-04-02	1992-04-10	unpublished
87	Andreae	Atlantic	89	1993-04-16	1993-05-03	Pfannkuche <i>et al.</i> [1993]
88	Boniforti	Mediterranean Sea	78	1992-04-28	1994-10-05	Boniforti <i>et al.</i> [1993], unpublished
89	Nguyen, Putaud,	Atlantic	70	1992-06-02	1992-06-21	Putaud and Nguyen [1996]
90	Mihalopoulos	Atlantic	76	1992-06-12	1992-06-20	Blomquist <i>et al.</i> [1996]
91	KettleD	Gulf of Maine	2	1992-07-12	1992-07-14	unpublished
92	KettleD	Atlantic Ocean	26	1992-09-20	1992-10-19	Groene [1995], unpublished
93	Curran, Jones	Great Barrier Reef	12	1992-09-19	1992-09-21	unpublished
94	Curran, Jones	Tasman Sea	18	1992-09-22	1992-10-04	unpublished
95	Turner	Southern Ocean	125	1992-10-29	1992-11-28	Turner <i>et al.</i> [1995]
96	KettleD	Southern Ocean	39	1992-11-24	1992-11-28	Turner <i>et al.</i> [1995]
97	Turner	Southern Ocean	101	1993-02-10	1993-03-14	Chuck <i>et al.</i> [2005]
98	KettleD	East China Sea	50	1993-02-28	1994-08-15	Uzuka <i>et al.</i> [1996]
99	Bates	Pacific	1308	1993-03-21	1993-05-07	Bates and Quinn [1997]
100	Matrai	Barents Sea	18	1993-05-13	1993-05-29	Matrai and Vernet [1997]
101	KettleD	Jiaozhou Bay, China	34	1993-01-15	1994-09-15	Ha <i>et al.</i> [1997]
102	Simo	Mediterranean Sea	53	1993-06-01	1994-07-21	Simo <i>et al.</i> [1997], Simo <i>et al.</i> [1995]
103	Rapsomanikis	Aegean Sea	55	1993-07-04	1993-07-15	unpublished
104	Levasseur	Gulf of St. Lawrence	64	1993-08-03	1993-08-09	Cantin <i>et al.</i> [1996]
105	KettleD	New Zealand	37	1993-08-31	1993-11-13	Lee and deMora [1996]
106	KettleD	Gulf Mexico	38	1993-09-17	1994-12-14	Kiene [1996]
107	Yang	East China Sea	14	1993-10-15	1994-10-15	Yang <i>et al.</i> [1996]
108	Bingemer	Southern	215	1993-10-21	1994-03-21	unpublished
109	Turner	Pacific	9	1993-10-22	1993-10-28	Turner <i>et al.</i> [1996b]
110	Turner	Pacific	9	1993-11-09	1993-11-19	Hatton <i>et al.</i> [1998]
111	Yang	South China Sea	19	1993-11-15	1993-11-15	Yang <i>et al.</i> [1999]
112	Bates	Pacific	1172	1993-11-23	1994-01-06	Bates and Quinn [1997]

... Table S1: (continued) ...

113	Berresheim	Southern	15	1994-01-20	1994-02-22	Berresheim <i>et al.</i> [1998]
114	Andrae,	Atlantic	41	1994-04-08	1994-05-06	unpublished
115	Schebeske	Atlantic, Arctic, Pacific	43	1994-07-18	1994-08-15	Sharma <i>et al.</i> [1999]
116	Uher,	Atlantic	208	1994-09-08	1994-09-19	Uher <i>et al.</i> [1995]
	Rapso-					
	manikis,					
	Andrae					
117	Curran, Jones	Southern	56	1994-09-01	1994-10-18	Curran <i>et al.</i> [1998]
118	KettleD	Indian	19	1994-09-09	1994-09-11	Hatton <i>et al.</i> [1996], Hatton <i>et al.</i> [1999]
119	Amouroux,	Pacific	89	1994-09-08	1994-09-16	unpublished
	Andrae					
120	Curran, Jones	Southern	21	1994-12-20	1995-01-31	Curran <i>et al.</i> [1998]
121	KettleD	California coast	10	1995-04-19	1995-05-01	Ledyard and Dacey [1996]
122	Turner	Pacific	19	1995-05-25	1995-06-07	Turner <i>et al.</i> [1996b]
123	Keller	Gulf of Maine	3	1995-06-17	1995-06-21	unpublished
124	Uher,	Atlantic	393	1995-07-15	1995-07-28	Uher <i>et al.</i> [1997], Uher <i>et al.</i> [1996]
	Schebeske,					
	Rapso-					
	manikis,					
	Andrae					
125	Roberts,	Black Sea	9	1995-07-26	1995-07-31	Amouroux <i>et al.</i> [2002]
	Amouroux,					
	Andrae					
126	Andrae,	Atlantic	49	1995-08-02	1995-08-12	unpublished
	Schebeske					
128	Bates	Pacific,Southern	1206	1995-10-21	1995-12-12	Bates and Quinn [1997], Bates <i>et al.</i> [1998]
129	Curran, Jones	Southern	28	1995-11-18	1995-12-05	Curran <i>et al.</i> [1998]
130	Bates	Pacific	1068	1996-03-15	1996-04-12	Bates and Quinn [1997]
131	Leck	Arctic	33	1996-07-15	1996-08-06	unpublished
132	DiTullio	Ross Sea	85	1996-12-16	1997-01-06	unpublished
133	Levasseur	Labrador Sea	37	1997-05-13	1997-06-09	unpublished
134	Kiene	Gulf of Mexico	13	1997-09-23	1997-10-01	unpublished
135	Belviso	Atlantic	909	1996-10-09	1996-11-05	Belviso <i>et al.</i> [2000]
136	Sciare	Indian	463	1997-12-03	1997-12-19	Sciare <i>et al.</i> [1999]
137	Sciare	Indian	157	1998-08-19	1998-08-30	unpublished
138	Bates	Atlantic	806	1997-06-20	1997-07-23	Bates and Quinn [1997]
139	Bates	Atlantic	666	1999-01-15	1999-02-08	Bates <i>et al.</i> [2001]
140	Bates	Indian	441	1999-02-11	1999-03-29	unpublished
141	Bates	Pacific, Sea of Japan	1535	2001-03-16	2001-04-19	unpublished

... Table S1: (continued) ...

142	Johnson	Bering Sea - Gulf of Alaska	879	2002-05-06	2002-05-31	unpublished	
143	Johnson	Bering Sea - Gulf of Alaska	577	2002-06-07	2002-06-22	unpublished	
144	Johnson	US West Coast	571	2002-11-07	2002-11-22	unpublished	
145	Johnson	Gulf of Alaska - Bering Sea	2128	2003-01-31	2003-03-31	unpublished	
146	Johnson	Gulf of Alaska - Bering Sea	2257	2003-04-30	2003-06-24	unpublished	
147	Johnson	Gulf of Alaska	1949	2003-06-27	2003-08-13	unpublished	
148	Johnson	Eastern Equatorial Pacific	1057	2003-10-27	2003-11-20	Huebert et al. [2004]	
149	Belviso	North Atlantic, Mediterranean Sea	552	1999-09-07	1999-09-23	Belviso et al. [2003]	
150	Wong	Northeast Pacific	20	1996-02-22	1996-08-31	Wong et al. [2006], Wong et al. [2005]	
151	Wong	Northeast Pacific	17	1997-02-13	1997-09-12	Wong et al. [2006], Wong et al. [2005]	
152	Wong	Northeast Pacific	17	1998-02-20	1998-09-04	Wong et al. [2006], Wong et al. [2005]	
153	Wong	Northeast Pacific	8	1999-02-10	1999-06-22	Wong et al. [2006], Wong et al. [2005]	
154	Wong	Northeast Pacific	11	2000-06-01	2000-09-15	Wong et al. [2006], Wong et al. [2005]	
155	Wong	Northeast Pacific	8	2001-06-18	2001-06-25	Wong et al. [2006], Wong et al. [2005]	
156	Kiene, Kieber	Southern Ocean	58	2003-10-31	2007-11-09	Kiene et al. [2007]	
157	Kiene, Kieber	Southern Ocean	45	2004-12-19	2004-12-27	Kiene et al. [2007]	
158	Kiene, Kieber	Southern Ocean	39	2005-10-26	2005-11-07	Kiene et al. [2007]	
159	Malin, Liss, Bell	Atlantic Ocean	132	1997-09-17	1997-10-16	Bell et al. [2006]	
160	Malin, Liss, Bell	Atlantic Ocean	107	1999-09-19	1999-10-12	Bell et al. [2006]	
161	Malin, Liss, Bell	Atlantic Ocean	57	2003-05-16	2003-06-12	Bell et al. [2006]	
162	Malin, Liss, Bell	Atlantic Ocean	26	2003-10-02	2003-10-11	Bell et al. [2006]	
163	Malin, Liss, Bell	Atlantic Ocean	66	2004-05-03	2004-05-26	Bell et al. [2006]	
164	Johnson	Gulf of Maine	1379	2004-07-09	2004-08-12	unpublished	
165	Johnson	Gulf of Mexico	431	2006-08-23	2006-09-11	unpublished	
166	Johnson	Eastern Equatorial Pacific	572	2006-10-14	2006-10-26	unpublished	
168	Baker	Northeast Atlantic	204	1997-05-12	1997-05-29	Baker et al. [2000]	
169	Saltzman	Equatorial, North Pacific Ocean	214	2004-05-23	2004-07-01	Marandino et al. [2007]	
170	Saltzman	Southeastern Pacific Ocean	82	2006-01-11	2006-01-24	Marandino et al. [2009]	

... Table S1: (continued) ...

171	Kiene, Kieber	Southern Ocean	21	2004-12-23	2005-01-19	<i>del Valle et al. [2009a]</i> , <i>del Valle et al. [2007]</i> , <i>del Valle et al. [2009b]</i>
172	Kiene, Kieber	Southern Ocean	11	2005-11-08	2005-11-29	<i>del Valle et al. [2009a]</i> , <i>del Valle et al. [2007]</i> , <i>del Valle et al. [2009b]</i>
173	Johnson	Atlantic Ocean	105	2007-10-09	2007-10-12	unpublished
174	Johnson	Eastern Tropical Pacific	1070	2007-10-16	2007-11-11	unpublished
175	Johnson	North Atlantic Ocean	1579	2008-03-21	2008-04-24	unpublished
176	Turner	East Atlantic Ocean	403	1996-06-08	1996-07-02	<i>Locarnini et al. [1998]</i>
177	Turner	East Atlantic Ocean	210	1998-06-10	1998-07-05	<i>Jickells et al. [2008]</i>
178	Turner	Southern Ocean, Atlantic Sector	39	2000-11-03	2000-11-06	<i>Turner et al. [2004]</i>
179	Lee, de Mora, Marsden, Gratton	North Water Polynya, Baffin Bay	98	1998-04-12	1998-06-24	<i>Bouillon et al. [2002]</i>
180	Lee, DiTullio, Bruland	Bering Sea	80	2003-08-12	2003-09-05	unpublished
181	Lee, DiTullio, Hutchins, Leblanc, Wilhelm	North Atlantic Ocean	76	2005-06-06	2005-07-03	unpublished
182	Lee, DiTullio, Dunbar, Smith	Ross Sea	188	2005-12-24	2006-01-23	unpublished
183	Lee, DiTullio, Dunbar, Smith	Ross Sea	110	2006-11-11	2006-12-06	unpublished
184	Lee, DiTullio	New Zealand Sector, Southern Ocean	212	2006-11-03	2006-12-11	unpublished
185	Lee, DiTullio	South Atlantic Ocean	57	2007-11-18	2007-12-11	unpublished
186	Simo	Mediterranean Sea	37	2003-01-13	2004-06-28	<i>Valina and Simo [2007]</i> , <i>Vila-Costa et al. [2008]</i>
187	Simo	Mediterranean Sea	11	2008-03-11	2008-09-17	unpublished
188	Simo	Arctic	17	2007-07-01	2007-07-22	<i>Gali and Simo [2010]</i>
189	Smythe-Wright	Mascarene Plateau, Indian Ocean	57	2002-06-18	2002-07-09	<i>Smythe-Wright et al. [2005]</i>
190	Simo	Mediterranean Sea	6	2007-09-18	2007-09-25	unpublished
191	Deal	Bering Sea	6	2001-08-29	2001-08-31	<i>Deal et al. [2005]</i>
192	Scarratt	NW Atlantic	139	2003-04-25	2003-05-15	<i>Merzouk et al. [2008]</i> , <i>Lizotte et al. [2008]</i>
193	Scarratt	NW Atlantic	110	2003-10-13	2003-10-30	unpublished
194	Scarratt	NW Atlantic	255	1999-09-11	1999-09-30	<i>Scarratt et al. [2007]</i>
195	Franklin, Martin	Mauritanian upwelling, Atlantic Ocean	59	2006-07-13	2006-08-02	unpublished
196	Archer	Southern Ocean	2984	2008-03-03	2008-04-07	unpublished
197	Kasamatsu	Southern Ocean (Indian sector)	19	2005-01-03	2005-01-20	unpublished

... Table S1: (continued) ...

198	Kasamatsu	Southern Ocean (Indian sector)	72	2006-01-06	2006-01-26	unpublished	
199	Watanabe, Kasamatsu	Okhotsk Sea	27	2000-06-13	2000-06-28	unpublished	
200	Kasamatsu, Odate, Watanabe	Southern Ocean (Indian sector)	10	2004-01-31	2004-02-10	unpublished	
201	Kasamatsu	Western North Pacific	60	2001-06-07	2001-07-07	unpublished	
202	Kasamatsu	Southern Ocean	7	2003-01-28	2003-03-06	<i>Kasamatsu et al.</i> [2004], <i>Kasamatsu et al.</i> [2005], <i>Preunkert et al.</i> [2007]	
203	Kasamatsu	Central Southern Pacific, Southern Ocean	46	2001-12-08	2002-01-17	<i>Kasamatsu et al.</i> [2004], <i>Kasamatsu et al.</i> [2005], <i>Preunkert et al.</i> [2007]	
204	Kasamatsu	Southern Ocean (Indian sector)	53	2007-12-27	2008-01-10	unpublished	
205	Kasamatsu	Southern Ocean	33	2003-01-24	2003-02-05	<i>Kasamatsu et al.</i> [2004], <i>Kasamatsu et al.</i> [2005], <i>Preunkert et al.</i> [2007]	
206	Kasamatsu	Southern Ocean	28	2002-02-13	2002-02-28	<i>Kasamatsu et al.</i> [2004], <i>Kasamatsu et al.</i> [2005], <i>Preunkert et al.</i> [2007]	
208	Kasamatsu	Southern Ocean (Indian sector)	23	2008-02-05	2008-02-22	unpublished	
209	Kiene	NW Atlantic	14	2002-04-06	2002-04-19	<i>Harada et al.</i> [2004]	
210	Simo	E Mediterranean, Black Sea	13	2000-10-06	2000-10-28	<i>Besiktepe et al.</i> [2004]	
211	Matrai	Arctic Ocean	55	2001-07-11	2001-08-17	<i>Matrai et al.</i> [2007], <i>Matrai et al.</i> [2008]	
212	Matrai, Ver-net	Balsfjord, Norway	10	1999-03-26	1999-05-18	unpublished	
213	Matrai	Sargasso Sea	42	2004-07-15	2004-08-01	<i>Bailey et al.</i> [2008], <i>Gabric et al.</i> [2008]	
214	Belviso	Northeast Atlantic Ocean	78	2001-02-03	2001-02-23	<i>Belviso et al.</i> [2004a], <i>Belviso et al.</i> [2004b]	
215	Belviso	Northeast Atlantic Ocean	80	2001-03-24	2001-04-12	<i>Belviso et al.</i> [2004a], <i>Belviso et al.</i> [2004b]	
216	Belviso	Northeast Atlantic Ocean	74	2001-08-26	2001-09-13	<i>Belviso et al.</i> [2004a], <i>Belviso et al.</i> [2004b]	
217	Belviso	Indian Sector of the Austral Ocean	26	2005-01-18	2005-02-12	<i>Bopp et al.</i> [2008], <i>Belviso et al.</i> [2008]	
218	Shenoy	Northern Arabian Sea	15	1998-01-04	1998-01-20	<i>Shenoy and Kumar</i> [2007]	
219	Shenoy	Central Indian Ocean	22	1998-02-22	1998-03-28	<i>Shenoy et al.</i> [2002]	
220	Shenoy	Arabian Sea (coastal)	33	1998-07-20	1998-08-14	<i>Shenoy and Kumar</i> [2007]	
221	Shenoy	Bay of Bengal	15	1998-10-30	1998-11-05	<i>Shenoy et al.</i> [2000]	
222	Shenoy	Arabian Sea	19	1998-12-01	1998-12-10	<i>Shenoy and Kumar</i> [2007]	
223	Shenoy	Central Indian Ocean	51	1999-01-27	1999-03-10	<i>Shenoy et al.</i> [2002]	
224	Shenoy	Bay of Bengal	32	1999-07-27	1999-08-05	<i>Shenoy and Kumar</i> [2007]	
225	Shenoy	Bay of Bengal	55	1999-08-11	1999-08-31	<i>Shenoy and Kumar</i> [2007]	
226	Shenoy	Arabian Sea (coastal)	21	1999-09-10	1999-10-10	<i>Shenoy and Kumar</i> [2007]	
227	Shenoy	Southern Bay of Bengal	42	2000-01-29	2000-02-19	<i>Shenoy and Kumar</i> [2007]	

... Table S1: (continued) ...

228	Shenoy	Arabian Sea	17	2000-11-06	2000-11-14	Shenoy and Kumar [2007]
229	Shenoy	Bay of Bengal	18	2001-07-10	2001-08-01	Shenoy et al. [2006]
230	Dacey	Bermuda Atlantic	126	1992-01-29	1992-11-24	Dacey et al. [1998]
231	Dacey	Bermuda Atlantic	276	1993-01-15	1993-11-11	Dacey et al. [1998]
232	Dacey	Bermuda Atlantic	71	1994-01-18	1994-11-15	Dacey et al. [1998]
233	Saltzman	North Atlantic Ocean	215	2007-07-17	2007-07-24	Marandino et al. [2008]
234	Lee, DiTullio, Balch	South Atlantic Ocean	125	2008-12-05	2008-12-31	unpublished
235	Bange	Mauritanian coast	43	2008-02-05	2008-02-19	unpublished
236	Simo	Antarctica	53	2009-01-28	2009-02-25	unpublished
237	Borges, Sciare	European Estuaries	16	1998-05-25	1998-05-29	Sciare et al. [2002]
238	Borges, Sciare	European Estuaries	9	1996-12-09	1996-12-11	Sciare et al. [2002]
239	Borges, Sciare	European Estuaries	14	1996-07-08	1996-07-11	Sciare et al. [2002]
240	Borges, Sciare	European Estuaries	7	1997-06-13	1997-06-15	Sciare et al. [2002]
241	Borges, Sciare	European Estuaries	13	1997-09-01	1997-09-04	Sciare et al. [2002]
242	Matrai, Dacey, DiT- ullio, Kieber, Kiene, Simo	Western Antarctic Peninsula	188	2005-11-17	2006-02-27	unpublished
243	Johnson	Eastern Eq. Pacific	1661	2008-10-20	2008-11-22	unpublished

Chapter II

Re-examination of global emerging patterns of ocean DMS concentration.

☒ bXXXXXXXX

During the last decade the number of seawater dimethylsulfide (DMS) concentration measurements has increased substantially. The importance this gas, emitted from the ocean to the atmosphere, may have in the cloud microphysics and hence in the Earth albedo and radiation budget, makes it necessary to accurately reproduce the global distribution. Recently, the monthly global DMS climatology has been updated taking advantage of the three-fold increased size and better resolved distribution of the observations available in the DMS database. Here, the emerging patterns found with the previous versions of the database and climatology are explored with the updated versions. The statistical relationships between the seasonalities of DMS concentrations and other variables are re-examined. The positive correlation previously found between surface seawater DMS and the daily-averaged climatological solar radiation dose in the upper mixed layer of the open ocean is confirmed with both the updated DMS database and climatology. Re-examination of the latitudinal match-mismatch between the seasonalities of DMS and phytoplankton, represented by the chlorophyll *a* concentration, reveals that they are highly positively correlated in latitudes higher than 40°, but anti-correlated in the 20°-40° latitudinal bands of both hemispheres. Overall, these global emerging patterns provide key information to further understanding the factors that control the emission of volatile sulfur from the ocean. The large uncertainties associated with the methodologies used in global computations, however, call for caution in using these emerging patterns as predictive tools, and prompt to the design of time series and process-oriented studies aimed at testing the validity of the observed relationships.



The emission of dimethylsulfide (DMS) from the ocean is the main natural source of volatile sulfur entering the atmosphere [Bates et al. 1992, Simó 2001]. Once in the air, DMS oxidation products contribute to the number of small-size atmospheric particles that are necessary for cloud formation [Andreae and Crutzen 1997]. These particles influence cloud microphysics and albedo over the oceans and hence have a potential to regulate the radiation budget of the Earth [Charlson et al. 1987]. The important role of DMS emissions on the radiation budget makes it necessary to accurately represent the global distribution of seawater DMS.

The DMS data coverage of the ocean is not enough to derive a reliable global distribution by direct interpolation/extrapolation of the very measurements. To be able to construct a climatology from the existing data, some kind of mapping criteria and objective analysis techniques have to be applied, and the resulting spatio-temporal distribution will carry an uncertainty inversely proportional to the number and coverage of the original data. During the last years several alternative methods for obtaining realistic global DMS fields have been proposed. Some of these are based on algorithms that derive surface DMS concentrations from other variables [Anderson et al. 2001, Aumont et al. 2002, Simó and Dachs 2002, or Belviso et al. 2004], while some other are totally or partially based on numerical models [Six 2006, Bopp et al. 2008, Elliott 2009, Vogt et al. 2010]. Both methods carry some uncertainties, which are mainly associated with the difficulties in the validation of the outputs, due to absence of an objective and well-covered global DMS distribution.

The DMS climatology that has been widely used hitherto was constructed a decade ago by Kettle et al. [Kettle et al. 1999, Kettle and Andreae 2000] after compiling the worldwide archived

measurements of DMS concentrations in the surface ocean, i.e., at depths shallower than 10 m. The number of data available for that climatology was approximately 17,000, and were the origin of what would become the Global Surface Seawater (GSS) DMS database. Since then, the scientific community has worked hard to enlarge the database: during the last decade the number of DMS measurements has increased threefold. Following this increase, a joint initiative of the SOLAS Project Integration, COST Action 735 and EUR-OCEANS was launched to produce an updated DMS climatology [Lana et al. 2011], which is now available and posted for open access at the SOLAS Project Integration webpage (www.bodc.ac.uk/solas_integration/).

There are notable differences between the updated (hereafter L10) and the former (K00) DMS climatologies in some regions of the ocean. The aim of this work is to re-examine in L10 some of the global emerging patterns that arose in K00 and past versions of the database and have been instrumental for better understanding the processes that regulate DMS production in the surface ocean and its emission to the atmosphere.

Methods

The seawater DMS concentration measurements used were those archived in the GSS DMS database (saga.pmel.noaa.gov/dms/) plus some additional measurements from the South Pacific [Lana et al. 2011]. This database is constructed from data contributions by individual scientists and maintained at the NOAA-PMEL. In February 2011, the DMS measurements amounted 48,164 and had been collected between March 1972 and June 2010. The data submitted after the year 2000 (hereafter postK00), i.e., not used in the construction of the K00 climatology, were also analyzed in this study (24,951 DMS measurements). The updated DMS climatology (named L10) was built using the database as for April 2010 (47,313 data). Data analysis and interpolation schemes, where our current knowledge of ocean biogeochemistry and DMS variability was applied, allowed us to construct monthly gridded maps of global sea surface DMS concentrations. The objective analysis procedures, detailed in Lana et al. [2011], were essentially the same as those employed by Kettle et al. for DMS [Kettle et al. 1999, Kettle and Andreae 2000] and those used for other variables (temperature, salinity, oxygen and nutrients) in the latest version of the World Ocean Atlas [Locarnini et al. 2010] and previous editions (WOA94, WOA98, WOA01, WOA05). In brief, the first step consists of monthly gridding the historical observations into 1°x1° (latitude x longitude) square means. Then, grid points were grouped

according to biogeographic provinces [Longhurst 1998], DMS concentrations were monthly averaged within each province, and gradients were smoothed at province borders. The resulting global monthly maps are called the first-guess fields. These are corrected at each grid point by the difference between the observed and the first-guess value, and also by the distance-weighted mean of all the grid points with observed data that lie within the area defined by a previously fixed influence radius. For comparative purposes, global monthly maps of surface DMS were also constructed using the algorithms of Simó and Dachs [2002], hereafter SD02, which parameterize the DMS concentration from the ratio of the chlorophyll *a* concentration (Chl_a) and the mixed layer depth (MLD). We recomputed SD02 using a SeaWiFS Chl_a climatology for the years 1997-2009, and the MLD climatology re-calculated from de Boyer Montégut et al. [2004] as in Vallina and Simó [2007a].

In all computations, DMS and Chl_a data were constrained within the 99.95 percentile. This way we wanted to avoid very high DMS and Chl_a values associated with very localized hotspots or potentially created by sampling and handling artifacts, which might have a disproportionate weight in global distributions. This imposed an upper limit of 220 nM for the GSS DMS data, 148 nM for the postK00 data, 34 nM for the L10 climatology, 95 nM for the K00 climatology, and 59 nM for the SD02 parameterization output. The upper limit for Chl_a was 10 mg m⁻³.

To re-examine the proposed proportionality found between DMS and the solar radiation dose (SRD) over most of the global surface ocean [Vallina and Simó 2007a, hereafter VS07], and assess the influence that the increased number of data has had on it, we computed the daily-averaged solar radiation in the upper mixed layer as in VS07, i.e., by: (a) calculating the solar irradiance at the top of the atmosphere [Brock 1981], (b) converting it into ocean-surface irradiance by a reduction by a half [Kiehl and Trenberth 1997], and (c) calculating the mean solar radiation in the mixed layer using a constant underwater light extinction coefficient (0.06 m⁻¹) and the aforementioned climatology of the MLD. Monthly DMS concentrations and SRD were averaged by boxes of either 10° x 20° (latitude x longitude), as in the original study by VS07. Monthly box DMS data were then paired with monthly box SRD data for regression and correlation analyses. We imposed an upper limit of 10 nM for the 10° latitude – 20° longitude box DMS averages (95 percentile) to avoid ephemeral patches of high DMS levels associated with eutrophic coastal systems and constrain the analysis into the large majority of the open ocean, also to compare to the original study.

An alternative calculation of the SRD was also done, with the incorporation of the following computations: (a) the conversion of the solar irradiance at the top of the atmosphere into ocean-surface irradiance was done taking into account the variable influence of clouds on reducing surface irradiance. To this aim, a cloud albedo climatology for the period 2001-2009 was obtained from CERES (Cloud and Earth's Radiant Energy System). At each $1^\circ \times 1^\circ$ pixel, the daily irradiance at surface was computed as: $EDAY_{surf} = (EDAY_{toa} * (1 - ALB_{toa})) * 0.72$. Where $EDAY_{toa}$ is the shortwave irradiance at the top of the atmosphere, ALB_{toa} is the cloud albedo at the top of atmosphere, and 0.72 is the average sunlight transmittance of a clear-sky atmosphere. (b) The mean solar radiation in the mixed layer depth was calculated using the computed $EDAY_{surf}$ and a climatology of the estimated underwater light extinction coefficient (at 490 nm) provided as an ocean colour product by the SeaWiFS Project.

Global maps of seasonal correlations were created with the following procedure [Vallina et al. 2007]: using a running window of $7^\circ \times 7^\circ$, we obtained for each position ($1^\circ \times 1^\circ$ pixel) of the global ocean a time series of 12 points (months) for paired of the two variable's data to compare. Each of the 12 points of the time series is the average of the 49 values taken by the pixel-centred running window in a given month. Then, for every $1^\circ \times 1^\circ$ grid box of the global ocean we calculate the seasonal Spearman correlation coefficient (ρ) between the two variables (12 degrees of freedom), generating a global map of seasonal correlations. Correlations were significant at 95% confidence level for $|\rho| > 0.5$.

To re-examine the extent of the connection between the DMS concentration and sea surface microbiota [Vallina et al. 2006], we used L10 and the monthly SeaWiFS Chla climatology derived from 1997-2009 data, and evaluate the global map of seasonal correlation. Regression and correlation analyses were also performed with monthly DMS and chlorophyll a concentration data averaged by boxes of $10^\circ \times 20^\circ$ (latitude x longitude).

RXXXXXX DXXXXXX

GbDMS XXXXX

Five representations of the global distribution of surface seawater DMS concentrations are compared by means of Hovmöller, latitude vs month diagrams (Figure 1). The subplots correspond to the GSS DMS data distribution (Figure 1a), with their associated gaps, the postK00 data (Figure 1b), with a higher number of gaps due to the reduced number of data, the two representations of the L10 and K00 climatologies (Figures 1c and 1d), and the distribution produced with the global SD02 parameterization (Figure 1e), with winter gaps at high latitudes reflecting lack of satellite Chl_a concentrations. The GSS data (total and after 2000), the two climatologies and the parameterization all show increased DMS concentrations at mid and high latitudes during the hemispheric summer months. In most cases, the maximum annual values for all 10° latitudinal bands are ≤ 15 nM.

As reported and discussed in Lana et al. [2011], the almost three fold increase in the number of data between K00 and L10 resulted in some remarkable differences in the climatologies despite the large similarity in the general pattern. K00 predicted much higher DMS concentrations than L10 in the high latitudes ($\geq 65^\circ$) in both hemisphere summers, whereas the situation is reversed in the 40°-60° bands. In the tropical/subtropical latitudinal bands (10°-40°), L10 predicts smoother seasonal patterns where K00 depicts larger differences between summer and winter. This is particularly so in 10°-40°S, and may be due to data inclusion in regions (South Indian Ocean and the Pacific Warm Pool) that were severely undersampled ten years ago. Most of the months of the year have data in that particular band in the updated database, due to the data submitted after the creation of the K00 climatology (see Figure 1b). Relatively high values can be observed in that latitudinal band for the GSS updated data (Figure 1a) and the postK00 data distribution (Figure 1b).

Interestingly, the SD02 parameterization, whose algorithms were derived from the same data as K00, predicts seasonal patterns more similar to L10 than to K00 in the lower latitudes. These regions are a large part of the ca. 80% of the global ocean where the algorithm used to calculate the DMS concentration depends only on the MLD [Simó and Dachs 2002]. This further supports the suggested fundamental role the MLD plays in controlling monthly surface DMS concentrations,

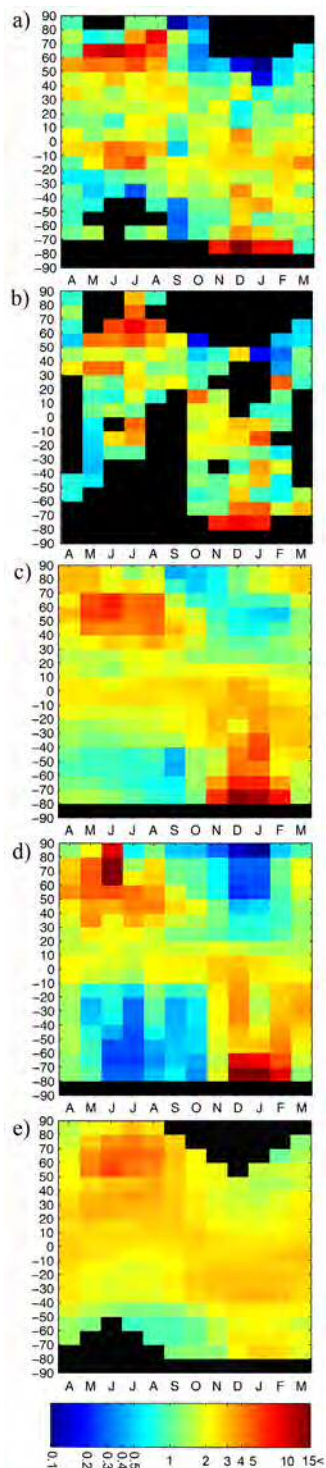


Figure 1. Monthly averages by 10° latitude bands of (a) Surface DMS seawater concentrations (GSS DMS database), (b) Surface DMS seawater concentrations from the GSS DMS database after the year 2000, (c) updated DMS climatology L10 (Lana et al. 2011), (d) DMS climatology K00 (Kettle and Andreae 2000), and (e) DMS distribution using SD02 algorithm (Simó and Dachs 2002).

through its effects either on plankton dynamics or on the solar radiation entering the mixed layer, or both [Simó and Pedrós-Alió 1999, Vallina and Simó 2007a]. In general, though, SD02 generates global monthly distributions that are more homogeneous than any of the climatologies, and fails at capturing the high summer DMS concentrations south of 60° S. As pointed out by Halloran et al. [2010], empirical parameterizations that are based on the knowledge of DMS production, such as SD02, should be appropriate to simulate present distributions of global DMS. However, they should be used with care as predictive tools in Earth-System models.

DMS vs SRD

To re-assess the global relationship between DMS and SRD reported by Vallina and Simó [2007a], we followed the same approach. We grouped the DMS data of either the GSS database, the postK00 data or the L10 climatology into boxes of 10° latitude x 20° longitude, and the same grouping was also applied to the SRD data. Box averages were calculated for each month, and the DMS averages were further grouped according to SRD bins of 15 W m⁻². Binned DMS means and standard deviations (accounting for approximately the 66% of the data set) are plotted against the corresponding SRD bins in Figures 2a, 2b and 2c, which correspond to the GSS DMS database, GSS DMS data measured after the year 2000, and L10, respectively. Analyzed this way, climatological SRD accounted for 96% of the variance of monthly regional surface DMS concentration in the GSS database, 91% for the postK00 data and 98% in L10. This confirms and even reinforces the findings of VS07. As in the previous study, standard deviations are quite large but the upper and lower contours of the scatter still show clear proportionality between DMS and the SRD.

As shown in Figure 3, the use of an alternative calculation to obtain the SRD produces changes in the statistical relationship between DMS and SRD. This alternative approach to the computation of the SRD includes the cloud albedo in the calculation of surface irradiance from the top-of-atmosphere insolation, and a satellite-derived parameterization of the underwater light extinction coefficient - see Methods. The L10 climatology and the alternative SRD were grouped into 10° x 20° boxes, and the DMS was averaged according to 20 W m⁻² SRD intervals. The regression coefficient is notably reduced, to a value of 0.76. Not only the metrics show a worse coupling, also the shape of the curve indicates linearity is notably lost and there seems not to be proportionality of DMS to SRD at intermediate SRD values (Figure 3). This poses some question mark on the otherwise linear relationship observed with either calculated climatological

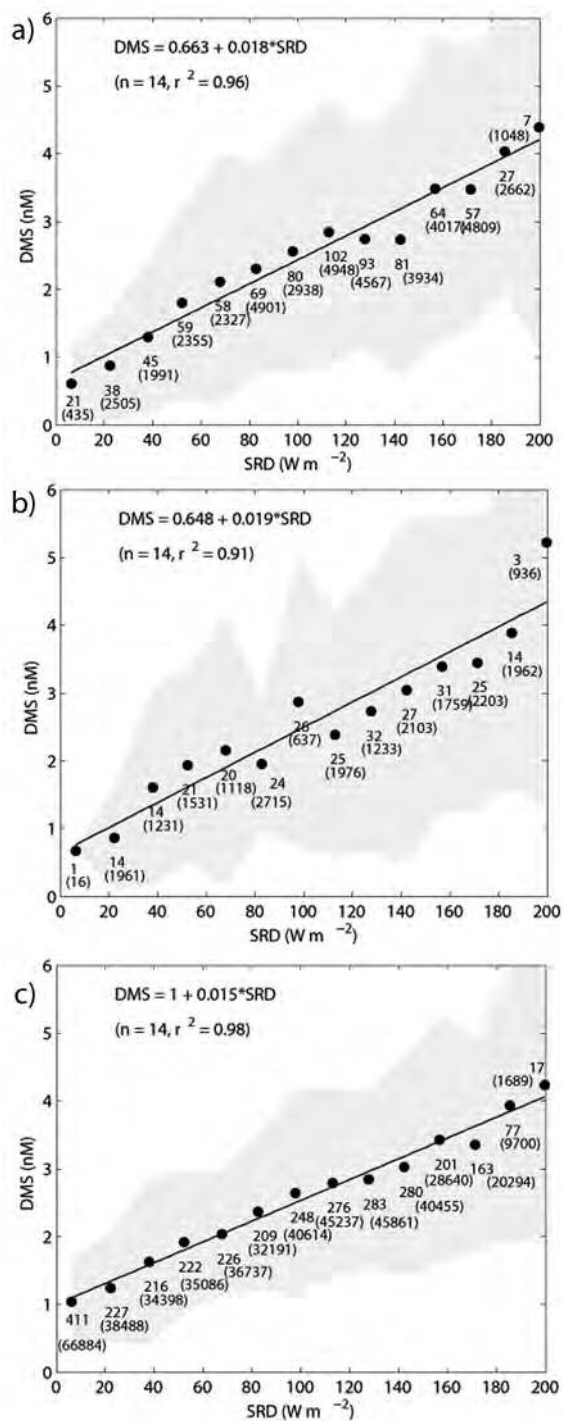


Figure 2. Linear regression against the Solar Radiation Dose (SRD) of the seawater DMS concentrations averages of 10° latitude by 20° longitude boxes, binned by SRD intervals of $15 W m^{-2}$; DMS data are obtained from: (a) updated GSS database; (b) data after the year 2000 from GSS database; (c) DMS climatology L10. The shaded area represents the standard deviations (accounting for approximately the 66% of the data set).

SRD with fixed atmospheric and underwater attenuation values, or with in situ DMS and SRD at two subtropical sampling sites [Vallina and Simó 2007a]. The objective of calculating SRD with inclusion of the cloud albedo was to account for regions of persistent cloudiness where the 50% atmospheric reduction of irradiance falls short (e.g., the Pacific intertropical convergence zone). It has to be noted, however, that the cloud albedo used is nothing but a climatology, and that for the most of the marine atmosphere cloudiness is very variable. The subsequent calculation of the atmospheric reduction is an approximate parameterization, and the same applies to the underwater light attenuation based on satellite measurements. Pretending these computations will show a more realistic relationship against non-contemporaneous DMS concentrations is almost as risky as the simple approach previously used.

The use of binned correlations between box averages is justified by the fact that the DMS data correspond to a combination of 40 years of measurements, and the SRD data are obtained with a climatological calculation. That is, DMS and SRD data are not contemporaneous and therefore they are not expected to be closely linked over a $1^\circ \times 1^\circ$ grid. With the aim at exploring to what extent climatological DMS concentration responds in proportionality to climatological SRD in the upper mixed layer, we apply a binning to reduce (smooth out) small scale variability and extract first order processes from the noisy data obtained with different spatial and temporal resolution. VS07 chose a binning interval of 15 W m^{-2} , which roughly is the range of SRD variation from month to month at mid latitudes. However, Derevianko et al. [2009] have noted that the use of box grouping and binning largely reduce the total variance in the data and result in exaggeratedly high coefficients of determination.

The window (or box) size we first used here is the same as that in VS07 because we wanted to compare the results. We further changed the size to evaluate its effect on the regression between SRD and DMS. We repeated the analysis with boxes of $7^\circ \times 7^\circ$, $5^\circ \times 5^\circ$ and $1^\circ \times 1^\circ$, always with a SRD binning interval of 15 W m^{-2} . The results show very similar regression coefficients. For the L10 climatology there is almost no variation in the regression coefficients for different windows. The GSS database had a regression coefficient reduced to 0.86 when the windows were $7^\circ \times 7^\circ$, but recovered (0.95) with $5^\circ \times 5^\circ$ windows. The DMS values obtained after the year 2000 showed more variable correlation coefficients against the SRD with changes in the window size: 0.82 for windows of $7^\circ \times 7^\circ$, 0.87 for $5^\circ \times 5^\circ$ and 0.96 for $1^\circ \times 1^\circ$. According to these results and those of Derevianko et al. [2009], the binning interval seems to have higher influence than the box averaged sizes in the correlation coefficients between DMS and SRD.

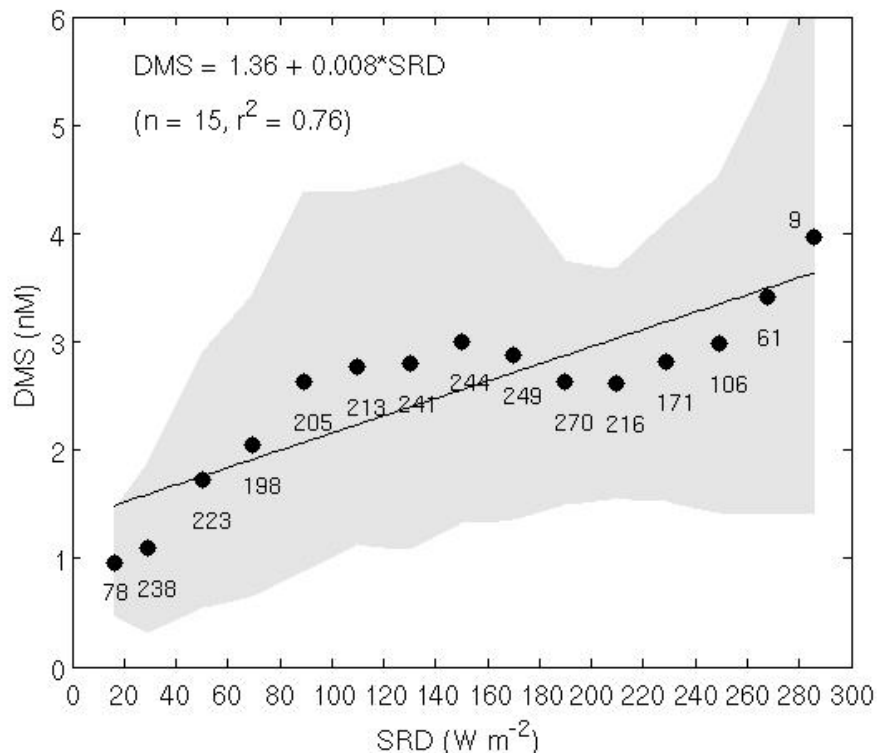


Figure 3. Linear regression against the alternative calculation of Solar Radiation Dose (SRD) of the seawater DMS concentrations values obtained from L10 climatology, averages of 10° latitude by 20° longitude boxes, binned by SRD intervals of 20 W m⁻².

It can be argued that even a smaller window, or a narrow-range binning does not provide a realistic assessment of the co-variation between variables, and that direct correlation of gridded data or boxes would be more appropriate. VS07 reported a Spearman's rank correlation coefficient of 0.47 for the monthly 10° x 20° boxes of the GSS database DMS and the SRD (n = 545). Using the latest version of the database, this coefficient becomes 0.45 (n = 806). After noting that the DMS concentrations do not follow a normal distribution, Lana et al. [2011] computed the correlation between the 1° x 1° gridded, log transformed climatological DMS and SRD data, and obtained a Pearson's correlation coefficient of 0.58 (n = 452,269). All these statistics, which are significant with a probability > 99.99%, suggest a certain degree of proportionality between DMS and SRD on a global scale.

For the sake of a further comparison between DMS and the alternative SRD, a global correlation map (Figure 4) was calculated using the updated DMS climatology, L10. The Spearman's correlation map shows that there is a strong seasonal coupling between both variables all over the global ocean. The seasonal coupling is broken in the equatorial area. We still do not have a sound explanation for the equatorial exception, but it has to be noted that seasonality is very weak around the equator. Negative or low correlation values may be produced by the low seasonality, since any uncertainty in the distribution of DMS may easily have a larger amplitude than the seasonal pattern.

Mechanisms behind the emerging pattern of proportionality between DMS and SRD, yet not fully resolved, are related to photobiological effects on DMS producers and consumers, and photophysical effects on the hydrodynamics of the upper ocean, and have been discussed elsewhere [Simó 2004, Toole and Siegel 2004, Vallina and Simó 2007a, 2007b, Vila-Costa et al. 2008]. A recent study by Galí et al. [2011] has shown that the exposure to solar radiation, UV included, increases gross DMS production, confirming sunlight as an important modulator of DMS. However, we have also shown that the relationship between climatological SRD and DMS data is influenced by the calculation of the SRD and the use of different DMS climatologies. Miles et al. [2009] used exclusively in situ data of irradiance and attenuation coefficient to calculate in situ SRD and compared them with DMS measurements in the Atlantic Ocean (they showed that, although DMS and light were significantly correlated, the correlation value was increased if they replace the in situ by climatological data for the calculation of SRD). Further studies should address this issue based solely on contemporaneous in situ measurements throughout seasons; only this way we will be able to evaluate the potential response of DMS production and emission to solar radiation, which is a required component of the hypothesized negative feedback that would link ocean biosphere and climate through atmospheric sulfur [Charlson et al. 1987].

DMS v Chl

Global $1^\circ \times 1^\circ$ maps of correlations between monthly DMS (K00 and L10) and Chl_a climatology concentrations are shown in Figure 5a and 5b. Seeing DMS as a biogenic trace gas, some degree of proportionality of its concentration to that of Chl_a (a commonly used measure of phytoplankton biomass) has often been sought, with success only at the regional scale but not at the global scale [Kettle et al. 1999; Lana et al. 2011]. Figures 5a and 5b show that, globally, a match-mismatch between the seasonalities of the two variables occurs largely depending on latitude: north of 40° N and south of 40° S, DMS shows a strong positive correlation to Chl_a, whereas in the 10° - 40° latitudinal bands of both hemispheres the relationship reverses into anti-correlation. This latitudinal distribution of correlations obtained with K00 (Figure 5a), and already reported by Vallina et al. 2006, occurs also with L10 (Figure 5b). It is remarkable how abrupt the transition is between positive and negative correlations at around 40° in both hemispheres. This is coincident with the upper latitudinal boundaries of the major subtropical ocean gyres.

The coincidence of the annual maxima of DMS concentrations with minima of phytoplankton biomass in subtropical and low temperate regions, where the stratification season is long and primary production is essentially limited by nutrient availability, has been called the 'summer DMS paradox' [Simó and Pedrós-Alió 1999], and has been attributed to a combination of plankton community succession and the effects of sunlight on plankton [Dacey et al. 1998, Simó and Pedrós-Alió 1999, Stefels 2000, Sunda et al. 2002, Simó 2004, Toole and Siegel 2004]. This feature is difficult to reproduce with numerical models [Le Clainche et al. 2010]. The production of the microalgal metabolite dimethylsulfoniopropionate (DMSP) seems to have much to tell about this paradox. DMSP is the main biogenic precursor of DMS in the ocean. One of the intracellular functions of DMSP in algal cells is as photoprotector. At some specific areas DMSP concentrations correlate with photo-protective pigments, instead of with chlorophyll *a* concentration [Bell et al., 2010]. Hence the correlation between chlorophyll *a* and DMSP is broken for those areas, and so is expected to be for DMS too. It has to be noted, though, that an important time lag between the annual maxima of DMSP and DMS has been reported in the subtropical waters of the Sargasso Sea [Dacey et al. 1998] and the Mediterranean [Vila-Costa et al. 2008]. The key to the understanding of the 'summer DMS paradox' is not to be found only in the understanding of the association of DMSP to phytoplankton ecotypes. Further studies of the multiple paths and players involved in determining the efficiency of the DMSP-to-DMS conversion at the community level are needed.

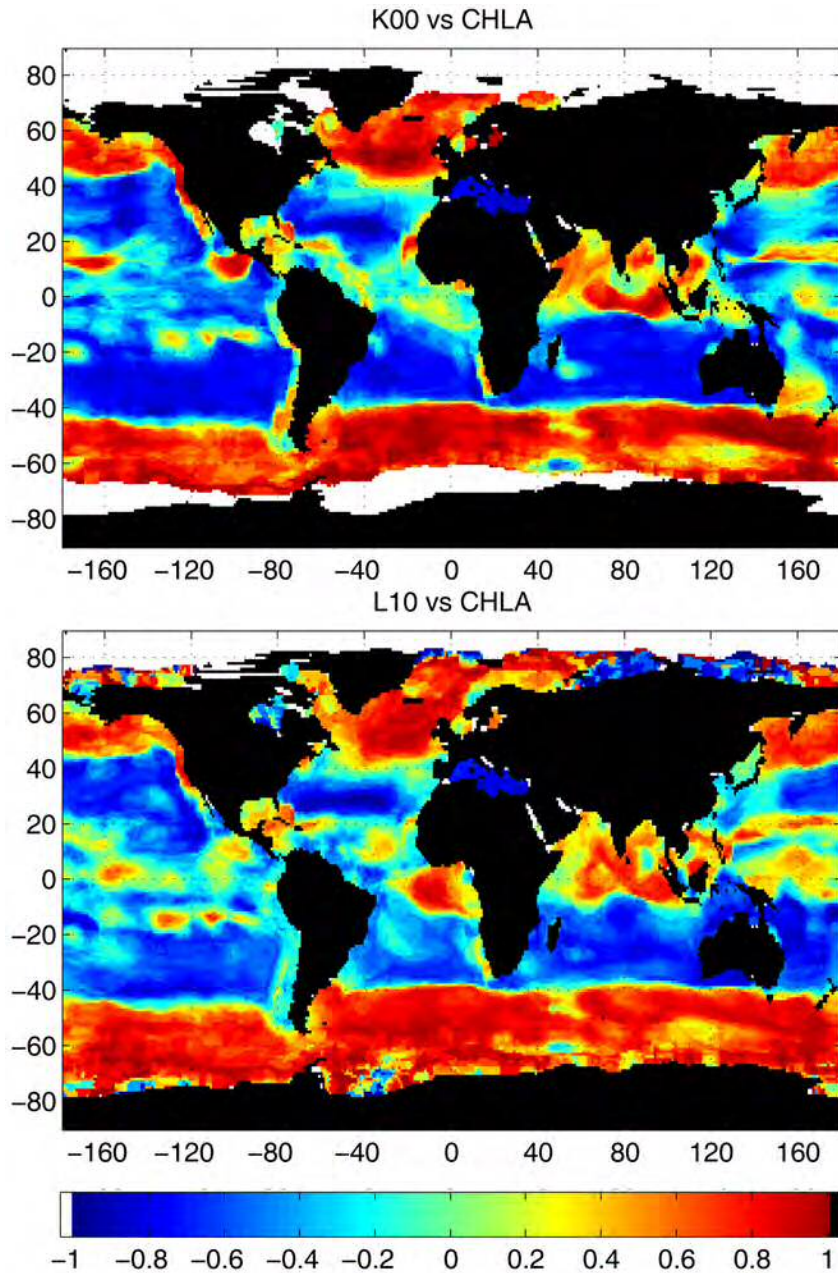


Figure 5. Global distribution of Spearman's rank coefficients of correlation between monthly series of Chla concentrations (SeaWiFS climatology of the years 1997-2009) and (a) DMS (climatology K00) and (b) DMS (updated climatology L10).

At high latitudes, conversely, where the stratification season is shorter and primary production is limited or co-limited by light, both phytoplankton and DMS peak in summer [Vallina et al. 2006, Kiene et al. 2007].

Differences between L10 and K00 with respect to their respective correlations to Chla occur in the equatorial Indian Ocean and in the eastern equatorial Atlantic. These areas, where there is less correlation with the K00 climatology (Figure 5a), confirming the results found with a different Chla climatology [Vallina et al., 2006], show a strong positive coupling with L10 (Figure 5b). In the equatorial and northern Indian Ocean, both phytoplankton biomass and DMS increase in phase in June through September at the pace dictated by the monsoons. In the northwest sector, this is due to the southwest monsoon wind [Dasgupta et al. 2009]; in the equatorial sector, high Chla levels come associated with the heavy precipitations of the monsoons, which transport silt and nutrients from land to sea through the rivers [Dasgupta et al. 2009]. In the eastern equatorial Atlantic off the coasts of Africa, DMS also appears to peak in the period from June to September, yet this seasonal pattern is largely uncertain due to a severe lack of data [Lana et al. 2011]. Water discharges by the Congo River, added to the direction of the South Equatorial Current, seem to be the causes of higher Chla levels in the same period [Dasgupta et al. 2009].

The same regression analysis used with L10 and the SRD was applied to the Chla climatology. Both L10 DMS and Chla data were averaged by $10^\circ \times 20^\circ$ boxes, and the box DMS means were plotted against box Chla concentration means binned into 0.1 mg m^{-3} intervals (Figure 6). An upper limit of 2 mg m^{-3} was imposed onto the box Chla means to exclude the coastal and local phytoplankton blooms that carry extremely high values. The regression coefficient is low ($r^2=0.47$, $n=20$) in agreement with the results of the distribution of the correlation between the two variables.

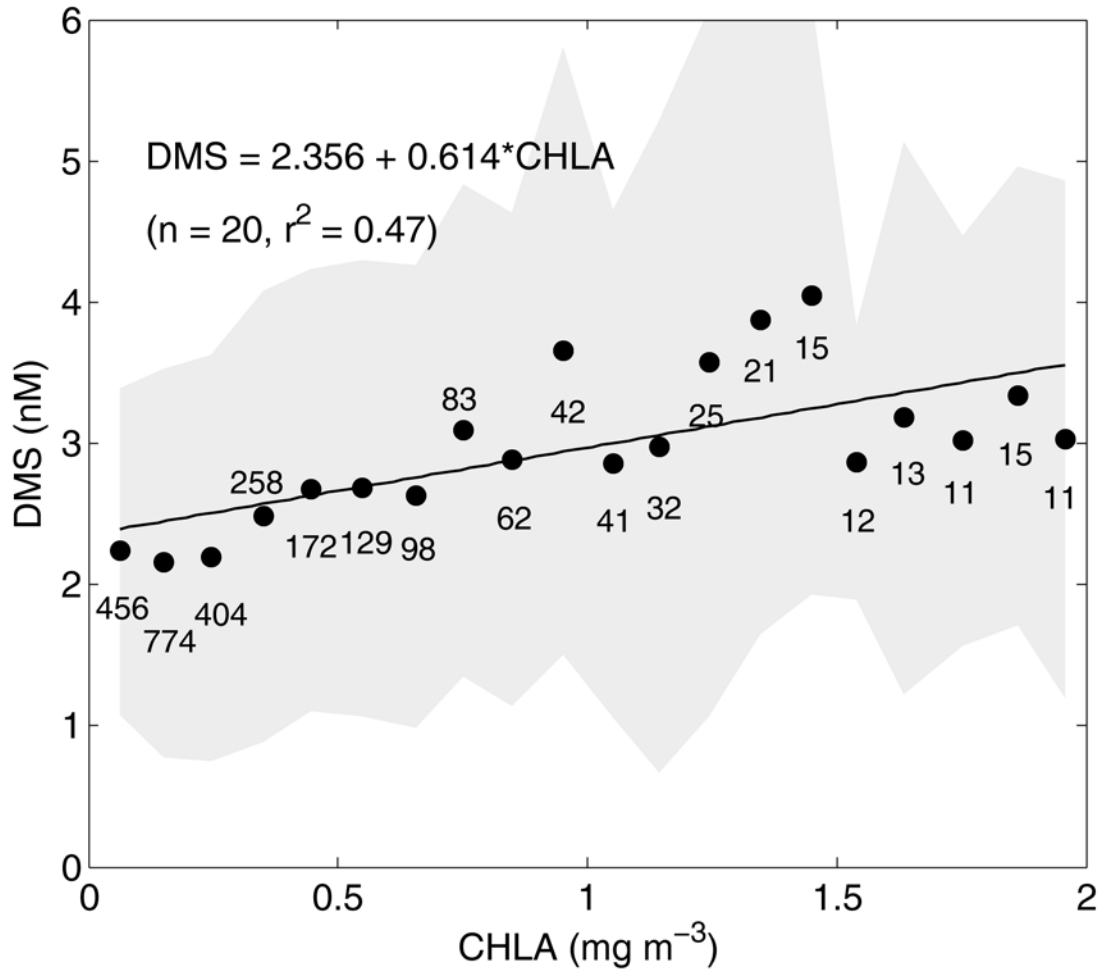


Figure 6. Linear regression of DMS concentrations (L10 climatology) averaged by 10° latitude x 20° longitude boxes against Chla concentrations binned in 0.1 mg m⁻³.



With the use of an increased number of DMS measurements and an updated global monthly climatology we have confirmed the salient features of the global monthly emerging patterns found in previous studies: (a) There is a general seasonal trend towards higher DMS concentrations in each hemispheric summer; (b) this seasonal pattern largely coincides with that of the daily solar radiation dose in the upper mixed layer of the ocean; (c) a proportionality between DMS and Chla only occurs north of 40° N and south of 40° S, while both variables are anti-correlated in most of the 40° N-40° S latitudinal band. These emerging patterns could be illustrative of some of the factors that control the ocean's source of volatile sulfur for the Earth system. Due to the large uncertainties associated with the computation of global variables, the reported relationships have to be taken with caution and as indicative of where further studies should be aimed to. In situ time series studies should be conducted to test these global emerging patterns, and the complexity of the interplay between physical, chemical, and biological processes that drive global DMS distributions should be investigated in process-oriented studies.

Acknowledgements. The authors want to thank each of the individual contributors that generously submitted their DMS data to the Global Surface Seawater Dimethylsulfide Database, and to J.E. Johnson and T.S. Bates for the maintenance of the database. We thank M. Galí and the two reviewers for their helpful comments. We thank the Ocean Biology Processing Group at GSFC for the production and distribution of the monthly chlorophyll a data. This work was supported by the Spanish Ministry of Science and Innovation through the projects MIMOSA, PRISMA and Malaspina 2010, and through a PhD studentship to A.L.

Chapter III

Natural and anthropogenic drivers of the seasonality of marine aerosol-cloud interactions.



A. Lana, R. Simó, E. Jurado and J. Dachs.

☒ b☒☒☒☒☒☒

Low marine clouds (LMC), which cover 40% of the oceans, act as powerful climate coolers because their ability to reflect sunlight (*albedo*) exceeds their ability to retain heat from below. The regional *albedo* of LMC increases with cloud amount and the zenith angle of sunlight, and inversely to cloud droplet size, which is related to the presence of small aerosols. We use nine years of global weekly satellite records to show that, over the unpolluted mid- and high-latitude ocean, LMC amounts increase as droplet size decreases from winter to summer, thus compensating for the lowering of the zenith angle and providing large negative radiative forcing. Disruption of this natural seasonality might cause a reduction of annual cloud-mediated cooling in the oceanic atmosphere regions heavily impacted by anthropogenic aerosols.



The timing of climatic seasons on Earth is set by well known orbital features, but their amplitude is internally modulated by positive and negative feedbacks in the radiation budget. Positive feedbacks (those that enhance seasonal transitions and amplitude) include heat retention by atmospheric water vapor [Wu et al. 2008], and snow and ice reflection [Hall and Qu 2006] and vegetation absorption [Liu et al. 2006] of solar radiation. Ocean's heat uptake, transport and release provide negative feedback that attenuates seasonal amplitude [Marshall and Plumb 2008]. Other potentially important seasonal feedbacks, either positive or negative, may result from clouds and their radiative behavior. Clouds are powerful climate players that both reflect shortwave radiation (SWR) from above to cause surface cooling and absorb longwave radiation (LWR) from below to cause surface warming [Harrison et al. 1990; Kim and Ramanathan 2008].

Clouds cover over 60% of the planet [Rossow and Schiffer 1999] and provide a negative net radiative forcing (cooling of the Earth-atmosphere system) of nearly -20 W m^{-2} [Harrison et al. 1990]. Among cloud types, low marine clouds (LMC, those occurring at the top of the marine boundary layer and composed of liquid droplets, Rossow and Schiffer 1999) are of major climate concern because they reduce insolation in the 40% of the highly absorbing dark ocean they overcast [Sassen and Wang 2008]. Main contributors to LMC are stratiform clouds, which are far more efficient at reflecting SWR than at absorbing LWR. Actually, LMC account for a dominant share of cloud negative forcing over the subtropical oceans [Klein and Hartmann 1993]. Despite their importance in the Earth radiative budget, LMC simulations represent one of the largest sources of uncertainty in model projections of global warming [Forster et al. 2007].

The seasonality of the abundance of LMC is principally governed by air column stability [Klein and Hartmann 1993], but their brightness or *albedo* is largely influenced by the presence of

aerosols. Small hygroscopic aerosols facilitate cloud droplet formation at atmospheric conditions that otherwise would be thermodynamically unfavorable for homogeneous water condensation [Andreae and Rosenfeld 2008]. Theory and observations concur to postulate that, given a fixed or low varying amount of liquid water, the more of these cloud condensation nuclei (CCN) occur, the more cloud droplets are formed and the smaller they are [Andreae and Rosenfeld 2008, Lohmann and Feichter 2005, Twomey 1991]. This is climatically relevant, because a cloud with more (fewer) and smaller (bigger) cloud droplets is a brighter (more transparent) cloud or, in other words, has a higher (lower) *albedo* [Twomey 1991]. Moreover, by being smaller, cloud droplets take longer to reach precipitable sizes; hence, a cloud formed on more CCN lives longer [Albrecht 1989] and its *albedo* is sustained longer. This is particularly important in air masses with low aerosol loads, like those over the oceans and far from continents, where CCN are scarce and cloud formation, brightness and duration are largely affected by variations in aerosol numbers.

Here we use nine years of global weekly satellite records to investigate the potential seasonal influence of natural and anthropogenic, marine and continental aerosols on cloud microphysics and albedo.

DATA METHODOLOGY

Marine clouds, cloud condensation nuclei and indirect effect (IE). The cloud optical and microphysical parameters, as well as derived statistics, were obtained from the Moderate resolution Imaging Spectroradiometer (MODIS) aboard the Terra Earth Observing System platform [Tanré et al., 1997, Platnick et al., 2003; Remer et al., 2005]. The data are from the Level 3 MODIS Terra Collection 5, available from the Atmosphere Archive Distribution System at the NASA Goddard Space Flight Center (ladsweb.nascom.nasa.gov/data/search.html). We used global weekly and monthly data of liquid cloud droplet effective radius (r_e , ratio of third to second moment of the cloud drop size distribution, important for radiative transfer, in μm) and liquid cloud fraction (A_c), with a $1^\circ \times 1^\circ$ latitude-longitude spatial resolution for the period 01 Jan 2001 – 31 Dec 2009 (9 years).

Column-integrated numbers of satellite-derived cloud condensation nuclei (N_{CCNs} , particles cm^{-2}) were also obtained from MODIS-Terra Collection 5. This variable is derived from aerosol

optical depths (AOD), the fraction of the AOD that corresponds to submicron aerosol (η), and the aerosol effective radius [Tanré et al., 1999; Gassó and Hegg, 2003]. N_{CCNs} represents the maximum columnar number of particles in the accumulation mode and provides an upper end estimate of the concentration of particles that may act as CCN at $\sim 0.2\%$ supersaturation.

The effect of aerosols on cloud microphysics was quantified using IE, the indirect effect index [Feingold et al. 2003], defined as:

$$IE = -\delta \log r_e / \delta \log N_{CCNs}$$

which was computed regionally as the slope of the linear regression between weekly $\log r_e$ and $\log N_{CCNs}$ values throughout the 2001-2009 period ($n = 414$). At each $1^\circ \times 1^\circ$ latitude-longitude grid pixel, IE was calculated with the logs of the means of r_e and N_{CCNs} within a $7^\circ \times 7^\circ$ box centered at the targeted position. According to theory [Twomey 1991], r_e is related to the number of cloud droplets (N_d) by:

$$r_e \sim (N_d)^{1/3}$$

and aircraft observations [Chuang et al. 2000] indicate that cloud droplets relate to the subset of aerosols with the appropriate size to act as CCN, namely the number of accumulation mode particles N_{ap} , by:

$$N_d \sim (N_{ap})^{(0.48 \pm 0.06)}$$

Therefore,

$$\log r_e \sim (0.16 \pm 0.02) \log N_{ap}$$

Derivation of N_{CCNs} by MODIS is based on the identification of CCN by size only [Remer et al. 2005, Gassó and Hegg 2003], with no clue to aerosol chemical composition or hygroscopicity. Therefore, N_{CCNs} is actually N_{ap} , the number of accumulation mode particles that may potentially act as CCN, and not the real number of CCN.

Marine aerosol characteristics, wind speed and continental aerosol source points. AOD (a measure of sunlight attenuation by the column of aerosols) was taken as an indication of total aerosol amount over the ocean. The standard deviation of the mean AOD (σ_{AOD}) within each $1^\circ \times 1^\circ$ latitude-longitude grid box was indicative of the existence of spatial gradients. The fine mode fraction (η) was used as an indication of aerosol size distribution. Ranging from 0 to 1, η is defined as the ratio of the AOD contributed by the small mode particles (or accumulation mode) to the total AOD ($\text{AOD}_{\text{small}}/\text{AOD}_{\text{total}}$) and can thus be viewed as a measure of the percentage of fine particles that contribute to the total aerosol burden. Wind speed values at 10 m over the surface (u_{10}), obtained from the National Center for Environmental Prediction (NCEP) / National Center for Atmospheric Research (NCAR) Reanalysis model, were used to identify the particles ejected to the atmosphere from the surface ocean as sea spray. Fire counts were taken from the World Fire Atlas of the European Space Agency (<http://dup.esrin.esa.it/!ionia/wfa/>). The Atlas is constructed with data obtained with the instrument Along Track Scanning Radiometer (ATSR), which localized the hot spots with night time data exceeding 308 K. The localizations of urban and industrial centers were taken from the MODIS-based International Geosphere-Biosphere Programme (IGBP) land cover classification data at the Land Processes Distributed Active Archive Center (US Geological Survey; <https://lpdaac.usgs.gov>). All these variables were used in a monthly resolution for 2001-2009, and interpolated (when needed) into $1^\circ \times 1^\circ$ latitudinal-longitudinal spatial resolution.

Dominant aerosol types over the oceans. In order to attribute marine aerosols to their dominant emission sources, we used satellite measurements of the optical characteristics of aerosols and modeled/assimilated analyses of atmosphere and land-associated variables. Source apportioning was conducted following the sequential threshold methodology of ref. [Jurado et al. 2008], see Table 1. We considered 6 aerosol types with alternate dominance over the oceans: mineral dust (DU), biomass burning aerosol (BB), urban, suburban and industrial aerosol (IN), sea-salt particles (SS), continentally influenced air masses in the distant marine atmosphere (BKc) and biogenic background marine aerosol (BKm). Note that ‘dominance’ is the key word here: several aerosol types co-exist at a given location and time; our method allows for attribution of the aerosol source or type that confers the optical properties observed from satellite. Thus, for instance, by attributing the aerosols of an air parcel over the Arabian Sea to DU we do not mean that those

Dominant aerosol	AOD	σ_{AOD}	η [0-1]	u_{10} (m s ⁻¹)	Other conditions
BB	≥ 0.1		≥ 0.6		Proximity to fire points.
IN	0.1-0.7		≥ 0.6		Proximity urban centers, not BB.
DU	≥ 0.3		< 0.6		Not BB, not IN.
SS			< 0.5	≥ 6	Distance from coast, not IN, not BB, not DU.
BKc		≥ 0.025			Not DU, not IN, not BB, not SS.
BKm					Not DU, not IN, not BB, not SS, not BKc.

Table 1. Criteria used for source apportioning of satellite derived aerosols. AOD: aerosol optical depth; σ_{AOD} : standard deviation of AOD; η : proportion of small aerosol; u_{10} : wind speed at 10 m height; BB: biomass burning aerosol; IN: urban, suburban and industrial aerosol; DU: mineral dust aerosol; SS: sea-salt aerosol; BKc: continentally-influenced remote marine aerosol; BKm: biogenic background marine aerosol.

aerosols are composed of dust only, but that the overall aerosol has the optical characteristics and source proximity of dust. We therefore refer to it as ‘dominated by dust’ yet we recognize it is most probably contributed also by sea salt, biogenic and anthropogenic aerosols.

Aerosol total abundance, size and proximity to potential source points were the main criteria used to distinguish among dominant types. To define these criteria (thresholds) we made use of average values reported in the literature for typical air-masses studied from satellite and ground stations, and by modeling (e.g., Husar et al., 1997; Tegen et al., 1997; Kaufman et al., 2001; Kaufman et al., 2002; Smirnov et al., 2002; Brasseur et al., 2003; Kinne et al., 2003; Cavalli et al., 2004; Kaufman et al., 2005). In first instance, large AOD values (≥ 0.1) accompanied by small size ($\eta \geq 0.6$) and connectivity to fire points were attributed to dominance of biomass burning particles (BB). If connected to urban and industrial centers, they were assigned to urban and industrial dominated aerosols (IN). Very large AOD (≥ 0.3) and large size ($\eta < 0.6$) were considered dust-dominated aerosol (DU). Large sized aerosols ($\eta < 0.5$) that did not meet the former criterion, occurred under high wind speeds ($\geq 6 \text{ m s}^{-1}$) and were not connected to coastland, were considered dominated by sea salt (SS). Among the remaining aerosols (at low AOD), those exhibiting large

$\sigma_{\text{AOD}} (\geq 0.025)$ were assigned a dominance of continental background aerosol. Finally, aerosols that did not meet any of the former criteria were considered dominated by the marine biogenic background aerosol.

Application of the sequential threshold method to monthly aerosol data from MODIS for the period 2001-2009 allowed constructing global monthly maps of the types/sources of oceanic aerosols.

A mask of the continental and anthropogenic influences on marine aerosols. In order to define the regions of the oceanic atmosphere that are heavily influenced by aerosols of continental origin (either natural or anthropogenic), we arbitrarily selected those $1^\circ \times 1^\circ$ latitude-longitude pixels where aerosol was dominated by either BB, IN, DU or BKc during 4 or more months a year, or in 36 months over the 9 years studied (see light grey areas in figure 2 of the main manuscript). Those regions with the same proportion of months dominated by BB or IN were considered the most heavily impacted by anthropogenic aerosols.

Solar radiation, cloud albedo and cloud shortwave radiative forcing. Climatological, daily-averaged solar irradiance at the top of atmosphere (S_{TOA} , W m^{-2}) was calculated according to Brock et al. [1981], and re-computed into weekly and monthly data on a $1^\circ \times 1^\circ$ latitude-longitude resolution grid. Cloud *albedo* was computed from total and clear sky albedos provided by Clouds and Earth's Radiant Energy System (CERES). The CERES instruments provide radiometric measurements that include both solar-reflected and Earth-emitted radiation from the top of the atmosphere to the Earth's surface. We used Level 3 daily data, with a $1^\circ \times 1^\circ$ latitude-longitude spatial resolution. Daily values were transformed into weekly and monthly means.

Cloud albedo (α_c) was calculated by subtracting the TOA clear-sky *albedo* (α_{clr}) from the TOA all-sky *albedo* (α):

$$\alpha_c = \alpha - \alpha_{\text{clr}}$$

Cloud shortwave radiative forcing (CRF_{sw} , W m^{-2}) was computed as the product of the TOA irradiance (S_{TOA}) and cloud albedo (α_c):

$$\text{CRF}_{\text{sw}} = S_{\text{TOA}} \times \alpha_c$$

Global maps of temporal correlations. Temporal co-variations between paired variables (namely N_{CCNs} and r_e , A_c and r_e , r_e and S_{TOA}) were explored by the running-window correlation method [Vallina et al. 2007]. For each month and each $1^\circ \times 1^\circ$ position, we substituted the value of the targeted variable for the average of the 49 values of a $7^\circ \times 7^\circ$ window located around the position. Then we constructed the weekly (8-day) series of the variable over the 2001-2009 period (9 years, 414 weeks) for each $1^\circ \times 1^\circ$ position. With these 414 data for each variable for each $1^\circ \times 1^\circ$ pixel we computed the Spearman's rank correlation (ρ) between paired variables, obtaining a global map of correlation coefficients. Correlations were significant at 95% confidence level when $|\rho| > 0.1$.

XXXXXXXXXX XXXXXXXXXXXXX

Studies of the global spread of the inverse proportionality between cloud droplet size and aerosol numbers that is observed at the local scale are feasible only with satellite data. We compared weekly global distributions of CCN numbers (N_{CCNs}) and cloud droplet effective radii (r_e) provided by the Moderate resolution Imaging Spectroradiometer (MODIS) for the period 2001 to 2009, and observed that they are anti-correlated over time in much of the oceanic atmosphere, particularly at mid and high latitudes (Figures 1a). This realization is consistent with previous works that attempted the same comparison simultaneously over time and space [Nakajima et al. 2001, Breón et al. 2002], and is a remarkable finding because MODIS derives N_{CCNs} as the number of small aerosols throughout the atmospheric column and not within the cloud layer [Remer et al. 2005]. We then calculated the indirect effect (IE, Feingold et al. 2003), obtaining values ranged between 0.12 and 0.17 (see Figure 2), with a global average of 0.14. Our observed IE are hence consistent with what is known and predicted about aerosol effects on droplet size. The global mean IE falls well within the expected range, and so do IE in midlatitude clean atmospheres (Figures 2, and 1d and 1e). Lower values (0.12-0.13) occur in polar regions where r_e is known to be particularly small [Bréon et al. 2002] and in regions where heavy loads of small

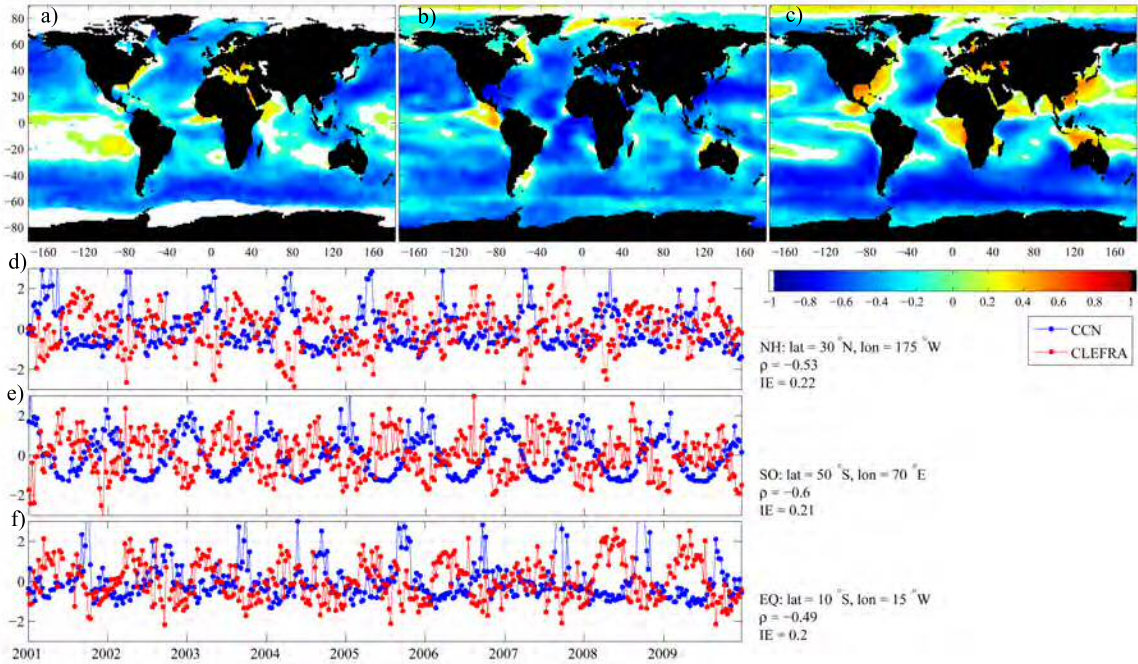


Figure 1. Seasonal aerosol-cloud coupling. **Top:** Global maps of Spearman’s rank correlation coefficients (ρ) between weekly data over the 2001-2009 period of (a) satellite-derived cloud droplet size r_e and number of accumulation mode particles N_{CCNs} , (b) satellite-derived liquid cloud fraction A_{cl} and r_e , and (c) r_e and the daily-averaged insolation S_{TOA} . Correlations are significant with a probability of 95% at $|\rho| > 1$ ($n = 414$). **Bottom (d,e,f):** Series of mean-normalized weekly data of r_e and N_{CCNs} at the three $7^\circ \times 7^\circ$ latitude-longitude windows indicated on map a. Central coordinates, ρ and indirect effect ($IE = -\delta \log r_e / \delta \log N_{CCNs}$) values are given next to each series.

continental aerosols may saturate the condensation effect [Rosenfeld 2000] or aerosol and cloud layers do not necessarily coincide in the vertical profile [Constantino and Bréon 2010].

Comparison of r_e with LMC abundance (liquid cloud fraction, A_{cl}) over time shows that, over the very most of the oceans, the more abundant LMC are, the smaller their droplets (Figure 1b). That is, the two variables that govern the contribution of LMC to planetary albedo vary, on a seasonal basis, in such a concert that they potentiate each other’s radiative effect. If we take daily-averaged insolation at the top of the atmosphere (S_{TOA}) as the marker of the pace of seasonality at every location on Earth, we observe that cloud droplets tend to be smaller in summer and

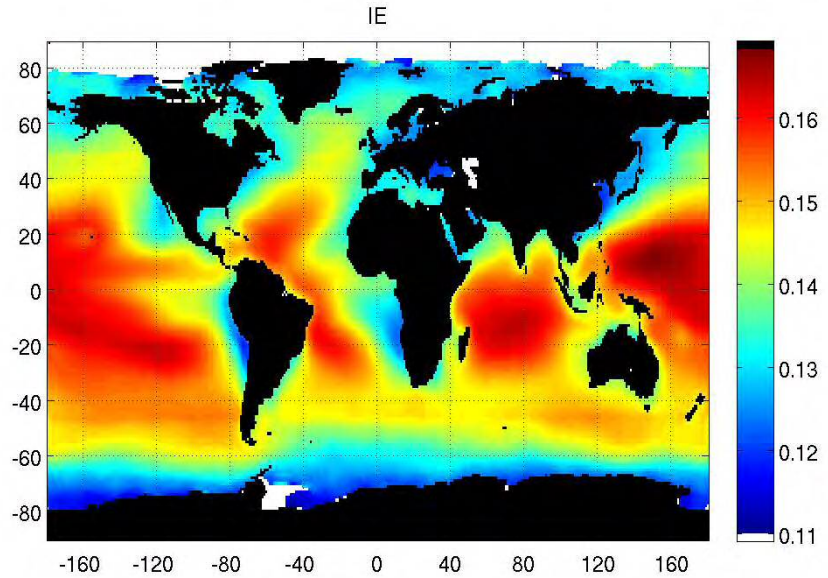


Figure 2. Global ocean distribution of IE calculated from weekly cloud droplet radius (r_e) and cloud condensation nuclei number (N_{CCNs}) values, in $7^\circ \times 7^\circ$ running windows, throughout the 2001-2009 period.

bigger in winter, as shown by the widespread anti-correlation between r_e and S_{TOA} (Figure 1c). This general seasonality of r_e breaks or even reverses in some particular regions of the oceans (yellow to red areas in Figure 1c) adjacent to known continental aerosol sources [Kaufman et al. 2002]. Surprisingly, however, not all major continental sources seem to produce the same effect, as revealed by the lack of effect of the typically thick dust plume over the tropical north Atlantic. It has been profusely documented that total aerosol mass is not the appropriate indicator of aerosol-cloud interaction because the ability of aerosols to act as CCN depends mainly on their size, but also on chemical composition and hygroscopicity [Andreae and Rosenfeld 2008, Twohy et al. 2008, Jones et al. 2009]. All these aerosol properties vary with source and transformation undertaken during transport. Unfortunately, satellites provide clues to size distribution but no surrogates of chemical composition and hygroscopicity [Kaufman et al. 2002]. Besides, aerosols of diverse nature and origin always coexist in the atmosphere, and source apportioning of marine aerosols using remote sensing is therefore a difficult task.

We used satellite measurements of optical parameters of aerosols and their proximity to localized sources to derive dominant aerosol types at any point and time over the oceans [Jurado et al. 2008]. The sequential threshold method (Table 1, description in Data and Methodology section)

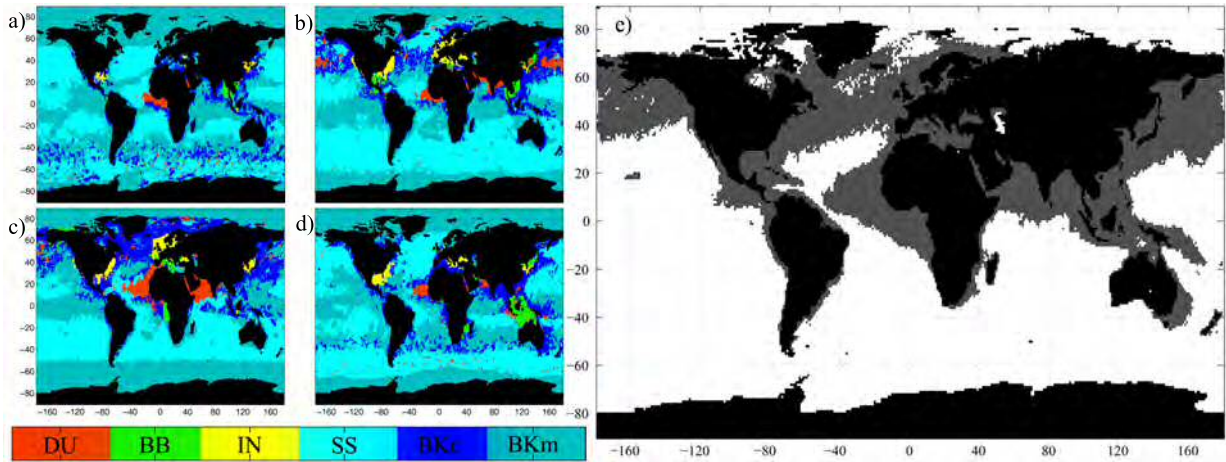


Figure 3. Natural and anthropogenic aerosols over the ocean. (a, b, c, d) Distribution of dominant aerosols types in January, April, July and October 2004, respectively. Aerosol types as in Table 1. Source attribution is based on sequential thresholds on satellite data (see further details in the Data and Methodology section). (e) Light and dark grey correspond to areas where continental (DU, BB, IN, BKc) and anthropogenic (BB, IN) aerosols, respectively, dominate in 30% or more of the 108 months between Jan 2001 and Dec 2009. Red squares indicate the positions of the study cases of fig. 5.

allowed identifying the global distribution of the dominant among the major aerosol types that concur in the marine atmosphere: mineral dust, biomass burning, urban and industrial, sea salt and marine biogenic particles (Figure 3). The method efficiently distinguishes between aerosols of marine and continental origins, and of natural and anthropogenic origins. See Figure 4 for an example year. Interestingly, those regions where small anthropogenic aerosols dominate during at least 1/3 of the year (Figure 3e) coincide with those where the seasonality of r_e is reversed (Figure 1c), namely the NW Atlantic off North America, the tropical Pacific off Central America, the tropical SE Atlantic off Africa, the S Indian around Madagascar, waters around Indonesia and NW Australia, the subtropical W Pacific off east Asia, and the continental European seas. The only exception occurs in the Arabian Sea, where anthropogenic aerosols are masked by co-occurring heavy loads of mineral dust [Jones et al. 2009]. Taken altogether, Figures 1 and 3 strongly suggest that aerosols indeed drive LMC droplet size through seasons, but natural marine aerosols bring this seasonality towards negative feedback on insolation, whereas anthropogenic aerosols provide positive feedback.

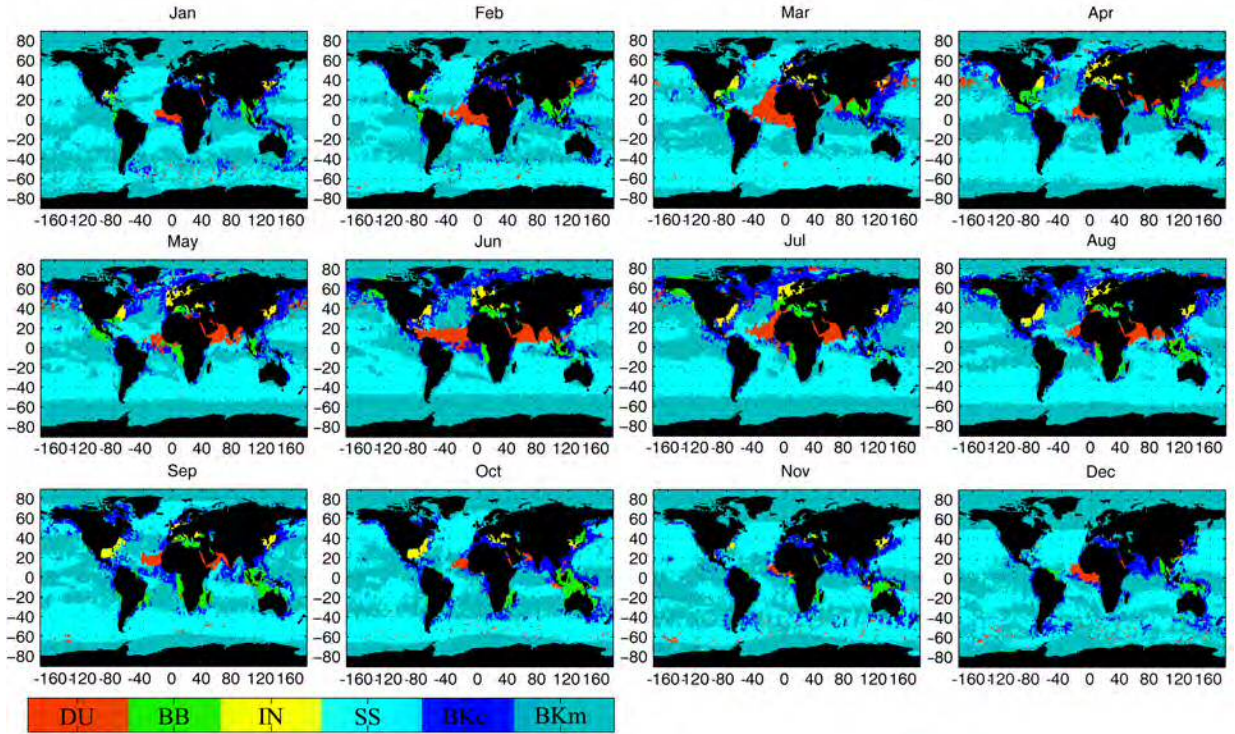


Figure 4. Monthly distribution of dominant aerosol types over the oceans in 2004, as estimated from satellite-derived aerosol optical characteristics with the sequential threshold method.

What are the potential consequences of these distinct natural and anthropogenic behaviors for the *albedo* and radiative forcing of LMC? Regional cloud *albedo* (α_c) is a positive function of the zenith angle of insolation, and solely because of that it would be higher in winter and lower in summer. This is not always the case because α_c is further modulated by cloud abundance (A_{cl}) and droplet size (r_e). We obtained weekly α_c data from the Clouds and Earth's Radiant Energy System (CERES) in two locations that we use as study cases because they are symmetric in latitude and have the same insolation and seasonality, similar mean annual A_{cl} and α_c (Figures 5a,c), but different aerosol amounts and sources. While aerosols in the South Pacific at 35°S are of natural marine origin all year round, the W Atlantic at 35°N is heavily impacted by urban and industrial aerosols. In the South Pacific, A_{cl} are higher and r_e are smaller coinciding with low zenith angles

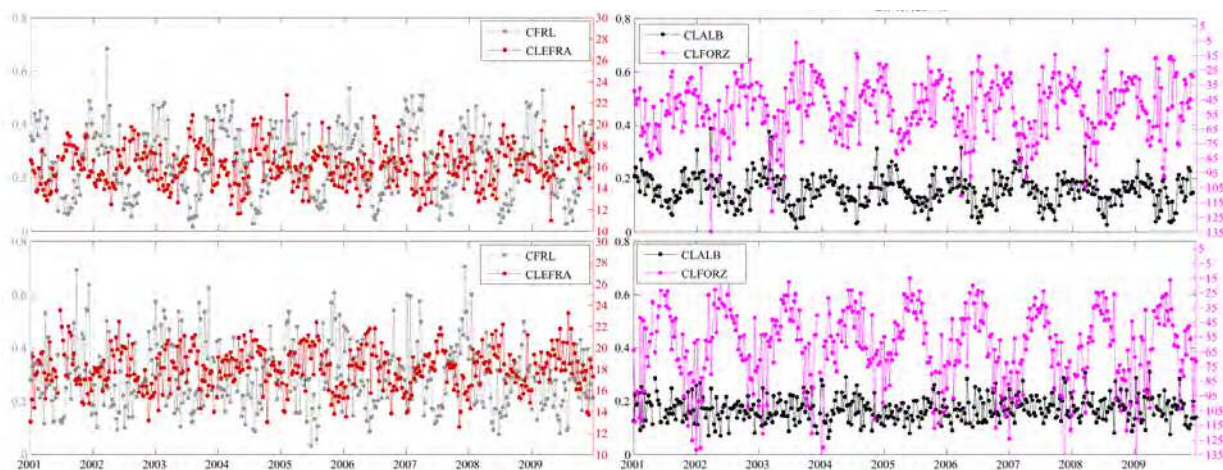
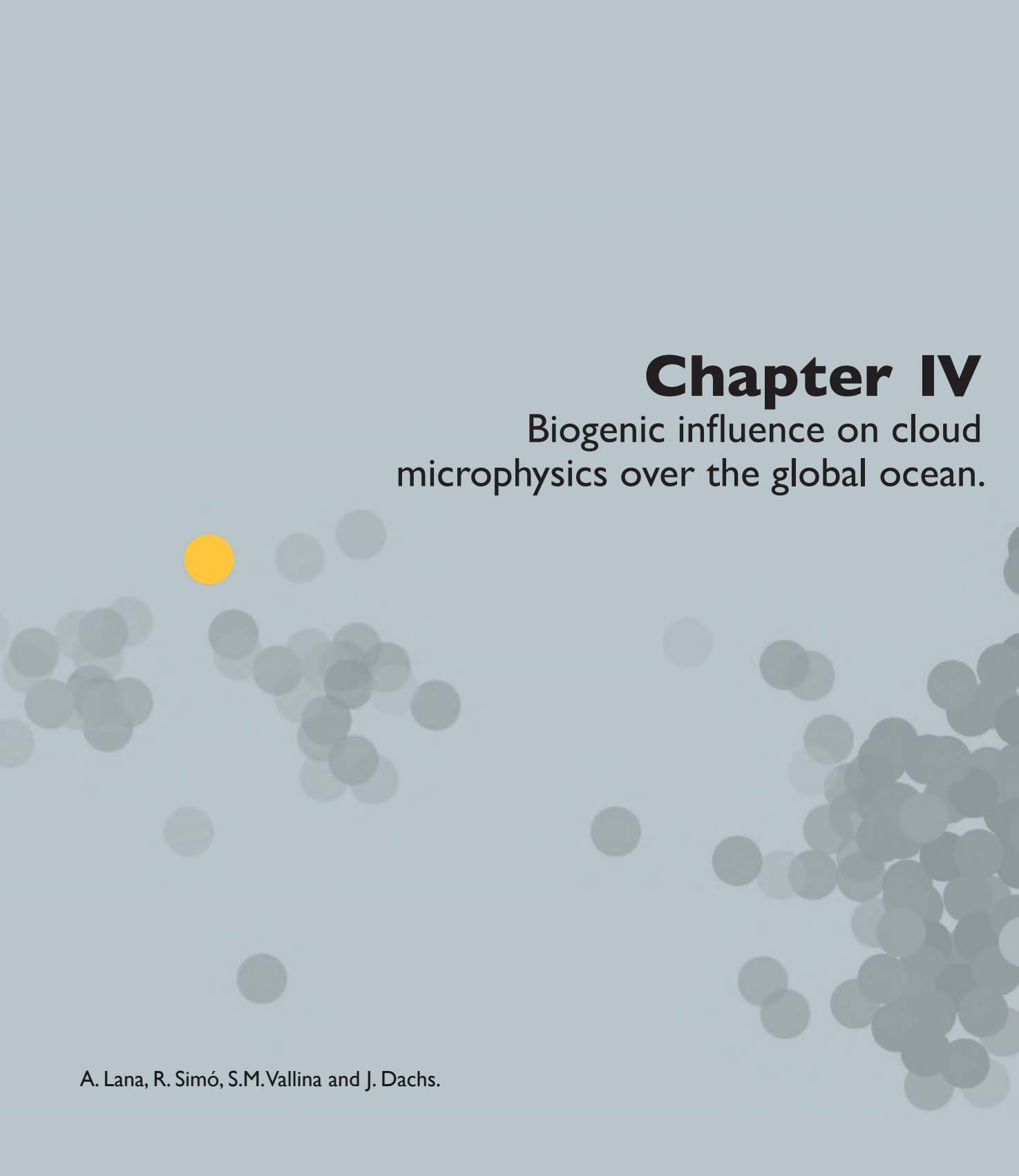


Figure 5. Cloud abundance, droplet size, and radiative effects. Series of weekly data of liquid cloud abundance A_{cl} , cloud droplet size r_e , cloud albedo α_c and cloud shortwave radiative forcing CRF_{sw} over the period 2001-2009 within two $7^\circ \times 7^\circ$ latitude-longitude windows centered at $35^\circ\text{N } 60^\circ\text{W}$ (a,b) and $35^\circ\text{S } 150^\circ\text{W}$ (c,d).

and higher insolation in summer (Figure 5c), thus resulting in almost invariant α_c , and cloud shortwave radiative forcing (CRF_{sw}) values that vary between -100 and -25 W m^{-2} from summer to winter (Figure 5d), with a 9-year mean of -62 W m^{-2} . In the NW Atlantic, A_{cl} are higher and r_e smaller in winter; together with the larger zenith angle, they give rise to higher α_c in winter, at the season of lower insolation. The resulting CRF_{sw} values vary between -75 and -20 W m^{-2} from late winter to fall (Figure 5b), with a 9-year mean of -51 W m^{-2} . Thus, CRF_{sw} in the anthropogenically perturbed air is lower than that in the clean air by as much as 11 W m^{-2} . Since in both cases the cloud LW radiative forcing exhibits a much narrower seasonal variability [Harrison et al. 1990], this difference in CRF_{sw} translates into a similar or even larger difference in cloud net radiative forcing, $10\text{-}15 \text{ W m}^{-2}$ [Harrison et al. 1990]. In other words, cloud cooling is notably reduced in the anthropogenically perturbed region. Similar patterns are observed in other polluted regions downwind of important emission sources, such as the Mediterranean and the Arabian Seas, the tropical S Indian off the NW of Australia, or the SE Atlantic off Angola, where annual mean CRF_{sw} are lower than those of pristine regions with similar annual cloudiness located at the same latitudes (data not shown).

Altogether, our results show that the two main drivers of cloud *albedo* over the oceans, namely meteorology-driven cloud abundance and aerosol-driven cloud droplet size, concur inversely in a unimodal seasonality. Over most of the clean marine atmosphere, this compensates the effects of the zenith angle on cloud *albedo* and provides strong annual cooling. Explanations for such a concurrence can be found in the seasonalities of the air column stability and the emission of natural marine aerosols, which are both stronger in summer [Klein and Hatmann 1993, Yum et al. 2004, Vallina et al. 2007]. It is most likely that this seasonal behavior was the general rule in the preindustrial Earth. Continent-to-ocean transport of anthropogenic aerosols interferes with the natural seasonality of the *albedo* of marine clouds, which may result in a reduction of their annual cooling potential.

Acknowledgements: We thank the NASA's MODIS-Atmosphere and the CERES teams, Level 1 and Atmosphere Archive and Distribution System (at GSFC) and Atmospheric Science Data Center (at LRC), the USGS' Land Processes Distributed Active Archive Center, the ESA's ATSR team, and the NCEP/NCAR Reanalysis Project for the production and free distribution of some of the data used in the present work. Funding was provided by the Spanish Ministry of Science and Innovation through the projects MIMOSA (CTM2005-06513), PRISMA (CTM2009-10193), Malaspina 2010 (CSD2008 – 00077), and a Ph.D. studentship to A.L. This is a contribution of the Research Group on Ocean Biogeochemistry and Global Change supported by the Generalitat de Catalunya.



Chapter IV

Biogenic influence on cloud
microphysics over the global ocean.

A. Lana, R. Simó, S.M. Vallina and J. Dachs.

Abstract

Aerosols have a large potential to influence climate through their effects on the microphysics and optical properties of clouds and, hence, on the Earth's radiation budget. Aerosol-cloud interactions have been intensively studied in polluted air, but the possibility that the marine biosphere plays an important role in regulating cloud brightness in the pristine oceanic atmosphere remains largely unexplored. We used 9 years of global satellite data and ocean climatologies to derive parameterizations of (a) production fluxes of sulfur aerosols formed by the oxidation of the biogenic gas dimethylsulfide emitted from the sea surface; (b) production fluxes of secondary organic aerosols from biogenic organic volatiles; (c) emission fluxes of biogenic primary organic aerosols ejected by wind action on sea surface; and (d) emission fluxes of sea salt also lifted by the wind upon bubble bursting. Series of global weekly estimates of these fluxes were correlated to series of cloud droplet effective radius data derived from satellite (MODIS). Similar analyses were conducted in more detail at 6 locations spread among polluted and clean regions of the oceanic atmosphere. The outcome of the statistical analysis was that negative correlation was common at mid and high latitude for sulfur and organic secondary aerosols, indicating they might be important in seeding cloud nucleation and droplet activation. Conversely, primary aerosols (organic and sea salt) showed more variable, non-significant or positive correlations, indicating that, despite contributing to large shares of the marine aerosol mass, they are not major drivers of the variability of cloud microphysics. Uncertainties and synergisms are discussed, and recommendations of research needs are given.



Aerosols have a great impact on the Earth's radiative budget by direct and indirect interactions with solar radiation. Direct effects occur through the absorption and the scattering of sunlight back into space, thus decreasing the solar energy that reaches the Earth's surface [Haywood and Boucher 2000]. Indirect effects occur through the big influence that aerosols have on the formation and optical properties of clouds. The concentration number, physical and chemical characteristics of aerosols modify cloud microphysics, namely the size and number of cloud droplets, and thereby influence cloud brightness [Twomey 1977] and longevity [Albrecht 1989], among other properties [Lohmann and Feichter 2005]. The most salient of these complex indirect effects is that clouds formed in the presence of larger amounts of small aerosols have larger albedo [Andreae and Rosenfeld 2008]. This influence is predicted more acute in air masses with fewer aerosols, such as those over the oceans away from continental influence [Twomey 1977; Andreae and Rosenfeld 2008].

Among the natural climate-regulation processes hypothesized to act through aerosol-cloud interactions, the most notorious was postulated as the CLAW hypothesis [Charlson et al. 1987]. CLAW suggested that oceanic emissions of dimethylsulfide (DMS) to the atmosphere could constitute a climate buffer through the regulation of the amount of solar radiation that reaches the Earth surface. DMS is formed in the surface ocean as a by-product of food-web processes and plankton ecophysiology [Simó 2001; Stefels et al. 2007]. Being a volatile compound, DMS is emitted from the ocean to the atmosphere where it is oxidized, mainly by OH radicals, to form H_2SO_4 , non-sea-salt SO_4^{2-} and other hygroscopic products that may nucleate into particles and grow to act as cloud condensation nuclei (CCN) or seeds for cloud drop formation [Andreae and Rosenfeld 2008]. If planktonic production of DMS increases with increasing temperature or sunlight, and its emission eventually reduces solar radiation, DMS might be the core of a negative (self-regulating) feedback between the marine biosphere and climate [Charlson et al. 1987]. The cross-discipline and cross-scale nature of the CLAW hypothesis has stimulated research

in and across fields as apparently distant as plankton ecophysiology, air-sea gas exchange and aerosol-cloud interactions [Simó 2001]. Even though some key aspects of the hypothesis have met strong support, notably through regional evidences for coupling between phytoplankton blooms cloud microphysics and optics [Meskhidze and Nenes 2006; Krüger and Graßl 2011], and global evidence for the sensitivity of DMS production to underwater light intensity [Vallina and Simó 2007a; Lana et al. 2011b], the existence and significance of the proposed feedback loop as a climate buffer remains elusive [Levasseur 2011].

Despite DMS has drawn much of the attention because of the CLAW hypothesis, there might be other secondary organic aerosol (SOA) precursors (as yet largely unidentified) that are produced by similar mechanisms and might therefore play analogous roles [Liss and Lovelock 2007]. Marine SOA precursors are natural volatile organic compounds produced by plankton and photochemical reactions all over the oceans. Their emissions are, however, poorly constrained [Dachs et al. 2005, Dachs et al. 2012, Simó 2011]. Initially it was suggested that biogenic isoprene fluxes could account for a significant fraction of SOA [Palmer and Shaw 2005; Meskhidze and Nenes 2006], as occurs over densely vegetated land. Recently, a number of other SOA precursors have been identified, namely iodomethanes, amines, monoterpenes and non-methane hydrocarbons (Simó 2011 and references therein). They cause increases in aerosol number and organic matter during periods of higher biological productivity [O'Dowd et al. 2004; Vaattovaara et al. 2006; Müller et al. 2009]. With these emissions being poorly quantified, combinations of modeling and observations indicate that known emission fluxes of marine volatiles cannot account for organic aerosol concentrations measured over the oceans, and important fluxes of primary organic aerosols (POA) are to be invoked (e.g., Arnold et al. 2009; Rinaldi et al. 2010). Actually, current estimates of POA and SOA precursor fluxes fall short at predicting organic aerosol levels through atmospheric models [Heald et al. 2005], thus calling for the existence of hitherto unaccounted marine sources of organic carbon. It is to be noted that emissions of hydrophobic semivolatile chemicals that accumulate in the surface microlayer and are released through volatilization or in association with sea-spray, such as alkanes and polycyclic aromatic hydrocarbons [Nizzetto et al. 2008, Dachs et al., unpublished data], have been overlooked as marine aerosol precursors.

Sea-spray is ejected into the atmosphere by the action of wind speed on the surface of the ocean. It is generated by bubble bursting and carries sea salt together with organic particles, both of which may act as CCN once in the atmosphere. These sea-spray POA are composed of virus, bacteria, biogenic polymeric organic material and associated semivolatiles [Bauer et al. 2003; Bowers et al. 2009; Russell et al. 2010; Orellana et al. 2011]. Being all of biological origin, it is likely

that POA precursors are somewhat proportional to plankton biomass and its most commonly used indicator, chlorophyll *a* concentration. Indeed, the scarce existing measurements of POA in small marine aerosols (e.g., O'Dowd et al., 2004; Leck and Bigg, 2007) suggest that they are more abundant in air masses downwind of chlorophyll *a* rich waters, particularly if strong winds enhance the lift of sea spray. The biological POA source may be reinforced by the action of surfactants exuded by phytoplankton, which lower surface tension and may facilitate the ejection of small aerosols.

Sea salt (SS) is also ejected off the sea surface as sea-spray. It has an important presence in the marine atmosphere, contributing 44% of the global aerosol optical depth [O'Dowd and De Leeuw, 2007]. Sea salt was overlooked in the original CLAW hypothesis, because it was thought to be composed of too few and too big particles to have a significant influence in cloud microphysics despite their high hygroscopicity [Le-Quéré and Saltzman 2009]. Today, however, it is known that a non-negligible proportion of sea salt particles belong in the small size fraction that makes them effective as CCN [Andreae and Rosenfeld 2008, de Leeuw et al. 2011]; moreover, sea salt aerosols play a role in the atmospheric chemistry of gaseous aerosol precursors [von Glasow 2007].

When the CLAW hypothesis was published [Charlson et al. 1987], DMS was suggested to be the main, if not the only, source of new CCN in the pristine ocean. This scenario has been complicated with the discovery of the aforementioned wide range of volatiles and particles with potential to influence cloud condensation [O'Dowd et al. 1997; Andreae and Rosenfeld 2008]. Further complication comes from the widespread occurrence of continental aerosols in the marine atmosphere, co-existing with marine aerosols in internal and external mixtures [Andreae and Rosenfeld 2008]. Any attempt to evaluate the role of the marine biosphere in cloud formation and the radiative budget on a global scale must therefore be able to distinguish between biotic and abiotic, and between autochthonous and continental sources of the marine aerosols, and describe their geographical, temporal, concentration and size distributions.

In the present paper, we make use of satellite data and ocean climatologies to parameterize the variability in the flux rates of aerosol formation from ocean-leaving DMS and SOA precursors. We also parameterize the emission fluxes of POA and sea salt from the surface ocean. These aerosol sources are compared with the satellite-derived size of cloud droplets on weekly and monthly bases over a 9-year period. Temporal correlations at both the global scale and representative locations are analyzed as a means to assess the potential role of each marine aerosol source in

driving the variability of cloud microphysics. Regions where the sought marine aerosol-cloud interactions are heavily interfered by continental aerosols are identified.

DMS and Methanology

Background and Data

The global ocean DMS concentration data used in this study is the L10 DMS climatology [Lana et al. 2011], which consists of global monthly maps of concentrations distributed in $1^\circ \times 1^\circ$ latitude-longitude pixels. This climatology, an update of that from 1999 [Kettle et al. 1999], was constructed using exclusively the surface DMS concentration measurements (approx. 47,000) available in the Global Surface Seawater DMS database (GSSDD), maintained at the NOAA-PMEL (<http://saga.pmel.noaa.gov/dms>) and fed with contributions of individual scientists from all over the world.

Ocean-to-atmosphere emission fluxes were computed with the climatological surface DMS concentrations and the corresponding gas transfer coefficients, which were parameterized taking into account both the water and the air side resistances, as described in McGillis et al. [2000]. The parameterization used for the water side DMS gas transfer coefficient is that used by Nightingale et al. [2000] corrected to the Schmidt number of DMS according to Saltzman et al. [1993]. The air side transfer coefficient calculation was based on the neutral stability water vapor bulk transfer coefficients from Kondo [1975]. The computation of the emission flux also considers the sea surface temperatures (SST) and the non-linear influence of wind speed on air-water mass transfer coefficients.

Monthly global, $1^\circ \times 1^\circ$ climatologies of SST and wind speed were obtained from the NCEP/NCAR reanalysis project (<http://www.esrl.noaa.gov>) for the period 1978-2008, as most of the DMS data available in the database are from that period. Because the water side gas transfer coefficient has a nonlinear dependence on wind speed, the use of monthly averaged wind speeds introduces a bias into the flux calculation. The flux was corrected for this effect assuming that instantaneous winds follow a Weibull distribution, using the approach of Simó and Dachs [2002].

To compute a proxy of DMS oxidation fluxes in the atmosphere we followed the same approach

as Vallina et al. [2006]. The hydroxylradical (OH) is the main atmospheric DMS oxidant [Savoie and Prospero 1989; Chin et al. 2000; Barrie et al. 2001, Kloster et al. 2006]. Daytime DMS oxidation initiated by OH produces, among other products, aerosol-forming methanesulphonic acid (MSA), sulfuric acid and its corresponding anion non-sea-salt sulfate (nss-SO_4^{2-}). Therefore the amount of DMS-derived aerosols that can act as CCN depends not only on the DMSflux but also on OH concentrations. We used a monthly global distribution of OH concentration data in the marine boundary layer (MBL) obtained from the GEOS-CHEM model run by the Atmospheric Chemistry Group at Harvard University for the year 2001 [Fiore et al. 2003].

The potential source function for DMS-derived CCN can be parameterized as follows:

$$\text{CCN}_{\text{DMS}} = b * \gamma * \text{DMSflux} \quad (1)$$

where b is a unit conversion constant and γ is a dimensionless parameter varying between 0 and 1 that gives the efficiency of DMS oxidation as function of the ratio between OH and DMSflux following an equation of the form:

$$\gamma = x / (k_s + x) \quad (2)$$

where,

$$x = \text{OH}/\text{DMSflux} \quad (3)$$

In the absence of OH (or very low OH) concentrations respect to the DMSflux, most (or at least part) of the DMSflux cannot be converted to CCN_{DMS} (in this situations γ will be low). On the other hand, if OH concentrations are in excess all the DMSflux can be oxidized to CCN_{DMS} (in this situations γ will be close to one). The form of the equation accounts for an asymptotic behavior; as the availability of OH for DMS oxidation (the variable x) increases, a higher fraction of the DMSflux can be converted to CCN_{DMS} approaching asymptotically the upper limit of gamma (for which all DMSflux is converted to CCN_{DMS}). Therefore $\gamma\text{DMSflux}$ gives the amount of biogenic sulfur potentially available for CCN production. Following Vallina et al. [2006], we took the value of k_s derived from the annual averages of OH, DMSflux and γ over the Southern Ocean. Note that Vallina et al. [2006] validated the capability of this parameterization to reproduce the seasonality of DMS oxidation by comparing it against monthly series of MSA concentrations in aerosols at 15 aerosol sampling stations of the world oceans. MSA is the

most appropriate for validation purposes because it is formed exclusively from DMS oxidation, whereas nss-SO₄ results from DMS, combustion sources and volcanic emissions altogether. For comparison purposes, we used the monthly aerosol MSA climatologies of Mace Head (Ireland), Hedo Okinawa (Japan), Palmer Station (Antarctica), Prince Edward Island (Southern Ocean) and Shemya Island (Aleutians) from the University of Miami network of aerosol sampling stations [Chin et al. 2000], and monthly rainwater MSA concentrations at Amsterdam Island [Sciare et al. 1998].

Marine SOA flux

We parameterized the variability of the SOA production rate with the same approach used for the DMS-derived aerosol, computing the emission flux and the oxidation rate of its precursor. Unlike biogenic sulfur aerosols, however, marine SOA has a number of potential precursors, namely a myriad of VOCs not yet fully characterized, which includes isoprene [Bonsang et al. 1992], terpenes [Yasaa et al. 2008], amines [Fachini et al. 2008], alkylnitrates [Chuck et al. 2002], alkanes [Dachs et al., unpublished data], among others [Bonsang et al. 2008]. Since no global climatology of surface ocean VOCs exists, and because both the air-sea transfer coefficient and the atmospheric oxidation are dependent on the chemical composition of the precursor mix, which is unknown and probably very variable, an accurate parameterization is impossible. To overcome this limitation, we considered that SOA-forming VOCs are closely associated with, and proportional to the concentration of chlorophyll *a* [Baker et al. 2000]. We took isoprene as a surrogate of SOA precursors, and parameterized the emissions of total volatile and semi-volatile precursors as it was isoprene. Isoprene concentration in the surface ocean has been found roughly proportional to chlorophyll *a*, at least much more so than that of DMS [Baker et al. 2000; Bonsang et al. 1992; Broadgate et al. 1997; Palmer and Shaw 2005]. Therefore, we computed the SOA-forming VOCs concentration in surface seawater as chlorophyll *a* as a proxy. The chlorophyll *a* weekly and monthly data for the period 2001-2009 were obtained from the SeaWiFS Project (GSFC, NASA), and transformed into 1°x1° latitude-longitude spatial resolution.

Then, we computed the VOC emission flux as:

$$F_{\text{voc}} = k_w(u, \text{SST}) * \text{CHL} \quad (4)$$

where k_w is the transfer coefficient of isoprene, calculated following Palmer and Shaw [2005].

SST and wind speed (u) climatologies were derived from the same data sources as for DMSflux, but over the 2001-2009 period only.

VOC oxidation into SOA was computed assuming OH is the main oxidant, which is the case for isoprene and most organics at the low NO_x levels of the marine atmosphere [Kroll et al. 2006; Carlton et al. 2009].

Model parameterization of submicron sea salt and POA

We parameterized the emission flux of submicron sea salt (F_{SS}) in sea spray as a function exclusively of the wind speed, following Geever et al. [2005]:

$$F_{SS} = (1.854 * 10^{-3}) * u^{2.706} \quad (5)$$

Where u is the wind speed taken from the same climatology as for the SOAflux.

Since POA is mainly constituted by phytoplankton and bacterioplankton-derived biopolymers [Facchini et al. 2008; Hawkins and Russell 2010] and biological particles such as virus, bacteria [Aller et al. 2005] and microalgae [Brown et al. 1964], it is reasonable to consider that POA precursors in the surface ocean occur in general proportionality to chlorophyll a [O'Dowd et al. 2004]. Indeed, an empirical parameterization has been suggested to estimate the amount of submicron organic matter lifted as primary particles by wind speed along with the sea spray as a function of the chlorophyll a concentration - CHL - [Vignati et al. 2010]:

$$\begin{aligned} \% \text{ organic mass} &= 43.5 * \text{CHL} + 13.805 & (6) \\ &\text{for CHL} < 1.43 \text{mgm}^{-3}; \text{ and} \end{aligned}$$

$$\begin{aligned} \% \text{ organic mass} &= 76 & (7) \\ &\text{for CHL} \geq 1.43 \text{mgm}^{-3}. \end{aligned}$$

With the calculation of the F_{ss} and the percentage of organic mass, we computed the POA flux emitted to the atmosphere:

$$\text{POAflux} = F_{ss} * (0.435 * \text{CHL} + 0.138) \quad (8)$$

for $\text{CHL} < 1.43\text{mgm}^{-3}$; and

$$\text{POAflux} = F_{ss} * 0.76 \quad (9)$$

for $\text{CHL} \geq 1.43\text{mgm}^{-3}$.

where CHL was taken from the same monthly $1^\circ \times 1^\circ$ SeaWiFS climatology used for the SOAflux.

Continental aerosols were defined as those with an aerosol optical depth (AOD) greater than 0.1 and an Angström exponent (AE) greater than 1.5.

To estimate the geographic extent of a heavy influence of continental aerosols to the marine atmosphere we used the approach of Jurado et al. [2008] and Lana et al. [2011c]. The aerosol classification procedure is mainly based on satellite optical measurements that are proxies for the amount and type of aerosol: the aerosol optical thickness, which describes the attenuation of sunlight by a column of aerosol, its standard deviation, indicative of the aerosol optical depth variability, and the Angström exponent, which is inversely related to the average size of the aerosol. These were all obtained from the Moderate Resolution Imaging Spectrometer Instrument (MODIS, <http://modis.gsfc.nasa.gov>). Complementary data used were wind speed and proximity to fire points, land vegetation and urban and industrial centers. Wind speed distributions were obtained from the NCEP/NCAR reanalysis project as mentioned above, and helped identify the conditions for large sea salt emissions. Firecounts were determined from nighttime ATSR data, identified where the signal exceeds 308 K, reported in the World Fire Atlas from the European Space Agency (<http://dup.esrin.esa.it/ionia/wfa/index.asp>). Urban centers and land vegetation were taken from the land cover classification map of the International Geosphere-Biosphere Programme (<http://edcdaac.usgs.gov/modis/mod12q1lv4.asp>). All parameters were computed into monthly means on a resolution of $1^\circ \times 1^\circ$ for the period 2001-2009.

The cloud microphysical property used in this study was the liquid cloud droplet effective radius (r_e , ratio of third to second moment of the satellite-derived cloud drop size distribution). It was obtained from the Level 3 MODIS Terra Collection 5, obtained from the NASA Goddard

Space Flight Center Level 1 and Atmosphere Archive Distribution System (DAADS Web, <http://ladsweb.nascom.nasa.gov/data/search.html>). The data resolution is 1° , with a quality assurance of 1 km. Both weekly and monthly data for the 2001-2009 period were used.

Temporal co-variations between paired variables

Temporal co-variations between paired variables (namely aerosol fluxes and r_e) were explored by the running-window correlation method [Vallina et al. 2006]. For each month and each $1^\circ \times 1^\circ$ position, we substituted the value of the targeted variable for the average of the 49 values of a $7^\circ \times 7^\circ$ window located around the position. Then we constructed the monthly series of the variable over the 2001-2009 period (9 years, 108 months) for each $1^\circ \times 1^\circ$ position. With these 108 data for each variable for each $1^\circ \times 1^\circ$ pixel we computed the Spearman's correlation between paired variables, obtaining a global map of correlation coefficients. Correlations were significant at 95% confidence level approximately when $\rho > 0.1$ (monthly and weekly temporal resolution) and when $\rho > 0.5$ (annual resolution).

For the Southern Ocean case study, we calculated the average of each variable over the 40° - 60° S latitudinal band, and compared the weekly data series of paired variables throughout the 9 years (414 weeks). We calculated the Spearman's correlation coefficient between the 414 data pairs of each aerosol flux and r_e . The time series were plotted in standardized form, since we were interested in the variability and co-variation of the variables and not in their absolute values.

For the aerosol sampling stations case studies, weekly aerosol fluxes and r_e values were averaged over a $7^\circ \times 7^\circ$ window located right upwind of each station. Paired variables were plotted in standardized form and correlated as for the Southern Ocean case study. When they were to be compared with in situ aerosol MSA concentrations, they were collapsed into monthly means over one climatological year by simple averaging.

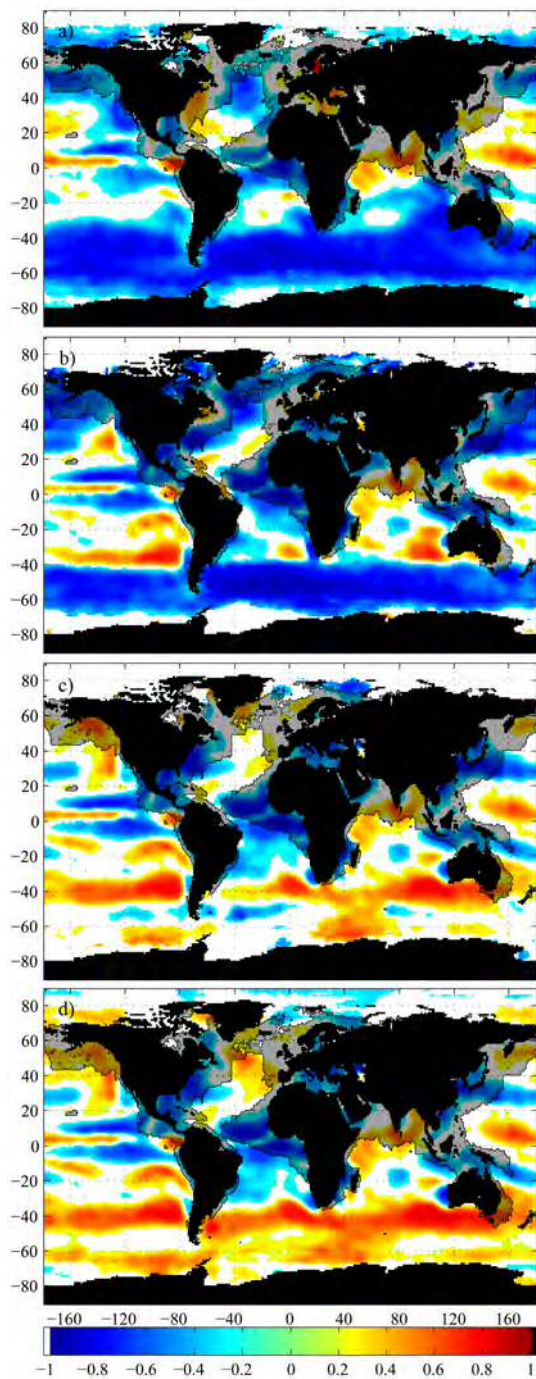


Figure 1. Global maps of Spearman's rank correlation coefficients between monthly series (2001-2009) of CLEFRA or r_c and the parameterized fluxes of: (a) DMS emission and oxidation in the atmosphere (γ DMSflux), (b) SOA formation in the atmosphere (SOAflux), (c) POA emission (POAflux) and (d) sea salt emission (SSflux). Superimposed on all maps is the mask that indicates the marine atmosphere heavily influenced by continental aerosols (see Methods).

RXXXXXX

GbMxpSXXXXXXXXXXCXXXXXXXXXX

DMS oxidation flux versus r_e : To investigate if there is a widespread seasonal relationship between secondary aerosol precursors or primary aerosols ejected from the ocean surface and cloud droplet size, we constructed global maps of correlation coefficients of monthly data over the period 2001-2009 (Figure 1). Superimposed on the plots is the area of the oceanic atmosphere heavily influenced by continental aerosols, according to Lana et al. [2011c]. Figure 1a shows that there is a strong negative correlation between the DMS oxidation flux ($\gamma\text{DMSflux}$) and r_e over temperate and high latitudes and in the subequatorial Atlantic and eastern Pacific oceans. A uniform negative correlation is particularly remarkable in the southern oceans south of 30°S. Negative correlation implies that the higher the DMS oxidation flux in the atmosphere is, such that there is larger potential for biogenic sulfur aerosol formation, the smaller the droplets of liquid clouds are, and vice versa. Indeed, over most of the global oceans $\gamma\text{DMSflux}$ increases from winter to summer as a result of a generalized increase of the seawater DMS concentration [Lana et al. 2011] and a concomitant increase in the OH concentration in the MBL [Vallina et al. 2006].

Correlation between $\gamma\text{DMSflux}$ and r_e turns non-significant in the subtropical southern Pacific and Atlantic, and slightly positive in the equatorial and the subtropical northern oceans. It is also non-significant or slightly positive downwind of major pollution sources, namely Europe (NE Atlantic and European seas), the eastern coast of North America (NW Atlantic), southern Asia (N Indian) and eastern Asia (NW Pacific). These are areas heavily influenced by continental aerosols, as shown by the mask on the map, and particularly by small combustion-derived aerosols [Lana et al., 2011c], which are as good as natural marine aerosols as CCN. The seasonality of combustion aerosols shows a maximum during winter, thus it is different from that of marine biogenic aerosols, and it has been shown that, in regions downwind of combustion foci, the seasonality of r_e differs from that in unpolluted oceanic regions and follows closely the timing of the dominant combustion aerosol [Lana et al. 2011c].

In the case of the equatorial and tropical N Pacific, the occurrence of positive correlations between $\gamma\text{DMSflux}$ and r_e is more puzzling. It is to be noted that this also occurs with the correlations of other types of natural aerosols to r_e (Figures 1b,c,d). This is a region most affected by the

intertropical convergence, where large ascending air fluxes feed the formation of a persistent band of high altitude-reaching thunderstorm clouds. There, the liquid cloud attribution of MODIS to the r_e measurements may have little to do with aerosols formed in the MBL.

In addition to the abundance of continental aerosols regions in the tropics and subtropics, it is to be noted that the low latitudes are characterized by low seasonality. Since our statistical analysis is mainly based on seasonal correlations, any uncertainty associated with the monthly variables can generate a noise with larger amplitude than the underlying seasonality, thus affecting the correlation coefficient. Only because of the low seasonality, hence, lower correlation coefficients are to be expected at lower latitudes, even if the underlying causal relationships were the same.

SOA precursors versus r_e : The correlation map between the chlorophyll *a* associated SOAflux and r_e (Figure 1b) is quite similar to that of the γ DMSflux (Figure 1a). Roughly, negative correlation (blue color) dominates and non-significant or positive correlation is most common at lower latitudes. Important differences occur in the southern oceans between 20°S and 40°S, where the SOAflux exhibits mostly positive correlation while the γ DMSflux gives non-significant or negative correlation. Also in the N Pacific between 20°N and 40°N, the SOAflux correlates negatively to r_e where γ DMSflux does not. Conversely, both γ DMSflux and SOAflux correlate negatively to r_e north of 40°N and south of 40°S.

Primary organic aerosol (POA) versus r_e : Unlike those of γ DMSflux and SOAflux, the correlation of marine submicron primary organic aerosols (POAflux) to r_e does not show a general pattern (Figure 1c). Correlation coefficients change from positive to negative through non-significant in a rather patchy way. Many of the regions with negative correlation, i.e., those where POA could be regarded as an important source of CCN and smaller cloud droplets, are regions with a heavy influence of continental aerosols. Since the POAflux was parameterized as a function of wind speed and the chlorophyll *a* concentration, the correlation map shows some similarities to that of the SOAflux. The important differences come from the fact that the SOAflux parameterization used also the OH concentration, which has a seasonality similar to that of r_e .

The correlation map of the submicron sea salt emission flux (SSflux) to r_e (Figure 1d) resembles that of the POAflux. This was expected because the parameterization of the POAflux is derived from that of the SSflux with intervention of the chlorophyll *a* concentration. The main difference between both occurs in the Southern Ocean south of 50°S, where the SSflux shows a rather uniform positive correlation to r_e . This strongly indicates that sea salt is not a main driver of CCN

variability in the pristine ocean, as already suggested by Vallina et al. [2007].

Weekly Evolution of the Upper Southern Ocean

Several authors have suggested that if a causal relationship between marine emissions and cloud microphysics occurs today, it should be most visible in the Southern Ocean [Menskindse and Nenes 2006; Krüger and Graßl 2011]. The reason is that, due to the lack of continental land masses and large pollution sources, and due to the strong circumpolar winds, the Southern Ocean underlies one of the most pristine atmospheres on Earth, with the additional particularity of being rather uniform over a broad latitudinal band and all throughout longitudes. Further, the seasonalities of both marine productivity and aerosol and cloud variables are very marked and repeated over years. Indeed, strong positive correlations have been reported between CCN numbers and the DMS oxidation fluxes in the Southern Ocean [Vallina et al. 2006]. Therefore, this region makes an interesting case study for a closer examination of correlations among marine aerosol emission and formation fluxes and cloud droplet size.

Weekly series of average γ DMSflux, SOAflux, POAflux and SSflux data were correlated to average r_e data over the full 40°-60°S band (Figure 2). Note that while SOA and primary aerosol fluxes were parameterized from weekly wind speed, SST and chlorophyll *a* data throughout the period 2001-2009, the parameterization of γ DMSflux used weekly seawater DMS concentration data deconvoluted from a climatological year; that is, the interannuality of the γ DMSflux series only reflects the interannuality of wind speed and SST, but not that of DMS.

Weekly r_e showed a clear annual pattern, repeated with great similarity year after year (Figure 2a): larger cloud droplets in austral winter (May through August) and smaller in summer (December-February). The series of γ DMSflux and r_e showed a close inverse relationship, with a Spearman's correlation coefficient of -0.93 (n=414). This agrees with the findings of Krüger and Graßl [2011] and is similar to the strong negative correlation found for monthly γ DMSflux and satellite-derived CCN numbers in the region [Vallina et al. 2006, 2007]. Also the SOAflux was strongly anti-correlated to r_e on a weekly basis (ρ =-0.92, n=414; Figure 2b). These results show that the more DMS and organic volatiles are emitted into the atmosphere and oxidized, the smaller cloud droplets are, which is consistent with the potential role of marine biogenic trace gases in aerosol nucleation and growth.

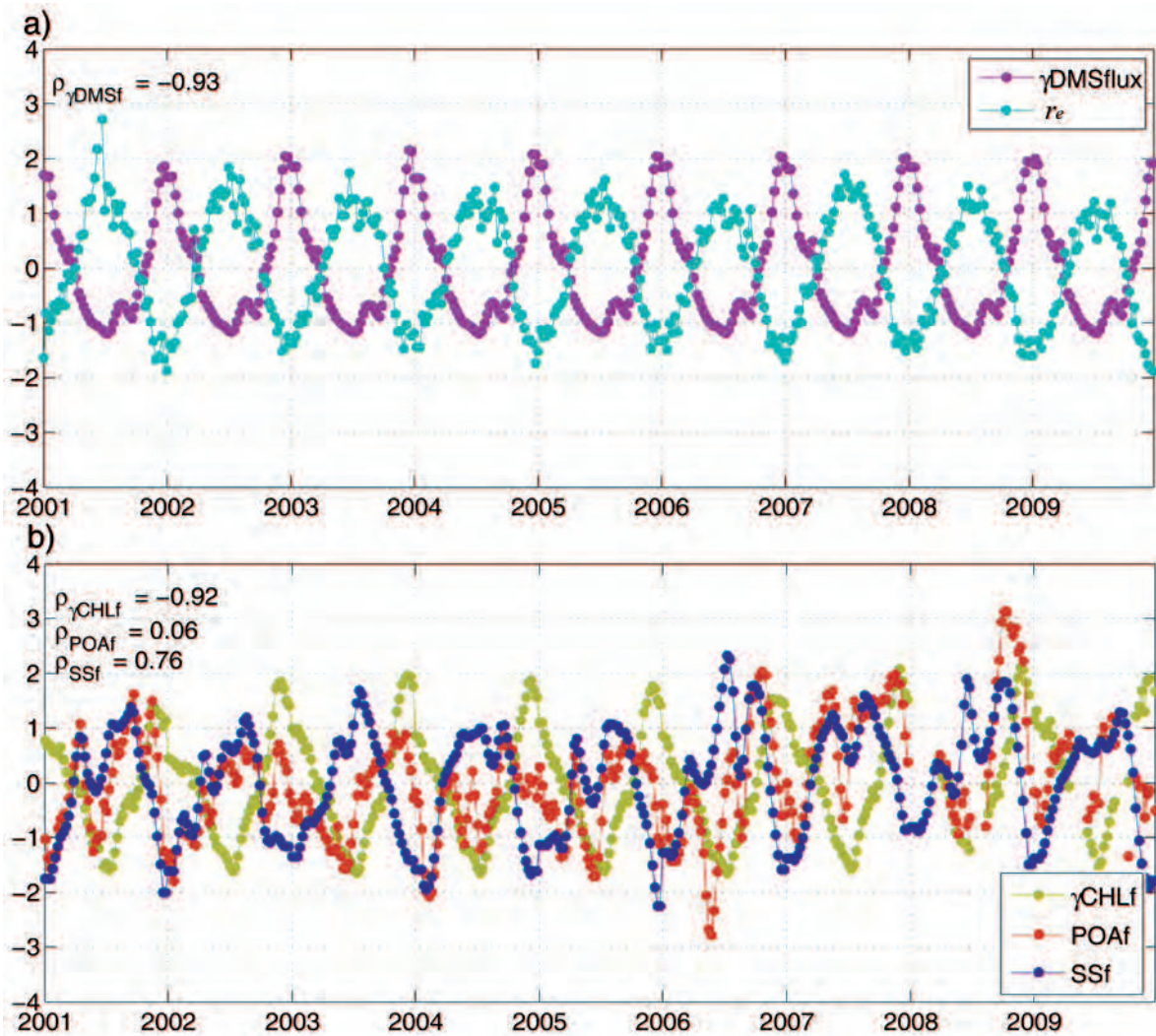


Figure 2. Temporal evolution (2001-2009) of (a) weekly satellite-derived r_e (CLEFRA) and $\gamma\text{DMSflux}$; (b) weekly SOA flux, POA flux and sea salt flux averaged over the entire Southern Ocean (40° - 60°S). The inset indicate the Spearman's correlation coefficient of each variable against r_e .

No correlation was found between the POAflux and r_e ($\rho=0.06$, $n=414$; Figure 2b). Even though POAflux exhibited some seasonality, this was less marked (less unimodal) than those of r_e , γ DMSflux and SOAflux, with minimal values in late summer, maximal values in late spring, and a lot of intra- and interannual variability. The SSflux, though also variable, showed more a marked seasonality, but in positive phase with that of r_e (Figure 2b). In fact, and according to its simple parameterization, SSflux followed the seasonality of wind speed. Consequently, the correlation coefficient was high but positive: 0.76 ($n=414$).

3.3.3.3. Localized areas of the ocean

With the aim to make a closer examination of the potential influence of marine biota on cloud microphysics we chose six localized areas of the ocean that represent different climate regimes and exhibit a range of quantitative influences of continental aerosol (Figure 3). These areas were defined as $7^\circ \times 7^\circ$ windows upwind of the Prince Edward Islands (Southern Ocean), Palmer Station (Antarctic Peninsula), Amsterdam Island (S Indian), Shemya Island (subarctic N Pacific), Mace Head (temperate NE Atlantic) and Hedo-Okinawa (temperate NW Pacific). All these areas contain an aerosol sampling station with a record of monthly atmospheric MSA measurements for at least one year. Since MSA originates exclusively from DMS oxidation and has no major continental source, it is a good metrics to which validate our representation of the γ DMSflux [Vallina et al. 2007]. Figure 3 shows the monthly series of MSA, γ DMSflux and r_e for a climatological year. Figures 4-6 show weekly series of γ DMSflux, r_e , SOAflux, POAflux and SSflux for the period 2001-2009. Note that, again, the γ DMSflux series was not constructed with actual weekly data but was calculated from deconvoluted, climatological monthly seawater DMS concentration and weekly wind speed and SST data.

Three of the stations are located in unpolluted regions: Prince Edward Island, Palmer and Amsterdam Island. Prince Edward Island (46.9°S - 37.3°E) is located in the Indian sector of the Southern Ocean. The annual variability of monthly aerosol MSA concentrations, which are maximal in summer and minimal in winter, agree well with that of the estimated γ DMSflux (Figure 3a), thus providing a ground-based test for the validity of the seawater DMS climatology and the associated emission and oxidation fluxes in the Southern Ocean. r_e showed an inverse seasonality, with larger cloud droplets in winter and smaller in summer, in the way it would be predicted by the indirect aerosol effect if the γ DMSflux would be a major source of CCN. As a result, the correlations of monthly MSA and γ DMSflux to r_e were strongly negative (Spearman's

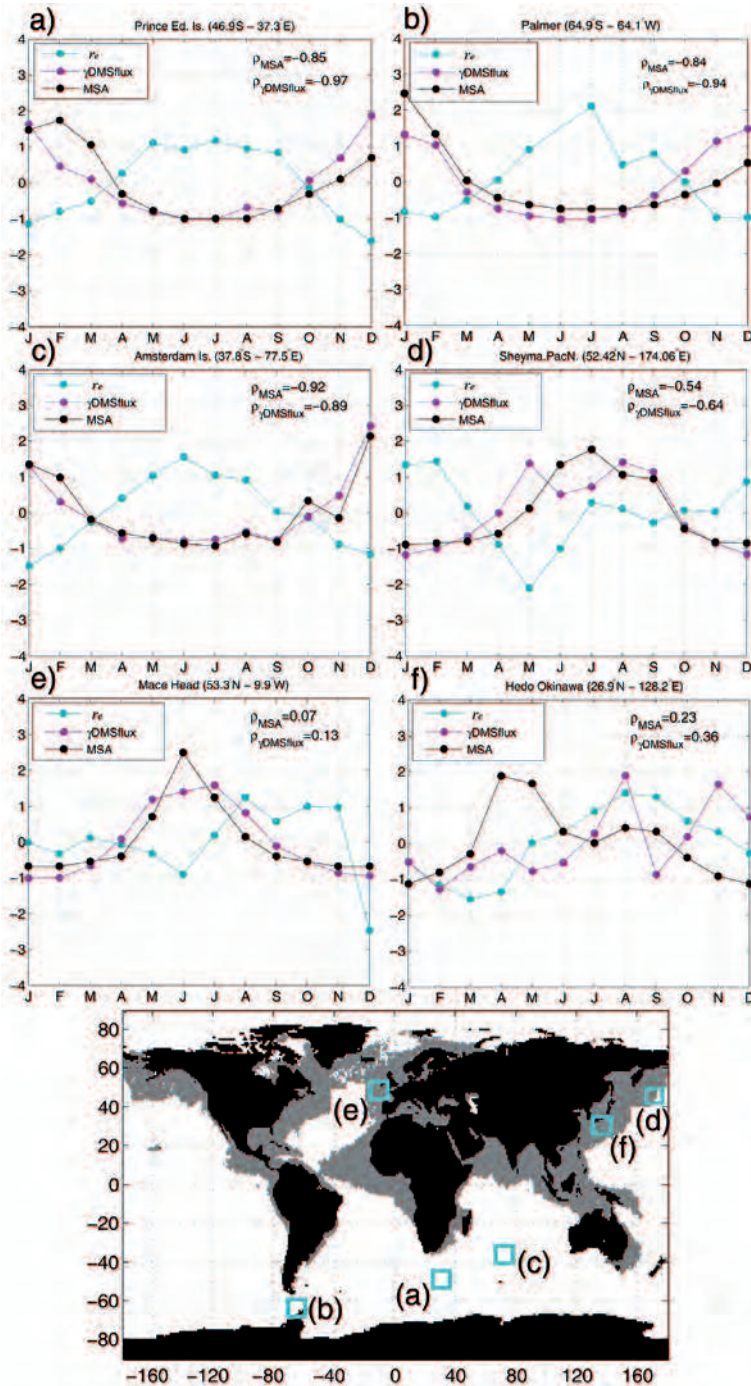


Figure3. Seasonal evolution of satellite-derived r_e (CLEFRA), SOA flux and ground-based aerosol MSA concentrations at six aerosol sampling stations: (a) Prince Edward Island, (b) Palmer Station, (c) Amsterdam Island, (d) Shemya Island, (e) Mace Head and (f) Hedo Okinawa. The bottom map shows the locations of the stations and the extension of the regions heavily impacted by continental aerosols.

coefficients of -0.85 and -0.97, respectively, $n=12$). On a weekly basis over the period 2001-2009, both γ DMSflux and SOAflux correlated significantly to r_e ($\rho=-0.64$ in both cases, $n=411$ and $n=376$). Conversely, the POAflux and the SSflux gave positive correlations (0.37 and 0.49, respectively, $n=381$ and $n=414$), contrary to the predictions if they were main sources of CCN (Figures 4a and 4b).

Palmer Station (64.9°S-64.1°W) is located on Anvers Island, midway down the western side of the Antarctic Peninsula. The seasonalities of aerosol MSA, γ DMSflux and r_e are very similar to those observed at Prince Edward Island, and the negative correlation of the two former to the latter was equally strong (-0.84 and -0.94, respectively, $n=12$; Figure 3b). Also weekly γ DMSflux correlated significantly to weekly r_e ($\rho=-0.66$, $n=411$; Figure 4c), and so did the SOAflux ($\rho=-0.6$, $n=322$; Figure 4d). The POA flux showed no significant correlation ($\rho=-0.16$, $n=324$) and the SSflux showed a slight positive correlation ($\rho=0.37$, $n=414$; Figures 4c and 4d).

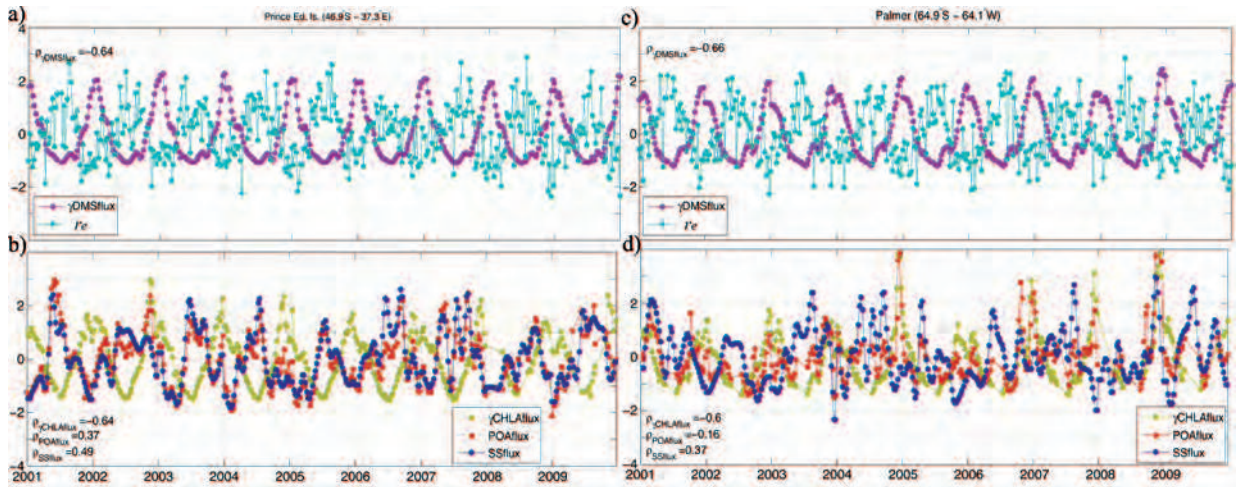


Figure 4. Same as Fig. 2 but for (a, b) Prince Edward Island, and (c, d) PalmerStation.

Amsterdam Island (37.8°S-77.5°E) is located in the S Indian Ocean. Monthly rainwater MSA from 1996 showed a marked seasonal variation with higher concentrations in summer, coincident with the seasonality of concurrent atmospheric DMS concentrations [Sciare et al. 1998]. We can observe in Figure 3c that the monthly variation of the MSA measurements agrees closely with that of the γ DMSflux derived from the updated seawater DMS climatology. Both MSA and γ DMSflux showed a strong negative correlation to r_e (Spearman's correlation coefficients of -0.92 and -0.89, respectively, n=12). On a weekly basis, the correlation between γ DMSflux and r_e was weaker (ρ =-0.49, n=411; Figure 5a) but still significant. SOAflux did not correlate significantly to r_e (ρ =-0.2, n=377), whereas POAflux and SSflux had similar positive correlations (0.43 and 0.45, respectively, n=381 and n=414; Figure 5b).

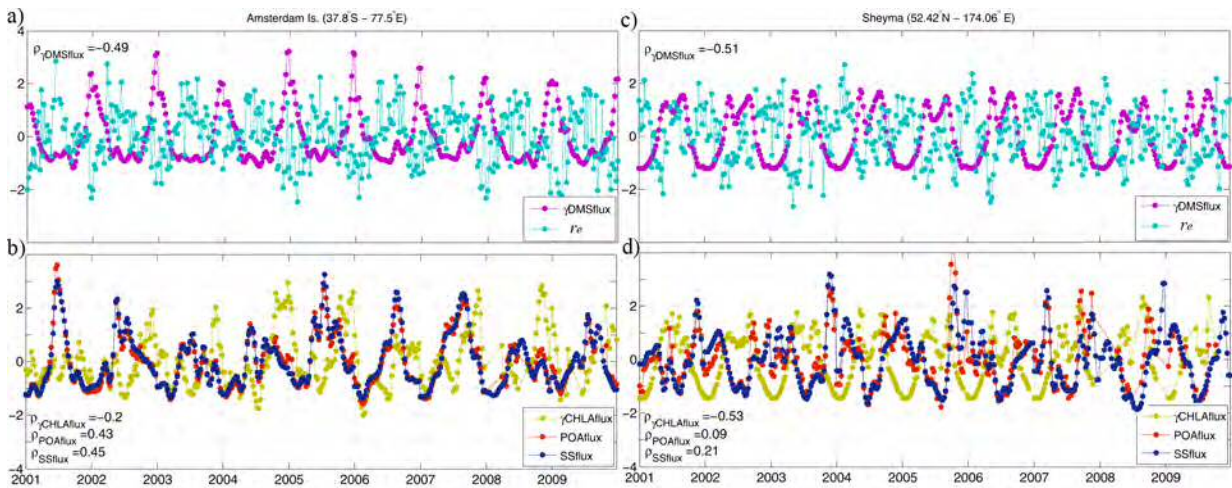


Figure5. Same as fig. 2 and 4 but for (a, b) Amsterdam Island, and (c,d) Shemya Island.

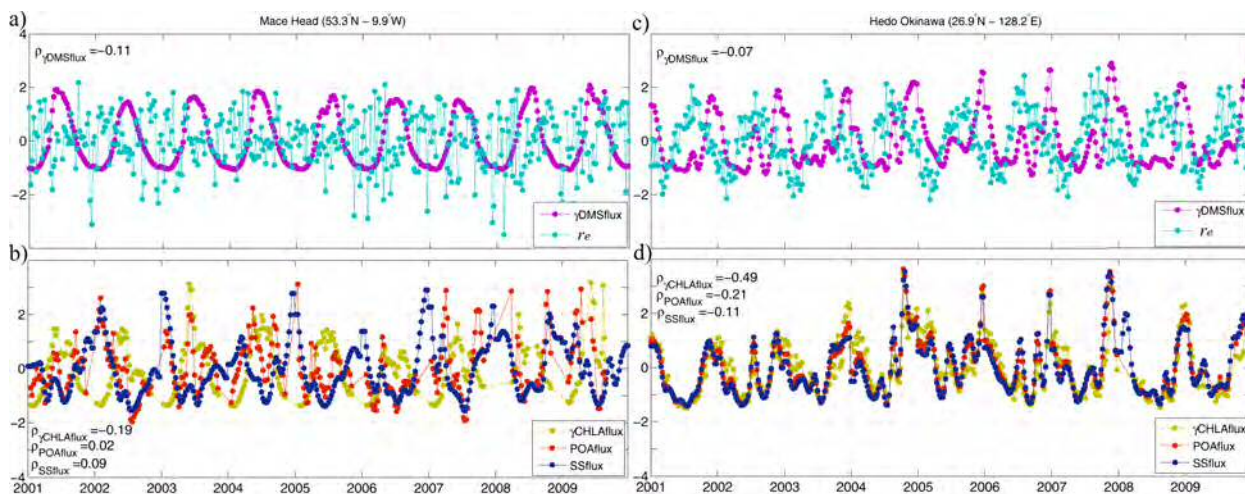


Figure 6. Same as Fig. 2, 4 and 5 but for (a, b) Mace Head, and (c, d) Hedo Okinawa.

Shemya (52.42°N - 174.06°E) is one of the Aleutian Islands located in the high-latitude central N Pacific. Aerosol MSA measurements were conducted by Saltzman et al. [1986] as part of a broader study over the Pacific Ocean. By computing the ratio $\text{MSA}/\text{nss-SO}_4^{-2}$, Savoie et al. [1989] concluded that marine biogenic sulfur accounts for ca. 80% of the annually averaged nss-SO_4^{-2} over the mid-latitude North Pacific. Shemya was the station with the highest MSA concentrations and the most dramatic seasonal cycle. In spite of a lack of local nss-SO_4^{-2} measurements, the authors estimated that the station is influenced by continental aerosol sources during the winter, when the input from biological sources is minimal. The monthly aerosol MSA series agreed closely with our estimate of monthly $\gamma\text{DMSflux}$ (Figure 3d). r_e showed a less unimodal seasonality than that in more pristine regions, and consequently the correlations of monthly MSA and $\gamma\text{DMSflux}$ to droplet size were lower, yet significant (-0.54 and -0.64 , respectively, $n=12$). On a weekly basis (Figures 5c and 5d), both $\gamma\text{DMSflux}$ and SOAflux were significantly inversely correlated to r_e ($\rho=-0.51$ and -0.53 , respectively, $n=410$ and $n=350$), whereas POAflux and SSflux were not ($\rho=0.09$ and 0.21 , respectively, $n=355$ and $n=414$).

We also chose two stations situated in polluted areas, i.e., heavily influenced by continental aerosols: Mace Head and Hedo-Okinawa. The aerosol MSA measurements at both stations were taken from Chin et al. [2000]. Mace Head (53.3°N-9.9°W) is located on the SW coast of Ireland. According to O'Dowd et al. [2004], this station allows for a sound sampling of air representative of the open ocean if precaution is taken to avoid land-crossing air masses. According to our satellite-using approach, a large part of the N Atlantic receives important loads of continental aerosols at least during 4 or more months a year [Lana et al. 2011c]. In the case of Mace Head, it often is under the influence of urban and industrial sources, especially during spring and summer. There was a close agreement between the seasonalities of MSA and γ DMSflux (Figure 3e), but they did not correlate significantly to r_e , which did not show any clear seasonal pattern. The correlation between γ DMSflux and r_e did not improve on a weekly basis ($\rho=-0.11$, $n=412$; Figure 6a). The SOAflux, POAflux and SSflux did not correlate either ($|\rho|<0.20$ in all cases, with $n=303$, $n=307$ and $n=414$ respectively; Figure 6b), indicating that the variation of r_e was driven by factors other than marine aerosols.

Cape Hedo is the northern tip of Okinawa Island (26.9°N-128°E), located between Japan main islands and Taiwan. The station is downwind of important urban and industrial aerosol sources, and it is also affected by biomass burning and Asian dust transport [Takami et al. 2006; Lana et al. 2011c]. This was the only examined station where monthly MSA and γ DMSflux data did not agree (Figure 3f); this had been observed by Vallina et al. [2007] using a former version of the seawater DMS climatology, and was attributed to the influence of polluted aerosols on particulate MSA through heterogeneous adsorption. Neither MSA nor γ DMSflux correlated significantly to r_e . This was also evident on a weekly basis, where the seasonalities of r_e and γ DMSflux were lagged by a few weeks ($\rho=-0.07$, $n=411$; Figure 6c). Among the other marine aerosol sources, only the SOAflux, but not POAflux and the SSflux, showed a significant negative correlation to r_e (correlation coefficients of -0.49, -0.21 and -0.11, respectively, $n=378$, $n=381$ and $n=414$).

DXXXXXXXXXX

SXXXXXXXXXX XXXXXXXXX

Our results show the spread of negative correlations of parameterized emission and oxidation fluxes of DMS and SOA precursors with cloud droplet size (r_e) over large regions of the ocean. In the case of DMS, this is consistent with the positive correlations reported for γ DMSflux and satellite-derived CCN burdens (N_{CCNs}) [Vallina et al. 2007] and for N_{CCNs} and r_e [Lana et al. 2011c] over the global oceans, particularly at mid and high-latitudes. Although correlation is never a proof of causality, it is a necessary condition for causality. The correlation map in fig. 1a provides support to the hypothesized importance of DMS emissions for cloud microphysics in the clean marine atmosphere.

Both the γ DMSflux and the SOAflux show a particularly high anti-correlation with r_e in the Southern Ocean, where there is a reduced number of CCN, and marine precursors must play an important role in cloud microphysics because the influence of continental aerosols is very low. However, there are also large areas in the tropics and subtropics where the seasonalities of the γ DMSflux and the SOAflux are non-significantly or even positively correlated to that of r_e . In some of these areas (e.g., the NW Atlantic, the N Indian and the westernmost N Pacific), the notable presence of continental aerosols is probably more influential on cloud microphysics than these natural secondary sources. But also in the cleaner equatorial and subtropical S Pacific, the lack of seasonal coupling discards marine secondary aerosols as the main divers of r_e . We should note, however, that the weak or absent seasonality in the tropics hampers the use of temporal correlation analyses that are mainly based on seasonal signals.

In the SH, the areas with non-significant or positive coupling between SOAflux and r_e extend further south than those for the γ DMSflux. This may reflect actual differences in the role of DMS and other organic volatiles as sources of CCN. But it could also be due to an inappropriate parameterization of the SOA precursor fluxes from the ocean. Based on multiple evidence (see section 2.2, and e.g. O’Dowd et al. 2004), we parameterized the SOAflux with the assumption that volatile and semivolatile precursors occur in the surface ocean in proportionality to the chlorophyll *a* concentration. At mid to high latitudes ($>40^\circ$), chlorophyll *a* concentrations increase in summer in parallel to an increase in CCN numbers [Vallina et al. 2007] and a decrease in cloud droplet size [Lana et al. 2011c]. At subtropical to mid latitudes, conversely, chlorophyll *a*

concentrations are maximal in late winter-early spring while CCN and r_e still peak in summer, thus giving rise to the observed mismatches in fig. 1b. Should SOA precursors have a seasonality less coupled to the chlorophyll *a* concentration (phytoplankton biomass) and more driven by, e.g., phytoplankton taxonomy, nutrient availability, oxidative stress and solar radiation, as is the case for DMS [Vallina and Simó 2007a; Lana et al. 2011, 2011b], the SOAflux might also show an annual maximum in summer and be more inversely proportional to r_e . There is a strong need to better identify the most important players among marine SOA precursors, beyond isoprene, and to conduct time series and manipulation studies aimed at deciphering the biological and environmental drivers of their seasonal variability. Also their volatilization and atmospheric chemical behavior (including SOA production yields in the marine atmosphere) need to be described if we are to assess their role in CCN formation and cloud microphysics over the ocean. Overall, the notion that SOA from marine biogenic precursors play in the size distribution and composition of remote marine aerosols is supported by aerosol studies [e.g., O’Dowd et al. 2004; Facchini et al. 2008; Sorooshian et al. 2009]. A significant influence of biogenic SOA on marine cloud microphysics is still an open question: regional, satellite-based studies have not agreed upon [Meskhidze and Nenes 2006; Miller and Yuter 2008].

A further complication for the interpretation of the differences and similarities between the SOAflux and the γ DMSflux with respect to r_e arises from the potential synergisms of volatile organics and biogenic sulfur in aerosol nucleation and CCN activation. Modeling [Meskhidze and Nenes 2006] and smog chamber studies [e.g., Zhang et al. 2004; Metzger et al. 2010] have suggested that mixtures of organic volatiles and ammonia enhance the nucleation of sulfuric acid into particles, their growth to the accumulation mode size, and their activation as CCN.

PM₁₀ and PM_{2.5}

POA emissions occur by bubble bursting formation of sea spray enriched with organic matter [Leck and Bigg 2005; Keene et al. 2007] or biological particles [Aller et al. 2005] that can be identified under the microscope. When only the chemical characterization of aerosols is feasible, POA are quantified as water-insoluble organic carbon [e.g. O’Dowd et al. 2004]. It has been shown [Leck and Bigg 2005; Leck and Bigg 2008] that those small insoluble organic aerosols are the seeds onto which acidic gases condense, a process that may lead to their activation as CCN.

Our statistical analyses yielded a patchy distribution of the correlation between the POAflux and

r_e (Figure 1c), with large regions with non-significant and positive correlations. Even though the parameterization of the POAflux related it to the chlorophyll a concentration, just like that of the SOAflux, their seasonal patterns were very different because of the larger influence wind speed has on the POAflux calculation. As a result, POA does not seem to play a role in driving the variability of cloud droplet size over most of the ocean. This is a little surprising, because water insoluble organic compounds have been seen to account for a dominant fraction of the organic mass of marine aerosols [Facchini et al. 2008; Russell et al. 2010]. A possible explanation would be the low hygroscopicity of most primary particles, including microorganism cells, unless they get internally mixed with hygroscopic condensates [Leck and Bigg 2005]. Another explanation would lie on the parameterization itself, where POA precursors are assumed to occur in some degree of proportionality to the chlorophyll a concentration. This is a reasonable assumption for biological particles such as viruses, bacteria and the smallest microalgae, but it is harder to predict for the algal polymers, mainly carbohydrates, that dominate the submicron aerosols [Facchini et al. 2008; Russell et al. 2010; Orellana et al. 2011]. It is known that this type of algal exudates do not only depend on total phytoplankton biomass but also on their species composition, physiological status and productivity [Verdugo et al. 2004]. As in the case of SOA precursors, hence, we should better know the geographic and seasonal distribution of POA-forming material and their environmental drivers before we can fully assess the significance of our results.

The sea salt lifted into the atmosphere with sea spray has been long recognized as the largest global source of primary aerosols [Woodcock 1948; de Leeuw et al. 2011]. In terms of mass, it represents the largest contributor to marine aerosols. Even though the concentration of small sized sea salt particles in the marine boundary layer is enough to represent an important, but highly variable, source of CCN [O'Dowd and Smith 1993; Lewis and Schwartz 2004; Caffrey et al., 2006; Pierce and Adams 2006], our correlation analysis shows that they do not seem to play an important direct role in driving the variability of cloud microphysics. At least, not the expected role, since the SSflux is positively or non-significantly correlated to r_e in most of the sea salt rich oceanic atmosphere (Figure 1d). This is consistent with the findings of Vallina et al. [2007] that sea salt contributes a large share of CCN numbers but does not drive their seasonality over the Southern Ocean. Our parameterization of the SSflux relates it exclusively to wind speed. Some modeling studies related the emission rate also with sea surface temperature [Caffrey et al. 2006; Pierce and Adams 2006; Korhonen et al. 2008] and confirmed the large contribution of sea salt to regional monthly mean CCN numbers in the marine boundary layer. It is important to notice that models are only as good as our knowledge of the underlying mechanisms is, and results

are difficult to validate because of the inherent difficulties associated with conducting in situ measurements of SS flux and realistically reproducing sea surface conditions in the laboratory. As for the POA, the influence of sea salt on the seasonal variability of cloud microphysics seems poor but remains uncertain.

CONCLUSIONS

Our correlation analyses at both the global and the regional scales and over a 9-year period provide a framework for potential causal relationships between marine aerosol source strengths and cloud microphysics. We have shown that the weekly flux of DMS emission and oxidation is significantly anti-correlated with cloud droplet size in most of the clean atmosphere over the mid and high latitude oceans. A similar result is found for the emission and oxidation of marine precursors of secondary organic aerosol, yet with differences in the subtropics. A remarkable result is the strong negative correlations found over the Southern Ocean, in the cleanest of current atmospheric regions. Conversely, primary organic and sea salt aerosols do not show a clear pattern against cloud droplet size, and in the case of the Southern Ocean they even show positive correlations, contrary to what would be expected if primary aerosols were direct drivers of cloud microphysics. Therefore we conclude that the observed patterns are consistent with a potential primary role of biogenic secondary aerosol precursors (DMS and organic volatiles) in determining the number and size of cloud droplets and, hence, having an impact on cloud radiative properties. Conversely, primary aerosols, even though they contribute to aerosol mass, do not seem to act as primary drivers of CCN numbers and droplet size.

Our efforts to distinguish among marine aerosol sources and types, deal with their distinct dynamics and seasonalities, and identify their areas of influence with respect to continental aerosols, overall represent a step forward towards the comprehension of aerosol-cloud interactions over the oceans. On first sight, however, our approach seems grounded on one major conceptual simplification: aerosol sources each contribute a proportion of an external mixture of marine aerosols, and the ones identified here to be the best coupled to cloud microphysics (namely the secondary aerosols) are hence the most climatically active through the indirect effects. A deeper interpretation of our data should take into account that most marine aerosols occur as internal mixtures from different sources and nature. Electron microscopy observations of marine aerosols depict a variety of heterogeneous particle constructions, with e.g. organic polymers internally

mixed with sulfuric acid or sea salt crystals [Leck and Bigg 1999, 2005, 2008]. The view that new aerosols and CCN are formed by homogeneous nucleation and further condensation of vapors is too simplistic; H_2SO_4 nucleation is enhanced by organics and ammonium, and growth to CCN activation occurs by organic condensation [e.g., Hegg et al. 1990; Covert et al. 1992; Kulmala et al. 2004; Zhang et al. 2004], but also tiny primary aerosols get activated as CCN by condensational growth or by absorption of surface active and hygroscopic compounds [Cavalli et al. 2004; Leck and Bigg 2005; O’Dowd and Leeuw 2007]. Our results should not be regarded as evidence for a unique role of DMS (and possibly other organic volatiles) in CCN formation, with dismissal of the primary aerosols, but point to a pivotal role of trace gas oxidation products in CCN activation of smaller secondary or primary particles [Andreae and Rosenfeld 2008].

A better knowledge of the biological and biogeochemical mechanisms that lead to the production of primary and secondary organic aerosol precursors, and particularly their spatio-temporal dynamics, is urgently needed if we are to better understand and parameterize their emission strengths. New information may change our current perception of the most important players in aerosol-cloud interactions in the pristine marine atmosphere that still covers a considerable area of our planet.

Acknowledgments. The authors wish to thank each of the individual contributors that generously submitted their data to the Global Surface Seawater Dimethylsulfide Database (GSSDD), and to J.E. Johnson and T.S. Bates (NOAA/PMEL) for the maintenance of the GSSDD. We thank the NCEP/NCAR Reanalysis Project for the production and free distribution of the SST and wind speed data used in the present work. The authors would also like to thank the SeaWiFS and MODIS-Atmosphere projects for the atmospheric variables and chlorophyll *a* concentrations values. Financial support was provided by the Spanish Ministry of Science and Innovation through the projects MIMOSA, PRISMA, Malaspina 2010, and a PhD studentship to A.L.



Discussion and Conclusions

The CLAW hypothesis 24 years later

In the context of the CLAW hypothesis [Charlson et al. 1987], this thesis aimed to contribute to the general knowledge of the biogeochemical-physical interactions and feedbacks between the ocean and the atmosphere as a coupled system. Aerosol-driven microphysical characteristics of clouds and their influence on the Earth's radiation budget were here analyzed, based on the emissions of marine aerosols and their precursors. The thesis has taken advantage of the recent huge increase in the number of marine volatile sulfur measurements and the long-term atmosphere satellite data record available.

The CLAW hypothesis suggests a simple mechanism that links the marine biota with climate regulation. According to this hypothesis, the biogenic DMS gas, produced by phytoplankton and emitted to the atmosphere, could be the major source of cloud condensation nuclei over the oceans. This implies that, before the industrial revolution, the formation and microphysics of clouds over the oceans, i.e. most of the Earth's clouds, would had been largely regulated by DMS emissions. Its simplicity and importance is what makes the hypothesis so attractive; however, thus far there is no concluding proof of its certainty.

This apparently simple hypothesis hides a huge intrinsic complexity. Under the surface of the ocean DMS is produced as a degradation product of the sulfur microalgal metabolite dimethylsulfoniopropionate (DMSP), which is a biogenic compound present in the photic zone. The efficiency of DMSP as DMS producer is mainly affected by solar radiation, the existent species of phytoplankton and the DMSP intracellular functions as an osmoregulator, cryoprotector or antioxidant, just to mention a few variables. DMS production, in turn, is affected by diverse environmental forcing factors by different paths. It can be enhanced under oxidative stress, nutrient limitation or high UV radiation, and is has a dependence on the phytoplankton groups and species present [Simó 2001; Stefels et al. 2007]. There is not a simple way to evaluate the DMS production in the ocean. In the first part of the thesis, we aimed at describing the global geographical and seasonal distribution of DMS and assessing its environmental regulators. A small part of the DMS produced under the oceans is emitted to the atmosphere [Simó, 2001; Vila-Costa et al., 2006]. The second part of the thesis focused on that moment onwards, when the DMS escapes from the ocean into the atmosphere. With regard to the atmospheric portion of the DMS cycle, there are many questions to be answered to understand the CLAW hypothesis: how DMS escapes to the atmosphere, its amount, its oxidation, its impact in the chemistry of

low troposphere, its interaction with other gases and compounds, its role in forming new cloud seeds or its relevance in the growth of pre-existing particles [Andreae and Rosenfeld 2008]. To answer these and other questions multidisciplinary studies are required. Chemists, physicists, biologists and oceanographers have involved in the study of the CLAW hypothesis. There is not yet a clear conclusion, and probably there will never be. That's probably what makes it so exciting, its complexity.

Since it was postulated, the available literature on this topic has opened many questions and has provided contrasting results, either supporting or rejecting the hypothesis.

Previous evidences supporting or against the CLAW hypothesis, published before the development of this thesis, are summarized bellow:

Previous evidences supporting or against the CLAW hypothesis

- Field measurements show strong relationships between atmospheric DMS, aerosol chemical composition (particularly methanesulfonate content), and cloud condensation nuclei, under unpolluted conditions. Some of these field measurements were performed over the tropical South Atlantic, over the Southern Indian Ocean, and at Cape Grim, situated in the Southern Ocean [Andreae et al., 1995; Baboukas et al., 2004; Andreae et al., 1999], just to mention a few examples. They suggested that DMS oxidation is the dominant sulfur source for aerosols during summer, indicating that over pristine areas of the ocean the atmospheric sulfur burden is mainly influenced by biogenic emissions.
- Anthropogenic sources of nss-SO₄ are mainly located in the North Hemisphere. Over most of the Southern Hemisphere, oceanic DMS emissions account for the majority of nss-SO₄ aerosols [Bates et al., 1992a].
- DMS concentrations are highly positively correlated with the solar radiation dose in the upper mixed layer of the open ocean, with independence of the latitude, plankton biomass or temperature [Vallina and Simó, 2006].
- There is an evidence of an impact of marine biota in cloud microphysics. Using satellite data, over a large phytoplankton bloom in the Southern Ocean cloud effective radius was

reduced, apparently, due to the increase of biogenic aerosols emissions from the ocean, with the consequent impact on the radiation flux at the top of the atmosphere. The reduction in the short-wave radiation at the surface was comparable to the indirect effect over highly polluted areas, which demonstrates the potential huge importance of biogenic emissions in climate regulation [Meskhidze and Nenes, 2006].

- A similar result is obtained using a circulation model: DMS emissions produce changes in cloud microphysical properties, both seasonally and globally. The model shows an increased number of smaller sized cloud droplets during the period of increased phytoplankton blooms [Thomas et al. 2010].

Field observations and the CLAW hypothesis

- Field observations show, at least in the Equatorial Pacific, no evidence of new particle formation in the marine boundary layer, in spite of the DMS emission and its conversion into sulfate aerosols [Clarke et al., 1996].

- The original simplification of the DMS cycle in the atmosphere hid key atmospheric processes that relate atmospheric DMS with the growth of pre-existing particles [Vaattovaara et al., 2006]. Those processes may imply a DMS effect on cloud albedo opposite of the one suggested by the CLAW hypothesis [von Glasow 2007].

- Adding aerosol physics processes on global models, a lower sensitivity of cloud condensation nuclei concentration is obtained to changes in DMS flux emissions [Woodhouse et al., 2010].

- MSA records from ice cores at high latitudes suggest that sulfur-climate feedback between glacial and interglacial periods was positive in sign [Saltzman et al., 2006, Legrand et al., 1997]. The sea ice extent, the origins of sulfur within the ice, or other sulfate sources such as continental or volcanic emissions could be the reason.

- According to the latter suggested reason for the no-evidence of the CLAW hypothesis in some regions, times and conditions, other aerosols are suggested to act as cloud condensation nuclei [Leck and Bigg, 2005, 2007; O'Dowd et al., 2004; Russell et al., 2010].

- A recent study, based in model simulations, suggests that the “plankton–DMS–clouds–earth albedo feedback” hypothesis is weak as a long-term thermostatic system but it may act as a seasonal mechanism that contributes to regulate the solar radiation doses reaching the Earth’s biosphere through seasons [Vallina et al., 2007, Vallina and Simó 2007c].

QUESTIONS

In this complex scenario, we tried to answer a handful of questions in order to provide a further insight into this mechanism. Although we partially answered them, some aspects remain unclear and open for further analyses and future investigation.

There are still a lot of uncertainties associated with the CLAW hypothesis, and big methodological challenges. One main difficulty is to segregate natural marine aerosols from anthropogenic and continental ones. This separation is a key requirement if we are to study the influence of marine biota on climate through aerosol production.

To facilitate approaching it, we can split the CLAW hypothesis in two main directions (Figure 1). On the one side, we have DMS production by the plankton food web, its ventilation to the atmosphere and its influence, once oxidized into aerosol-forming species, on cloud formation (Figure 1a). On the other side, solar radiation has an influence on plankton and physics of the photic zone, where DMS is produced, and, at the same time, it is influenced by cloud albedo, which reduces the amount of sunlight that reaches the ocean surface (Figure 1b). These two main process directions are highly influenced by the physical, chemical and meteorological characteristics of the atmosphere. We focused our studies on the seasonality of the two halves of the CLAW hypothesis, using correlation analyses of regional and global data. Spatio-temporal correlations between seasonally changing variables are a necessary, but not sufficient, condition for the feasibility of the potential feedbacks between marine biota and climate. The correlations do not provide the final answer, but they are a very useful approach.

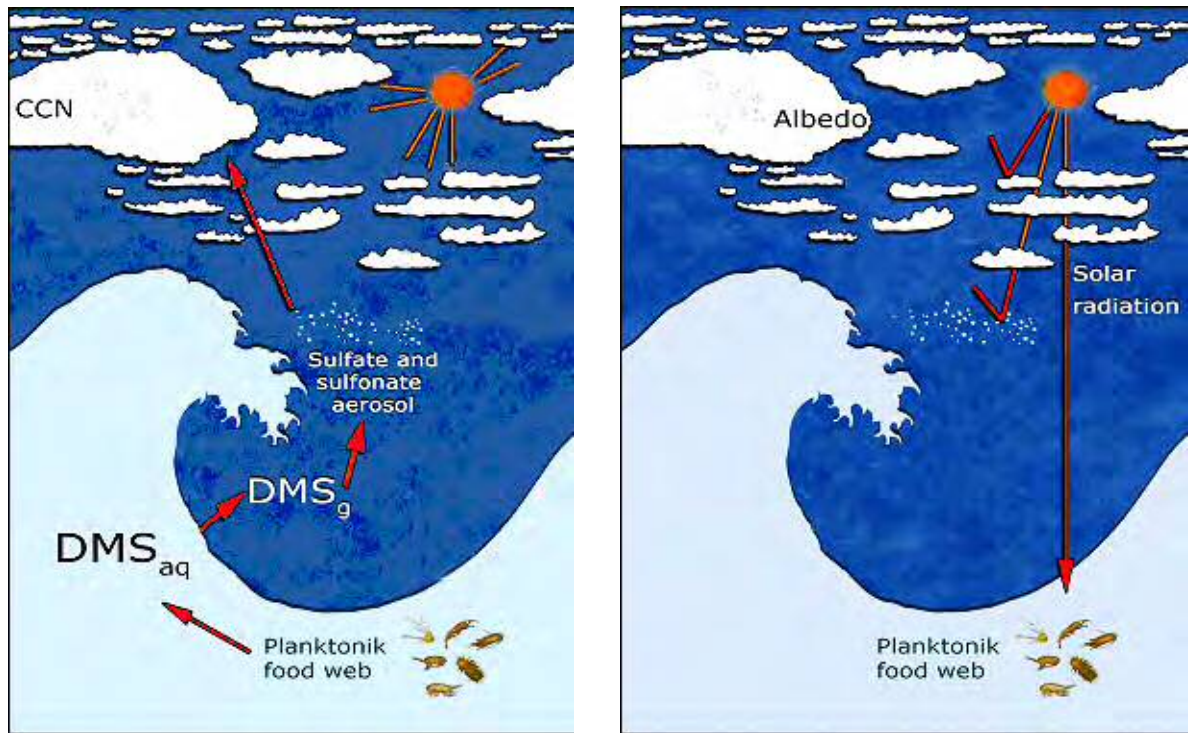


Figure 1. Scheme of the CLAW hypothesis loop: (a) the first part of the loop relates the emission of DMS from the ocean to cloud formation and brightness (albedo); (b) the second part deals with how solar radiation, affected by the albedo of clouds affects DMS production in the surface ocean.

DMS concentration in the ocean surface (Chapter 1)?

The first objective of the thesis was to create an accurate updated DMS global distribution as a follow up to the hitherto widely used DMS climatology, created in 1999 [Kettle et al., 1999], and updated one year later [Kettle and Andreae, 2000]. Over the last decade, the amount of data in the global DMS database has tripled. Using this enlarged data set, we have applied objective analysis techniques [Barnes, 1964; Locarnini et al., 2010] to create monthly global maps of DMS concentration in the ocean surface (**Chapter 1**).

The scarcity of data over space and time makes it very difficult to construct a uniform global distribution with high temporal and spatial resolutions. The extreme under-sampling of many regions of the ocean, and the uneven temporal coverage obligated us to make use of interpolation and extrapolation techniques, based on our knowledge of the biogeography of the oceans, to construct a monthly global DMS distribution with a $1^\circ \times 1^\circ$ latitudinal-longitudinal resolution. With the new climatology we created an spatio-temporal framework for future DMS process studies to address the relevant scales of variability.

The new DMS climatology was instrumental to address both sides of the CLAW hypothesis: the variability of DMS concentration and emission told us both about the distribution of aerosol sources to be compared with aerosol numbers and cloud microphysics (Figure 1a), and about the factors controlling DMS production, including cloud albedo (Figure 1b).

Previous studies [Vallina and Simó, 2007a] found a strong positive relationship between sea surface DMS and the solar radiation dose received in the upper mixed layer of the ocean. The analysis was based on the DMS database and local time-series measurements. We revisited this global analysis taking advantage of the updated DMS database and climatology, with the aim to re-examine the seasonal coupling between SRD and DMS. Our results confirm the tight relationship between both variables over the global ocean (**Chapter 2**) that had been seen in previous studies. However, the statistical analyses seem to be very sensitive to the SRD binning intervals and the methodology used to calculate SRD. Other studies, such as Derevianko et al. [2009], had pointed out this concern, namely that the use of box grouping and binning largely reduces the total variance in the data and results in exaggeratedly high coefficients of determination. However, the use of the updated climatology in the linear regression, using a

smaller averaged box and a reduced binning interval for the SRD than that used in **Chapter 2**, shows a high coefficient of determination— see Figure 2. In the results shown in **Chapter 2**, and in the latter calculations, standard deviations are quite large but the upper and lower contours of the range still show clear proportionality between DMS and the SRD.

The surface seawater DMS concentration is linked to plankton organisms living within the upper mixed layer. Using the surface chlorophyll *a* concentration as a proxy of the phytoplankton biomass in the surface ocean, we re-evaluated the potential links between DMS and plankton. The link had been previously studied by Vallina et al. [2006]. Re-examination of the latitudinal match-mismatch between the seasonality of DMS and phytoplankton, represented by the chlorophyll *a* concentration, reveals that they are highly positively correlated in latitudes higher than 40°, but anti-correlated in the 20°-40° latitudinal bands of both hemispheres.

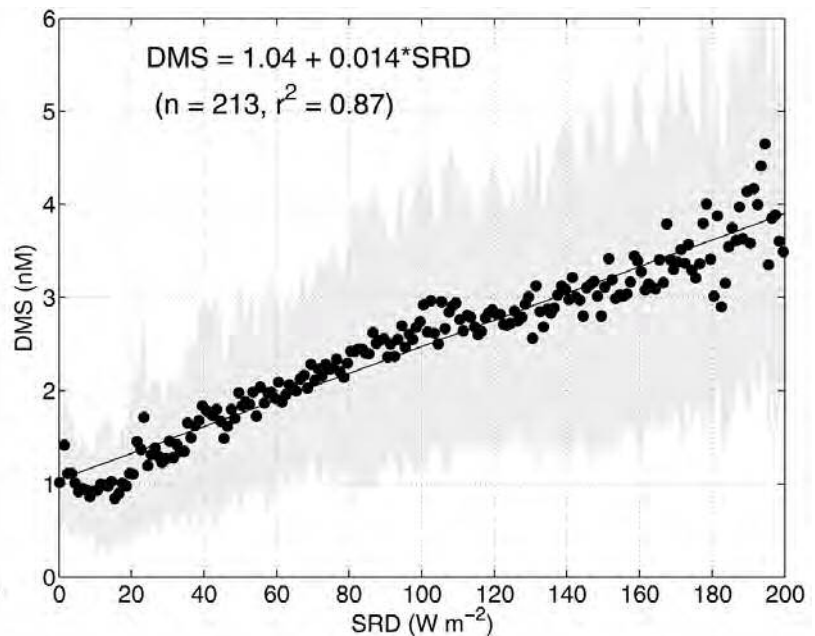


Figure 2. Linear regression of the seawater DMS concentrations from the updated DMS climatology L10 against the daily-averaged Solar Radiation Dose (SRD) in the upper mixed layer of the ocean. Dots are averages of 5° latitude by 5° longitude boxes, binned by SRD intervals of 1 W m⁻². SRD calculated as in Vallina and Simó (2007).

In spite of the differences between the updated and the previous DMS climatology (**Chapter 1**), very few differences have been found in the global and seasonal emerging patterns with the use of the updated DMS database and climatology. This is probably due to the use of updated versions of the other variables employed in the re-examination of the patterns, when there was an updated version available. These global emerging patterns provide key information about the factors that control the emission of volatile sulfur from the ocean. Sunlight and phytoplankton concentration seem to be important modulators of DMS production. However, further work is still required to understand DMS production and emission.

DMS emission and microphysical properties of clouds

We analyzed the hypothesized relationship between emitted DMS and cloud formation. To this aim, we explored the relationship between a parameterization of the DMS emission and oxidation flux and cloud droplet radius with the use of satellite-derived data. When it was possible, the resolution was brought to weekly and local (**Chapter 4**). We focused our attention on the cloud droplet effective radius as the significant cloud microphysical property for our purpose. The size of the cloud droplets influences the solar radiative properties of clouds in two ways. Firstly, if the size of the cloud droplets becomes smaller, the cloud albedo increases [Twomey, 1977]. Secondly, smaller droplets stay longer in the atmosphere before reaching the size needed to become a rain droplet and precipitate [Albrecht, 1989]. In other words, smaller droplets make longer-lasting clouds. Both phenomena contribute to reduce the solar radiation that reaches the Earth's surface, and both produce a cooling effect.

We evaluated the seasonality of low clouds over the global ocean, and found a temporal coupling (correlation) between their coverage and the size of the cloud droplets. These two cloud properties (one macrophysical, cloud cover fraction, and one microphysical, droplet size) vary in concert and in proportionality to the incident solar radiation. When the solar radiation is higher, the cloud droplet radius is smaller, and cloud coverage is higher. These relationships imply that two of the factors that contribute to cloud *albedo* increase their positive contribution with higher solar irradiances. The third main driver of cloud albedo, solar zenith angle, influences in such a way that it increases albedo with an increase in the angle. Therefore, if for the zenith angle alone, cloud albedos would be higher in winter and lower in summer, thus providing positive feedback on insolation and a modest annual cooling of the ocean surface. But the seasonality of both cloud cover and cloud droplet size is such that it decreases cloud albedo in winter and

to secondary aerosols, and any attempt to quantify secondary aerosol formation has to rely on parameterizations of an idealized or ‘average’ bulk precursor. A parameterization of the oxidation flux of biogenic isoprene (as a surrogate of the secondary organic aerosol, SOA, formation in the marine atmosphere) showed a similar seasonal variability to that of the inverse of the cloud droplet radius at mid and high latitudes. Therefore, at these latitudes it is difficult to discriminate the relative roles of DMS and SOA precursors in regulating droplet size because they all vary in concert. As a matter of fact, we observed a close coupling between chlorophyll *a* concentration and cloud droplet effective radius over marine areas not affected by continental aerosols – see Figure 3a. However, where the oceanic atmosphere is strongly affected by continental aerosols, this relation is broken – see Figure 3b – because cloud droplet size is largely controlled by pollution aerosols.

We parameterized SOA precursor emission and oxidation as a function of the chlorophyll *a*

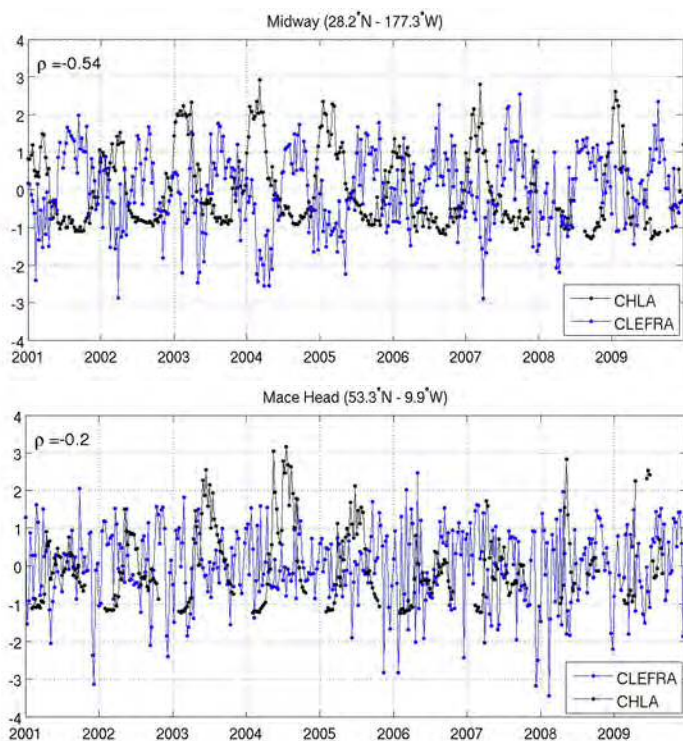


Figure 3. Temporal evolution of satellite-derived weekly chlorophyll *a* concentrations (Chla) and cloud droplet effective radius (CLEFRA) over the years 2001-2009, at (a) Midway Islands (pristine area of the subtropical North Pacific atmosphere) and (b) Mace Head, Ireland (situated in the North-East Atlantic Ocean, affected by continental aerosols).

concentration (proxy of plankton biomass), the wind speed, the sea surface temperature and their main oxidant, the OH radical. Although a myriad of compounds are potential SOA precursors (see Table 1, obtained from Simó [2011], for more details), we use isoprene as a surrogate, and base our parameterization on the properties of this compound [Palmer and Shaw 2005]. However, *in situ* measurements are needed to validate the parameterizations with the real data series of the amounts of aerosols formed by biogenic flux emissions from the ocean. Correlation maps and temporal evolution plots show a tight coupling, over large regions of the high latitude oceans, between cloud droplet effective radius and the parameterization of the two biogenic secondary aerosol precursors studied (DMS and organic volatiles). Unfortunately, during this thesis it was not possible to evaluate which of them would be the main player. Further studies therefore are needed to address this issue.

Parameterized emission fluxes of primary aerosols (primary organic aerosols – POA - and sea salt) do not vary in anti-correlation with cloud droplet effective radius as would be predicted if there were a strong influence of the former on the latter. Rather, POA fluxes show a patchy correlation to cloud droplet effective radius, and sea salt fluxes show a mainly positive correlation in large regions such as the Southern Ocean (**Chapter 4**). These results suggest that particles emitted directly from the ocean as aerosols do not seem to have a large/direct impact on the variability of cloud microphysics.

Apparently, at the mixed boundary layer (MBL) sea salt aerosols provide much of the surface area for cloud condensation [Pirjola et al. 2000], and particle nucleation is highly sensitive to the presence of those primary particles. Aerosol nucleation is affected by short-term meteorological phenomena [O’Dowd et al., 1998; Petters et al., 2006; Chen et al., 2011] that cannot be deeply analyzed with the temporal and spatial scale used for our studies. The nucleation process, classically assumed to occur only via homogeneous condensation of H_2SO_4 clusters, has been observed in areas affected by the incursion of a wide range of aerosols, as in the tropical marine boundary layer, MBL [Clarke et al., 1998], or close to shore [Covert et al., 1992; Hoppel et al., 1994; O’Dowd et al., 2002]. The occurrence of nucleation in the remote MBL remains unclear. The chemical composition of the formed particles can be influenced by their transport through the atmosphere, and by the original composition of the precursor. Transport of particles from other areas, such as the free troposphere [Covert et al., 1996; Clarke et al. 1998, Russel et al. 1998], seems to play an important role in providing new cloud-seeding aerosols to the remote MBL. However, other studies show that sulfuric nucleation can indeed occur in the remote MBL [Petters et al. 2006]. Laboratory experiments show that SOA exist mostly as internally mixed

COMPOUND	MAIN ENVIRONMENTAL ROLE ^a	OCEANIC EMISSION		OTHER SOURCES ^c	TOKEN REFERENCES
		MAGNITUDE	CONTRIBUTION TO TOTAL EMISSION ^b		
CH ₄	Greenhouse	0.6-15 Tg/yr	0.1-2%	Wetlands, livestock, rice fields, landfills, natural gas	Bates et al. 1996, Denman et al. 2007, Rhee et al. 2009
N ₂ O	Greenhouse	0.9-7 TgN/yr	4-20%	Soils, fertilizers, combustion	Nevison et al. 1995, Bange 2006, Rhee et al. 2009
Sulfur volatiles: Dimethylsulfide (DMS)	Global sulfur budget Aerosol precursor: atmospheric acidity and cloud nucleation	20-35 TgS/yr	90%	Soils, plants	Kettle & Andreae 2000, Simó & Dachs 2002
COS	Precursor of stratospheric aerosol	0.60 TgS/yr	20%	Soils, combustion	Kettle et al. 2002, Uher 2006, Sutharalingam et al. 2008
CS ₂	COS precursor	0.15 TgS/yr	?	Soils, wetlands	Xie & Moore 1999, Kettle et al. 2002
Selenium volatiles (methyl selenides)	Global selenium budget	≤35 GgSe/yr	50-75%	Soils, plants, wetlands	Amoroux et al. 2001
Halogenated volatiles: CH ₃ I, CH ₂ I ₂	Global iodine budget, tropospheric photochemistry, coastal aerosol precursor, cloud nucleation	1 TgI/yr	>50%	Rice fields, combustion	Moore & Groszko 1999, O'Dowd et al. 2002
CH ₃ Br	Stratospheric ozone destruction	20-46 GgBr/yr	10-40%	Agriculture, combustion, salt marshes	Lobert et al. 1995, Pilinis et al. 1996, Butler 2000, Yvon-Lewis et al. 2009
CH ₃ Cl	Tropospheric photochemistry, acidity, stratospheric ozone destruction	0.1-0.3 TgCl/yr	10%	Combustion, industrial	Moore et al. 1996, Khalil & Rasmussen 1999, Butler 2000
Other halomethanes and haloethanes	Tropospheric photochemistry, acidity, stratospheric ozone destruction	?	?	Combustion	Moore et al. 1995, Butler 2000
NH ₃ and methylamines (mono-, di-, tri-)	Aerosol acidity-alkalinity	?	?	Soils, wetlands, plants?	Quinn et al. 1988, Gibb et al. 1999, Jickells et al. 2003, Facchini et al. 2008
Alkyl nitrates	Tropospheric photochemistry	?	?	Combustion, photo-reactions	Chuck et al. 2002, Moore & Blough 2002
Volatile hydrocarbons (e.g., C ₂ -C ₆ , isoprene, monoterpenes)	Tropospheric photochemistry, aerosol precursors	2.1 TgC/yr	minor	Plants, combustion	Plass-Dülmer et al. 1995, Broadgate et al. 1997, Yassaa et al. 2008, Arnold et al. 2009, Gantt et al. 2009

a Impact of the oceanic emission on the Earth System, mainly through atmospheric chemistry.

b Estimated contribution of the oceans to the global emission from all sources (natural + anthropogenic).

c Main sources to the atmosphere, other than the ocean.

Table 1. (obtained from Simó 2011) The breath of the sea. Volatile compounds (other than CO₂ and O₂) produced in the surface ocean by biological and photochemical reactions, which are emitted into the atmosphere and affect its chemical properties and dynamics. In most cases a 'positive' net annual flux has been observed, but this does not mean that the surface ocean is always supersaturated in these trace everywhere. In some cases, such as COS or CH₃Br, throughout the year the oceans change their role as a source or a sink depending on the accumulation rates in the troposphere caused by variability in all sources. The list is intended comprehensive but not complete.

organic-inorganic particles [Prenni et al., 2007], and organics facilitate the nucleation of H_2SO_4 clusters and make them grow [Kulmala et al. 2004; Metzger et al. 2010]. Moreover, condensation of organic volatiles or their surface-active oxidation products make POA significantly more hygroscopic, to the extent that they can become activated with atmospheric ageing [Leck and Bigg 2005].

Our data indicate that the main player on the cloud microphysics variation seems to be biogenic emissions from the ocean, affecting directly by providing new secondary particles that can act as cloud condensation nuclei, or indirectly by growth and activation of pre-existing particles. The latter process calls for a revision of the contribution of sea salt and POA to marine aerosols, where they account for much of the variability of the total mass and size distribution [Quinn and Coffman, 1999; O'Dowd et al., 2004; Russell and Singh, 2006; Facchini et al., 2008], but, according to our study, not for the variability of the amount of cloud condensation nuclei. This calls for a revision of the CLAW hypothesis into an enriched formulation with the inclusion of other sources of marine aerosol [Leck and Bigg 2007].

MAIN CONCLUSIONS by ChapXXXX

Chapter 1. Efforts have been conducted to accurately represent the global DMS distribution. With some limitations, we have now updated a monthly global DMS climatology based exclusively on DMS measurements. The increase amount of DMS data used to construct the updated DMS climatology has produced an increase in the DMS concentration values in the regions of the ocean and months that were severely under-sampled in the previous study. Conversely, data additions have substantially decreased climatological concentrations in regions that had enough data coverage, but extremely high values, as the Polar Regions. Those changes in the updated DMS global distribution have produced an increase in the updated estimates of the DMS flux emissions of 17%. The best estimate suggests an annual DMS emission flux of 28.1 TgS.

Chapter 2. We investigated the factors that have the main influence in DMS production, and how the environmental variables affect DMS variation. An evaluation of the emerging patterns found in the updated DMS distribution, confirms previous results in spite of the regional changes observed. The monthly global DMS distribution coupled closely with that of the daily solar radiation dose in the upper mixed layer of the ocean. The seasonal proportionality between DMS and chlorophyll *a* concentration at high latitudes of both hemispheres and the inverse

proportionality in the subtropical and low temperate ocean - the so-called ‘summer paradox’ - is confirmed as a global emerging pattern.

Chapter 3. We used nine years of satellite-derived aerosol and cloud data to investigate the seasonality of aerosol-cloud interactions over the global ocean and its natural and anthropogenic drivers. We observed a strong negative correlation between the weekly evolution of cloud droplet effective radius and the fraction of liquid clouds, mainly corresponding to low clouds. That is, the higher occurrence of low clouds, the smaller their droplets are, and vice-versa. A strong negative correlation is also found between solar irradiance at the top of the atmosphere and cloud droplet size. Therefore, aerosol-driven microphysical characteristics (namely cloud droplet size) of low marine clouds concur seasonally with liquid cloud cover and solar irradiance in such a

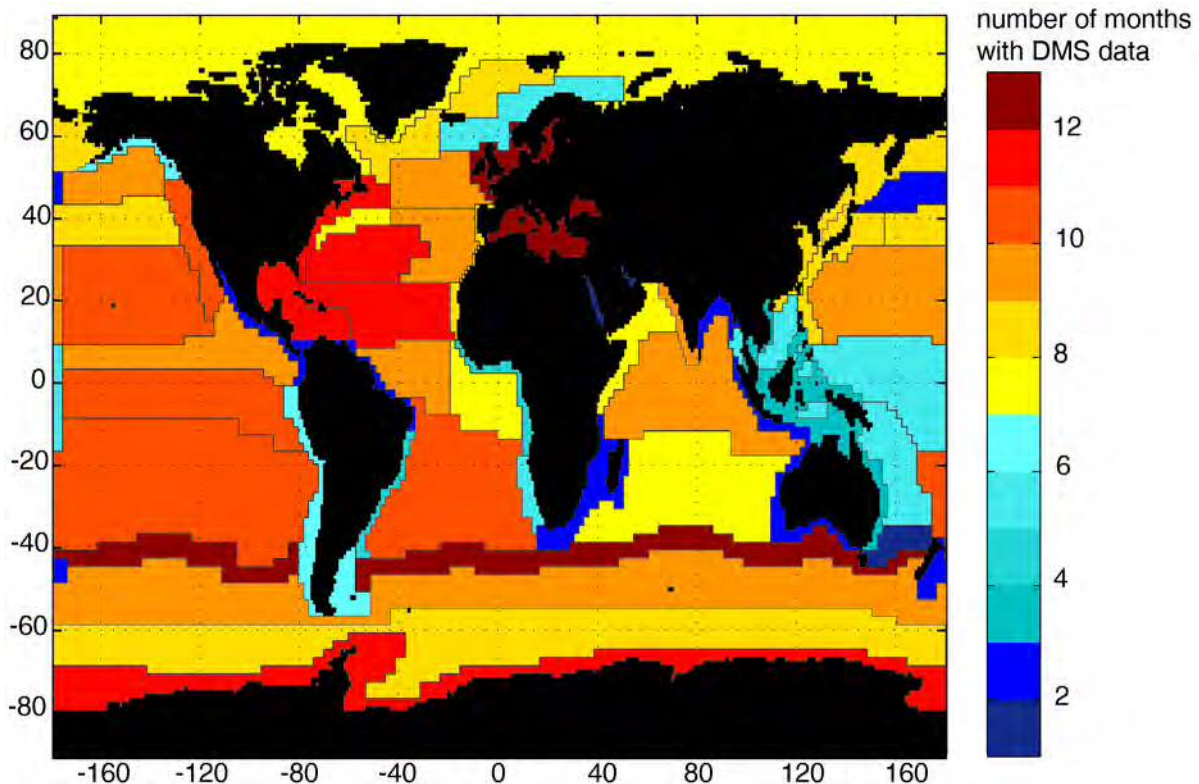


Figure 4. Ocean divided by Longhurst provinces (Longhurst, 2007), with the representation of the number of months with DMS data.

way that they compensate for the variations of solar zenith angle and provide strong cooling of the ocean surface. This natural seasonal couplings found in the pristine marine atmosphere are clearly broken in regions heavily influenced by continental aerosols, and particularly by putative anthropogenic aerosols (industrial, urban and biomass burning sources). As a result of seasonal perturbation, anthropogenic aerosols locally reduce annual surface cooling by low clouds.

Chapter 4. Correlation analyses with satellite data and empirical parameterizations revealed that, over pristine region such as the Southern Ocean, sulfate secondary aerosols formed from DMS emissions and secondary organic aerosols vary seasonally in concert with the cloud droplet effective radius, in the way expected if they were providing new cloud condensation nuclei. Regions where big loads of continental aerosols dominate during a significant part of the year did not show this correlation between marine biogenic secondary aerosols and cloud microphysics. Parameterized emission fluxes of primary organic aerosols and sea salt did not vary in anti-correlation with cloud droplet size as would be predicted if there was a mechanistic relationship between the variables: there was a patchy correlation in the case of the primary organic aerosol, and a mainly positive correlation in the case of sea salt over the pristine ocean. These results suggest that particles emitted directly from the ocean as aerosols do not seem to have a large direct impact on the variability of cloud microphysics.

FUTURE PERSPECTIVES

The CLAW hypothesis formulated almost 25 years ago has caused something even more valuable than a concise result: a huge interest of the scientific community in the investigation of ocean and atmosphere exchanges, and thousands of interdisciplinary studies. We probably will not reach a definitive conclusion, but the results obtained from each study are increasing the pieces of this puzzle.

During the thesis we realized of the importance of the amount of DMS measurements available, and how valuable they are. The development of automatic and semi-automatic systems to measure DMS concentration are changing the perspective on DMS studies. Having a global, homogeneously spatial and temporal DMS measurements distribution would resolve most of the limitations found in the construction of the updated DMS climatology. We have to be conscious of the regions of the ocean severely undersampled, shown in our study (**Chapter 1**) and schematically in Figure 4. This situation should motivate the proposals of new projects to improve our knowledge of DMS distribution and dynamics.

Simultaneous measurements of seawater DMS concentrations and cloud microphysical properties would contribute to improve our knowledge in this field. Those areas without continental influence are of special interest, where the studies can focus on the marine aerosols and their precursors, without interferences from continental sources. Studies should be dedicated to improve the current parameterizations of the emission fluxes of aerosols and precursors from the ocean.

The use of remote sensing data was extremely valuable for the present thesis. However, the data were limited to certain satellites that provide long time series, but limited in spatial resolution, solely available in a two dimensional format. The further use of alternative remote sensing tools, such as CALIPSO (Cloud-Aerosol Lidar and Infrared Pathfinder Satellite Observation), which provides data on the vertical dimension of the atmosphere, would improve our knowledge of aerosol sources and cloud formation. CALIPSO provides a three-dimensional perspective of how clouds and aerosols are formed and transported, and should be an invaluable tool for studying weather and climate. Currently the sensor launching is so recent that there is no long-term series, but this will obviously be solved in a few years time.

Accurate and consistent quantification of aerosol precursors in the ocean and their chemical transformations in the atmosphere are critically needed in order to better understand how ocean biogeochemistry influences the atmosphere. The collaboration between the oceanographic and atmospheric communities, which provides in situ data assimilation systems, with the Earth Observation technology community, which provides global satellite measurements, should render an unprecedented potential to observe and predict the processes that govern the ocean-atmosphere interactions and their impacts from local to global scales.

- Aitken J. (1880-1881) On dust, fogs, and clouds, *Proceedings of the Royal Society of Edinburgh* 11(108):14-18; 122-126.
- Albrecht, B. A. (1989), Aerosols, cloud microphysics, and fractional cloudiness, *Science*, 245(4923), 1227–1230.
- Aller, J.Y., M. R. Kuznetsova, C. J. Jahns, and P. F. Kemp (2005), The sea surface microlayer as a source of viral and bacterial enrichment in marine aerosols, *Journal of Aerosol Science*, vol. 36, 801–812.
- Alvain, S., C. Moulin, Y. Dandonneau, and H. Loisel (2008), Seasonal distribution and succession of dominant phytoplankton groups in the global ocean: A satellite view, *Global Biogeochemical Cycles*, 22, GB3001, doi:10.1029/2007GB003154.
- Amoroux, D., P.S. Liss, E Tessier, M Hamren-Larsson and OFX Donard (2001). Role of oceans as biogenic sources of selenium. *Earth and Planetary Science Letters* 189, 277-283.
- Amouroux, D., G. Roberts, S. Rapsomanikis, and M. O. Andreae (2002), Biogenic gas (CH₄, N₂O, DMS) emission to the atmosphere from near-shore and shelf waters of the North-Western Black Sea, *Estuarine Coastal And Shelf Science*, 54(3), 575–587.
- Anderson T. R., Spall S. A., Yool A., Cipollini P., Challenor P. G., and Fasham M. J. R.. (2001). Global fields of sea surface dimethylsulfide predicted from chlorophyll, nutrients and light. *Journal of Marine Systems*, 30(1-2):1–20.
- Andreae, M. O. (1985), Dimethylsulfide in the water column and the sediment porewaters of the Peru upwelling area, *Limnology And Oceanography*, 30(6), 1208–1218.
- Andreae, M. O., and D. Rosenfeld (2008), Aerosol-cloud-precipitation interactions. Part 1. The nature and sources of cloud-active aerosols, *Earth Science Reviews*, 89(1–2), 13–41, doi:10.1016/j.earscirev.2008.03.001.
- Andreae, M. O., and H. Raemdonck (1983), Dimethyl sulfide in the surface ocean and the marine atmosphere - a global view, *Science*, 221(4612), 744–747.
- Andreae, M. O., and P. J. Crutzen (1997), Atmospheric aerosols: biogeochemical sources and role in atmospheric chemistry, *Science*, 276(5315), 1052–1058.
- Andreae, M. O., and W. R. Barnard (1984), The marine chemistry of dimethylsulfide, *Marine Chemistry*, 14(3), 267–279.
- Andreae, M. O., W. Elbert, and S. J. Demora (1995), Biogenic sulfur emissions and aerosols over the tropical South Atlantic: 3. Atmospheric dimethylsulfide, aerosols and cloud condensation nuclei, *Journal of Geophysical Research*, 100(D6), 11,335–11,356.
- Andreae, M. O., W. Elbert, Y. Cai, T. W. Andreae, and J. Gras (1999), Nonsea-salt sulfate, methanesulfonate, and nitrate aerosol concentrations and size distributions at Cape Grim, Tasmania, *J. Geophys. Res.*, 104(D17), 21,695– 21,706, doi:10.1029/1999JD900283.
- Andreae, M.O. (2007) Aerosols Before Pollution. *Science*, Vol. 315, no. 5808, pp. 50-51. doi: 10.1126/science.1136529.
- Andreae, T. W., M. O. Andreae, and G. Schebeske (1994), Biogenic sulfur emissions and aerosols over the tropical South-Atlantic .1. dimethylsulfide in seawater and in the atmospheric boundary-layer, *Journal of Geophysical Research - Atmos.*, 99(D11), 22,819–22,829.
- Andreas, E. L. (2002), A review of the sea spray generation function for the open ocean, in *Atmosphere-Ocean Interactions*, vol. 1, edited by W. A. Perrie, pp. 1 – 46, WIT Press, Southampton, UK.

-
- Archer, S. D., D. G. Cummings, C. A. Llewellyn, and J. R. Fishwick (2009), Phytoplankton taxa, irradiance and nutrient availability determine the seasonal cycle of DMSP in temperate shelf seas, *Marine Ecology Progress Series*, 394, 111–124, doi:10.3354/meps08284.
- Arnold, S. R., D.V. Spracklen, J. Williams, N. Yassaa, J. Sciare, B. Bonsang, V. Gros, I. Peeken, A. C. Lewis, S. Alvain, C. Moulin (2009), Evaluation of the global oceanic isoprene source and its impacts on marine organic carbon aerosol, *Atmospheric Chemistry and Physics*, 9, 1253–1262.
- Aumont O., Belviso S., and Monfray P. (2002). Dimethylsulfoniopropionate (DMSP) and dimethylsulfide (DMS) sea surface distributions simulated from a global three-dimensional ocean carbon cycle model. *Journal of Geophysical Research Oceans*, 107(C4):3029. doi: 10.1029/1999JC000111.
- Baboukas, E., J. Sciare, and N. Mihalopoulos (2004), Spatial, temporal and interannual variability of methanesulfonate and non-sea-salt sulfate in rainwater in the southern Indian Ocean (Amsterdam, Crozet and Kerguelen Islands), *Journal of Atmospheric Chemistry*, 48, 35–37.
- Bailey, K. E., DA Toole, B Blomquist, RG Najjar, B Huebert, DJ Kieber, RP Kiene, P Matrai, GR Westby, DA del Valle (2008), Dimethylsulfide production in Sargasso Sea eddies, *Deep Sea Research. Part II*, 55(10-13), 1491–1504, doi: 10.1016/j.dsr2.2008.02.011.
- Baker, A. R., S. M. Turner, W. J. Broadgate, A. Thompson, G. B. McFiggans, O. Vesperini, P. D. Nightingale, P. S. Liss, and T. D. Jickells (2000), Distribution and sea-air fluxes of biogenic trace gases in the Eastern Atlantic Ocean, *Global Biogeochemical Cycles*, 14(3), 871–886.
- Bange, H.W. (2006). New Directions: The importance of oceanic nitrous oxide emissions. *Atmospheric Environment* 40, 198-199.
- Barnard, W. R., M. O. Andreae, and R. L. Iverson (1984), Dimethylsulfide and *Phaeocystis poucheti* in the southeastern Bering Sea, *Continental Shelf Research*, 3(2), 103–113.
- Barnard, W. R., M. O. Andreae, W. E. Watkins, H. Bingemer, and H. W. Georgii (1982), The flux of dimethylsulfide from the oceans to the atmosphere, *Journal Of Geophysical Research Oceans And Atmospheres*, 87(NC11), 8787–8793.
- Barnes I., Hjorth J., Mihalopoulos N. (2006). Dimethyl sulfide and dimethyl sulfoxide and their oxidation in the atmosphere. *Chemical Reviews*, 106, 3, pp. 940-975 doi: 10.1021/cr020529.
- Barnes, I., Bastian, V., Becker, K. H., and Overath, R. D. (1991) Kinetic studies of the reactions of IO, BrO and ClO with DMS, *International Journal of Chemical Kinetics*, 23, 579–591.
- Barnes, S. L. (1964), A technique for maximizing details in numerical weather map analysis, *Journal of Applied Meteorology*, 3(4), 396–409.
- Barnes, S. L. (1994), Applications of the Barnes Objective Analysis Scheme. Part III: Tuning for minimum error, *Journal of Atmospheric and Oceanic Technology*, 11(6), 1459–1479.
- Barrie, L. A., Y.Yi, WR Leach, U. Lohmann, P. Kasibhatla, G.-J. Roelofs, J. Wilson, F. McGovern, C. Benkovitz, MA Melieres, K. Law, J. Prospero, M. Kritz, D. Bergmann, C. Bridgeman, M. Chin, J Christensen, R. Easter, J. Feichter, C. Land, A. Jeuken, E. Kjellstrom, D. Koch, P. Rasch (2001), A comparison of large-scale atmospheric sulphate aerosol models (COSAM): overview and highlights, *Tellus Series B-Chemical And Physical Meteorology*, 53 (5), 615–645.
- Bates, T. S., K. C. Kelly, J. E. Johnson, and R. H. Gammon (1996), A reevaluation of the open ocean source of methane to the atmosphere, *Journal of Geophysical Research*, 101(D3), 6953–6961.

- Bates T.S, Calhoun J.A., Quinn P.K., (1992a), Variations in the methanesulfonate to sulfate molar ratio in submicrometre marine aerosol particles over the Pacific Ocean. *Journal of Geophysical Research* 1992, 97, 9859.
- Bates T.S., Lamb B.K., Guenther A., Dignon J., and Stoiber R.E. (1992). Sulfur emissions to the atmosphere from natural sources. *Journal of Atmospheric Chemistry*, 14:315–337.
- Bates, T. S., and J. D. Cline (1985), The role of the ocean in a regional sulfur cycle, *Journal of Geophysical Research Oceans*, 90(NC5), 9168–9172.
- Bates, T. S., and P. K. Quinn (1997), Dimethylsulfide (DMS) in the equatorial Pacific Ocean (1982 to 1996): Evidence of a climate feedback?, *Geophysical Research Letters*, 24, 861–864.
- Bates, T. S., P.K. Quinn, D.J. Coffman, J.E. Johnson, T.L. Miller, D.S. Covert, A. Wiedensohler, S. Leinert, A. Nowak and C. Neusüss (2001), Regional physical and chemical properties of the marine boundary layer aerosol across the Atlantic during AEROSOLS99: An overview, *Journal of Geophysical Research Atmos.*, 106(D18), 20,767–20,782.
- Bates, T. S., J. A. Calhoun, and P. K. Quinn (1992), Variations in the methanesulfonate to sulfate molar ratio in submicrometer marine aerosol-particles over the South-Pacific Ocean, *Journal of Geophysical Research Atmos.*, 97(D9), 9859–9865.
- Bates, T. S., J. D. Cline, R. H. Gammon, and S. R. Kellyhansen (1987), Regional and seasonal-variations in the flux of oceanic dimethylsulfide to the atmosphere, *Journal of Geophysical Research Oceans*, 92(C3), 2930–2938.
- Bates, T. S., J. E. Johnson, P. K. Quinn, P. D. Goldan, W. C. Kuster, D. C. Covert, and C. J. Hahn (1990), The biogeochemical sulfur cycle in the marine boundary-layer over the Northeast Pacific- Ocean, *Journal Of Atmospheric Chemistry*, 10(1), 59–81.
- Bates, T. S., K. C. Kelly, and J. E. Johnson (1993), Concentrations and fluxes of dissolved biogenic gases (DMS, CH₄, CO, CO₂) in the equatorial Pacific during the SAGA-3 experiment, *Journal of Geophys Res Atmos*, 98(D9), 16,969–16,977.
- Bates, T. S., R. P. Kiene, G. V. Wolfe, P. A. Matrai, F. P. Chavez, K. R. Buck, B. W. Blomquist, and R. L. Cuhel (1994), The cycling of sulfur in surface seawater of the Northeast Pacific, *Journal of Geophysical Research Oceans*, 99(C4), 7835–7843.
- Bates, T. S., V. N. Kapustin, P. K. Quinn, D. S. Covert, D. J. Coffman, C. Mari, P. A. Durkee, W. J. De Bruyn, and E. S. Saltzman (1998), Processes controlling the distribution of aerosol particles in the lower marine boundary layer during the first aerosol characterization experiment (ACE 1), *Journal of Geophysical Research Atmosphere*, 103(D13), 16,369–16,383.
- Bauer, H., Giebl, H., Hitzenberger, R., Kasper-Giebl, A., Reischl, G., Zibuschka, F., Puxbaum, H. (2003), Airborne bacteria as cloud condensation nuclei. *Journal of Geophysical Research (Atmosphere)* 108 (D21) AAC 2/1-AAC 2/5.
- Bedjanian, Y., Poulet, G., and Bras, G. L. (1996) Kinetic study of the reaction of BrO radicals with dimethylsulfide, *International Journal of Chemical Kinetics*, 28, 383–389.
- Bell, T. G., G. Malin, C. M. McKee, and P. S. Liss (2006), A comparison of dimethylsulphide (DMS) data from the Atlantic Meridional Transect (AMT) programme with proposed algorithms for global surface dms concentrations, *Deep Sea Research. Part II*, 53(14-16), 1720–1735, doi:10.1016/j.dsr2.2006.05.013.
- Bell, T.G., A.J. Poulton, and G. Malin. (2010). Strong linkages between dimethylsulphoniopropionate (DMSP) and phytoplankton community physiology in a large subtropical and tropical Atlantic

-
- Ocean data set, *Global Biogeochem. Cycles*, 24, GB3009, doi:10.1029/2009GB003617.
- Belviso S., Moulin C., Bopp L., and Stefels J. (2004). Assessment of a global climatology of oceanic dimethylsulfide (DMS) concentrations based on SeaWiFS imagery (1998-2001). *Canadian Journal of Fisheries and Aquatic Sciences*. 61:804–816(13). doi: 10.1139/F04-001.
- Belviso, S., A. Sciandra, and C. Copin-Montegut (2003), Mesoscale features of surface water DMSP and DMS concentrations in the Atlantic Ocean off Morocco and in the Mediterranean Sea, *Deep Sea Research. Part I*, 50(4), 543–555.
- Belviso, S., and G. Caniaux (2009), A new assessment in North Atlantic waters of the relationship between DMS concentration and the upper mixed layer solar radiation dose, *Global Biogeochemical Cycles*, 23, GB1014, doi:10.1029/2008GB003382.
- Belviso, S., C. Moulin, L. Bopp, and J. Stefels (2004a), Assessment of a global climatology of oceanic dimethylsulfide (DMS) concentrations based on SeaWiFS imagery (1998-2001), *Canadian Journal Of Fisheries And Aquatic Sciences*, 61(5), 804–816. doi:10.1139/F04-001.
- Belviso, S., L. Bopp, I. C. Moulin, J.C. Orr, T.R. Anderson, O. Aumont, S. Chu, Elliott, M.E. Maltrud, R. Simó (2004b), Comparison of global climatological maps of sea surface dimethyl sulfide, *Global Biogeochemical Cycles*, 18, GB3013, doi:10.1029/2003GB002193.
- Belviso, S., L. Bopp, J. Mosseri, M. Tedetti, N. Garcia, B. Griffiths, F. Joux, I. Obernosterer, J. Uitz, M. J. W. Veldhuis (2008), Effect of natural iron fertilisation on the distribution of DMS and DMSP in the Indian sector of the Southern Ocean, *Deep Sea Research. Part II*, 55(5-7), 893–900.
- Belviso, S., P. Buatmenard, J. P. Putaud, B. C. Nguyen, H. Claustre, and J. Neveux (1993), Size distribution of dimethylsulfoniopropionate (DMSP) in areas of the Tropical Northeastern Atlantic-Ocean and the Mediterranean-Sea, *Marine Chemistry*, 44(1), 55–71.
- Belviso, S., R. Morrow, and N. Mihalopoulos (2000), An Atlantic Meridional Transect of surface water dimethyl sulfide concentrations with 10-15 km horizontal resolution and close examination of ocean circulation, *Journal of Geophysical Research Atmospheres*, 105(D11), 14,423–14,431.
- Berresheim, H. (1987), Biogenic sulfur emissions from the Sub-Antarctic and Antarctic Oceans, *Journal of Geophysical Research Atmospheres*, 92(D11), 13,245–13,262.
- Berresheim, H., J. W. Huey, R. P. Thorn, F. L. Eisele, D. J. Tanner, and A. Jefferson (1998), Measurements of dimethyl sulfide, dimethyl sulfoxide, dimethyl sulfone, and aerosol ions at Palmer station, Antarctica, *Journal Of Geophysical Research-Atmospheres*, 103(D1), 1629–1637.
- Berresheim, H., M. O. Andreae, G. P. Ayers, and R. W. Gillett (1989), Distribution of biogenic sulfur-compounds in the remote Southern-Hemisphere, *ACS Symposium Series*, 393, 352–366.
- Berresheim, H., M. O. Andreae, R. L. Iverson, and S. M. Li (1991), Seasonal-variations of dimethylsulfide emissions and atmospheric sulfur and nitrogen species over the Western North-Atlantic Ocean, *Tellus Series B-Chemical And Physical Meteorology*, 43(5), 353–372.
- Besiktepe, S., K. W. Tang, M. Vila, and R. Simo (2004), Dimethylated sulfur compounds in seawater, seston and mesozooplankton in the seas around turkey, *Deep Sea Research Part I*, 51(9), 1179–1197.
- Bingemer, H. (1984), Dimethylsulfid in ozean und mariner atmosphere - experimentelle untersuchung einer natuerlichen schwefelquelle for die atmosphere., Ph.D. thesis, Univ. Frankfurt/Main, Frankfurt, Germany.
- Bingemer, H. W. G. S. B., H., and G. Ockelmann (1987), Die Bedeutung biogener Schwefelemissionen

- for den tropospherischen Schwefelkreislauf, in *Atmosphärische Spurenstoffe*, Dtsch. Forsch., Weinheim. Germany.
- Blando, J.D., Turpin, B.J. (2000), Secondary organic aerosol formation in cloud and fog droplets: a literature evaluation of plausibility. *Atmospheric Environment* 34, 1623–1632.
- Blomquist, B. W., A. R. Bandy, and D. C. Thornton (1996), Sulfur gas measurements in the eastern North Atlantic Ocean during the Atlantic stratocumulus transition experiment marine aerosol and gas exchange, *Journal of Geophysical Research Atmospheres*, 101(D2), 4377–4392.
- Boniforti, R., P. Emaldi, R. Ferraroli, M. Maspero, R. Nair, and A. Novo (1993), Preliminary data on DMS concentration in seawater samples collected from the la-spezia Gulf (Ligurian sea), *Dimethylsulfide: Oceans, Atmosphere And Climate*, pp. 163–172.
- Bonsang, B., A. A. Aarbaoui, and J. Sciare (2008), Diurnal variation of non-methane hydrocarbons in the subantarctic atmosphere, *Environmental Chemistry*, 5(1), 16–23, doi:10.1071/EN07018.
- Bonsang, B., C. Polle, and G. Lambert (1992), Evidence for marine production of isoprene, *Geophysical Research Letters*, 19, 1129–1132, doi:10.1029/92GL00083.
- Bopp, L., O. Aumont, S. Belviso, and S. Blain (2008), Modelling the effect of iron fertilization on dimethylsulphide emissions in the Southern Ocean, *Deep Sea Research Part II-Topical Studies in Oceanography*, 55(5-7), 901–912.
- Bouillon, R. C., P. A. Lee, S. J. de Mora, M. Levasseur, and C. Lovejoy (2002), Vernal distribution of dimethylsulphide, dimethylsulphonioacetate, and dimethylsulphoxide in the North water in 1998, *Deep-Sea Research Part II-Topical Studies in Oceanography*, 49(22-23), 5171–5189.
- Bowers, R.M., Lauber, C.L., Wiedinmyer, C., Hamady, M., Hallar, A.G., Fall, R., Knight, R., Fierer, N. (2009), Characterization of airborne microbial communities at a high-elevation site and their potential to act as atmospheric ice nuclei. *Applied and Environmental Microbiology* 75, 5121–5130.
- Brasseur, G.P., R.G. Prinn, and A.A.P. Pszenny (2003), *Atmospheric Chemistry in a Changing World*. Springer Verlag, Berlin.
- Bréon F.M., D. Tanré, S. Generoso (2002), Aerosol effect on cloud droplet size monitored from satellite. *Science* 295, 834-838.
- Brimblecombe, P., and D. Shooter (1986), Photooxidation of dimethylsulfide in aqueous-solution, *Marine Chemistry*, 19(4), 343–353.
- Broadgate, W., Liss, P., and Penkett, S. (1997), Seasonal emissions of isoprene and other reactive hydrocarbon gases from the ocean, *Geophysical Research Letters*, 24(21), 2675–2678.
- Brock T.D.(1981). Calculating solar radiation for ecological studies. *Ecol Model*, 14 (1- 2).
- Brown, R. M., Larson, D. A. and Bold, H. C. (1964), Airborne algae: Their abundance and heterogeneity. *Science* 143, 583-585.
- Butler, J.H. (2000). Better budgets for methyl halides? *Nature* 403, 260-261.
- Burgermeister, S., R. L. Zimmermann, H. W. Georgii, H. G. Bingemer, G. O. Kirst, M. Janssen, and W. Ernst (1990), On the biogenic origin of dimethylsulfide - relation between Chlorophyll, ATP, organismic DMSP, phytoplankton species, and DMS distribution in Atlantic surface-water and atmosphere, *Journal Of Geophysical Research-Atmospheres*, 95(D12), 20,607–20,615.
- Caffrey, P. F., Hoppel, W. A., and Shi, J. J.(2006), A one-dimensional sectional aerosol model integrated with mesoscale meteorological data to study marine boundary layer aerosol dynamics, *Journal Of Geophysical Research* , 111, D24201, doi:10.1029/2006JD007237.

-
- Cantin, G., M. Levasseur, M. Gosselin, and S. Michaud (1996), Role of zooplankton in the mesoscale distribution of surface dimethylsulfide concentrations in the Gulf of St Lawrence, Canada, *Marine Ecology-Progress Series*, 141(1-3), 103–117.
- Carlton, A. G., C. Wiedinmyer, and J. H. Kroll (2009), A review of secondary organic aerosol (SOA) formation from isoprene, *Atmospheric Chemistry and Physics*, 9, 4987–5005, doi:10.5194/acp-9-4987-2009.
- Carslaw, K. S., O. Boucher, D. V. Spracklen, G. W. Mann, J.G.L. Rae, S. Woodward, M. Kulmala (2010), A review of natural aerosol interactions and feedbacks within the Earth system, *Atmospheric Chemistry and Physics*, 10(4), 1701–1737, doi:10.5194/acp-10-1701-2010.
- Cavalli, F. M.C. Facchini, S. Decesari, M. Mircea, L. Emblico and S. Fuzzi (2004), Advances in characterization of size-resolved organic matter in marine aerosol over the North Atlantic, *Journal of Geophysical Research* 109, D24215, doi:10.1029/2004JD005137.
- Charlson, R. J., J. E. Lovelock, M. O. Andreae, and S. G. Warren (1987), Oceanic phytoplankton, atmospheric sulfur, cloud albedo and climate, *Nature*, 326(6114), 655–661.
- Charlson, R. J., S. E. Schwartz, J. M. Hales, R. D. Cess, J. Coakley, J. A., J. E. Hansen, and D. J. Hofmann (1992), Climate forcing by anthropogenic aerosols, *Science*, 255 (5043), 423–430.
- Chen J.-P., T.-S. Tsai, and S.-C. Liu (2011), Aerosol nucleation spikes in the planetary boundary layer. *Atmospheric Chemistry and Physics*, 11, 7171–7184. doi:10.5194/acp-11-7171-2011.
- Chin, M., R. B. Rood, S. J. Lin, J. F. Muller, and A. M. Thompson (2000), Atmospheric sulfur cycle simulated in the global model GOCART: Model description and global properties, *Journal Of Geophysical Research-Atmospheres*, 105 (D20), 24,671-24,687,doi:10.1029/2000JD900384.
- Christner, B. C., C. E. Morris, C. M. Foreman, C. Rongman, and D. C. Sands (2008), Ubiquity of biological ice nucleators in snowfall, *Science*, 319, 1214, doi:10.1126/science.1149757.
- Chu, S. P., S. Elliott, and M. E. Maltrud (2003), Global eddy permitting simulations of surface ocean nitrogen, iron, sulfur cycling, *Chemosphere*, 50(2), 223-235.
- Chuang PY., DR Collins, H. Pawlowska, JR Snider, HH Jonsson, JL Brenguier, RC Flagan, JH Seinfeld (2000), CCN measurements during ACE-2 and their relationship to cloud microphysical properties. *Tellus* 52B, 843–867.
- Chuck, A. L., S. M. Turner, and P. S. Liss (2005), Oceanic distributions and air-sea fluxes of biogenic halocarbons in the open ocean, *Journal Of Geophysical Research-Oceans*, 110(C10).
- Chuck, A.L., S.M. Turner, and P.S. Liss (2002), Direct evidence for a marine source of C₁ and C₂ alkyl nitrates. *Science* 297, 1151-1154.
- Clarke A.D., Li Z., and Litchy M. (1996), Aerosol dynamics in the equatorial Pacific Marine boundary layer: Microphysics, diurnal cycles and entrainment. *Geophysical Research Letters*, 23, 7, pp. 733-736.
- Clarke, A. D., J. L. Varner, F. Eisele, R. L. Mauldin, D. Tanner, and M. Litchy (1998), Particle production in the remote marine atmosphere: Cloud outflow and subsidence during ACE 1, *Journal Of Geophysical Research*, 103, 16,397–16,409, doi:10.1029/97JD02987.
- Cline, J. D., and T. S. Bates (1983), Dimethyl sulfide in the equatorial Pacific-Ocean - a natural source of sulfur to the atmosphere, *Geophysical Research Letters*, 10(10), 949–952.
- Costantino L., F.M. Bréon (2010), Analysis of aerosol-cloud interaction from multi-sensor satellite observations. *Geophysical Research Letters* 37, L11801, doi:10.1029/2009GL041828.
- Coulier P.J. (1875) Note sur une nouvelle propriete de l'air, *Journal de Pharmacie et de Chimie* 4:165-

- 172.
- Covert, D. S., V. N. Kapustin, P. K. Quinn, and T. S. Bates (1992), New particle formation in the marine boundary layer, *Journal Of Geophysical Research*, 97, 20,581–20,589.
- Crahan, K. K., D. Hegg, D. S. Covert, and H. Jonsson (2004), An exploration of aqueous oxalic acid production in the coastal marine atmosphere, *Atmospheric Environment*, 38, 3757–3764, doi:10.1016/j.atmosenv.2004.04.009.
- Cressman, G. (1959), An operational objective analysis system, *Mon. Weather Rev.*, 87, 367–374.
- Curran, M. A. J., G. B. Jones, and H. Burton (1998), Spatial distribution of dimethylsulfide and dimethylsulfoniopropionate in the Australasian sector of the Southern Ocean, *Journal Of Geophysical Research*, 103, 16,677–16,689.
- Dacey J.W.H., Howse F.A., Michaels A.F., Wakeham S.G. (1998). Temporal variability of dimethylsulfide and dimethylsulfoniopropionate in the Sargasso Sea. *Deep-Sea Research Pt I*. 45 (12) 2085.
- Dacey, J. W. H., S. G. Wakeham, and B. L. Howes (1984), Henry Law constants for dimethylsulfide in fresh-water and seawater, *Geophysical Research Letters*, 11(10), 991–994.
- Dachs, J. Encinar, C., Galbán-Malagón, C., Zúniga, J. Berrojalbiz, N. (2012). Large volatilization fluxes of aliphatic hydrocarbons from the Mediterranean Sea and implications for secondary aerosol formation. In preparation.
- Dachs, J., Calleja, M.LL., C.M. Duare, S. Del Vento, B. Turpin, A. Polidori, G. J. Herndl, S. Agustí. (2005). High atmosphere-ocean exchange of organic carbon in the NE subtropical Atlantic. *Geophysical Research Letters* 32, L21807, doi:10.1029/2005GL023799.
- Daley, R. (1993), *Atmospheric Data Analysis*, Cambridge Univ Press, Cambridge, U.
- Darwin C. (1846) An account of the Fine Dust which often falls on Vessels in the Atlantic Ocean. *Q. J. Geol. Soc. London* 2, 26–30.
- Dasgupta S., Singh R.P, and Kafatos M. (2009). Comparison of global chlorophyll concentrations using MODIS data. *Advances in Space Research*, 43(7):1090–1100. doi: 10.1016/j.asr.2008.11.009.
- de Boyer Montégut C., Madec G., Fischer A.S., Lazar A., and Iudicone D. (2004). Mixed layer depth over the global ocean: An examination of profile data and a profile-based climatology. *Journal Of Geophysical Research*, 109, C12003. doi: 10.1029/2004JC002378
- de Leeuw, G., E. L. Andreas, M. D. Anguelova, C. W. Fairall, E. R. Lewis, C. O’Dowd, M. Schulz, and S. E. Schwartz (2011), Production flux of sea spray aerosol, *Reviews of Geophysics*, 49, RG2001, doi:10.1029/2010RG000349.
- Deal, C. J., D. J. Kieber, D. A. Toole, K. Stamnes, S. Jiang, and N. Uzuka (2005), Dimethylsulfide photolysis rates and apparent quantum yields in Bering Sea seawater, *Continental Shelf Research*, 25(15), 1825–1835.
- del Valle, D. A., D. J. Kieber, D. A. Toole, J. Bisgrove, and R. P. Kiene (2009a), Dissolved DMSO production via biological and photochemical oxidation of dissolved DMS in the Ross Sea, Antarctica, *Deep-Sea Research Part I-Oceanographic Research Papers*, 56(2), 166–177.
- del Valle, D. A., D. J. Kieber, D. A. Toole, J. Brinkley, and R. P. Kiene (2009), Biological consumption of dimethylsulfide (DMS) and its importance in DMS dynamics in the Ross Sea, Antarctica, *Limnology And Oceanography*, 54(3), 785–798.
- del Valle, D. A., D. J. Kieber, J. Bisgrove, and R. P. Kiene (2007), Light-stimulated production of dissolved DMSO by a particle-associated process in the Ross Sea, Antarctica, *Limnology And*

-
- Oceanography, 52, 2456–2466.
- Delort, A.-M., Vařtilingom, M., Amato, P., Sancelme, M., Parazols, M., Mailhot, G., Laj, P., and Deguillaume, L. (2010), A short overview of the microbial population in clouds: Potential roles in atmospheric chemistry and nucleation processes, *Atmospheric Research*, 98, 249–260, doi:10.1016/j.physletb.2003.10.071.
- Denman, K.L. et al. (2007). Couplings Between Changes in the Climate System and Biogeochemistry. In: *Climate Change 2007: The Physical Science Basis. Contribution of Working Group I to the Fourth Assessment Report of the Intergovernmental Panel on Climate Change* [Solomon, S., D. Qin, M. Manning, Z. Chen, M. Marquis, K.B. Averyt, M. Tignor and H.L. Miller (eds.)]. Cambridge University Press, Cambridge, United Kingdom and New York, NY, USA.
- Derevianko G. J., Deutsch C., and Hall A. (2009). On the relationship between ocean DMS and solar radiation. *Geophysical Research Letters* 36:L17606. 10.1029/2009GL039412.
- Devred, E., S. Sathyendranath, and T. Platt (2007), Delineation of ecological provinces using ocean colour radiometry, *Marine Ecology Progress Series*, 346, 1–13, doi:10.3354/meps07149.
- DiTullio, G. R., and W. O. Smith (1993), Dimethyl sulfide concentrations near the Antarctic Peninsula: November, 1992, *Antarct., J. U. S.*, pp. 130–132.
- DiTullio, G. R., and W. O. Smith (1995), Relationship between dimethylsulfide and phytoplankton pigment concentrations in the Ross Sea, Antarctica, *Deep-Sea Research Part I-Oceanographic Research Papers*, 42(6), 873–892.
- Ehrenberg (1830). *Ann. Phys. U. Chem.*, Vol. 17-18, pp. 477-514. 1829-1830.
- Elliott S. (2009). Dependence of DMS global sea-air flux distribution on transfer velocity and concentration field type. *Journal Of Geophysical Research Biogeosci.*, 114:G02001. doi: 10.1029/2008JG000710.
- Elliott, S. (2009), Dependence of DMS global sea-air flux distribution on transfer velocity and concentration field type, *Journal Of Geophysical Research*, 114, G02001, doi:10.1029/2008JG000710.
- Ervens, B., G. Feingold, G. J. Frost, and S. M. Kreidenweis (2004), A modeling study of aqueous production of dicarboxylic acids: 1. Chemical pathways and speciated organic mass production, *Journal Of Geophysical Research*, 109, D15205, doi:10.1029/2003JD004387.
- Facchini (2008), A combined organic-inorganic sea-spray source function, *Geophysical Research Letters*, 35, L01801, doi:10.1029/2007GL030331.
- Facchini MC, M. Rinaldi, S. Decesari, C. Carbone, E. Finessi, M. Mircea, S. Fuzzi, D. Ceburnis, R. Flanagan, E.D. Nilsson, G. de Leeuw, M. Martino, J. Woeltjen, C.D. O’Dowd (2008), Primary submicron marine aerosol dominated by insoluble organic colloids and aggregates. *Geophysical Research Letters* 35(L17814).
- Feingold, G. WL Eberhard, DE Veron, and Michael Previdi (2003), First measurements of the Twomey indirect effect using ground-based remote sensors, *Geophysical Research Letters* 30(6), 1287, doi:10.1029/2002GL016633
- Fiore, A., D. J. Jacob, H. Liu, R. M. Yantosca, T. D. Fairlie, and Q. Li (2003), Variability in surface ozone background over the united states: Implications for air quality policy, *Journal Of Geophysical Research-Atmospheres*, 108 (D24), 4787.
- Forster, P., V. Ramaswamy, P. Artaxo, T. Berntsen, R. Betts, D.W. Fahey, J. Haywood, J. Lean, D.C. Lowe, G. Myhre, J. Nganga, R. Prinn, G. Raga, M. Schulz and R. Van Dorland (2007) Changes

- in Atmospheric Constituents and in Radiative Forcing. In: *Climate Change 2007: The Physical Science Basis. Contribution of Working Group I to the Fourth Assessment Report of the Intergovernmental Panel on Climate Change* [Solomon, S., D. Qin, M. Manning, Z. Chen, M. Marquis, K.B. Averyt, M. Tignor and H.L. Miller (eds.)]. Cambridge University Press, Cambridge, United Kingdom and New York, NY, USA.
- Fritsch, F. N., and R. E. Carlson (1980), Monotone piecewise cubic interpolation, *SIAM J. Num. Anal.*, 17(2), 238-246.
- Froelich, P. N., L. W. Kaul, J. T. Byrd, M. O. Andreae, and K. K. Roe (1985), Arsenic, barium, germanium, tin, dimethylsulfide and nutrient biogeochemistry in Charlotte Harbor, Florida, a phosphorus-enriched estuary, *Estuarine Coastal And Shelf Science*, 20(3), 239–264.
- Froyd, K.D., D. M. Murphy, T. J. Sanford, D. S. Thomson, J. C. Wilson, L. Pfister, and L. Lait. (2009) Aerosol composition of the tropical upper troposphere. *Atmospheric Chemistry and Physics*, 9, 4363–4385
- Gabric, A. J., PA Matrai, RP Kiene, RM Cropp, JWH Dacey, GR DiTullio, RG Najjar, R Simó, DA Toole, DA del Valle, D Slezak (2008), Factors determining the vertical profile of dimethylsulfide in the Sargasso Sea during summer, *Deep-Sea Research Part I-Topical Studies In Oceanography*, 55(10-13), 1505–1518.
- Gabric, A., P. H. Whetton, and R. Cropp (2001), Dimethylsulphide in the subantarctic Southern Ocean under enhanced greenhouse conditions, *Tellus, Ser. B*, 53, 273–287, doi:10.1034/j.1600-0889.2001.01244.x.
- Galí, M., and R. Simó (2010), Occurrence and cycling of dimethylated sulfur compounds in the Arctic during summer receding of the ice edge, *Marine Chemistry*, doi:10.1016/j.marchem.2010.07.003.
- Galí, M., V. Saló, R. Almeda, A. Calbet, and R. Simó (2011), Stimulation of gross dimethylsulfide (DMS) production by solar radiation, *Geophysical Research Letters*, 38, L15612, doi:10.1029/2011GL048051.
- Gantt B., N. Meskhidze, and D. Kamykowski (2009). A new physically-based quantification of marine isoprene and primary organic aerosol emissions. *Atmospheric Chemistry and Physics* 9, 4915–4927.
- Garcia, H. E., R. A. Locarnini, J. I. Antonov, and T. P. Boyer (2010), *World Ocean Database 2009*, NOAA Atlas NESDIS 71, edited by S. Levitus, U.S. Govt. Print. Off., Washington, D. C.
- Gassó S., D.A. Hegg (2003), On the retrieval of columnar aerosol mass and CCN concentration by MODIS. *Journal Of Geophysical Research*, 108(D1), 4010, doi:10.1029/2002JD002382.
- Geever, M., C. D. O’Dowd, S. van Ekeren, R. Flanagan, E. D. Nilsson, G. de Leeuw, and U. Rannik (2005), Submicron sea spray fluxes, *Geophysical Research Letters*, 32(15), L15,810.
- Gibb, S.W., R.F.C. Mantoura, P.S. Liss, and R.G. Barlow (1999). Distributions and biogeochemistries of methylamines and ammonium in the Arabian Sea. *Deep Sea Research II* 46, 593-615.
- Gibson, J. A. E., R. C. Garrick, H. R. Burton, and A. R. McTaggart (1988), Dimethylsulfide concentrations in the ocean close to the Antarctic continent, *Geomicrobiology Journal*, 6(3-4), 179–184.
- Gondwe, M, M. Krol, W. Gieskes, W. Klaassen, and H. de Baar (2003), The contribution of ocean-leaving DMS to the global atmospheric burdens of DMS, MSA, SO₂, and NSS SO₄⁼, *Global Biogeochem. Cycles*, 17, 1056, doi:10.1029/2002GB001937.

-
- Greenberg JP; Guenther AB; Turnipseed A (2005). Marine organic halide and isoprene emissions near Mace Head, Ireland, *Environmental chemistry* [1448-2517] vol.:2 num.:4 pp.:291 -294.
- Groene, T. (1995), Biogenic production and consumption of dimethylsulfide (DMS) and dimethylsulfoniopropionate (DMSP) in the marine epipelagic zone - a review, *Journal Of Marine Systems*, 6(3), 191–209.
- Hall A., X. Qu (2006), Using the current seasonal cycle to constrain snow albedo feedback in future climate change. *Geophysical Research Letters* 33, L03502, doi:10.1029/2005GL025127.
- Halloran P.R., Bell T.G., and Totterdell I.J. (2010). Can we trust empirical marine DMS parameterisations within projections of future climate?. *Biogeosciences*, 7, 1645–1656, doi:10.5194/bg-7-1645-2010.
- Harada, H., M. A. Rouse, W. Sunda, and R. P. Kiene (2004), Latitudinal and vertical distributions of particle-associated dimethylsulfoniopropionate (DMSP) lyase activity in the Western North Atlantic Ocean, *Canadian Journal Of Fisheries And Aquatic Sciences*, 61(5), 700–711.
- Hardman-Mountford, N. J., T. Hirata, K. A. Richardson, and J. Aiken (2008), An objective methodology for the classification of ecological pattern into biomes and provinces for the pelagic ocean, *Remote Sensing of Environment*, 112(8), 3341–3352, doi:10.1016/j.rse.2008.02.016.
- Harrison, E.F., P. Minnis, B.R. Barkstrom, V. Ramanathan, R.D. Cess, and G.G. Gibson (1990). Seasonal variation of cloud radiative forcing derived from the Earth Radiation Budget Experiment. *Journal Of Geophysical Research*, 95, 18687-19730.
- Hatton, A. D., G. Malin, and P. S. Liss (1999), Distribution of biogenic sulphur compounds during and just after the Southwest Monsoon in the Arabian Sea, *Deep-Sea Research Part I-Topical Studies In Oceanography*, 46(3-4), 617–632.
- Hatton, A. D., G. Malin, S. M. Turner, and P. S. Liss (1996), DMSO - a significant compound in the biogeochemical cycle of DMS, *Biological And Environmental Chemistry Of DMSP And Related Sulfonium Compounds*, pp. 405–412.
- Hatton, A. D., S. M. Turner, G. Malin, and P. S. Liss (1998), Dimethylsulphoxide and other biogenic sulphur compounds in the Galapagos Plume, *Deep-Sea Research Part Ii-Topical Studies In Oceanography*, 45(6), 1043–1053.
- Hawkins, L.N. and L. M. Russell (2010), Polysaccharides, Proteins, and Phytoplankton Fragments: Four Chemically Distinct Types of Marine Primary Organic Aerosol classified by Single Particle Spectromicroscopy. *Advances in Meteorology*, Volume 2010, Article ID 612132, doi:10.1155/2010/612132.
- Haywood, J. and Boucher, O. (2000). Estimates of the direct and indirect radiative forcing due to tropospheric aerosols: a review. *Reviews of Geophysics*, 38, 4.
- Heald, C., D.J. Jacob, R.J. Park, L.M. Russell, B.J. Huebert, J.H. Seinfeld, H. Liao, R. J. Weber. (2005). A large organic aerosol source in the free troposphere missing from current models. *Geophysical Research Letters* 32, L18809, doi: 10.1029/2009GL023831.
- Hegg, D. A., L. F. Radke, and P. V. Hobbs (1990), Particle-production associated with marine clouds, *J. Geophysical Research Letters* 95(D9), 13,917-13,926, doi:10.1029/JD095iD09p13917.
- Herrmann, H., Tilgner, A., Barzaghi, P., Majdik, Z., Gligorovski, S., Poulain, L., Monod, A. (2005), Towards a more detailed description of tropospheric aqueous phase organic chemistry: CAPRAM 3.0. *Atmospheric Environment* 39, 4351–4363.

- Holligan, P. M., E Fernandez, J Aiken, W M Balch, P Boyd, P H Burkill, M Finch, S B Groom, G Malin, K Muller, D A Purdie, C Robinson, C C Trees, S M Turner, P Vanderwal (1993), A biogeochemical study of the coccolithophore, *emiliania-huxleyi*, in the North-Atlantic, *Global Biogeochemical Cycles*, 7(4), 879–900.
- Holligan, P., S. Turner, and P. Liss (1987), Measurements of dimethyl sulphide in frontal regions, *Continental Shelf Research*, 7(2), 213–224.
- Hoppel, W. A., G. M. Frick, J. W. Fitzgerald, and B. J. Wattel (1994), A cloud chamber study of the effect that nonprecipitating water clouds have on the aerosol size distribution, *Aerosol Science and Technology*, 20, 1–30, doi:10.1080/02786829408959660.
- Hoppel, W. A., G. M. Frick, J. W. Fitzgerald, and R. E. Larson (1994), Marine boundary layer measurement of new particle formation and effects nonprecipitating clouds have on aerosol size distribution, *Journal Of Geophysical Research*, 99, 14,443–14,459.
- Howard, E. C., S. L. Sun, E. J. Biers, and M. A. Moran (2008), Abundant and diverse bacteria involved in DMSP degradation in marine surface waters, *Environmental Microbiology*, 10(9), 2397–2410, doi:10.1111/j.1462-2920.2008.01665.x.
- Hu, M., X. Tang, J. Li, and Z. Yu (1997), Flux of dimethylsulfide in the Jiaozhou Bay, China., *Journal of Environmental Science (China)*, 9, 80–85.
- Huebert, B. J., B. W. Blomquist, J. E. Hare, C. W. Fairall, J. E. Johnson, and T. S. Bates (2004), Measurement of the sea-air DMS flux and transfer velocity using eddy correlation, *Geophysical Research Letters*, 31(23), L23,113.
- Hughes, C., Malin, G., Turley, C.M., Keely, B.J., Nightingale, P.D., Liss, P.S. (2008). The production of volatile iodocarbons by biogenic marine aggregates. *Limnology and Oceanography*, 53, 867-872.
- Husar, R.B. J.S. Prospero and LL Stowe (1997), Characterization of tropospheric aerosols over the oceans with the NOAA advanced very high resolution radiometer optical thickness operational product, *Journal of Geophysical Research* 102, 16889-16909
- Iida, T., S. I. Saitoh, T. Miyamura, M. Toratani, H. Fukushima, and N. Shiga (2002), Temporal and spatial variability of coccolithophore blooms in the eastern Bering Sea, 1998–2001, *Progress in Oceanography*, 55(1–2), 165–175.
- Ingham, T., Bauer, D., Sander, R., Crutzen, P. J., and Crowley, J. N. (1999). Kinetics and products of the reactions BrO+DMS and Br+DMS at 298 k, *Journal of Physical Chemistry A*, 103, 7199–7209.
- Iverson, R. L., F. L. Nearhoof, and M. O. Andreae (1989), Production of dimethylsulfonium propionate and dimethylsulfide by phytoplankton in estuarine and coastal waters, *Limnology And Oceanography*, 34(1), 53–67.
- Jickells, T. D., S. D. Kelly, A. R. Baker, K. Biswas, P. F. Dennis, L. J. Spokes, M. Witt, and S. G. Yeatman (2003). Isotopic evidence for a marine ammonia source, *Geophysical Research Letters* 30(7), 1374, doi:10.1029/2002GL016728.
- Jickells, T. D., Liss, PS, Broadgate, W, Turner, S, Kettle, AJ, Read, J, Baker, J, Cardenas, LM, Carse, F, Hamren-Larssen, M, Spokes, L, Steinke, M, Thompson, A, Watson, A, Archer, SD, Bellerby, RGJ, Law, CS, Nightingale, PD, Liddicoat, MI, Widdicombe, CE, Bowie, A, Gilpin, LC, Moncoiffe, G, Savidge, G, Preston, T, Hadziabdic, P, Frost, T, Upstill-Goddard, R, Pedros-Alio, C, Simo, R, Jackson, A, Allen, A and DeGrandpre, MD (2008), A lagrangian biogeochemical study of an eddy in the Northeast Atlantic, *Progress In Oceanography*, 76(3),

366–398.

- Johnson, M. T., P. S. Liss, T. G. Bell, T. J. Lesworth, A. R. Baker, A. J. Hind, T. D. Jickells, K. F. Biswas, E. M. S. Woodward, and S. W. Gibb (2008), Field observations of the ocean-atmosphere exchange of ammonia: Fundamental importance of temperature as revealed by a comparison of high and low latitudes, *Global Biogeochemical Cycles*, 22, GB1019, doi:10.1029/2007GB003039.
- Jones T.A., S.A. Christopher, J. Quaas (2009), A six year satellite-based assessment of the regional variations in aerosol indirect effects. *Atmospheric Chemistry and Physics* 9, 4091–4114.
- Jurado, E., J. Dachs, C. M. Duarte, and R. Simo (2008), Atmospheric deposition of organic and black carbon to the global oceans, *Atmospheric Environment*, 42 (34), 7931–7939, doi:10.1016/j.atmosenv.2008.07.029.
- Kasamatsu, N., O. T., and M. Fukuchi (2005), Dimethylsulfide and dimethylsulfoniopropionate production in the Antarctic pelagic food web, *Ocean and Polar Research*, 27, 197–203.
- Kasamatsu, N., S. Kawaguchi, S. Watanabe, T. Odate, and M. Fukuchi (2004), Possible impacts of zooplankton grazing on dimethylsulfide production in the Antarctic Ocean, *Canadian Journal Of Fisheries And Aquatic Sciences*, 61(5), 736–743.
- Kaufman, YJ, A. Smirnov, BN Holben and O. Dubovik (2001), Baseline maritime aerosol: Methodology to derive the optical thickness and scattering properties, *Geophysical Research Letters* 28, 3251-3254.
- Kaufman, Y., D. Tanré, and O. Boucher (2002), A satellite view of aerosols in the climate system, *Nature* 419, 215–223.
- Kaufman, Y.J., Boucher, O., Tanre, D., Chin, M., Remer, L.A., Takemura, T. (2005). Aerosols anthropogenic component estimated from satellite data. *Geophysical Research Letters*, 32,17, L17804, doi: 10.1029/2005GL023125.
- Keene, WC, H Maring, JR Maben, DJ Kieber, AAP Pszenny, EE Dahl, MA Izaguirre, AJ Davis, MS Long, X Zhou, L Smoydzin and R Sander (2007), Chemical and physical characteristics of nascent aerosols produced by bursting bubbles at a model air-sea interface, *Journal Of Geophysical Research*, 112, D21202, doi:10.1029/2007JD008464.
- Kettle A.J., Andreae M.O., Amouroux D., Andreae T.W., Bates T. S., Berresheim H., Bingemer H., Boniforti R., Curran M.A.J., DiTullio G.R., Helas G., Jones G.B., Keller M.D., Kiene R.P., Leck C., Lévassieur M., Malin G., Maspero M., Matrai P., McTaggart A. R., Mihalopoulos N., Nguyen B.C., Novo A., Putaud J. P., Rapsomanikis S., Roberts G., Schebeske G., Sharma S., Simó R., Staubes R., Turner S., and Uher G. (1999). A global database of sea surface dimethylsulfide (DMS) measurements and a procedure to predict sea surface DMS as a function of latitude, longitude, and month. *Global Biogeochemical Cycles*, 13(2):399–444.
- Kettle, A. J., and M. O. Andreae (2000), Flux of dimethylsulfide from the oceans: A comparison of updated data seas and flux models, *Journal Of Geophysical Research*, 105(D22), 26,793–26,808.
- Kettle, A. J., U. Kuhn, M. von Hobe, J. Kesselmeier, and M. O. Andreae (2002). Global budget of atmospheric carbonyl sulfide: Temporal and spatial variations of the dominant sources and sinks, *Journal of Geophysical Research*, 107(D22), 4658, doi:10.1029/2002JD002187.
- Khalil, M.A.K., and R.A. Rasmussen (1999). Atmospheric methyl chloride. *Atmospheric Environment* 33, 1305-1321.

- Kieber, D. J., J. F. Jiao, R. P. Kiene, and T. S. Bates (1996), Impact of dimethylsulfide photochemistry on methyl sulfur cycling in the equatorial Pacific ocean, *Journal Of Geophysical Research-Oceans*, 101(C2), 3715–3722.
- Kiehl J.T. and Trenberth K.E. (1997). Earth's annual global mean energy budget. *B American Meteorological Society*, 78(2):197–208.
- Kiene R.P., Kieber D.J., Slezak D., Toole D.A., del Valle D.A., Bisgrove J., Brinkley J., and Rellinger A. (2007). Distribution and cycling of dimethylsulfide, dimethylsulfoniopropionate, and dimethylsulfoxide during spring and early summer in the Southern Ocean south of New Zealand. *Aquatic Sciences* 69(3). 305-319. doi: 10.1007/s00027-007-0892-3.
- Kiene, R. P. (1996), Turnover of dissolved DMSP in the estuarine and shelf waters of the northern Gulf of Mexico, in *Biological and Environmental Chemistry of DMSP and Related Sulfonium Compounds*, Plenum, New York.
- Kiene, R. P., L. J. Linn, and J. A. Bruton (2000), New and important roles for DMSP in marine microbial communities, *Journal of Sea Research*, 43(3–4), 209–224.
- Kim D., V. Ramanathan (2008), Solar radiation budget and radiative forcing due to aerosols and clouds. *Journal Of Geophysical Research* 113, D02203, doi:10.1029/2007JD008434.
- Kinne S., U Lohmann, J Feichter, M Schulz, C Timmreck, S Ghan, R Easter, M Chin, P Ginoux, T Takemura, I Tegen, D Koch, M Herzog, J Penner, G. Pitari, B Holben, T Eck, A Smirnov, O Dubovik, I Slutsker, D Tanre, O. Torres, M Mishchenko, I Geogdzhayev, DA Chu, and Y Kaufman (2003). Monthly averages of aerosol properties: A global comparison among models, satellite data, and AERONET ground data. *Journal of Geophysical Research-Atmospheres*, 108, D20, 4634. doi: 10.1029/2001JD001253.
- Kirst, G. O., M. Wanzek, R. Haase, S. Rapsomanikis, S. de Mora, G. Schebeske, and M. O. Andreae (1993), Ecophysiology of ice algae (Antarctica): dimethylsulfoniopropionate content and release of dimethylsulfide during ice melt, in *Dimethylsulphide: Oceans, Atmosphere, and Climate.*, Kluwer, Dordrecht. Germany.
- Klein S.A., D.L. Hartmann (1993), The seasonal cycle of low stratiform clouds. *J. Climate* 6, 1587-1606.
- Kloster, S., J. Feichter, E. M. Reimer, K. D. Six, P. Stier, and P. Wetzel (2006), DMS cycle in the marine ocean-atmosphere system - a global model study, *Biogeosciences*, 3 (1), 29–51.
- Koch, S. E., M. desJardins, and P. J. Kocin (1983), An interactive Barnes Objective Map Analysis Scheme for use with satellite and conventional data, *Journal of Applied Meteorology*, 22(9), 1487–1503.
- Kondo, J. (1975), Air-sea bulk transfer coefficients in diabatic conditions, *J. Meteorol.*, 9, 91–112.
- Korhonen, H., Carslaw, K. S., Spracklen, D. V., Mann, G. W., and Woodhouse, M. T. (2008), Influence of oceanic dimethyl sulphide emissions on cloud condensation nuclei concentrations and seasonality over the remote southern hemisphere oceans: A global model study, *Journal of Geophysical Research*, 113, D15204, doi:10.1029/2007JD009718.
- Kreidenweis, S., G. Tyndall, M. Barth, F. Denterner, J. Lelieveld, and M. Mozurkewich (1999). Aerosols and clouds, in *Atmospheric Chemistry and Global Change*, edited by J.J.O.G.P. Brasseur and G.S. Tyndall, pp. 117-155, Oxford Univ. Press, New York.
- Kroll, J. H., N. L. Ng, S. M. Murphy, R. C. Flagan, and J. H. Seinfeld (2006), Secondary organic aerosol formation from isoprene photooxidation, *Environmental Science and Technology*, 40,

-
- 1869–1877, doi:10.1021/es0524301.
- Krüger, O., and H. Graßl (2011), Southern Ocean phytoplankton increases cloud albedo and reduces precipitation, *Geophysical Research Letters*, 38, L08809, doi:10.1029/2011GL047116.
- Kulmala, M., V.M. Kerminen, T. Anttila, A. Laaksonen, and C.D. O’Dowd (2004). Organic aerosol formation via sulphate cluster activation. *Journal Of Geophysical Research* 109 (D4), D04205. doi:10.1029/2003JD003961.
- Kwint, R. L. J., and K. J. M. Kramer (1996), Annual cycle of the production and fate of DMS and DMSP in a marine coastal system, *Marine Ecology-Progress Series*, 134(1-3), 217–224.
- Lana A., Bell T.G., Simó R, Vallina S.M., Ballabrera-Poy J., Kettle A.J., Dachs J., Bopp L., Saltzman E.S., Stefels J., Johnson J.E, and Liss P.S. (2011). An updated climatology of surface dimethylsulfide concentrations and emission fluxes in the global ocean. *Global Biogeochemical Cycles*, 25(1):GB1004. doi: 10.1029/2010GB003850
- Lana, A., R. Simó, E. Jurado, and J. Dachs (2011c), Natural and anthropogenic drivers of the seasonality of marine aerosol-cloud interactions. In preparation.
- Lana, A., R. Simó, S.M. Vallina, and J. Dachs (2011b). Re-examination of global emerging patterns in DMS concentration. *Biogeochemistry*, doi 10.1007/s10533-011-9677-9.
- Le Clainche Y., Vecina A., Levasseur M., Cropp R., Gunson J., Vallina S.M., Vogt M., Lancelot C., Allen I., Archer S., Bopp L., Deal C., Elliott S., Jin M., Malin G., Schoemann V., Simó R., Six K. and Stefels J. (2010). A first appraisal of prognostic ocean DMS models and prospects for their use in climate models. *Global Biogeochemel Cycles*, 24, GB3021. doi: 10.1029/2009GB003721
- Leck C and Bigg EK (2007), A modified aerosol-cloud-climate feedback hypothesis. *Environmental Chemistry* 4:400–403.
- Leck, C., and C. Persson (1996), The central Arctic ocean as a source of dimethyl sulfide - seasonal variability in relation to biological activity, *Tellus Series B-Chemical And Physical Meteorology*, 48(2), 156–177.
- Leck, C., and E. K. Bigg (1999), Aerosol production over remote marine areas - A new route, *Geophysical Research Letters*, 26, 3577–3580, doi:10.1029/1999GL010807.
- Leck, C., and E. K. Bigg (2005), Source and evolution of the marine aerosol: A new perspective, *Geophysical Research Letters*, 32, L19803, doi:10.1029/2005GL023651.
- Leck, C., and E. K. Bigg (2008), Comparison of sources and nature of the tropical aerosol with the summer high arctic aerosol, *Tellus B*, doi: 10.1111/j.1600-0889.2007.00315.x
- Leck, C., and H. Rodhe (1991), Emissions of marine biogenic sulfur to the atmosphere of Northern Europe, *Journal of Atmospheric Chemistry*, 12(1), 63–86.
- Leck, C., U. Larsson, L. E. Bgander, S. Johansson, and S. Hajdu (1990), Dimethyl sulfide in the Baltic Sea: Annual variability in relation to biological activity, *Journal Of Geophysical Research*, 95, 3353–3363.
- Ledyard, K. M., and J. W. H. Dacey (1996), Kinetics of DMSP-Iyase activity in coastal seawater, in *Biological and Environmental Chemistry of DMSP and Related Sulfonium Compounds*, Plenum, New York,.
- Lee, G., J. Park, Y. Jang, M. Lee, K.-R. Kim, J.-R. Oh, D. Kim, H.-I. Yi, and T.-Y. Kim (2010), Vertical variability of seawater DMS in the South Pacific Ocean and its implication for atmospheric and surface seawater DMS, *Chemosphere*, 78(8), 1063-1070, doi:10.1016/j.

- chemosphere.2009.10.054.
- Lee, P. A., and S. J. deMora (1996), DMSP, DMS and DMSO concentrations and temporal trends in marine surface waters at Leigh, New Zealand, *Biological And Environmental Chemistry Of DMSP And Related Sulfonium Compounds*, pp. 391–404.
- Legrand, M., C. Hammer, M. De Angelis, J. Savarino, R. Delmas, H. Clausen, and S. J. Johnsen (1997), Sulfur-containing species (methanesulfonate and SO_4) over the last climatic cycle in the Greenland Ice Core Project (central Greenland) ice core, *Journal of Geophysical Research*, 102(C12), 26,663–26,679, doi:10.1029/97JC01436.
- Le-Quéré, C., and E. Saltzman (2009), *Surface Ocean Lower Atmosphere Processes*, Geophysical Monograph Series.
- Levasseur, M. (2011), If Gaia could talk, *Nature Geoscience* 4, 351–352.
- Lewis, E. R., and S. E. Schwartz (2004), *Sea salt Aerosol Production: Mechanisms, Methods, Measurements and Models—A Critical Review*, Geophysical Monograph Series, vol. 152, 413 pp., AGU, Washington, D. C. *Limnol. Oceanogr.*, 53(2), 2008, 867–872.
- Liss, P. S., A. D. Hatton, G. Malin, P. D. Nightingale, and S. M. Turner (1997), Marine sulphur emissions, *Philosophical Transactions Of The Royal Society B-Biological Sciences*, 352(1350), 159–168.
- Liss, P. S., A. J. Watson, M. I. Liddicoat, G. Malin, P. D. Nightingale, S. M. Turner, and R. C. Upstillgoddard (1993), Trace gases and air-sea exchanges, *Philosophical Transactions Of The Royal Society Of London Series A-Mathematical Physical And Engineering Sciences*, 343(1669), 531–541.
- Liss, P. S., A. L. Chuck, S. M. Turner, and A. J. Watson (2004), Air-sea gas exchange in Antarctic waters, *Antarctic Science*, 16(4), 517–529, doi:10.1017/S0954102004002299.
- Liss, P. S., and P. G. Slater (1974), Flux of gases across air-sea interface, *Nature*, 247, 181–184.
- Liss, P., and J.N. Galloway (1993). Air-sea exchange of sulphur and nitrogen and their interaction in the marine environment, in *Interactions of C, N, P and S Biogeochemical Cycles and Global Change*, edited by R. Wollast, F.T. Mackenzie and L. Chou. Pp. 258–281, Springer.
- Liss, P., and L. Merlivat (1986), Air-sea gas exchange rates: Introduction and synthesis, in *The Role of Air-Sea Exchange in Geochemical Cycling*, edited by P. Buat-Ménard, pp. 113–128, D. Reidel, Dordrecht, Netherlands.
- Liss, P.S., and J. E. Lovelock (2007), Climate change: the effect of DMS emissions. *Environmental Chemistry* 2007 4, 377–378
- Liu Z., M. Notaro, J. Kutzbach, N. Liu, (2006) Assessing global vegetation–climate feedbacks from observations. *Journal of Climate* 19, 787–814.
- Lizotte, M., M. Levasseur, M. G. Scarratt, S. Michaud, A. Merzouk, M. Gosselin, and J. Pommier (2008), Fate of dimethylsulfoniopropionate (DMSP) during the decline of the Northwest Atlantic Ocean spring diatom bloom, *Aquatic Microbial Ecology*, 52(2), 159–173. doi:10.3354/ame01232.
- Lobert, J.M., J.H. Butler, S.A. Montzka, L.S. Geller, R.C. Myers, and J.W. Elkins (1995). A net sink for atmospheric CH_3Br in the East Pacific Ocean. *Science* 267, 1002–1005.
- Locarnini, R., A. Mishonov, J. Antonov, T. Boyer, and H. Garcia (2010), *WorldOceanDatabase 2009*, NOAA Atlas NESDIS 68, edited by S. Levitus, U.S. Govt. Print. Off., Washington, D.C.
- Locarnini, S. J. P., S. M. Turner, and P. S. Liss (1998), The distribution of dimethylsulfide, DMS, and

-
- dimethylsulfoniopropionate, DMSP, in waters off the Western coast of Ireland, *Continental Shelf Research*, 18(12), 1455–1473.
- Lohmann, U. (2009), Marine Boundary Layer Clouds, in *Surface Ocean-Lower Atmosphere Processes*, Geophys. Monogr. Ser., doi: 10.1029/2008GM000769.
- Lohmann, U. and J. Feichter (2005). Global indirect aerosol effects: a review. *Atmospheric Chemistry and Physics*, 5, 715–737.
- Longhurst, A. (1998), *Ecological Geography of the Sea*, Acad. Press, London.
- Longhurst, A. (2007), *Ecological Geography of the Sea*, 2nd ed., Acad. Press, Burlington, Mass.
- Loose, B., W. R. McGillis, P. Schlosser, D. Perovich, and T. Takahashi (2009), Effects of freezing, growth, and ice cover on gas transport processes in laboratory seawater experiments, *Geophysical Research Letters*, 36, L05603, doi:10.1029/2008GL036318.
- Lovelock and Margulis (1974). Atmospheric homeostasis by and for the biosphere: the gaia hypothesis. *Tellus XXVI*, 1-2.
- Lovelock, J. E., R. J. Maggs, and Rasmussen, R.A (1972), Atmospheric dimethyl sulfide and natural sulfur cycle, *Nature*, 237(5356), 452–&.
- Lovelock, J.E. (1972). Atmospheric Dimethyl Sulphide and the Natural Sulphur Cycle. *Nature*, 237.
- Lovelock, J.E. (2003). The living Earth. *Nature*, 426.
- Marandino, C. A., W. J. De Bruyn, S. D. Miller, and E. S. Saltzman (2007), Eddy correlation measurements of the air/sea flux of dimethylsulfide over the North Pacific Ocean, *Journal Of Geophysical Research-Atmospheres*, 112(D3), D03,301.
- Marandino, C. A., W. J. De Bruyn, S. D. Miller, and E. S. Saltzman (2008), DMS air/sea flux and gas transfer coefficients from the North Atlantic summertime coccolithophore bloom, *Geophysical Research Letters*, 35(23), L23,812.
- Marandino, C. A., W. J. De Bruyn, S. D. Miller, and E. S. Saltzman (2009), Open ocean DMS air/ sea fluxes over the Eastern South Pacific Ocean, *Atmospheric Chemistry and Physics*, 9(2), 345–356.
- Marshall J., R.A. Plumb (2008) *Atmosphere, ocean, and climate dynamics: an introductory text* (Elsevier Academic Press, USA).
- Martensson, E. M., E. D. Nilsson, G. de Leeuw, L. H. Cohen, and H. C. Hansson (2003), Laboratory simulations and parameterization of the primary marine aerosol production, *Journal Of Geophysical Research*, 108(D9), 4297, doi:10.1029/2002JD002263.
- Matrai, P. A., and M. D. Keller (1993), Dimethylsulfide in a large-scale coccolithophore bloom in the Gulf of Maine, *Continental Shelf Research*, 13(8-9), 831–843.
- Matrai, P. A., and M. Vernet (1997), Dynamics of the vernal bloom in the marginal ice zone of the Barents Sea: Dimethyl sulphide and dimethylsulfoniopropionate budgets, *Journal Of Geophysical Research-Oceans*, 102(C10), 22,965–22,979.
- Matrai, P. A., D. J. Cooper, and E. S. Saltzman (1996), Frontal enhancement of dimethylsulfide concentrations across a gulf stream meander, *Journal Of Marine Systems*, 7(1), 1–8.
- Matrai, P. A., L. Tranvik, C. Leck, and J. C. Knulst (2008), Are high Arctic surface microlayers a potential source of aerosol organic precursors?, *Marine Chemistry*, 108(1-2), 109–122.
- Matrai, P. A., W. M. Balch, D. J. Cooper, and E. S. Saltzman (1993), Ocean color and atmospheric dimethyl sulfide - on their mesoscale variability, *Journal Of Geophysical Research-Atmospheres*, 98(D12), 23,469–23,476.

- Matrai, P., M. Vernet, and P. Wassmann (2007), Relating temporal and spatial patterns of DMSP in the Barents Sea to phytoplankton biomass and productivity, *Journal of Marine Systems*, 67(1–2), 83–101, doi:10.1016/j.jmarsys.2006.10.001.
- McGillis, W. R., J. W. H. Dacey, N. M. Frew, E. J. Bock, and R. K. Nelson (2000), Water-air flux of dimethylsulfide, *Journal Of Geophysical Research-Oceans*, 105 (C1), 1187–1193.
- McTaggart, A. R., and H. Burton (1992), Dimethyl sulfide concentrations in the surface waters of the Australasian Antarctic and Sub-Antarctic oceans during an austral summer, *Journal Of Geophysical Research-Oceans*, 97(C9), 14,407–14,412.
- McTaggart, A. R., and H. Burton (1992), Dimethyl Sulfide concentrations in the surface waters of the Australasian Antarctic and Subantarctic Oceans during an austral summer, *Journal Of Geophysical Research*, 97, 14,407–14,4412.
- Meier, F.C. (1935). Collecting micro-organisms from the Arctic atmosphere. *The Scientific Monthly*.
- Merzouk, A., M. Levasseur, M. Scarratt, S. Michaud, M. Lizotte, R. B. Rivkin, and R. P. Kiene (2008), Bacterial DMSP metabolism during the senescence of the spring diatom bloom in the Northwest Atlantic, *Marine Ecology-Progress Series*, 369, 1–11, doi: 10.3354/meps07664.
- Meskhidze, N. and A. Nenes (2006), Phytoplankton and cloudiness in the Southern Ocean. *Science* 2006, 314, 1419. doi:10.1126/SCIENCE.1131779.
- Metzger, A., B Verheggenb, J Dommerna, J Duplissya, ASH Prevota, E Weingartnera, I Riipinenc, M Kulmalac, DV Spracklend, KS Carslawd and U Baltenspergera (2010), Evidence for the role of organics in aerosol particle formation under atmospheric conditions, *Proceedings of the National Academy of Sciences USA*, 107, 6646–6651.
- Mihalopoulos, N. (1989), Contribution a l'étude du cycle biogéochimique de l'oxy-sulfure de carbone dans l'atmosphère, Ph.D. thesis, Univ. de Paris VII, Paris.
- Mihalopoulos, N., B. C. Nguyen, J. P. Putaud, and S. Belviso (1992), The oceanic source of carbonyl sulfide (COS), *Atmospheric Environment Part A-General Topics*, 26(8), 1383–1394.
- Miles C.J., Bell T.G., and Lenton T.M. (2009). Testing the relationship between the solar radiation dose and surface DMS concentrations using in situ data. *Biogeosciences*, 6, 1927–1934.
- Miller, M. A., and S. E. Yuter (2008), Lack of correlation between chlorophyll a and cloud droplet effective radius in shallow marine clouds, *Geophysical Research Letters*, 35, L13807, doi:10.1029/2008GL034354.
- Miyazaki, Y., K. Kawamura, and M. Sawano (2010), Size distributions of organic nitrogen and carbon in remote marine aerosols: Evidence of marine biological origin based on their isotopic ratios, *Geophysical Research Letters*, 37, L06803, doi: 10.1029/2010GL042483.
- Moore, R.M., and W. Groszko (1999). Methyl iodide distribution in the ocean and fluxes to the atmosphere, *Journal of Geophysical Research* 104(C5), 11,163–11,171.
- Moore, R.M., and N.V. Blough (2002). A marine source of methyl nitrate. *Geophysical Research Letters* 29, 10.1029/2002GL014989.
- Moore, R.M., Groszko, W., Niven, S. (1996). Ocean-atmosphere exchange of methyl chloride: results from N.W. Atlantic and Pacific Ocean studies. *Journal of Geophysical Research* 101, 28,529–28,538.
- Müller, C., Y. Iinuma, J. Karstensen, D. van Pinxteren, S. Lehmann, T. Gnauk, and H. Herrmann (2009), Seasonal variation of aliphatic amines in marine sub-micrometer particles at the Cape Verde islands, *Atmospheric Chemistry and Physics*, 9, 9587–9597.

-
- Nakajima T., A. Higurashi, K. Kawamoto, J.E. Penner (2001), A possible correlation between satellite-derived cloud and aerosol microphysical parameters. *Geophysical Research Letters* 28, 1171-1174.
- Nakano, Y., Goto, M., Hashimoto, S., Kawasaki, M., and Wallington, T. J. (2001) Cavity ring-down spectroscopic study of the reactions of Br atoms and BrO radicals with dimethyl sulfide, *Journal of Physical Chemistry A*, 105, 11 045–11 050
- Nevison, C. D., R. F. Weiss, and D. J. Erickson III (1995). Global oceanic emissions of nitrous oxide, *Journal of Geophysical Research*, 100(C8), 15,809–15,820.
- Nguyen, B. C., A. Gaudry, B. Bonsang, and G. Lambert (1978), Re-evaluation of role of dimethyl sulfide in sulfur budget, *Nature*, 275(5681), 637–639.
- Nguyen, B. C., N. Mihalopoulos, and S. Belviso (1990), Seasonal-variation of atmospheric dimethylsulfide at Amsterdam Island in the Southern Indian-ocean, *Journal Of Atmospheric Chemistry*, 11(1-2), 123–141.
- Nguyen, B. C., N. Mihalopoulos, J. P. Putaud, A. Gaudry, L. Gallet, W. C. Keene, and J. N. Galloway (1992), Covariations in oceanic dimethyl sulfide, its oxidation-products and rain acidity at Amsterdam Island in the Southern Indian-ocean, *Journal Of Atmospheric Chemistry*, 15(1), 39–53.
- Nightingale, P. D., G. Malin, C. S. Law, A. J. Watson, P. S. Liss, M. I. Liddicoat, J. Boutin, and R. C. Upstill-Goddard (2000), In situ evaluation of air-sea gas exchange parameterizations using novel conservative and volatile tracers, *Global Biogeochemical Cycles*, 14(1), 373–387.
- Nizzetto, L., Lohmann, R., Gioia, R., Jahnke, A., Temme, C., Dachs, J., Herckes, P., DiGuardo, A., Jones, K., (2008) PAHs in air and seawater along a north-south Atlantic transect: trends, processes and possible sources. *Environmental Science and Technology* 42, 1580–1585.
- O’Dowd, C. D. and Smith, M. H.(1993), Physicochemical properties of aerosols over the Northeast Atlantic – Evidence for wind-speedrelated submicron sea-salt aerosol production, *Journal Of Geophysical Research*, 98, 1137–1149.
- O’Dowd, C. D., and G. De Leeuw (2007), Marine aerosol production: a review of the current knowledge, *Philosophical Transactions Of The Royal Society A-Mathematical Physical And Engineering Sciences*, 365 (1856), 1753–1774.
- O’Dowd, C. D., B. Langmann, S. Varghese, C. Scannell, D. Ceburnis, and M. C. Facchini (2008), A combined organic-inorganic sea-spray source function, *Geophysical Research Letters*, 35 (1), L01,801.
- O’Dowd, C. D., Geever, M., Hill, M. K., Smith, M. H., and Jennings, S. G. (1998) New particle formation: Nucleation rates and spatial scales in the clean marine coastal environment, *Geophysical Research Letters*, 25, 1661–1664.
- O’Dowd, C. D., M. C. Facchini, F. Cavalli, D. Ceburnis, M. Mircea, S. Decesari, S. Fuzzi, Y. J. Yoon, and J.-P. Putaud (2004), Biogenically driven organic contribution to marine aerosol, *Nature*, 431 (7009), 676–680.
- O’Dowd, C. D., M. H. Smith, I. E. Consterdine, and J. A. Lowe (1997), Marine aerosol, sea-salt, and the marine sulphur cycle: A short review, *Atmospheric Environment*, 31, 73–80, doi:10.1016/S1352-2310(96)00106-9.
- O’Dowd, C.D., J.L. Jimenez, R. Bahreini, R.C. Flagan, J.H. Seinfeld, K. Hameri, L. Pirjola, M. Kulmala, S.G. Jennings, T. Hoffmann (2002). Marine aerosol formation from biogenic

- iodine emissions. *Nature*. Vol. 417, pp. 632-636. doi: 10.1038/nature00775.
- Oliver, M. J., and A. J. Irwin (2008), Objective global ocean biogeographic provinces, *Geophysical Research Letters*, 35, L15601, doi:10.1029/2008GL034238.
- Orellana, M.V., P.A. Matrai, C. Leck, C.D. Rauschenberg, A.M. Lee, and E. Coz (2011), Marine microgels as a source of cloud condensation nuclei in the high Arctic, *Proceedings of the National Academy of Sciences USA*, 108, 13612-13617.
- Palmer, P. I., and S. L. Shaw (2005), Quantifying global marine isoprene fluxes using MODIS chlorophyll observations, *Geophysical Research Letters*, 32 (9), L09,805.
- Penner, J. E., Hegg, D., and Leaitch, R. (2001), Unraveling the role of aerosols in climate change, *Environmental Science & Technology*, 35, 332A– 340A.
- Pérez, V., E. Fernandez, E. Maranon, P. Serret, and C. Garcia-Soto (2005), Seasonal and interannual variability of chlorophyll a and primary production in the equatorial Atlantic: In situ and remote sensing observations, *Journal of Plankton Research*, 27(2), 189–197.
- Petters, M. D., J. R. Snider, B. Stevens, G. Vali, I. Faloona, and L. Russell (2006), Accumulation mode aerosol, pockets of open cells, and particle nucleation in the remote subtropical Pacific marine boundary layer, *Journal Of Geophysical Research*, 111, D02206, doi:10.1029/2004JD005694.
- Pfannkuche, O., J. C. Duinker, G. Graf, R. Henrich, H. Thiel, , and B. Zeitzschel (1993), Meteor-berichte, in Inst. for Meereskunde der Univ. Hamburg, Hamburg, Germany.
- Pierce, J. R. and Adams, P. J. (2006), Global evaluation of CCN formation by direct emission of sea salt and growth of ultrafine sea salt, *Journal Of Geophysical Research*, 111, D06203, doi:10.1029/2005JD006186.
- Pilinis, C., D. B. King, and E. S. Saltzman (1996), The oceans: A source or a sink of methyl bromide? *Geophysical Research Letters* 23(8), 817–820.
- Pirjola L; O'Dowd CD; Brooks IM; and Kulmala M. (2000) Can new particle formation occur in the clean marine boundary layer? *Journal of Geophysical Research- Atmospheres* Vol:105, Issue:D21, pp: 26531-26546, doi: 10.1029/2000JD900310.
- Plass-Dülmer, C., R. Koppmann, M. Ratte, and J. Rudolph (1995). Light nonmethane hydrocarbons in seawater, *Global Biogeochemical Cycles* 9, 79–100.
- Platnick, S. MD King, SA Ackerman, WP Menzel, BA Baum, JC Riédi and RA Frey (2003), The MODIS cloud products: Algorithms and examples from Terra, *IEEE Transactions on Geoscience & Remote Sensing*. 41, 459–473, doi:10.1109/TGRS.2002.808301.
- Prenni, A. J., M. D. Petters, S. M. Kreidenweis, P. J. DeMott, and P. J. Ziemann (2007), Cloud droplet activation of secondary organic aerosol, *Journal Of Geophysical Research*, 112, D10223, doi:10.1029/2006JD007963.
- Preunkert, S., M. Legrand, B. Jourdain, C. Moulin, S. Belviso, N. Kasamatsu, M. Fukuchi, and T. Hirawake (2007), Interannual variability of dimethylsulfide in air and seawater and its atmospheric oxidation by-products (methanesulfonate and sulfate) at Dumont d'Urville, Coastal Antarctica (1999-2003), *Journal Of Geophysical Research-Atmospheres*, 112(D6), D06,306.
- Putaud, J. P., and B. C. Nguyen (1996), Assessment of dimethylsulfide sea-air exchange rate, *Journal Of Geophysical Research- Atmospheres*, 101(D2), 4403–4411.
- Putaud, J. P., B. Nguyen, S. Belviso, and N. Mihalopoulos (1993a), Are dimethylsulfide and condensation nuclei connected over the tropical Northeastern Atlantic Ocean? in

-
- Dimethylsulphide: Oceans, Atmosphere, and Climate., Kluwer, Dordrecht, Germany.
- Putaud, J. P., S. Belviso, B. C. Nguyen, and N. Mihalopoulos (1993b), Dimethylsulfide, aerosols, and condensation nuclei over the tropical Northeastern Atlantic-ocean, *Journal Of Geophysical Research-Atmospheres*, 98(D8), 14,863–14,871.
- Quinn, P., R.J. Charlson, and T.S. Bates (1988). Simultaneous observations of ammonia in the atmosphere and ocean. *Nature* 335, 336-338.
- Quinn P.K., D.J. Coffman. (1999), Comment on “Contribution of different aerosol species to the global aerosol extinction optical thickness: Estimates from model results” by Tegen et al. *Journal of Geophysical Research-Atmospheres*. Vol. 104 (D4) pp: 4241-4248. doi:10.1029/1998JD200066.
- Quinn, P. K., T. S. Bates, J. E. Johnson, D. S. Covert, and R. J. Charlson (1990), Interactions between the sulfur and reduced nitrogen cycles over the central Pacific-ocean, *Journal Of Geophysical Research-Atmospheres*, 95(D10), 16,405–16,416.
- Quinn, PK, Coffman DJ, Kapustin VN, Bates TS, and Covert, DS. (1998) Aerosol optical properties in the marine boundary layer during the First Aerosol Characterization Experiment (ACE 1) and the underlying chemical and physical aerosol properties. *Journal of geophysical research* [0148-0227] vol.:103 núm.:D13 pp.:16547 -16563.
- Ramanathan, V., R.D. Cess, E.F. Harrison, P. Minnis, B.R. Barkstrom, E. Ahmad, and D. Hartmann (1989). Cloud-radiative forcing and climate: Results from the Earth Radiation Budget Experiment. *Science*, 243, 57-63.
- Remer, L.A. Y.J. Kaufman, D. Tanré, S. Mattoo, D.A. Chu, J.V. Martins, R.-R. Li, C. Ichoku, R.C. Levy, R.G. Kleidman, T.F. Eck, E. Vermote, and B.N. Holben (2005), The MODIS aerosol algorithm, products, and validation, *Journal of the Atmospheric Sciences* 62, 947–973, doi:10.1175/JAS3385.1.
- Rhee, T. S., A. J. Kettle, and M. O. Andreae (2009). Methane and nitrous oxide emissions from the ocean: A reassessment using basin-wide observations in the Atlantic, *Journal of Geophysical Research*, 114, D12304, doi:10.1029/2008JD011662.
- Rinaldi, M., S. Decesari, E. Finessi, L. Giulianelli, C. Carbone, S. Fuzzi, C.D. O’Dowd, D. Ceburnis, and MC. Facchini. (2010), Primary and secondary organic marine aerosol and oceanic biological activity: Recent results and new perspectives for future studies. *Advances in Meteorology*, Article ID 310682, doi:10.1155/2010/310682.
- Rinaldi, M., S. Decesari, C. Carbone, E. Finessi, S. Fuzzi, D. Ceburnis, C.D. O’Dowd, J. Sciare, J.P. Burrows, M. Vrekoussis, B. Ervens, K. Tsigaridis, and M.C. Facchini, (2011), Evidence of a natural marine source of oxalic acid and a possible link to glyoxal, *Journal of Geophysical Research*, 116, D16204, doi:10.1029/2011JD015659.
- Roesler, E. L., and J. E. Penner (2010), Can global models ignore the chemical composition of aerosols?, *Geophysical Research Letters*, 37, L24809, doi:10.1029/2010GL044282.
- Rosenfeld D. (2000), Suppression of rain and snow by urban and industrial air pollution. *Science* 287, 1793-1796.
- Rossow W.B., R.A. Schiffer (1999), Advances in understanding clouds from ISCCP. *Bulletin of the American Meteorological Society* 80, 2261–2287.
- Russell, L. M., and E. G. Singh (2006), Submicron salt particle production in bubble bursting, *Aerosol Science and Technology*, 40, 664 – 671, doi:10.1080/02786820600793951.

- Russell, L. M., D. H. Lenschow, K. K. Laursen, P. B. Krummel, S. T. Siems, A. R. Bandy, D. C. Thornton, and T. S. Bates (1998), Bidirectional mixing in an ACE 1 marine boundary layer overlain by a second turbulent layer, *Journal Of Geophysical Research*, 103, 16,411 – 16,432.
- Russell, L.M., L.N. Hawkins, A.A. Frossard, P.K. Quinn, and T.S. Bates (2010), Carbohydrate-like composition of submicron atmospheric particles and their production from ocean bubble bursting. *Proceedings of the National Academy of Sciences*, vol. 107, no. 15, 6652–6657.
- Saiz-Lopez, A., and J. M. C. Plane (2004), Novel iodine chemistry in the marine boundary layer, *Geophysical Research Letters*, 31, L04112, doi:10.1029/2003GL019215.
- Saltzman, E. S., D. B. King, K. Holmen, and C. Leck (1993), Experimental determination of the diffusion coefficient of Dimethylsulfide in water, *Journal Of Geophysical Research*, 98(C9), 16,481–16,486.
- Saltzman, E. S., D. L. Savoie, J. M. Prospero and R. G. Zika (1986), Methanesulfonate and non-sea-salt sulfate in Pacific air: regional and seasonal variations. *Journal of Atmospheric Chemistry* 4, 227-240.
- Saltzman, E. S., I. Dioumaeva, and B. D. Finley (2006), Glacial/interglacial variations in methanesulfonate (MSA) in the Siple Dome ice core, West Antarctica, *Geophysical Research Letters*, 33, L11811, doi:10.1029/2005GL025629.
- Saltzman, E. S., W. J. De Bruyn, M. J. Lawler, C. A. Marandino, and C. A. McCormick (2009), A chemical ionization mass spectrometer for continuous underway shipboard analysis of dimethylsulfide in near-surface seawater, *Ocean Science*, 5(4), 537–546.
- Saltzman, E.S. (2009a), Marine aerosols, in *Surface Ocean-Lower Atmosphere Processes*, *Geophysical Monograph Series*, doi: 10.1029/2008GM000769.
- Sassen, K., and Z. Wang (2008), Classifying clouds around the globe with the CloudSat radar: 1-year of results, *Geophysical Research Letters*, 35, L04805, doi:10.1029/2007GL032591.
- Savoie, D. L., and J. M. Prospero (1989), Comparison of oceanic and continental sources of non-sea-salt sulfate over the pacific-ocean, *Nature*, 339 (6227), 685–687, doi:10.1038/339685a0.
- Scarratt, M. G., M. Levasseur, S. Michaud, and S. Roy (2007), DMSP and DMS in the Northwest Atlantic: Late-summer distributions, production rates and sea-air fluxes, *Aquatic Sciences* 69, 292–304, doi:10.1007/s00027-007-0886-1.
- Sciare, J., E. Baboukas, R. Hancy, N. Mihalopoulos, and B. C. Nguyen (1998), Seasonal variation of dimethylsulfoxide in rainwater at Amsterdam Island in the Southern Indian Ocean: Implications on the biogenic sulfur cycle, *Journal Of Atmospheric Chemistry*, 30 (2), 229–240.
- Sciare, J., N. Mihalopoulos, and B. C. Nguyen (2002), Spatial and temporal variability of dissolved sulfur compounds in European estuaries, *Biogeochemistry*, 59(1-2), 121–141.
- Sciare, J., N. Mihalopoulos, and B. Nguyen (1999), Summertime seawater concentrations of dimethylsulfide in the Western Indian ocean: Reconciliation of fluxes and spatial variability with long-term atmospheric observations, *Journal of Atmospheric Chemistry*, 32, 357–373(17).
- Sharma, S., L. A. Barrie, D. Plummer, J. C. McConnell, P. C. Brickell, M. Levasseur, M. Gosselin, and T. S. Bates (1999), Flux estimation of oceanic dimethyl sulfide around North America, *Journal Of Geophysical Research-Atmospheres*, 104(D17), 21,327–21,342.

-
- Shenoy, D. M., and M. D. Kumar (2007), Variability in abundance and fluxes of dimethyl sulphide in the Indian Ocean, *Biogeochemistry*, 83(1-3), 277–292, doi:10.1007/s10533-007-9092-4.
- Shenoy, D. M., J. T. Paul, M. Gauns, N. Ramaiah, and M. D. Kumar (2006), Spatial variations of DMS, DMSP and phytoplankton in the Bay of Bengal during the summer monsoon 2001, *Marine Environmental Research*, 62(2), 83–97.
- Shenoy, D. M., M. D. Kumar, and V. V. S. S. Sarma (2000), Controls of dimethyl sulphide in the Bay of Bengal during bobmex-pilot cruise 1998, *Proceedings Of The Indian Academy Of Sciences-Earth And Planetary Sciences*, 109(2), 279–283.
- Shenoy, D. M., S. Joseph, M. D. Kumar, and M. D. George (2002), Control and interannual variability of dimethyl sulfide in the Indian Ocean, *Journal Of Geophysical Research-Atmospheres*, 107(D19), 8008.
- Shon, Z. H., D D Davis, G. Chena, G. Grodzinskya, A. Bandyb, D. Thorntonb, S. Sandholma, J. Bradshawa, R. Stickela, W. Chameidesa, G. Kokc, L. Russelld, L. Mauldinc, D. Tannerc, F. Eiselec (2001), Evaluation of the DMS flux and its conversion to SO₂ over the Southern Ocean, *Atmospheric Environment*, 35 (1), 159–172.
- Shuman, F. G. (1957), Numerical methods in weather prediction: II. Smoothing and filtering, *Monthly Weather Review*, 85(11), 357–361.
- Siegel, D. A., and A. F. Michaels (1996), Quantification of non-algal light attenuation in the Sargasso Sea: Implications for biogeochemistry and remote sensing, *Deep-Sea Research Part Ii-Topical Studies In Oceanography*, 43(2-3), 321–345.
- Simó R. (2004). From cells to globe: approaching the dynamics of DMS(P) in the ocean at multiple scales. *Canadian Journal of Fisheries and Aquatic Sciences*, 61(5), 673-684. doi: 10.1139/F04-030.
- Simó R. and Pedrós-Alió C. (1999). Role of vertical mixing in controlling the oceanic production of dimethyl sulphide. *Nature*, 402(6760):396–399.
- Simó, R. (2001), Production of atmospheric sulfur by oceanic plankton: biogeochemical, ecological and evolutionary links, *Trends in Ecology & Evolution*, 16(6), 287–294.
- Simó, R. (2011). The role of marine microbiota in short-term climate regulation. In *The role of marine biota in the functioning of the biosphere*, C. Duarte (ed.), Fundación BBVA and Rubes Editorial, Bilbao, pp. 107-130.
- Simó, R., and J. Dachs (2002), Global ocean emission of dimethylsulfide predicted from biogeophysical data, *Global Biogeochem.Cycles*, 16(4), 1078, doi: 10.1029/2001GB001829.
- Simó, R., J. O. Grimalt, and J. Albaiges (1997), Dissolved dimethylsulphide, dimethylsulphoniopropionate and dimethylsulphoxide in Western Mediterranean waters, *Deep-Sea Research Part Ii-Topical Studies In Oceanography*, 44(3-4), 929–950.
- Simó, R., J. O. Grimalt, C. Pedros-Alio, and J. Albaiges (1995), Occurrence and transformation of dissolved dimethyl sulfur species in stratified seawater (Western Mediterranean-Sea), *Marine Ecology-Progress Series*, 127(1-3), 291–299.
- Six K.D. (2006). What controls the oceanic dimethylsulfide (DMS) cycle? A modeling approach. *Global Biogeochemical Cycles* 20(4) GB4011. doi: 10.1029/2005GB002674
- Six, K. D., and E. Maier-Reimer (2006), What controls the oceanic dimethylsulfide (DMS) cycle? A modeling approach, *Global Biogeochem. Cycles*, 20, GB4011, doi:10.1029/2005GB002674.
- Smirnov, A. BN Holben, YJ Kaufman, O Dubovik, TF Eck, I Slutsker, C Pietras, and RN Halthoreet

- (2002), Optical properties of atmospheric aerosol in maritime environments, *Journal of Atmospheric Science* 59, 501-523
- Smythe-Wright, D., S. M. Boswell, C. H. Lucas, A. L. New, and M. S. Varney (2005), Halocarbon and dimethyl sulphide studies around the mascarene plateau, *Philosophical Transactions Of The Royal Society Of London Series A-Mathematical Physical And Engineering Sciences*, 363(1826), 169–185.
- Sorooshian, A., L. T. Padró, A. Nenes, G. Feingold, A. McComiskey, S.P. Hersey, H. Gates, H.H. Jonsson, S.D. Miller, G.L. Stephens, R.C. Flagan, J.H. Seinfeld (2009), On the link between ocean biota emissions, aerosol, and maritime clouds: Airborne, ground, and satellite measurements off the coast of California, *Global Biogeochemical Cycles*, 23, GB4007, doi:10.1029/2009GB003464.
- Staubes, R., and H. W. Georgii (1993), Biogenic sulfur-compounds in seawater and the atmosphere of the Antarctic region, *Tellus Series B-Chemical And Physical Meteorology*, 45(2), 127–137.
- Staubes-Diederich, R. (1992), Veneilung von dimethylsulfid, carbonylsulfid und schwefelkohlenstoff in ozean und mariner atmosphere, Ph.D. thesis, Johann Wolfgang Goethe-Universitat, Frankfurt am Main, Gernany.
- Stauhes, R., and H.-W. Georgii (1993), Measurements of atmospheric and seawater DMS concentrations in the Atlantic, the Arctic, and the Antarctic region, in *Dimethylsulfide: Oceans, Atmosphere, and Climate.*, G. Restelli and G. Angeletti.
- Stefels, J. (2000). Physiological aspects of the production and coverision of DMSP in marine algae and higher plants. *Journal of Sea Research* 43 (3-4), 183-197.
- Stefels, J., and L. Dijkhuizen (1996), Characteristics of DMSP-lyase in *Phaeocystis* sp (prymnesiophyceae), *Marine Ecology Progress Series*, 131(1–3), 307–313.
- Stefels, J., M. Steinke, S. Turner, G. Malin, and S. Belviso (2007), Environmental constraints on the production and removal of the climatically active gas dimethylsulphide (DMS) and implications for ecosystem modelling, *Biogeochemistry*, 83(1–3), 245–275, doi:10.1007/s10533-007-9091-5.
- Sunda W., Kieber D.J., Kiene R.P., and Huntsman S. (2002). An antioxidant function for DMSP and DMS in marine algae. *Nature*, 418(6895):317–320.
- Suntharalingam, P., A. J. Kettle, S. M. Montzka, and D. J. Jacob (2008). Global 3-D model analysis of the seasonal cycle of atmospheric carbonyl sulfide: Implications for terrestrial vegetation uptake. *Geophysical Research Letters* 35, L19801, doi:10.1029/2008GL034332.
- Takami, A., W. Wang, D. Tang, and S. Hatakeyama (2006), Measurements of gas and aerosol for two weeks in northern China during the winterspring period of 2000, 2001 and 2002, *Atmospheric Research*, 82, 688–697, doi:10.1016/j.atmosres.2006.02.023.
- Tanré, D. Y. J. Kaufman, M. Herman, and S. Mattoo (1997), Remote sensing of aerosol properties over oceans using the MODIS/EOS spectral radiances, *Journal Of Geophysical Research* 102, 16,971–16,988, doi:10.1029/96JD03437
- Tanré, D. L.A. Remer, Y.J. Kaufman, S. Mattoo, P.V. Hobbs, J.M. Livingston, P.B. Russell and A. Smirnov (1999), Retrieval of aerosol optical thickness and size distribution over ocean from the MODIS airborne simulator during TARFOX, *Journal Of Geophysical Research* 104(D2), 2261–2278

-
- Tanré, D., F. M. Breon, J. L. Deuze, M. Herman, P. Goloub, F. Nadal, and A. Marchand (2001), Global observation of anthropogenic aerosols from satellite, *Geophysical Research Letters*, 28 (24), 4555–4558.
- Tanzer, D., and K. G. Heumann (1992), Gas-chromatographic trace-level determination of volatile organic sulfides and selenides and of methyl-iodide in Atlantic surface-water, *International Journal Of Environmental Analytical Chemistry*, 48(1), 17–31.
- Tegen, I., P Hollrig, M Chin, I Fung, D Jacob and J Penner (1997), Contribution of different aerosol species to the global aerosol extinction optical thickness: Estimates from model results, *Journal Of Geophysical Research* 102, 23895-23915
- Thomas M.A., P. Suntharalingam, L. Pozzoli, S. Rast, A. Devasthale, S. Kloster, J. Feichter, and T. M. Lenton (2010), Quantification of DMS aerosol-cloud-climate interactions using the ECHAM5-HAMMOZ model in a current climate scenario. *Atmospheric Chemistry and Physics* 10, 7425–7438, doi:10.5194/acp-10-7425-2010.
- Toole D.A. and Siegel D.A.(2004). Light-driven cycling of dimethylsulfide (DMS) in the Sargasso Sea: Closing the loop. *Geophysical Research Letters*, 31(9):L09308. doi: 10.1029/2004GL019581.
- Toole, D. A., D. J. Kieber, R. P. Kiene, D. A. Siegel, and N. B. Nelson (2003), Photolysis and the dimethylsulfide (DMS) summer paradox in the Sargasso Sea, *Limnology and Oceanography*, 48(3), 1088–1100.
- Trevena, A. J., and G. B. Jones (2006), Dimethylsulphide and dimethylsulphonio propionate in Antarctic sea ice and their release during sea ice melting, *Marine Chemistry*, 98(2–4), 210–222, doi:10.1016/j.marchem. 2005.09.005.
- Turner, S. M., G. Malin, and P. S. Liss (1989), Dimethyl sulfide and (dimethylsulfonio) propionate in European coastal and shelf waters, in *Biogenic Sulfur in the Environment*, American Chemical Society, Washington, D. C.
- Turner, S. M., G. Malin, P. D. Nightingale, and P. S. Liss (1996a), Seasonal variation of dimethyl sulphide in the North Sea and an assessment of fluxes to the atmosphere, *Marine Chemistry*, 54(3-4), 245–262.
- Turner, S. M., G. Malin, P. S. Liss, D. S. Harbour, and P. M. Holligan (1988), The seasonal-variation of dimethyl sulfide and dimethylsulfonylpropionate concentrations in nearshore waters, *Limnology And Oceanography*, 33(3), 364–375.
- Turner, S. M., M. J. Harvey, C. S. Law, P. D. Nightingale, and P. S. Liss (2004), Iron-induced changes in oceanic sulfur biogeochemistry, *Geophysical Research Letters*, 31(14), L14,307.
- Turner, S. M., P. D. Nightingale, L. J. Spokes, M. I. Liddicoat, and P. S. Liss (1996b), Increased dimethyl sulphide concentrations in sea water from in situ iron enrichment, *Nature*, 383(6600), 513–517.
- Turner, S. M., P. D. Nightingale, W. Broadgate, and P. S. Liss (1995), The distribution of dimethyl sulfide and dimethylsulphonylpropionate in Antarctic waters and sea-ice, *Deep-Sea Research Part Ii-Topical Studies In Oceanography*, 42(4-5), 1059–1080.
- Twohy C.H., J.R. Anderson (2008), Droplet nuclei in non-precipitating clouds: composition and size matter. *Environmental Research Letters* 3, 045002.
- Twomey, S. (1974), Pollution and the planetary albedo, *Atmospheric Environment*, 8, 1251-1256.
- Twomey S. (1991), Aerosols, clouds and radiation. *Atmospheric Environment*. 25A, 2435-2442.
- Twomey, S. (1977), Influence of pollution on shortwave albedo of clouds, *Journal Of The Atmospheric*

- Sciences, 34(7), 1149–1152.
- Uchida, A., T. Ooguri, and Y. Ishida (1992), The distribution of dimethylsulfide in the waters off Japan and in the subtropical and tropical Pacific-Ocean, *Nippon Suisan Gakkaishi*, 58(2), 261–265.
- Uher, G. (2006). Distribution and air–sea exchange of reduced sulphur gases in European coastal waters. *Est. Coastal and Shelf Science* 70, 338–360.
- Uher, G., G. Schebeske, S. Rapsomanikis, and M. O. Andreae (1995), Measurements of dimethyl sulfide in surface waters of the Northeast Atlantic ocean, in *Ann. Geophys.*, 13. suppl.II, Part II, C394, Hamburg, Germany.
- Uher, G., G. Schebeske, S. Rapsomanikis, and M. O. Andreae (1996), The distribution of dissolved dimethyl sulfide at the European continental margin, in *Ann. Geophys.*, 14. suppl. II, C590, Den Haag, Netherlands.
- Uher, G., G. Schebeske, S. Rapsomanikis, and M. O. Andreae (1997), The distribution of dissolved dimethylsulfide at the European continental margin., in *OMEX I final report, Subproject Carbon Cycling and Biogases*, Brussels, European Union Marine Science and Technology (MAST) program.
- Uzuka, N., S. Watanabe, and S. Tsunogai (1996), Dimethylsulfide in coastal zone of the East China sea, *Journal of Oceanography*, 52(3), 313–321.
- Vaattovaara, P., P. E. Huttunen, Y. J. Yoon, J. Joutsensaari, K. E. J. Lehtinen, C. D. O’Dowd, and A. Laaksonen (2006), The composition of nucleation and aiten modes particles during coastal nucleation events: evidence for marine secondary organic contribution, *Atmospheric Chemistry And Physics*, 6, 4601–4616.
- Vallina S.M. and Simó R. (2007b). Re-visiting the CLAW hypothesis. *Environmental Chemistry* 4: 384–387. doi: 10.1071/EN07055.
- Vallina S.M., Simó R, Gasso S., de Boyer-Montegut C., del Rio E., Jurado E., and Dachs J. (2007). Analysis of a potential ‘solar radiation dose-dimethylsulfide-cloud condensation nuclei’ link from globally mapped seasonal correlations. *Global Biogeochemical Cycles* , 21(2):B2004–B2004. doi: 10.1029/2006GB002787.
- Vallina S.M., Simó R., and Gasso S. (2006). What controls CCN seasonality in the southern ocean? A statistical analysis based on satellite-derived chlorophyll and CCN and model-estimated OH radical and rainfall., *Global Biogeochemical Cycles* 20(1):B1014–B1014. doi: 10.1029/2005GB002597.
- Vallina, S. M., and R. Simó (2007a), Strong relationship between DMS and the solar radiation dose over the global surface ocean, *Science*, 315(5811), 506–508, doi:10.1126/science.1133680.
- Vallina, S. M., R. Simó, and M. Manizza (2007c), Weak response of oceanic dimethylsulfide to upper mixing shoaling induced by global warming, *Proceedings of the National Academy of Sciences U. S. A.*, 104(41), 16,004–16,009, doi:10.1073/pnas.0700843104.
- Verdugo, P., A.L. Alldredge, F. Azam, D.L. Kirchman, U. Passow, and P.H. Santschi (2004), The oceanic gel phase: a bridge in the DOM-POM continuum. *Marine Chemistry*, 92, 67–85.
- Vignati E; Facchini MC; Rinaldi M; Scannell C; Ceburnis D; Sciare J; Kanakidou M; Myriokefalitakis S; Dentener F; O’Dowd CD (2010) Global scale emission and distribution of sea-spray aerosol: Sea-salt and organic enrichment. *Atmospheric Environment* Vol: 44 (5) pp: 670–677. doi: 10.1016/j.atmosenv.2009.11.013.
- Vila-Costa M., Kiene R.P., and Simó R. (2008). Seasonal variability of the dynamics of dimethylated

-
- sulfur compounds in a coastal northwest Mediterranean site. *Limnology and Oceanography* 53: 198-211.
- Vila-Costa, M., J. Pinhassi, C. Alonso, J. Pernthaler, and R. Simó (2007), An annual cycle of dimethylsulfoniopropionate-sulfur and leucine assimilating bacterioplankton in the coastal NW Mediterranean, *Environmental Microbiology*, 9(10), 2451–2463, doi:10.1111/j.1462-2920.2007.01363.x.
- Vila-Costa, M., R. Simó, H. Harada, J. M. Gasol, D. Slezak, and R. P. Kiene (2006), Dimethylsulfoniopropionate uptake by marine phytoplankton, *Science*, 314(5799), 652–654, doi:10.1126/science.1131043.
- Vogt, M., S. M. Vallina, E. T. Buitenhuis, L. Bopp, and C. Le Quere (2010), Simulating Dimethylsulphide seasonality with the Dynamic Green Ocean Model PlankTOM5, *Journal of Geophysical Research*, 115, C06021, doi:10.1029/2009JC005529.
- von Glasow R. and P. J. Crutzen (2004). Model study of multiphase DMS oxidation with a focus on halogens. *Atmospheric Chemistry and Physics*, 4, 589–608, ref: 1680-7324/acp/2004-4-589
- von Glasow, R. (2007) A look at the CLAW hypothesis from an atmospheric chemistry point of view, *Environmental Chemistry*, 4, 379–381,
- Wanninkhof, R. (1992), Relationship between wind speed and gas exchange over the ocean, *Journal of Geophysical Research*, 97, 7373–7382.
- Warneck, P. (2003), In-cloud chemistry opens pathway to the formation of oxalic acid in the marine atmosphere, *Atmospheric Environment*, 37, 2423–2427, doi:10.1016/S1352-2310(03)00136-5.
- Watanabe, S., H. Yamamoto, and S. Tsunogai (1995), Relation between the concentrations of DMS in surface seawater and air in the temperate North Pacific region, *Journal Of Atmospheric Chemistry*, 22(3), 271–283.
- Weber, R. J., P. H. McMurry, L. Mauldin, D. J. Tanner, F. L. Eisele, S. M. Brechtel, F. Kreidenweis, G.L. Kok, R. D. Schillawski, and D. Baumgardner (1998), A study of new particle formation and growth involving biogenic and trace gas species measured during ACE 1, *Journal of Geophysical Research*, 103, 16,285–16,396.
- Wong, C. S., S. E. Wong, W. A. Richardson, G. E. Smith, M. D. Arychuk, and J. S. Page (2005), Temporal and spatial distribution of dimethylsulfide in the Subarctic Northeast Pacific ocean: a high-nutrient-low-chlorophyll region, *Tellus B*, 57(4), 317–331.
- Wong, C. S., S. K. E. Wong, A. Pena, and M. Levasseur (2006), Climatic effect on DMS producers in the NE sub-Arctic Pacific: ENSO on the upper ocean, *Tellus Series B-Chemical And Physical Meteorology*, 58(4), 319–326.
- Woodcock, A. H. (1948), Note concerning human respiratory irritation associated with high concentrations of plankton and mass mortality of marine organism, *Journal of Marine Research*, 7, 56–62.
- Woodhouse, M. T., Carslaw, K. S., Mann, G. W., Vallina, S. M., Vogt, M., Halloran, P. R., and Boucher, O. (2010), Low sensitivity of cloud condensation nuclei to changes in the sea-air flux of dimethyl-sulphide, *Atmospheric Chemistry and Physics Discuss.*, 10, 3717-3754, doi:10.5194/acpd-10-3717-2010.
- Wu Q., D.J. Karoly, G.R. North (2008), Role of water vapor feedback on the amplitude of season cycle in the global mean surface air temperature. *Geophysical Research Letters* 35, L08711,

- doi:10.1029/2008GL033454.
- Xie, H., and R. M. Moore (1999). Carbon disulfide in the North Atlantic and Pacific Oceans, *Journal of Geophysical Research* 104(C3), 5393–5402.
- Yang, G. P., M. Lévassieur, S. Michaud, A. Merzouk, M. Lizotte, and M. Scarratt (2009), Distribution of dimethylsulfide and dimethylsulfoniopropionate and its relation with phytoplankton in the surface microlayer of the western North Atlantic during summer, *Biogeochemistry*, 94, 243–254, doi:10.1007/s10533-009-9323-y.
- Yang, G. P., X. T. Liu, L. Li, and Z. B. Zhang (1999), Biogeochemistry of dimethylsulfide in the South China Sea, *Journal Of Marine Research*, 57(1), 189–211.
- Yang, G. P., Z. B. Zhang, L. Li, and X. Liu (1996), Study on the analysis and distribution of dimethyl sulfide in the East China Sea, *Chinese Journal of Oceanology and Limnology*, 14(2), 141–147.
- Yassaa, N., I. Peeken, E. Zöllner, K. Bluhm, S. Arnold, D. Spracklen, and J. Williams (2008), Evidence for marine production of monoterpenes, *Environmental Chemistry*, 5, 391–401, doi:10.1071/EN08047.
- Yoch, D. C. (2002), Dimethylsulfoniopropionate: its sources, role in the marine food web, and biological degradation to dimethylsulfide, *Applied and Environmental Microbiology*, 68(12), 5804–5815, doi:10.1128/AEM.68.12.5804-5815.2002.
- Yu, J. Z., S. F. Huang, J. H. Xu, and M. Hu (2005), When aerosol sulfate goes up, so does oxalate: Implication for the formation mechanisms of oxalate, *Environmental Science & Technology*, 39, 128–133, doi:10.1021/es049559f.
- Yum S.S., J.G. Hudson (2004), Wintertime/summertime contrasts of cloud condensation nuclei and cloud microphysics over the Southern Ocean. *Journal Of Geophysical Research* 109, D06204, doi:10.1029/2003JD003864.
- Yvon-Lewis, S.A., E.S. Saltzman, and S.A. Montzka (2009). Recent trends in atmospheric methyl bromide: analysis of post-Montreal Protocol variability. *Atmospheric Chemistry and Physics* 9, 5963–5974.
- Yvon, S. A., E. S. Saltzman, D. J. Cooper, T. S. Bates, and A. M. Thompson (1996), Atmospheric sulfur cycling in the tropical Pacific marine boundary layer (12 degrees S, 135 degrees W): A comparison of field data and model results. 1. Dimethylsulfide, *Journal Of Geophysical Research-Atmospheres*, 101(D3), 6899–6909.
- Zemmelink, H. J., J. W. H. Dacey, L. Houghton, E. J. Hints, and P. S. Liss (2008), Dimethylsulfide emissions over the multi-year ice of the western Weddell Sea, *Geophysical Research Letters*, 35(6), L06603, doi:10.1029/2007GL031847.
- Zhang, R.Y., I. Suh, J. Zhao, D. Zhang, E.C. Fortner, X. Tie, L.T. Molina and M.J. Molina (2004). Atmospheric new particle formation enhanced by organic acids, *Science*, 304 (5676), 1487–1490.